Defining conditions required for the derivation of midbrain dopaminergic neurons from embryonic stem cells using stem cell reporter lines

A thesis submitted in fulfillment of the requirements for the degree of

DOCTOR OF PHILOSOPHY (PhD)

By

Brigham Jay Hartley, B. Sc (Hons)

Drug Discovery Biology

Faculty of Pharmacy and Pharmaceutical Sciences

Monash University

Australia

May 2013

Table of Contents

Declaration

I hereby declare that this thesis contains no content that has been accepted for the award of any other degree or diploma at any university or equivalent institution. Additionally, to the best of my knowledge and belief, this thesis contains no material previously published, presented or written by another person, except where due reference is made in the text of this thesis.

This thesis contains one original paper published in a peer-reviewed journal. The inclusion of co-authors reflects the fact that the work came from a collaborative effort between researchers.

Chapter 3 "**Implantation of mESC-derived *Lmx1a* positive neural progenitors in an MPTP Mouse Model of Parkinson's disease**" is part of a paper published in the journal Stem Cells (2012).

_____

Signature

_____

Date

In the case of Chapter 3 contribution to the work was as follows:

Name	Nature of contribution (est. % contribution)
Brigham Hartley	Study design, planning, collection and assembly of data (60%)
Christian Nefzger	Planning, collection and/or assembly of data (15%)
Colin Su	Collection and/or assembly of data (10.5%)
Stewart Fabb	Generation of reporter cell lines (10.5%)
Siew Beh	Collection and/or assembly of data (2%)
Wendy Zeng	Collection and/or assembly of data (2%)
John Haynes	Conception and design, advice, manuscript reviewing
Colin Pouton	Conception and design, advice, manuscript reviewing

In the case of Chapter 4 and 5 contributions to the work were as follows:

Name	**Nature of contribution (est. % contribution)**
Brigham Hartley	Study design, planning, collection and/or assembly of data (85%)
Stewart Fabb	Cloning and reporter cell line screening (5%)
Ben Finnin	Help with reporter cell line generation (5%)
Marina Schmidt	Collection and/or assembly of data (5%)
John Haynes	Conception and design, advice, manuscript reviewing
Colin Pouton	Conception and design, advice

Declaration by co-authors

The undersigned authors hereby certify that:

- they meet the criteria for authorship in that they have participated in the conception, execution, or interpretation of at least that part of the publication in their field of expertise;
- they take public responsibility for their part of the publication, except for the responsible author who accepts overall responsibility for the publication;
- there are no other authors of the publication according to these criteria;
- potential conflicts of interest have been disclosed to (a) granting body, (b) the editor or publisher of journal or other publications, and (c) the head of the responsible academic unit; and
- The original date are stored at the following location and will be held for at least five years from the date indicated above

Location

Drug Discovery Biology, Faculty of Pharmacy and Pharmaceutical Sciences, Monash University, Parkville, Vic, Australia

Name	**Signature**	**Date**
Brigham Hartley		27/05/13
Ben Finnin		27/05/13
Stewart Fabb		27/05/13
Christian Nefzger		21/05/13
Colin Su		21/05/13
Siew Beh		21/05/13
Wendy Zeng		21/05/13
John Haynes		27/05/13
Colin Pouton		27/05/13

Acknowledgements

The last four years have been the worst and best times of my life and wouldn't have been possible with out a number of supportive people in my life.

First and foremost I would to thank my mother, Rosemary, who has been my biggest fan and support, both emotionally and financially! She really is the best! Also my big little bro Dari for his muscles and words of encouragement; and my father, Donald for my random phone calls here and there!.. oh and also money.

My supervisors, John and Jen. Thank you both for your support and our little chats over the years (and putting up with me). Also Colin who has provided me with tremendous insight into the realm of science with his scientific tidbits.

I would also like to thank my rock and fantastic mentor in both life and the politics of science Erica, with out whom, I would have probably thrown the "towel" in a long time ago.

How could I forget my surrogate molecular biology daddy, Stewart! Also Ben, my Mr. known-it-all and a great philosophizing buddy. Oh the places you will go. Both Louise and Christian, who have provided me with hours of timewasting and thoughtful discussion, but who have also importantly gone off into the big bad world of science and have engendered me with inspiration and hope for making it.

Numerous other people in the Stem Cell Lab. Of note Cam, who has really been my thesis buddy of the last 6 months of late nights. Poor Cam. Brad, my hESC buddy. My "students" Marina and Pradeep for not providing me with to many headaches! Durgesh for this worldly optimism. Other stem cell members Colin and Wendy.

A special mention also goes to Adrian and his friendly banter!

Thank you all so much!

Communications

The following communications, resulting form studies conducted in this thesis were presented as conference abstracts, posters or presentations.

- **Hartley B.J.** Watmuff, B., Finnin, B.A., Fabb, S.A., Pouton, C.W., & Haynes, J.M., (2012) **"Modelling neuroinflammation in Parkinson's disease using human pluripotent stem cell derived midbrain dopaminergic neurons"** Selected oral presentation at the Australian Society for Stem Cell Research part of the 6th Annual Australian Health and Medical Research Congress, November 25-28 2012, Adelaide, Australia
- **Hartley B.J.** Schmidt, M.E., Finnin, B.A., Fabb, S.A., Pouton, C.W., & Haynes, J.M., (2012) "***LMX1A*** **defines midbrain dopaminergic neurons from differentiating human pluripotent stem cells: FACS and fiction"** poster presented at the 10th annual International Society for Stem Cell Research (ISSCR) Conference, June 13-16, 2012, Yokohama, Japan
- **Hartley B.J.** Schmidt, M.E., Finnin, B.A., Fabb, S.A., Nefzger, C.M., Su, C., Pouton, C.W., & Haynes, J.M., (2011) "***LMX1A*** **defines midbrain dopaminergic neurons: FACS and fiction"** poster presented at the 1st Joint Cold Spring Harbor (CSH) Asia/International Society for Stem Cell Research (ISSCR) Conference on Cellular Programs & Reprogramming, Oct 24-28 2011, Suzhou, China
- **Hartley B.J.** Schmidt, M.E., Finnin, B.A., Fabb, S.A., Pouton, C.W., & Haynes, J.M., (2011) "**Using a *LMX1A* reporter cell line to isolate midbrain dopaminergic precursors from human embryonic stem cells"** oral presentation at the 1st Student Brain Symposium, Florey Neurosciences Institute, Melbourne, VIC, Australia, Oct 6, 2011 -

- **Hartley B.J.** Schmidt, M.E., Finnin, B.A., Fabb, S.A., Pouton, C.W., & Haynes, J.M., (2011) "**Using a *LMX1A* reporter cell line to isolate midbrain dopaminergic precursors from human embryonic stem cells"** oral presentation at the 6th Annual Higher Degree by Research Symposium, Monash University, Melbourne, VIC, Australia, Oct 3, 2011
- Watmuff B.,* **Hartley B.J.,*** Pouton, C.W., & Haynes, J.M., (2010) **"mES Cell Derived Pitx3^{+} Dopaminergic Neurons Display Signs of Functional Maturity After *In vitro* Differentiation"** poster presentation at 8th Annual International Society for Stem Cell Research Conference, June 16-19, San Francisco, CA, United States of America
- **Hartley B.J.,*** Watmuff B.,* Pouton, C.W., & Haynes, J.M., (2009) **"mES Cell Derived Pitx3^{+} Dopaminergic Neurons Display Signs of Functional Maturity After *In vitro* Differentiation"** poster presentation at 1st Annual Monash University Neuroscience and Mental Health Early Career Researchers Network Symposium. Clayton, VIC, Australia – awarded 1st prize for poster competition

Publications

- Nefzger, C.M*., Su, C*., Fabb, S.A., **Hartley, B.J.,** Beh, S.J., Haynes, J.M., Pouton, C.W., (2012) **"*Lmx1a* allows context-specific isolation of progenitors of GABAergic or dopaminergic neurons during neural differentiation of embryonic stem cells"** *Stem Cells* 2012;30 1349-1361
- **Hartley, B.J.,** Watmuff, B., Hunt, C.P., Haynes, J.M. & Pouton, C.W. (in press, 2013) "***In vitro* differentiation of pluripotent stem cells towards either forebrain GABAergic or midbrain dopaminergic neurons"** *Book titled "Neural Stem Cells Assays" to be published by Wiley-Blackwell*
- Hunt, C.P., Watmuff, B., **Hartley, B.J.,** Haynes, J.M. & Pouton, C.W. (in press, 2013) **"Genetic reporter cell lines: tools for stem cell biology and drug discovery"** *Book titled "Neural Stem Cells Assays" to be published by Wiley-Blackwell*

* These authors contributed equally

Summary

The ability of pluripotent stem cells (ESCs) to self-renew and generate somatic phenotypes of the adult human make them an attractive cell source for both *in vitro* disease modelling and cell replacement therapy (CRT). The efficient and robust derivation of midbrain dopaminergic (mbDA) cells from PSCs may pave the way for CRT, for PD patients whose disease is refractory to current pharmacotherapy or physical intervention such as DBS. Moreover, the derivation of functional *bona fide* mbDA neurons may also help interrogate molecular processes that underlie pathogenesis of PD, through *in vitro* PD modelling. However, a major hindrance to the application of PSC-derived cells to CRT and disease modelling is that current differentiation protocols produce cultures containing a mixture of neural phenotypes, with low yields of the target cell type. Reporter cell lines offer the ability to readily isolate cells from differentiating PSC cultures based on the expression of a gene of interest. The LIM homeobox transcription factor 1 α (*Lmx1a*) is a prominent regulator of early mbDA specification. In this study I utilize both mouse and human PSCs expressing EGFP under the control of the endogenous *Lmx1a*-promoter to investigate aspects of mbDA cell fate specification following FACS, subsequent to derivation under chemically defined monolayer (CDML) or PA6 stromal cell differentiation protocols. The survival, integration and functional regenerative capacity of mESC-derived *Lmx1a* positive progenitors in a MPTP mouse model of PD were also assessed.

In the first experimental Chapter (Chapter 3) I demonstrated that the MPTP mouse model of PD was not suitable to assess the functional regenerative capacity of grafted *Lmx1a* positive precursors due to the absence of behavioural deficits. Grafted FACS-isolated *Lmx1a* positive precursors survived sorting and grafting, but they did not appear to differentiate or integrate in the host striatum of MPTP treated mice. In an effort to

understand the differentiational potential of *Lmx1a*+ progenitors, FACS-isolated *Lmx1a*+ cells from both CDML and PA6 differentiation conditions were replated for terminal differentiation. It was shown that the isolation of mbDA progenitors using *Lmx1a* reporter cell line from differentiating mESCs was context dependent. Indicating that *Lmx1a* positive cells isolated from CDML conditions gave rise to rostral GABA+/GAD67+/SatB2+ neurons, where as *Lmx1a* positive cells isolated from PA6 differentiation conditions gave rise to mbDA cells at high frequency following terminal differentiation.

As mouse PSCs are not a suitable cell source for CRT or *in vitro* disease modelling due to differences in function and neurochemistry compared to human mbDA neurons, Chapter 4 explored whether the isolation of *LMX1A* positive cells from human PSCs differentiating under PA6 conditions would also give rise to high yields of mbDA neurons. In contrast to mESC differentiation, PA6 differentiation of hESCs did not yield neural or mbDA precursors to a similar extent. Following inhibition of TGFβ (ALK4, 5 and 7) and BMP (ALK2 and 3) receptors using small molecules, robust neural induction was achieved. However in the absence of regionalisation cues, neuroepithelial progenitors defaulted to a mixed culture containing cells with rostral and dorsal midbrain phenotypes. Floor plate specification of progenitors was achieved with a small molecule activator of SHH signalling, but this did not induce widespread mbDA progenitor differentiation and suggested a requirement for caudalisation signals. Caudalisation agents were tested for their ability to specify a midbrain phenotype. Fibroblast factor 8b, upregulated the expression of mbDA progenitor genes, and thus was used in the directed differentiation of neural precursors before FACS isolation. Quantitative PCR following FACS isolation of *LMX1A*-promoter driven EGFP positive cells demonstrated a transcriptional profile indicative of mbDA progenitors. Following protracted maturation in defined medium, high yields of mbDA

neurons were observed. Thus, work in Chapter 4 provided a proof of principle that mbDA neurons can be generated from hESCs in high yields, demonstrating a more clinically relevant cell population.

The final experimental Chapter (Chapter 5) defined the conditions required for the derivation of mbDA neurons under CDML conditions free of animal products or cell lines or via the use of FACS isolation techniques. Small molecules inhibitors of TGFβ and BMP signalling provided robust neural induction in the absence of PA6 cells. Using the hLMX1A-AIG reporter cell line as a screening tool for the commitment to a mbDA phenotype, it was shown that exposure to morphogens important for mbDA neuron specification (SHH and WNT signalling), enabled the derivation of regionally specified mbDA progenitors. The commitment to mbDA neural phenotype was subsequently confirmed with a hPITX3-EGFP reporter cell line. In summary work in this chapter provided evidence that mbDA neurons can be generated from hESCs in high yields under CDML conditions, demonstrating a more clinically and industrial relevant cell population, that can be used for either CRT or *in vitro* PD modelling.

Abbreviations

$[Ca2+]_i$	intracellular calcium ion concentration
°C	degrees Celsius
α-MEM	alpha modified Eagle's medium
6-OHDA	6-hyrdoxydopamine
5-HT	5-hydroxytryptamine/serotonin
AA	ascorbic acid
AADC	aromatic L-amino acid decarboxylase
AF	Alexa Fluor® secondary antibodies
AIG	AMP/IRES/EGFP
ALDH1	aldehyde dehydrogenase 1
AMP	ampicillin resistance gene
APC	adenomatosis polyposis coli
ATP	adenosine triphosphate
BAX	B-cell lymphoma 2 associated protein
BCL-2	B-cell lymphoma 2
bHLH	basic-helix-loop-helix
BMP	bone morphogenic protein
BDNF	brain-derived neurotrophic factor
BSA	bovine serum albumin
CDML	chemically defined monolayer
CHIR99021	6-(2-(4-(2,4-dichlorophenyl)-5-(4-methyl-1H-imidazol-2yl)pyrimidin- 2-ylamino)ethylamino)nicotinonitrile
CM	conditioned medium
CNS	central nervous system
COMT	catechol-O-methyltransferase
CRT	cell replacement therapy
d	day of differentiation
DβH	dopamine beta hydroxylase

DA	dopamine
DAergic	dopaminergic
DAG	diacylglycerol
DAPI	4',6-diamidino-2-phenylindole
DAPT	N-[N-(3,5-Difluorophenacetyl)-L-alanyl]-S-phenylglycine t-butyl ester
DAAM1	DSH-associated activator of morphogenesis 1
DAT	dopamine active transporter
db-cAMP	dibutyryl cyclic AMP
DBS	deep brain stimulation
DKK1	dickkopf 1 homolog
DSH	dishevelled cytoplasmic phosphoprotein
DMEM	Dulbecco's modified eagle's medium
DMEM/F12	Dulbecco's modified eagle's medium: nutrient xix F12
DMSO	dimethyl sulfoxide
DNA	deoxyribonucleic acid
DOPAC	3,4-dihydroxy-phenylacetic acid
EB	embryoid bodies
EFNB1	ephrin B-1
EGFP	enhanced green fluorescent protein
EN1/2	engrailed 1/2
EpiSC	epiblast stem cell
ERK	extracellular signal-regulated kinases
FACS	fluorescence-activated cell sorting
FBS	fetal bovine serum
FGF	fibroblast growth factor
FLUO-4 AM	FLUO 4 acetoxymethyl ester
FOXA2	forkhead box protein a2
FOXG1	Forkhead box protein G1
FRT	flippase recognition target sites
FP	floorplate
FZD	frizzled receptor

g	grams
GABA	γ-Aminobutyric acid
GAD65/67	glutamic acid decarboxylase 65/67
GDF	growth differentiation factor
GDNF	glial-cell derived neurotrophic factor
GFAP	glial fibrillary acidic protein
GIRK2	G-protein-gated inwardly rectifying K+ channel 2
GFRα1	glial-cell derived neurotrophic factor receptor α1
GMEM	Glasgow minimum essential medium
GPi	globus pallidus internal
GSK3β	glycogen synthase kinase 3 beta
HBSS	Hank's buffered salt solution
hESC	human embryonic stem cell
HVA	homovanillic acid
ICM	inner cell mass
iCM	induced cardiomyocyte
iDA	induced dopaminergic neuron
IGF2	insulin like growth factor 2
iN	induced neuron
IP3	inositol trisphosphate
iPSC	induced pluripotent stem cell
IRES	internal ribosomal entry site
IZ	intermediate zone
JNK	c-Jun N-terminal kinases
KO	knockout
KO-DMEM	knockout Dulbecco's modified eagle's medium
KSR	knockout serum replacement
L	litre
L-DOPA	L-3,4-dihydroxyphenylalanine

LB	Lewy body
LEF1	lymphoid enhancer-binding factor 1
LIF	leukemia inhibitory factor
LMX1A/B –	LIM homeobox transcription factor 1 alpha/beta
LRP5/6 –	low-density lipoprotein receptor-related proteins 5/6
LSB	LDN193189 and SB431542
M	molar
MAO	monoamine oxidase
MAPK	mitogen-activated protein kinase
mbDA	midbrain dopaminergic neuron
mC	mCherry fluorescent protein
MEF	mouse embryonic fibroblast
mESC	mouse embryonic stem cell
MPP+	1-Methyl-4-phenylpyridinium
MPDP	1-Methyl-4-phenyl-2,3- dihydropyridinium
MPPP	1-Methyl-4-phenyl-4-propionoxypiperidine
MPTP	1-Methyl-4-phenyl-1,2,3,6-tetrahydropyridine
MSX	msh homebox
NBM	neurobasl media
Neo	neomycin
NET	norepinephrine transporter
NGN2	neurogenin 2
NR4A2	nuclear receptor subfamily 4, group A, member 2
NSB	noggin and SB431542
OCT4	octamer-binding transcription factor 4
OTX2	orthodenticle homologue 2
PBS	phosphate buffered saline
P/S	penicillin/streptomycin
PAX2/6/7 -	paired box gene 2/6/7
PD	Parkinson’s disease

PI	propidium iodide
PITX3	pituitary homeobox 3
PLC	phospholipase C
PLO	poly-L-ornithine
PTN	pleiotrophin
qRT-PCR	quantitative PCR with reverse transcription
RA	retinoic acid
RAC1	Ras-related C3 botulinum toxin substrate 1
ROCK	rho-associated protein kinase
R-NSC	rosette neural stem cell
ROS	reactive oxygen species
RRF	retrorubal field
RNA	ribonucleic acid
SAG	smoothened agonist
SANT-1	N-[(3,5-dimethyl-1-phenyl-1H-pyrazo-l-4-yl)methylene]-4-(phenylmethyl)-1-piperazinamin-e
SDF-1	stromal cell-derived factor 1
SDIA	stromal derived inducing activity
SEM	standard error of the mean
sFRP	secreted frizzled-related protein
SGZ	subgranular zone
SHH	sonic hedgehog
SMAD	mothers against decapentaplegic (MAD) and the Caenorhabditis elegans protein SMA.
SN	Substantia Nigra
SNpc	Substantia Nigra pars compacta
SNpr	Substantia Nigra pars reticulata
SOX2	sex determining region Y box 2
SOD	superoxide dismutase
SSEA1/4	stage-specific embryonic antigen 1/4
STN	subthalamic nuclei
SVZ	sub ventricular zone

TALEN	transcription activator–like effector nuclease
TCF	transcription factor 3
TGF	transforming growth factor
TH	tyrosine hydroxylase
TO-PRO®-3	Quinolinium,4-[3-(3-methyl-2(3H)-benzothiazolylidene)-1-propenyl]-1-[3-(trimethylammonio)propyl]-, diiodide
TUJ1	neuron-specific class III beta-tubulin
U	
VM	ventral midbrain
VMAT2	vesicular monoamine transporter 2
VTA	ventral tegmental area
VZ	ventricular zone
v/v	volume per unit volume
WNT	wingless-type MMTV integration site family
w/v	weight per unit volume
X	
Y	
ZFN	zinc finger nuclease

List of Figures

List of Tables

Chapter One: General Introduction

1.1 Stem cells

Embryonic stem cells (ESCs) are a remarkable group of cells derived from the isolation of and *in vitro* cultivation of the inner cell mass (ICM) of a blastocyst (Evans & Kaufman, 1981; Martin 1981; Thomson et al., 1998). Under appropriate culture conditions ESCs self-renew and posses the potential to differentiate into all somatic cell types, a feature known as pluripotency (Pan, 2007). These two characteristics, self-renewal and pluripotency, make ESCs and their differentiated progeny attractive tools for studying developmental and cellular biology, pharmacological and toxicological screens; as well as for potential clinical applications such as cell replacement therapy (CRT)(Pouton & Haynes, 2007; Wobus, 2001).

Current research into the etiology, mechanisms of disease progression and treatment of neurological diseases such as Parkinson's disease (PD) is hampered by the necessity to use animal or cellular models that do not fully recapitulate the human disease. Embryonic stem cell-derived midbrain dopaminergic (mbDA) neurons, the same neurons lost in PD (see Section 1.4), could circumvent such issues and allow disease modelling, target identification and validation in a physiologically relevant human system (Pouton & Haynes, 2007). Furthermore, as current therapeutic approaches in PD are only symptomatic, PSC-derived cellular sources could be used for CRT to possibly halt or retard disease progression (Wu & Boyd, 2007).

1.1.1 Mouse embryonic stem cells

Mouse ESCs (mESCs), isolated from the inner cell mass (ICM) of the blastocyst were initially maintained on mitotically inactivated mouse embryonic fibroblasts (MEFs, also referred to as feeders) cells (Evans & Kaufman, 1981; Martin 1981). Mouse ESCs divide

symmetrically every 12 hrs, grow in dome-shaped colonies (Niwa et al., 1998) and are defined by the expression of the transcription factors octamer-binding transcription factor 4 (Oct4) and Nanog (Chambers et al., 2003). The key cytokine secreted by MEFs demonstrated to enable mESC self-renewal was originally identified as Differentiation inhibiting activity (DIA)(Williams et al., 1988; Rathjen, Toth, Willis, Heath, & Smith, 1990) but now has been shown to be leukemia inhibitory factor (LIF) (Williams et al., 1988; Smith et al., 1988). Since then, mESCs have been maintained under *in vitro* culture conditions in the absence of MEFs, but in the presence of LIF together with serum (Ying, Nichols, Chambers, & Smith, 2003). Following withdrawal of LIF, mESCs continue to proliferate, but begin to differentiate into the three germ layers, the endoderm, the mesoderm and the ectoderm (Niwa et al., 1998).

Numerous pathways play a role in the maintenance of mESC self-renewal (Ying et al., 2008), however, the most clearly established pathway is the STAT3 signaling pathway, which is only activated in the presence of serum and LIF (Niwa et al., 1998; Ying et al., 2003). Fetal bovine serum (FBS) is a commonly used media supplement and contains many growth factors, however the indispensable factor for self-renewal of mESCs, BMP4, induces Inhibitor of differentiation (Id) genes (Ying et al., 2003).

After almost three decades of maintaining mESCs using LIF and serum, it has been recently demonstrated that the inhibition of glycogen synthase kinase 3 beta (GSK3β) and mitogen activated protein kinase (MAPK – MEK1/2) signals is sufficient for self-renewal (Ying et al., 2008). Modulating these pathways using a two inhibitor cocktail known as 2i in the presence of LIF can maintain mESCs for numerous passages (Ying et al., 2008), in what has been coined a stem cell "naïve" state, because it closely resembles the most primitive state, or ground state of the mouse blastocyst (see Ying et al., 2008).

1.1.2 Human embryonic stem cells

Due to the fact that they were derived 17 years after mESCs (Thomson et al., 1998), the understanding, manipulation and differentiation of human embryonic stem cells (hESCs) is considerably inferior. hESCs were initially isolated under culture conditions, similar to mESCs (using feeders and serum) and are also defined by the expression of the pluripotency factors, OCT4 and Nanog, although other markers such as TRA-1-60 and stage-specific embryonic antigen-4 (SSEA-4) can also be used (Thomson et al., 1998). In contrast to mESCs, hESCs are dependent on fibroblast growth factor (FGF) and transforming growth factor β (TGFβ/Activin/Nodal) signaling pathways to maintain pluripotency (Dahéron et al., 2004; James, Levine, Besser, & Hemmati-Brivanlou, 2005; Schatten, Smith, Navara, Park, & Pedersen, 2005; Vallier, Alexander, & Pedersen, 2005). FGF2 is the key cytokine that maintains the self-renewal and pluripotency capacity of hESCs (Diecke, Quiroga-Negreira, Redmer, & Besser, 2008; Eiselleova, Matulka, Kriz, & Kunova, 2009; Greber et al., 2010; Levenstein et al., 2006). The action of FGF2 is mainly mediated through the MAP-ERK pathway, however other reports show that MAP-ERK independent FGF2 signaling can contribute to hESC self renewal and pluripotency (Diecke, Quiroga-Negreira, Redmer, & Besser, 2008; Dvorak et al., 2005; Li et al., 2007). FGF signaling works in conjunction with wingless-type MMTV integration site family (WNT), TGFβ, Hedgehog and Notch signalling, but antagonises BMP signalling (Greber, Lehrach, & Adjaye, 2007), which is known to promote differentiation of hESCs towards trophoblast (Xu et a., 2002).

The TGFβ superfamily consists of more than 40 members, including activin, nodal and BMPs (Gray et al., 2000). TGFβ1, via the TGFβ1 receptor (activin A receptor type II-like kinase 5, Alk5)(Vallier, Alexander, & Pedersen, 2005) and activin and nodal (Gray et al.,

2000) activates mothers against decapentaplegic (MAD) and the Caenorhabditis elegans protein SMA (SMAD)2/3 signaling (James, Levine, Besser, & Hemmati-Brivanlou, 2005; Vallier, Alexander, & Pedersen, 2005). Activin A, in concert with FGF2 maintains hESCs in an undifferentiated state without the need for feeder cells, conditioned medium (CM) or STAT3 activation (Beattie et al., 2005). Although activin/nodal signaling is essential for hESC maintenance, it is insufficient to maintain pluripotency or self-renewal when used alone (Vallier, Alexander, & Pedersen, 2005). Delineation of these signaling pathways has allowed the maintenance of hESC cultures under feeder free/animal product free conditions (Amit, Shariki, & Margulets, 2004).

Humans ESCs also show differences in clonal propagation (hESCs are susceptible to apoptosis following single cell dissociation)(Brimble et al., 2004; Ginis et al., 2004; Minkovsky & Patel, 2011; Ohgushi & Sasai, 2011; Rao, 2004; Watanabe et al., 2007), colony morphology and growth characteristics (hESCs grow slowly [36 hr doubling time] and as flat colonies)(Amit and Itskovitz-Eldor, 2002), and in their X inactivation status, with female hESCs retaining one inactive X chromosome (although this varies from hESC line to hESC line)(Hoffman et al., 2005).

1.1.3 Induced cell types

1.1.3.a Induced pluripotent stem cells

Although heralded as a cure to numerous biological afflictions, a number of political, sociological and ethical concerns remain that need to be overcome before the true translational potential of ESCs can be realised. Some of these concerns include the destruction of the embryo in the procurement of ESCs and immune rejection following transplantation (Bradley, Bolton, & Pedersen, 2002; Landry & Zucker, 2004; Swijnenburg

et al., 2005; Thomson et al., 1998). Such concerns have forced investigators to search for alterative sources of cells suitable for *in vivo* and *in vitro* use.

In 2006, the Yamanaka lab first reported the successful reprogramming of adult mouse fibroblasts back to a "ESC-like phenotype" via the forced expression of *Oct4*, Kruppel-like factor 2 (*Klf2*), sex determining region Y-box 2 (*Sox2*) and myelocytomatosis viral oncogene homolog (*myc*)(Takahashi & Yamanaka, 2006). Human somatic cells were subsequently reprogrammed in 2007 with the same four factors (Takahashi et al., 2007; Yu et al., 2007). Termed induced pluripotent stem cells (iPSCs), the generation of these "ESC-like" cells represented a breakthrough for both disease modeling and CRT since patient-specific iPSC lines could be generated that would provide disease specific *in vitro* models or abate the need for immunosuppressive (Dimos, Rodolfa, Niakan, & Weisenthal, 2008; Lee et al., 2009).

Generally, iPSC generation is an inefficient process (0.1% for conventional iPSC generation; Anokye-Danso et al., 2011). This together with the fact that viral integration into the host genome increases the risk of tumorigenicity has so far restricted the widespread adoption of iPSC based technology (Okita, Nakagawa, Hyenjong, Ichisaka, & Yamanaka, 2008). Thus, the present focus of the iPSC field is the generation of safer and more efficient re-programming strategies through the use of excisable viral cassettes (Soldner et al., 2009; Somers et al., 2010; Woltjen, Hämäläinen, Kibschull, Mileikovsky, & Nagy, 2011), proteins (Cho et al., 2010; Kim, Kim, Moon, & Chung, 2009; Zhou et al., 2009), micro RNAs (Anokye-Danso et al., 2011; Miyoshi et al., 2011), small molecules (Huangfu et al., 2008; Shi et al., 2008; Yuan et al., 2011b) or synthetic messenger RNA (Plews et al., 2010; Rosa & Brivanlou, 2010; Warren et al., 2010).

In terms of morphology and the expression of pluripotency markers, iPSCs appear identical to ESCs (Kim et al., 2011a), however, there is increasing evidence that discrepancies in epigenetic and genetic signatures exist (Chin, Mason, Xie, Volinia, & Singer, 2009; Guenther et al., 2010; Kim et al., 2011a; Lagarkova et al., 2010; Laurent et al., 2011; Sullivan, Bai, Fletcher, & Wilmut, 2010). Lamentably, the biggest advantage of iPSCs, the immuno-tolerability by the host, has recently been questioned by the demonstration that *in vitro* autologous transplantation of iPSCs in mice generates an immune reaction (Zhao, Zhang, & Rong, 2011).

1.1.3.b Transdifferentiated cells

A more recent source of cells for CRT and experimental disease modelling, which negates the need to generate a pluripotent intermediate, is via transdifferentiation from one adult somatic cell type to another. This method has generated both neurons (induced neurons, iNs) and cardiomyocytes (induced cardiomyocytes; iCM), using either the forced expression of lineage specific genes (Ambasudhan et al., 2011; Efe et al., 2011; Kim et al., 2011b; Liu, Li, Stubblefield, & Blanchard, 2011; Marro et al., 2011; Meng, Chen, Miao, Zhou, & Lao, 2011; Pang et al., 2011; Perrier et al., 2004; Pfisterer et al., 2011) or whole transcriptome transfer (Kim et al., 2011c; Sul et al., 2009). As advantageous as this strategy appears to be, the non-proliferative nature of transdifferentiated cells raises issues of efficiency, and the ability to generate sufficient cell numbers for experimental and clinical applications is questionable. To this end, a number of groups have now shown that it is possible to transdifferentiate self-renewing tripotent precursor populations (for the neural lineage), which can be expanded and differentiated into neurons, astrocytes and oligodendrocytes (Han et al., 2012; Lujan, Chanda, Ahlenius, Südhof, & Wernig, 2012; Matsui et al., 2012; Thier et al., 2012).

Although iPSC generation and transdifferentiation to direct phenotypes represent exciting alternatives to ESCs, to date the highest differentiation yields are from ESCs (Chambers et al., 2012; Kattman et al., 2011; Kim et al., 2011a; Kriks et al., 2011). Thus, this thesis will focus on the use of ESC-derived mdDA progenitors, precursors and neurons. However, a key challenge to the stem cell field remains the development of a reproducible, practical, economically viable protocol for directing differentiation of ESCs to a mbDA phenotype.

1.2 *In vivo* neurodevelopment

1.2.1 Early brain organisation

The development of the central nervous system (CNS) commences at the gastrula stage of embryogenesis. This process, known as neural induction, was first demonstrated in amphibians by Spemann and Mangold in 1924 (as reviewed in Weinstein & Hemmati-Brivanlou, 1999). Analogous neural inductive capacity was later demonstrated for the organising centres of amniotes, indicating a conserved method of neural induction across species (Waddington & Schmidt, 1933). Since this pioneering work, the molecular mechanisms that govern neural induction have been elucidated. Rather than acting via receptor mediated signalling events to promote neural induction, organiser factors antagonise local epidermal inducers, in particular members of the TGFβ superfamily, such as BMPs and activin/nodal (Hemmati-Brivanlou, Kelly, & Melton, 1994; Sasai, Lu, Steinbeisser, & De Robertis, 1995). Noggin, follistatin and chordin all antagonise BMP and/or activin/nodal signals to induce neuralisation within the ectoderm, in turn forming the neuroepithelium (Hawley & Wünnenberg-Stapleton, 1995; Hemmati-Brivanlou et al., 1994; Lamb, Knecht, Smith, & Stachel, 1993; Sasai et al., 1995; Xu, Kim, Taira, & Zhan, 1995). Following neural induction, the neuroepithelium, also known as the neuroectoderm, thickens as a result of cellular division to form the neural plate (Patthey & Gunhaga, 2011; Wurst & Bally-Cuif, 2001). As the neural plate develops, it invaginates, giving rise to the neural tube, in a process known as neurulation (Sakai, 1989).

Prior to neural tube closure, the rostral aspect expands and is segregated into three vesicles that form the prosencephalon, mesencephalon and rhombencephalon (Donkelaar, 2006; Vermeren & Keynes, 2001), which eventually form the forebrain, midbrain and hindbrain, respectively. These early structures further divide and generate distinct

anatomical regions of the adult brain: the prosencephalon divides into the telencephalon, which in turn gives rise to corpus striatum (globus pallidus and striatum), the paleocortex and neocortex, and the diencephalon, which becomes the epithalamus, thalamus, hypothalamus and infundibulum (Rubenstein, 1994). The rhombencephalon gives rise to the metencephalon and myelencephalon. The metencephalon becomes the cerebellum and pons, and the myelencephalon forms the medulla oblongata (Vermeren & Keynes, 2001). Unlike the prosencephalon and rhombencephalon, the mesencephalon does not divide into secondary vesicles but rather gives rise to the tectum, tegmentum and cerebral peduncles (Wassef & Joyner, 1997). Together with the spinal cord, these brain structures align along the rostrocaudal (R/C) and dorsoventral (D/V) axes to form the CNS (Vermeren & Keynes, 2001). CNS development hinges on the activity of a number of morphogens that direct developing neural precursors to specific phenotypes. These signals include Sonic hedgehog (SHH) and the WNT family of signalling molecules.

1.2.2 Specification of neural axes by signalling molecules

1.2.2.a SHH signalling

Sonic hedgehog is one of the three main proteins of the mammalian hedgehog signalling pathway (Ingham & McMahon, 2001). In regards to VM development, SHH is secreted from cells in the notochord, a structure ventral to the neural tube (see Fig. 1.1), where it induces the formation of the floor plate (FP)(Jessell, Bovolenta, Placzek, Tessier-Lavigne, & Dodd, 1989). The FP is a structure that extends along the midline of the ventral neural tube from its most caudal aspect in the spinal cord, through the midbrain into the diencephalon, with its rostral limit being below a region known as the zona limitans intrathalamica (Chiang et al., 1996; Jessell et al., 1989) SHH signalling from the underlying notochord induces the expression of SHH in the FP, thereby creating a secondary ventral organising signalling centre (Ericson, Briscoe, Rashbass, van Heyningen, & Jessell, 1997). The gradient of SHH is thought to specify the D/V identity of cells throughout the developing neural tube (Briscoe, Pierani, Jessell, & Ericson, 2000)(see Fig. 1.1). This hypothesis was exemplified by Chamberlain et al., (2008), where SHH transcriptional activity was visualised in the developing neural tube using a SHH-eGFP reporter mouse, and eGFP was observed to be concentrated at the most ventral domain of the neural tube with a decreasing intensity of fluorescence up to the most dorsal domain (Chamberlain, Jeong, Guo, Allen, & McMahon, 2008). In the FP, where SHH concentrations are the highest, SHH activates forkhead box protein A2 (FOXA2; Echelard, Epstein, St-Jacques, & Shen, 1993), which in turn induces a number of downstream genes important in the specification of the ventral midbrain and thus can be used to identify FP cells (Bonilla et al., 2008; Kittappa, Chang, Awatramani, & McKay, 2007; Nelander, Hebsgaard, & Parmar, 2009).

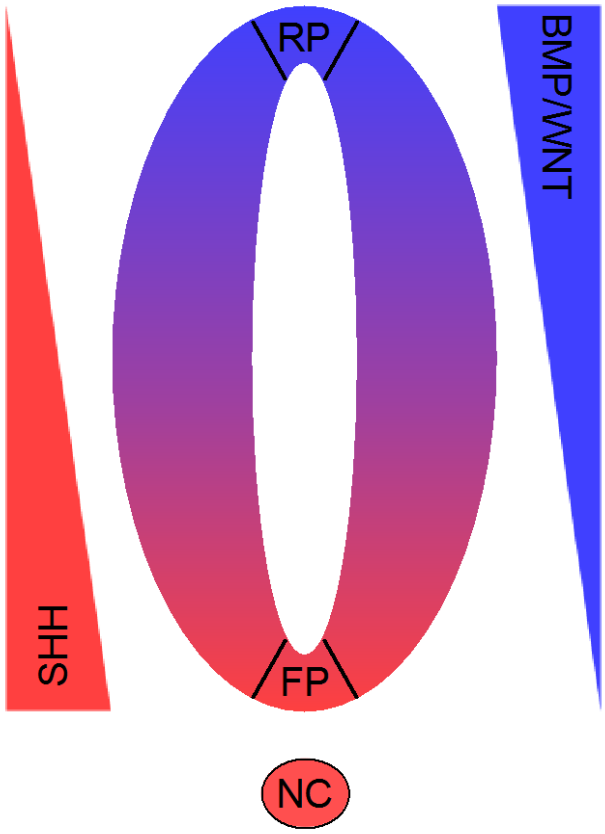

Figure 1.1 Morphogen Specification of the Neural Tube. The roof plate (RP) secretes BMP and WNTs (blue), while the notochord (NC) secretes SHH (red) in turn inducing SHH expression in the floorplate FP.

1.2.2.b WNT signalling

The WNT family of signalling molecules modulate many cellular processes, including neurogenesis (Logan & Nusse, 2004; Wilson & Edlund, 2001). The levels and regions of WNT expression during neurogenesis are complex and differ tremendously between the 19 isoforms. WNT1, WNT3, WNT3a and WNT8 are all expressed in the roofplate of the developing neural tube (Fig 1.2; Capdevila, Tabin, & Johnson, 1998; Hollyday & McMahon, 1995; Ikeya & Takada, 1998; Marcelle & Stark, 1997; Parr, Shea, & Vassileva, 1993). WNT5a and WNT7a are expressed in the FP of the developing neural tube, except in the developing myelencephalon, which contains only WNT7a. WNT1 is also found in the FP of the midbrain (Parr et al., 1993), whereas WNT4 is expressed in both the roofplate and the FP (McGrew & Otte, 1992; Ungar, Kelly, & Moon, 1995).

WNT signalling occurs via one major and two less common pathways, following the binding of WNT to the cell surface receptor Frizzled (FZD)(Bhanot et al., 1996; Wilson & Edlund, 2001; Yang-Snyder, Miller, Brown, & Lai, 1996). Each pathway involves different intracellular signalling proteins and downstream effectors.

For canonical signalling, WNT binds to FZD, leading to the formation of a protein complex between the WNT co-receptor, low-density lipoprotein receptor-related proteins 5/6 (LRP5/6; Pinson, Brennan, Monkley, Avery, & Skarnes, 2000; Tamai, Zeng, Liu, Zhang, & Harada, 2004; Wehrli et al., 2000), the cytoplasmic phosphoprotein Dishevelled (DSH; (Cliffe, Hamada, & Bienz, 2003; Tamai et al., 2004) and Adenomatous polyposis coli (APC; (Hart, de los Santos, Albert, & Rubinfeld, 1998; Kishida et al., 1998). This protein complex inhibits the activity of GSK3β, which in the absence of WNT signalling phosphorylates β-catenin leading to its proteolytic degradation (Aberle, Bauer, Stappert, Kispert, & Kemler, 1997; Nakamura, Hamada, Ishidate, & Anai, 1998). Following the inhibition of the "β-

catenin destruction complex" by WNT, levels of β-catenin increase within the cytoplasm (Munemitsu, Albert, Souza, Rubinfeld, & Polakis, 1995; Tolwinski & Wieschaus, 2004). β-catenin translocates to the nucleus where it interacts with transcription factors, such as lymphoid enhancer-binding factor 1/T-cell-specific transcription factor (LEF1/TCF) to affect WNT target gene expression (Behrens, Kries, Kühl, Bruhn, & Wedlich, 1996; van de Wetering et al., 1997).

The other WNT signal transduction pathways, the planar cell polarity (PCP) and WNT/calcium pathways are β-catenin independent. In the PCP pathway, WNT recruits DSH following interaction with FZD, which in turn forms a complex with DSH-associated activator of morphogenesis 1 (DAAM1)(Habas, Kato, & He, 2001). DAAM1 then activates the small G-protein Rho, which subsequently activates Rho-associated protein kinase (ROCK). DSH also complexes with Ras-related C3 botulinum toxin substrate 1 (RAC1) which in turn activates c-Jun N-terminal kinases (JNK), leading to cytoskeletal rearrangement (Winter et al., 2001). WNT modulates the levels of Ca^{2+} by activating phospholipase C (PLC), leading to the generation of diacylglycerol (DAG) and inositol trisphosphate (IP3), causing Ca^{2+} release from intracellular Ca^{2+} stores (Kohn & Moon, 2005).

WNT signalling was initially shown to inhibit BMP4-signalling, causing pronounced neural induction (Baker, Beddington, & Harland, 1999). This was further corroborated by a demonstration that the microinjection of β-catenin mRNA increased noggin and chordin expression and subsequently promoted neural induction (Wessely, Agius, & Oelgeschläger, 2001). Conversely, Heeg-Truesdell and LaBonne have argued that inhibition of WNT-associated β-catenin signalling was required for neural induction (Heeg-Truesdell & LaBonne, 2006). Since then, it has been revealed that the dynamic expression of WNT

leads to the precise spatiotemporal control in neural induction. In addition, downstream transcriptional mediation of the WNT pathway may confer distinct phenotypic outcomes in different cellular contexts (Heeg-Truesdell & LaBonne, 2006).

WNT signalling also plays a role in patterning, in both the D/V and R/C axes of the developing neural tube. XWNT-3a (a Xenopus laevis WNT-3a homologue), together with noggin and follistatin were shown to potentiate the expression of caudalising genes while suppressing rostralising genes (McGrew & Lai, 1995). Further studies using dominant negative XWNT8 (McGrew, Hoppler, & Moon, 1997) or through modulation of WNT signalling (Leyns, Bouwmeester, Kim, Piccolo, & De Robertis, 1997), gave impetus to the notion that WNTs act as caudalising agents. Consistent with this notion, later evidence showed that increased expression of secreted WNT antagonists and thus decreased WNT signalling, increased the incidence of rostral markers at the expense of caudal markers (Peng & Westerfield, 2006). A number of WNT antagonists such as Dickkopf1 (DKK1) (Brott, 2002; del Barco Barrantes, Davidson, Gröne, Westphal, & Niehrs, 2003; Diep, Hoen, Backman, Machon, & Krauss, 2004; Glinka et al., 1998; Hashimoto et al., 2000), secreted Frizzled-related proteins (sFRPs) (Bradley et al., 2000; Dennis, Aikawa, & Szeto, 1999; Finch et al., 1997; Kim & Lowenstein, 2001; Leimeister, Bach, & Gessler, 1998; Leyns et al., 1997; Rattner et al., 1997) and cerberus (Biben, Stanley, Fabri, & Kotecha, 1998; Bouwmeester, Kim, Sasai, & Lu, 1996; Piccolo, Agius, Leyns, & Bhattacharyya, 1999), which are expressed in the anterior ectoderm, have decisive roles in patterning. Thus, the caudalising activity of WNTs, together with the expression of WNT modulators such as DKK1, sFRPs and cerebus contribute to a WNT signalling gradient that regulates the specification of progenitors along the R/C axis much like SHH does in the D/V axis (Kiecker & Niehrs, 2001)(see Fig. 1.2).

1.2.3 Midbrain dopaminergic neurogenesis

Owning to the difficulty in obtaining human tissue the majority of studies examining the development of mbDA neurons to date has been conducted using mice, thus the following section outlines the development of the mouse vMB unless otherwise stated.

Mammalian mbDA neurons reside in three distinct nuclei; the substantia nigra pars compacta (SNpc; A9), the ventral tegmental area (VTA; A10) and the retrorubal field (RRF; A11)(Bjorklund & Dunnett, 2007). Three major axonal projections arise from the A9 and A10 nuclei; the nigrostriatal pathway, from the SNpc to the dorsal striatum, and both the mesolimbic and mesocortical pathways, projections from the VTA to the ventral striatum and the frontal cortex, respectively (Bjorklund & Dunnett, 2007). The DAergic cells of the A8 are a dorsal and caudal extension of the A9 group and project to striatal, limbic and cortical areas (Bentivoglio & Morelli, 2005).

1.2.3.a Transcriptional control of midbrain dopamine neurogenesis

Following the molecular signals that shape the embryonic brain along the D/V and R/C axes, local developmental programs are initiated. The genesis of mbDA neurons occurs in response to gradients of two diffusible secreted factors, Shh and Fgf8 (Ericson et al., 1997; Lee, Danielian, Fritzsch, & McMahon, 1997). As discussed earlier Shh is secreted from the notochord, and subsequently from the FP (see Section 1.2.2.a). Fgf8 is secreted from the isthmus organiser also known as the mid-hindbrain organiser (MHO)(Lee et al., 1997), which is present at the mid-hindbrain boundary. The location of the MHO engenders it with a unique ability to control the size and location of the field where mbDA neurons will be generated (Brodski et al., 2003). Early in development, the MHO is established in response to the mutual repression of two transcription factors, orthodenticle

homologue 2 (Otx2) and gastrulation brain homeobox 2 (Gbx2)(Joyner & Liu, 2000). Notably, Otx2 and Gbx2 are not required for the induction of MHO genes, but are essential for the correct position of the MHO (Brodski et al., 2003; Li & Joyner, 2001; Puelles et al., 2004).

Following the establishment of the MHO, a second wave of transcription factors begin to further regionalise the mid and hindbrain. Pair-ruled gene 2 (Pax2; (Urbánek, Fetka, Meisler, & Busslinger, 1997) the LIM homeobox transcription factor 1-beta (Lmx1b; (Adams, Maida, Golden, & Riddle, 2000) and Wnt1 (Prakash, Brodski, Naserke, & Puelles, 2006) all participate in the regionalisation process. Subsequently, engrailed (En-1, En2 and Pax5 are expressed around the developing MHO (Danielian & McMahon, 1996; Urbánek et al., 1997). In addition to Shh, Fgf8 and Wnt1 signalling, retinoic acid (RA) is also essential for determining where the mid-hindbrain boundary will form, and thus is an important signalling molecule in the development of mbDA neurons (Niederreither, Fraulob, & Garnier, 2002).

In response to Shh signalling, the FP becomes populated with radial glia-like progenitors positive for Foxa2 (Bonilla et al., 2008; Kittappa et al., 2007; Lin et al., 2009) and Sox2, a transcription factor important for the regulation of embryonic and neural development (Graham, Khudyakov, Ellis, & Pevny, 2003). The expression of LIM homeobox transcription factor 1-alpha (Lmx1a) in the Foxa2+ floorplate cells marks the first sign of mbDA progenitors (Andersson, Tryggvason, Deng, Friling, Alekseenko, Robert, Perlmann, & Ericson, 2006b; Ono et al., 2007; Terzioglu & Galter, 2008)(see Fig. 1.3). Lmx1a is involved in the specification of a neural and dopaminergic fate (Andersson et al., 2006b; Deng et al., 2011; Yan, Levesque, Claxton, Johnson, & Ang, 2011), presumably through the transcriptional repression of other cell fates in the developing midbrain (Nakatani, Kumai,

Mizuhara, Minaki, & Ono, 2010), although this remains to be explored fully. Lmx1a and Lmx1b are important in the maintenance and survival of mbDA neurons (Smidt et al., 2000; Yan et al., 2011), while the latter is also important for the specification of serotonergic neurons (Cheng et al., 2003; Ding et al., 2003b; Nefzger, Haynes, & Pouton, 2011). Wnt1 signalling induces Lmx1a expression, which in turn induces Wnt1 expression, forming an auto regulatory feedback loop (Chung et al., 2009). Neurogenin 2 (Ngn2) is the foremost proneural factor essential for the neurogenesis of mbDA progenitors (Andersson, Jensen, Parmar, Guillemot, & Bjorklund, 2006a; Kele et al., 2006; Lindholm et al., 2007; Shachar, Kahana, Kampel, Warshawsky, & Youdim, 2004; Thompson, Grealish, Kirik, & Björklund, 2009). Using chick embryos and mouse mutants, Lmx1a has been shown to regulate neurogenesis by inducing Msx11 expression, which subsequently activates Ngn2 (Andersson et al., 2006b). Consistent with this observation, Ngn2 expression was reduced to 70% of wildtype levels in Lmx1a dreher mutant mice (Ono et al., 2007). In addition, Lmx1a has been demonstrated to repress Nkx6.1 expression, another Shh responsive gene expressed broadly in progenitor cells of the ventral midbrain (Andersson et al., 2006b), important for motor neuron and ventral interneuron fates (Sander et al., 2000). However, as Lmx1a induces Msx1, it has been suggested that Lmx1a-mediated suppression of Nkx6.1 is most likely indirect. Indeed when Lmx1a was overexpressed in chick embryos at a time point when Lmx1a has not induced Msx1 expression, Nkx6.1 repression was not observed (Andersson et al., 2006b). Corin, a transmembrane serine protease and marker of the ventral midline is also expressed at this time (Ono et al., 2007).

After this initial wave of specification, mbDA progenitors begin to migrate ventrally and express nuclear receptor subfamily 4, group A, member 2 (Nr4a2), a member of the nuclear receptor family of transcription factors (Zetterström, Williams, Perlmann, & Olson,

1996). NR4A2 expression occurs as the mbDA progenitors leave the cell cycle, where NR4A2 interacts with the cyclin-dependent kinase inhibitor p57Kip2 (Joseph et al., 2003), tyrosine hydroxylase (Th), aromatic L-amino acid decarboxylase (Aadc), vesicular monoamine transporter 2 (VMAT2), the DA transporter (DAT)(Smits, Ponnio, Conneely, Burbach, & Smidt, 2003), as well as the axonal transport motor protein, kinesin family member 1A (KIF1A), and the neuronal-specific regulator of semaphorin 3A signalling in growth cones, collapsing response mediator 1 (CRMP1)(Johnson, Michelhaugh, Bouhamdan, Schmidt, & Bannon, 2011). Remarkably, this NR4A2 mediated control of protein expression is restricted to DA neurons of the midbrain and is not required in any other TH-expressing cell populations (Zetterström et al., 1997). The regulation of TH via Nr4a2 is due to a direct interaction of Nr4a2 with a Nr4a2 binding response element (NBRE) in the 5' untranslated region of the Th gene (Kim, Kim, Hwang, & Seo, 2003). A NBRE sequence has also been found in the DAT gene, indicating similar regulation (Sacchetti, Brownschidle, Granneman, & Bannon, 1999).

Following the expression of Nr4a2, another transcription factor, Pitx3, a member of the bicoid class of homeodomain proteins, is observed in developing post-mitotic mbDA progenitors (Smidt et al., 1997). Pitx3 is important for the maintenance and survival of mbDA neurons (Nunes, Tovmasian, Silva, Burke, & Goff, 2003; Semina, Murray, Reiter, Hrstka, & Graw, 2000). Furthermore, Pitx3, like Nr4a2, regulates the expression of Th at the genetic level, as there is a high affinity Pitx3 binding site present in the Th promoter (Cazorla, Smidt, O'Malley, & Burbach, 2000; Lebel, Gauthier, & Moreau, 2001). In addition to its role of regulating Th expression, there is evidence suggesting that Pitx3 regulates a microRNA feedback circuit important for the stability of the mbDA phenotype (Kim et al., 2007).

During the above-mentioned transcriptional specification phase, mbDA neurogenesis and subsequent expansion of the mbDA domain is proceeding at a remarkable rate. Anatomically, the mbDA region ends up comprising three distinct zones (see Fig 1.3): the ventricular zone (VZ; uppermost domain) containing proliferative Sox2+ progenitors, the intermediate zone (IZ) containing migrating post-mitotic Lmx1a+/Nr4a2+ DA neuroblasts, and the mantle zone (MZ, lower-most domain) containing mature DA neurons (Jönsson, Ono, Björklund, & Thompson, 2009; Villaescusa & Arenas, 2010).

Following expansion and migration, the newly formed mbDA neurons begin to integrate into the neuronal circuitry and form the nigrostriatal pathway. At this point A9 neurons can be delineated from other mdDA neurons via the preferential expression of G-protein-gated inwardly rectifying K+ channel 2 (Girk2), aldehyde dehydrogenase 1 family, member A1 (Aldh1a1) and the low level expression of calbindin, which is mainly expressed in mbDA neurons of the A10 region (Thompson, Barraud, Andersson, Kirik, & Björklund, 2005).

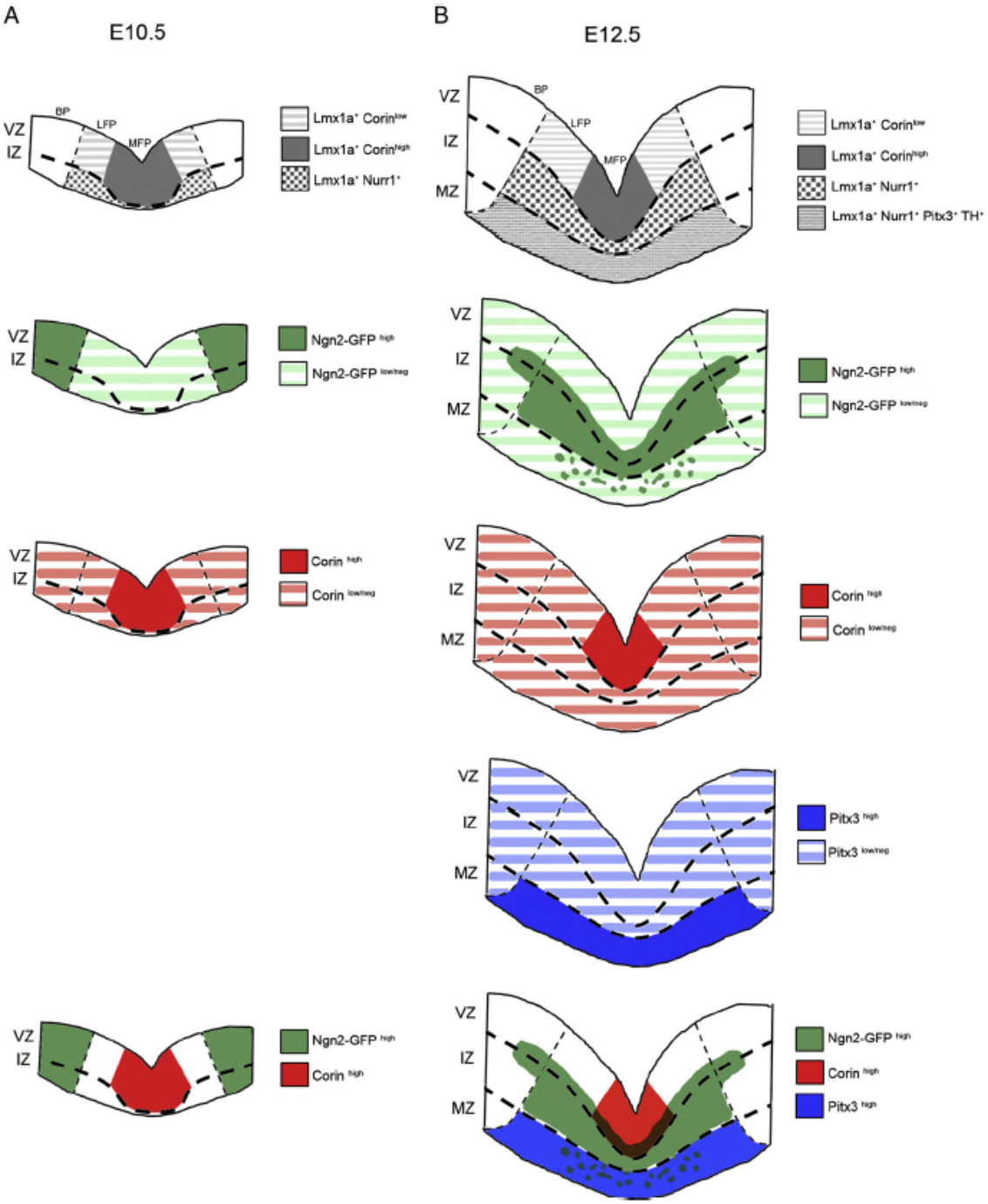

Figure 1.2 Schematic of marker expression during (**A**) early and (**B**) late ventral midbrain neurogenesis. Marker expression in each area is indicated by colour and different textures. Striped areas indicate low/negative expression. Solid areas indicate high expression. Lmx1a expression is shown in grey, Ngn2 expression is depicted in green, Corin expression is in red and the expression domain of Pitx3 is shown in blue. In early ventral midbrain neurogenesis only the ventral zone (VZ) and intermediate zone (IZ) are shown, where as in late neurogenesis all three domains, the VZ, IZ and mantle zone (MZ) are present. From this schematic it is clear that Lmx1a expression appears in early mbDA progenitor (grey areas, A) and its expression is maintained in maturing mbDA neurons as they migrate ventrally to form Lmx1a+/Nurr1 (Nr4a2)+/Pitx3+/Th+ mbDA neurons (B).

- image taken from (Villaescusa & Arenas, 2010)

1.3 *In vitro* neural specification

The differentiation of ESCs into cells of the neural lineage attempts to mimic *in vitro* neurodevelopment, whereby extrinsic cytokines induce neural commitment as well as specify neuronal phenotypes. As endogenous neurogenesis in the adult human brain is largely restricted to the subventricular zone (SVZ) and subgranular zone (SGZ) (Arsenijevic et al., 2001; Kirschenbaum et al., 1994; Kukekov et al., 1999; Pagano et al., 2000; Pincus & Keyoung, 1998; Taupin, 2002), the capacity for endogenous regeneration in response to damage, disease and/or degeneration is limited. Thus ESC-derived neural phenotypes have been proposed as a potential exogenous therapeutic replacement.

1.3.1 Early methods for the in vitro differentiation of DA neurons from ESCs

Over the years, many protocols have been established to direct ESC differentiation into specific neural lineages. Initial efforts utilised embryoid bodies (EBs), which contain multicellular multi-differentiated structures, of which neural derivatives are present but only in limited amounts (Bain, Kitchens, Yao, Huettner, & Gottlieb, 1995). The study of neural induction using EB formation is complicated as cell-cell interactions occur and growth factor expression is not controlled. Furthermore, due to the three dimensional nature of EBs, the extraction of neural subtypes is problematic. To combat these problems, a five-stage, modified version of the EB protocol was developed (Lee et al., 2000). In this modification, ESCs are first expanded (stage 1), EBs are formed (stage 2), neural precursors are selected for using a chemically defined media (stage 3), the neural precursors are expanded (stage 4), and finally the precursors are patterned and then matured into functional post mitotic neurons (stage 5). Using this protocol, moderate numbers of mbDAergic neurons (>30%) from mESCs can be obtained (Lee et al., 2000).

An alternative to the five-stage protocol is the co-culture of ESCs on top of a monolayer of bone marrow stromal cells, such as PA6 or MS5 cells. When cultured at a low density in chemically defined media, mESCs colonise and undergo efficient neuralisation (Kawasaki et al., 2000). In addition, the stromal monolayer induces a modest proportion of mbDAergic cells from ESCs (30%). Interestingly, as patterning factors such as SHH, FGF8, RA or WNTs (see section 1.2) are not added to cultures during differentiation, the inference has been made that PA6/MS5 cells secrete/express their own patterning factors (Kawasaki et al., 2000; Perrier et al., 2004), an effect now known as stromal derived inducing activity (SDIA; Kawasaki et al., 2000). In an effort to ascertain the factors responsible for SDIA, Vazin and co-workers identified a combination of four proteins termed SPIE factors; stromal cell-derived factor 1 (SDF-1), pleiotrophin (PTN), insulin like growth factor 2 (IGF2) and ephrin B1 (EFNB1), which are secreted from PA6 cells and able to mimic the mbDA phenotype-inducing properties of SDIA (Vazin et al., 2009).

Stromal co-culture systems can also be used to generate other neural subtypes. Barberi et al., (2003) demonstrated that by altering the concentration, type and timing of cytokines added to a MS5 co-culture of hESCs, GABAergic, serotoninergic, cholinergic and motor neurons, as well as astrocytes and oligodendrocytes could be selectively generated (Barberi et al., 2003). Although this techniques offers a way of generating subtype specified cells from neural lineages, the presence of undifferentiated ESCs, the difficulty separating ESCs-derived cells from the stromal cell layer and the undefined nature of the differentiation process represent major drawbacks in the utilisation of the stromal co-culture method (Barberi et al., 2003).

Lastly, regardless of whether differentiation is induced by SDIA from stromal co-cultures, SPIE factors or the five-stage selection EB protocol, factors underlying neural specification remain unknown.

As an alternative, Ying and Smith (2003) developed an adherent chemically defined monolayer (CDML) differentiation protocol utilising serum free neural basal media together with a supportive extracellular matrix (laminin, gelatin or poly L-ornithine). A key feature of the CDML protocol was that it allowed the observation, analysis and manipulation of neural specification independent of multicellular aggregates, co-culture, serum, uncharacterized media constituents or cell selection methods (Ying & Smith, 2003). Using the CDML protocol, ESCs efficiently convert into neural precursors in the absence of any additional extrinsic factors, and by day 4 of differentiation more than 60% of cells are positive for SOX1, a marker of ectodermal cells committed to the neural lineage (Nefzger et al., 2012; Pevny, Sockanathan, & Placzek, 1998; Ying & Smith, 2003). This increases to over 75% of cells by day 7 (Nefzger et al., 2012; Ying & Smith, 2003). The early neuroepithelial cells organise themselves into structures known as rosettes, and consequently have been termed rosette neural stem cells or R-NSCs (Elkabetz et al., 2008). R-NSCs are a type of NSCs that can be derived from both mouse and human ESCs or neural plate stage embryos (Elkabetz et al., 2008). R-NSCs possess differentiation potential for both CNS and peripheral nervous system fates and give rise to a number of neural lineages (Elkabetz et al., 2008). These neural precursors can be expanded in suspension as neurospheres, or as adherent cultures (Zeng, Fabb, Haynes, & Pouton, 2011). The mitogen FGF-2 plays a major role in the expansion and survival of the neural precursors at this stage. Alternatively, the precursors can be plated in media with reduced or no FGF2 at all onto a substrate of

laminin/poly-L-ornithine/fibronectin, which induces them to terminally differentiate into glial cells or functional neurons (Nefzger et al., 2012; Ying & Smith, 2003).

1.3.2 Recent methods for the derivation of mbDA neurons from ESCs

Due to problems in obtaining mature mbDA neurons from an adult brains (either mouse or human), it has been difficult to compare the genetic, proteomic and functional characteristics of ESC-derived mbDA neurons to their *in vivo* counterparts. Until recently (see section 1.2), TH was used solely as a marker for mbDA neurons. Given the widespread expression of TH in the brain (Bjorklund & Dunnett, 2007) this approach is inadequate for defining *bona fide* mbDA neurons. Moreover, recent functional studies conducted on slice preparations of mouse midbrains have demonstrated functional characteristics specific to mdDA neurons, such as slow (1–3 Hz) spontaneous spiking (Guzman et al., 2010).

Armed with these new cell subtype specific assays (mbDA specific markers e.g. Foxa2/Th and functional characteristics e.g. slow (1–3 Hz) spontaneous spiking), stem cell biologists have recently demonstrated the derivation of b*ona fide* mbDA neurons from numerous cell sources, ESCs (Kirks et al., 2011), iPSCs (Kirks et al., 2011), and iNs (Pfisterer et al., 2011) utilising various patterning protocols and genetic manipulations. However, as outlined above, homogenous cultures have never been observed. As exogenous factor based protocols have not consistently generated large amounts of mbDA neurons, investigators have recently utilised the forced expression of genes associated with the mbDA phenotype as a means of generating high purity cultures.

Andersson and colleagues demonstrated that following the transfection of a mESC line generated to drive LMX1A and MSX1 from the NESTIN FP enhancer, moderate numbers (~37%) of mbDA neurons were generated (Andersson, et al., 2006b). Using a

similar approach, together with extrinsic factor patterning, Friling and co-authors observed that 75-95% of total cells were positive for TH, of which 98% of the TH+ cells also co-expressed other midbrain markers (Friling et al., 2009), although this study has never been repeated. A more recent study enriched for ventral midbrain precursors using FACS together with an OTX2-eGFP reporter line and CORIN antibody surface labeling, and demonstrated terminal cultures of which 82% were positive for TH and co-expressed other midbrain markers (Chung et al., 2011).

Regardless of which protocol is used to generate specific neural subtypes, issues of heterogeneity still exist within terminally differentiated cultures (Elkabetz et al., 2008; Gaspard & Vanderhaeghen, 2010; Denhamn et al., 2010). To date no reports demonstrate pure cultures of neurons or neural subtypes, particular mbDA progenitors or neurons. To overcome this limitation, a number of strategies have been employed to enrich the number of cells of interest. One method uses fluorescence activated cell sorting (FACS), an approach used in conjunction with reporter cell lines (Chung, Shin, & Hedlund, 2006; Hedlund et al., 2008; Nefzger et al., 2012) or cell surface antigen immunofluorescence labeling (Yuan et al., 2011a). FACS can be used to extract progenitors (Chung et al., 2006; 2011; Nefzger et al., 2012), or purify terminal cultures for a specific post mitotic subtype (Hedlund et al., 2008).

1.4 Parkinson's disease

Parkinson's disease (PD) was first described in 1817 by James Parkinson, and is a profoundly debilitating disease affecting the CNS. This neurodegenerative disease is second only to Alzheimer's disease in prevalence, and affects 1-2% of individuals over the age of 60 (Beal, 2001). PD usually manifests in a gradual onset between the ages of 50 and

70, and progresses slowly with death occurring within 10 to 20 years (Hoehn & Yahr, 1998). Traditionally, PD is characterised by four principal motor symptoms: the absence (akinesia) or slowness (bradykinesia) of movement, tremors at rest, and postural instability (Shahed & Jankovic, 2007). Less pronounced symptoms include a shuffling gait, minimal facial expressions, hypophonia (soft speech), dystonia and a stooped posture (Shahed & Jankovic, 2007).

At a neuropathological level, PD is characterised by the progressive loss of DA neurons in the SNpc (Fearnley & Lees, 1991). Although inheritable forms of PD (which account for 5-10% of patients) have been documented (Zimprich, 2011), the cause of the majority of cases remains unknown, 150 years following Parkinson's seminal paper. This has left one resounding question: why are mdDA neurons of the SNpc specifically affected in PD?

1.4.1 Dopamine biosynthesis:

Dopamine (DA) is the chief catecholaminergic neurotransmitter controlling voluntary movement, motivation, cognition and reward in the adult mammalian brain. DA is produced in a two-step reaction beginning with the conversion of dietary L-tyrosine to 3,4-dihydrocyphenylanine (L-DOPA) by TH, the rate-limiting enzyme in DA synthesis (Fitzpatrick, 1991). This is followed by the conversion of L-DOPA to DA by AADC. Newly synthesised cytosolic DA is rapidly transported into vesicles by VMAT2. Action potentials then cause increases in intracellular Ca^{2+} leading to the release of DA into the synaptic cleft.

Interestingly, AADC is not specific to DA neurons and is involved in the conversion L5-hydroxytryptophan to 5-hydroxytryptamine in serotonergic neurons (Boadle-Biber, 1993). Intriguingly, it has been shown that serotonergic neurons can take up L-DOPA from

the extracellular space and convert it to DA, and thus DA can be stored and released in an activity dependent manner (Arai, Karasawa, Geffard, & Nagatsu, 1994). However, the uptake of L-DOPA and the subsequent uncontrolled release of DA from serotonergic terminals is also related to the increased incidence of dyskinesias (Carlsson et al., 2009; Carta et al., 2007; Politis et al., 2011).

With respect to the degradation of DA, two major pathways exist. In most brain regions, including the basal ganglia, the inactivation of DA begins via reuptake mechanisms involving the DAT (Nirenberg et al., 1996). Once transported inside the cell, DA is broken down by monoamine-oxidases (MAOs).

In the prefrontal cortex however, where there is low-level DAT expression, DA is inactivated by reuptake mechanisms involving the norepinephrine transporter (NET) and subsequent breakdown by catechol-O-methyltransferase (COMT)(Morón, Brockington, Wise, Rocha, & Hope, 2002).

1.4.2. Neuropathophysiology

In the adult human there are an estimated 250,000 to 500,000 DAergic neurons in the ventral midbrain (Bjorklund & Dunnett, 2007). Normal aging in humans is accompanied by the loss of 0.5% DAergic cell bodies in the SNpc per year (McGeer, Itagaki, Akiyama, & McGeer, 1988). This normal cell loss is evenly distributed across all DA cell bodies of the SNpc, however the degeneration observed in PD is localised to the ventrolateral and ventromedial regions of the SNpc (Fearnley & Lees, 1991). Meta-analysis of post mortem SNpc counts imply that the disease onset occurs begins, on average, 4.6 years before the presentation of clinical symptoms (Fearnley & Lees, 1991).

The onset of symptoms has been correlated with the degeneration of 50-60% of SNpc DAergic neurons, and a striatal DA depletion of 60-80% (Bernheimer, Birkmayer, Hornykiewicz, Jellinger, & Seitelberger, 1973, Fearnley & Lees, 1991). Such a high loss of DAergic SNpc neurons before the presentation of symptoms is thought to be due to adaptive neural responses, such as increased activity and sprouting of remaining SNpc DAergic neurons, and changes in the density and/or sensitivity of DAT and striatal post-synaptic dopamine receptors (Bezard, Gross, & Brotchie, 2003; Song & Haber, 2000).

Motor deficits associated with PD are due to the dysregulation of signals emanating from the basal ganglia, specifically the nigrostriatal pathway (Price, Farley, & Hornykiewicz, 1978 as reviewed in Dauer & Przedborski, 2003). The basal ganglia are a group of highly interconnected subcortical nuclei, which send projections to the cerebral cortex and thalamus. There are four main nuclei in the basal ganglia, the SN, the striatum, the globus pallidus (GPi) and the subthalamic nucleus (STN)(Albin & Young, 1989). Neurons within the basal ganglia receive afferent inputs from the cortex and thalamus, and send efferent information back to the cortex via the thalamus and the brain stem (Lee & Tepper, 2009). This is commonly referred to as "the basal ganglia motor loop". The SN consists of the pc and pars reticulata (pr). The pr is mainly comprised of GABAergic neurons, whereas the pc is dominated by DAergic neurons (Celada & Paladini, 1999).

All nuclei of the basal ganglia send afferents to the SN where they synapse with both mbDA neurons of the SNpc and GABAergic neurons of the SNpr (Lee & Tepper, 2009). With the exception of the STN, which is glutamatergic (Smith & Parent, 1988), the predominant input into the SN is GABAergic (Lee & Tepper, 2009). As a whole, the afferent inputs, which modulate the activity of mbDA neurons, are complex and involve many different neuronal subtypes, ionotropic and metabotropic receptors, and as such are out of the scope of this

review (for a detailed discussion see Misgeld, 2004). Suffice it to say, mbDA mediated signalling through the basal ganglia results in altered striatal DA levels (Besson, Cheramy, Feltz, & Glowinski, 1969).

The SNpc lies dorsal to the SNpr and DA neurons found here contain neuromelanin (Moses, Ganote, Beaver, & Schuffman, 1966). This characteristic pigment results from oxidised and polymerised DA that accumulate in large lysosomal granules inside mdDA neurons with age (Van Woert, Prasad, & Borg, 1967). DAergic neurons are also found within the VTA, a medial extension of the pc (Bjorklund & Dunnett, 2007). The VTA is less affected in PD where mbDA neuron loss in PD patients is 50% of age matched controls (Hirsch, Graybiel, & Agid, 1988), whereas in the SNpc of advanced PD patients a loss of 80% is observed (Fearnley & Lees, 1991).

Another defining neuropathological feature of PD is the presence of "Lewy bodies" (LBs)(Gibb & Lees, 1988). PD-associated Lewy bodies are abnormal cytosolic aggregates of protein of which α-synuclein is the primary component (Gibb & Lees, 1988). Alpha-synuclein is a fibrillar protein which is liable to aggregation and it is believed to contribute to the disease progression of PD due to a toxic gain of function mutation (Xilouri, Vogiatzi, Vekrellis, Park, & Stefanis, 2009).

PD also affects areas outside of the nigrostriatal system. Degeneration and the presence of LBs have been observed in the raphe nucleus (Halliday, Blumbergs, & Cotton, 1990), locus coeruleus (German, Manaye, & White, 1992), as well as the nucleus basalis of Meynert (Nakano, 1984) and dorsal motor nucleus of the vagus (Mann & Yates, 1983) which lead to the non-motor symptoms of PD.

1.4.3 Etiology

Mitochondrial dysfunction is the prevailing dogma to explain the etiology of idiopathic PD (Schapira & Jenner, 2011). Numerous divergent hypotheses exist to explain the role of mitochondrial dysfunction in PD (as reviewed in Exner et al., 2012). Much of the support for mitochondrial dysfunction comes from mutations or misexpression in animal models or genetic linkage analysis of either α-synuclein (Hsu et al., 2000; Klivenyi et al., 2006), Parkinson protein 2, E3 ubiquitin protein ligase (PARK2 also known as Parkin; (Palacino et al., 2004), PTEN-induced putative kinase 1 (PINK1; Clark et al., 2006; Exner et al., 2007), Parkinson disease autosomal recessive, early onset 7 (PARK7 also known as DJ-1; Canet-Avilés & Wilson, 2004; Irrcher et al., 2010) and Leucine-rich repeat kinase 2 (LRRK2; Mortiboys, Johansen, Aasly, & Bandmann, 2010; Saha et al., 2009). Dysfunction or misregulation these proteins contribute directly or indirectly to aberrant mitochondrial function, providing impetus to the hypothesis that malfunctioning mitochondrial can lead to SNpc DA cell death in idiopathic PD.

The discovery that the mitochondrial toxin 1-methyl-4-phenyl-1,2,3,6-tetrahydropyridine (MPTP) caused Parkinsonian symptoms in humans following self-administration provided the initial stimulus for the proposed role of mitochondrial dysfunction in idiopathic PD. MPTP-induced Parkinsonism was first observed in 1976 (Langston, Ballard, Tetrud, & Irwin, 1983). However, MPTP toxicity could not be demonstrated experimentally, as investigators used rats as model animals, a species later found to be resistant to MPTP intoxication (Boyce, Kelly, Reavill, & Jenner, 1984). The relationship between PD and MPTP was confirmed in 1983, when several drugs users took MPTP in the hope that it was a synthetic analogue of heroin, (Langston et al., 1983), and soon after exhibited Parkinsonian like symptoms.

A plethora of animal studies using known mitochondrial toxins, such as pesticides with structural similarities to MPTP, then ensued. Paraquat (McCormack et al., 2002; Thiruchelvam, Richfield, Baggs, Tank, & Cory-Slechta, 2000) and rotenone (Alam & Schmidt, 2002; Sherer et al., 2003a; 2003b), both routinely used pesticides, were shown to cause mdDA neuronal loss in the SNpc following long term exposure in rodents, inferring that exposure to environmental factors plays a role in PD. Consistent with this idea, the incidence of PD in farming areas has risen since the introduction of pesticides (Gorell, Johnson, Rybicki, Peterson, & Richardson, 1998). Indeed an epidemiological study carried out in Taiwan indicated that exposure to paraquat for more than 20 years was associated with an increasing risk of PD (Liou et al., 1997). Other studies have also suggested that rural living and drinking well water is strongly correlated with an increased risk of PD (Jiménez & Mateo, 1992; Priyadarshi, Khuder, Schaub, & Priyadarshi, 2001; Semchuk, Love, & Lee, 1991; Zorzon, Capus, & Pellegrino, 2002). Although these case studies were retrospective and have potential methodological limitations (de Lau, 2006), a meta-analysis of the evidence reported a positive association between risk factors (such as living in a rural area, drinking well water, farming, and exposure to pesticides) and PD (Priyadarshi et al., 2001).

A significant caveat however is the finding that although paraquat and rotenone selectively lesion mdDA neurons (Sherer et al., 2003a; Thiruchelvam et al., 2000) and cause α-synuclein inclusions (Manning-Bog et al., 2002; Sherer et al., 2003a), neither compound enters mdDA neurons via the DAT (Richardson, Quan, Sherer, Greenamyre, & Miller, 2005). This lack of molecular a basis in the selective lesioning of mdDA neurons remains inexplicable and further complicates the etiology with regards to PD.

1.5 Experimental models of Parkinson's disease

Parkinson's disease does not arise in animals. However, the DAergic neuronal pathology observed in the Parkinsonian midbrain can be mimicked experimentally both, *in vitro* or *in vivo*, by a number of neurotoxins or genetic aberrations (Terzioglu & Galter, 2008). As current hypotheses impute an environmental toxin(s) in the etiology of idiopathic PD (Schapira & Jenner, 2011), neurotoxin models have been the most widely used and provide the most relevant and robust animal models of experimental Parkinsonism to date (Terzioglu & Galter, 2008). More recently, the links between familial PD and specific genetic mutations have been elucidated, and a number of genetic models have arisen from these findings (Guzman et al., 2010; Itier et al., 2003; Li et al., 2009). The genetic based animal models of PD are out of the scope of this review however, and will not be discussed further. For a recent comprehensive review, see (Dawson & Ko, 2010).

Animal models of PD concentrate on lesions of the nigrostriatal DA pathway and study the resultant sensorimotor function and neuropathology. While providing a useful starting point, these models do not recapitulate the clinical disorder, which has many non-motor features and non-DAergic, extra-nigral pathologies (Chaudhuri & Schapira, 2009; Meredith et al., 2008). Nevertheless, these DAergic lesion models are useful in evaluating the utility of DAergic therapies such as cell grafts and novel pharmacotherapies (Lindholm et al., 2007; Shachar et al., 2004; Thompson et al., 2009).

1.5.1 6-hydroxydopamine

6-hydroxydopamine (6-OHDA), a hydroxylated analogue of DA, was the first chemical substance shown to kill monoaminergic neurons in the mammalian brain (Ungerstedt, 1968). Although 6-OHDA-induced pathology differs from that of PD it has

been used extensively to model PD both, *in vitro* and *in vivo*. Due to 6-OHDA's inability to cross the blood brain barrier it must be administered by local stereotaxic injection into the SNpc, median forebrain bundle (which carries ascending DAergic and serotonergic projections to the forebrain) or the striatum, to target the nigrostriatal pathway (Javoy, Sotelo, Herbet, & Agid, 1976; Jonsson, 1983). Although 6-OHDA can be delivered bilaterally, it is usually injected unilaterally, as bilaterally lesioned animals require high levels of care and often die. The asymmetrical rotations that result in the unilateral model, or 'hemi-parkinsonian model", can be quantified; which in the past has provided an ability to assess the anti-PD properties of new pharmacotherapies (Jiang et al., 1993; Robinson & Becker, 1983), or other disease management strategies (Bjorklund et al., 2002; Kozlowski, Connor, Tillerson, Schallert, & Bohn, 2000).

Post administration, 6-OHDA enters the cytosol via the DAT where it auto-oxidises, generating the reactive oxidative species (ROS) responsible for the initiation of neurodegenerative processes (Choi et al., 1999; Kulich & Chu, 2003). 6-OHDA induced lesions result in rapid decreases in striatal DA levels within the first 24 hours of administration, with cell death progressing in the weeks following toxin injection (Jeon et al., 1995).

Nonetheless, the use of 6-OHDA draws controversy, as it does not replicate the slow degeneration of the nigrostriatal pathway observed in PD patients and (Jeon et al., 1995), as mentioned above, nor does it recapitulate the cardinal feature of LB inclusions (Meredith, Halliday, & Totterdell, 2004).

1.5.2 1-Methyl-4-phenyl-1,2,3,6-tetrahydropyridine (MPTP)

As reviewed earlier (see Section 1.4.3), MPTP causes PD-like symptoms when administered intravenously. Due to its highly lipophilic nature, MPTP crosses the blood-brain barrier within minutes of intravenous administration (Markey, Johannessen, Chiueh, Burns, & Herkenham, 1984). Once in the brain, MPTP is oxidised to MPDP+ by MAO-B, most likely extraneuronally, in glia (Jenner & Marsden, 1986). MPDP+ then spontaneously oxidises into the active toxic molecule, MPP+ (Jackson-Lewis & Przedborski, 2007). MPP+ is released into the extracellular space, by an unknown mechanism, where it is transported into DAergic neurons by the DAT(s) (Javitch, D'Amato, Strittmatter, & Snyder, 1985). This uptake mechanism has been confirmed using DAT inhibitors such as mazindol (Javitch et al., 1985) or complete DAT gene ablation (Bezard et al., 1999). Conversely, transgenic mice over-expressing the DAT, as driven by the TH promoter, are more sensitive to MPTP (Donovan et al., 1999).

Inside DAergic neurons, MPP+ is translocated into synaptosomal vesicles via VMAT2 (Staal, Hogan, Liang, German, & Sonsalla, 2000), transported to, and becoming concentrated in, the mitochondria (Ramsay, Dadgar, Trevor, & Singer, 1986b) or, MPP+ can remain in the cytosol, where it affects dynamic cellular processes (Klaidman, Adams, Leung, Kim, & Cadenas, 1993). The vesicular sequestration of MPP+ via VMAT2 appears to protect cells from MPTP-induced toxicity, since VMAT2 knock out mice have enhanced MPTP toxicity (Takahashi, Miner, & Sora, 1997), and VMTA2 overexpressing mice have reduced sensitivity (Liu et al., 1992).

The uptake of polar MPP+ into mitochondria is thought to compromise adenosine triphosphate (ATP) synthesis via inhibition of the electron transport enzyme nicotinamide adenine dinucleotide plus hydrogen:ubiquinone oxidoreductase (complex 1)(Ramsay,

Salach, Dadgar, & Singer, 1986a). Whether this inhibition of complex I activity is the sole cause underlying MPTP-induced DA death in the midbrain, is unclear though, as complex I activity must be reduced by 70% or more to cause severe ATP depletion (Davey & Clark, 1996). Taken together with data demonstrating only a transient 20% reduction in mouse striatal and midbrain ATP levels following the addition of MPTP (Chan, DeLanney, Irwin, Langston, & Di Monte, 1991), it seems improbable that the inhibition of ATP synthesis is the sole mechanism underlying MPTP toxicity.

So what causes MPTP-induced DA cell death? Complex I inhibition by MPP+ leads to an increased production of ROS, especially superoxide (Choi et al., 1999; Choi, Palmiter, & Xia, 2011; Cleeter, Cooper, & Schapira, 1992; Smith, 1997). MPP+ associated ROS formation seems to be an essential step in the *in vitro* toxicity of DA neurons, as copper/zinc superoxide dismutase (SOD1- a key ROS scavenging enzyme) over expressing transgenic mice are significantly more resistant to MPTP toxicity than control animals (Przedborski et al., 1992). The fluorescent tag, dihydroethidium, has also been used to label superoxide radicals following MPTP administration (Wu et al., 2003). However ROS may not be solely responsible for all the detrimental MPTP toxicities, as several lines of evidence now support the hypothesis that ROS exerts its effects together with other reactive species such as nitric oxide (NO) (Iravani, Kashefi, Mander, & Rose, 2002; Liberatore et al., 1999; Przedborski et al., 1996; Schulz, Matthews, & Muqit, 1995). NO and the superoxide radical interact to form peroxynitrite (OONO-), one of the most destructive oxidising molecules (IschiropoulosAl-Mehdi, 1995).

In response to depleted ATP and the production of ROS and NO, death signals which result in apoptotic pathway activation are induced in MPTP intoxicated neurons (Jackson-Lewis, Jakowec, Burke, & Przedborski, 1995). Knock-out of B-cell lymphoma 2 (BCL2)–

associated X protein the pro-apoptotic member of the BCL-2 family (Vila et al., 2001), or over expression of BCL-2, attenuates MPTP neurotoxicity, which supports the notion of apoptotic cell death (Yang et al., 1998).

Additionally, the loss of DA neurons from the SNpc in the MPTP mouse model is associated with both microglial activation and reactive astrocytes (Czlonkowska & Kohutnicka, 1996; Kohutnicka et al., 1998). The microglial response has been suggested to indicate an active, continuing process of cell death (Przedborski & Vila, 2003; Teismann & Schulz, 2004). The presence of activated microglia has been observed in Parkinsonian patients (Gerhard, Pavese, Hotton, & Turkheimer, 2006) and also in post-mortem samples of subjects decades after being exposed to MPTP (Langston et al., 1999). This challenges the idea that the toxic insult from MPTP contributes only to rapid cell death, and demonstrates that MPTP toxicity is more reminiscent of clinical PD.

1.6 Clinical and experimental therapies for Parkinson's disease

Currently, there is no cure for PD, however numerous symptom-alleviating therapeutic approaches have been tested in rodents, non-human primates and humans. These treatments fall into four broad categories, (1) pharmacotherapy, (2) physical intervention, (3) gene therapy and (4) cell replacement therapy.

1.6.1 Pharmacotherapy

Pharmacological intervention using treatments that increase DA synthesis have dominated the market since the early 1960's. Beginning with the discovery that administration of L-DOPA to Parkinsonian animals resulted in the reduction of behavioural

deficits (Birkmayer & Hornykiewicz, 1961 as reviewed in Barbeau, 1969), to this day L-DOPA therapy remains the mainstay treatment for PD patients; effective in managing the early stages of the disease. L-DOPA based pharmacotherapy is not with out its drawbacks however, as L-DOPA-associated complications arise with systemic delivery at high doses, as peripheral decarboxylation to DA by AADC leads to subsequent activation of DA receptors outside the CNS (Butcher & Engel, 1969). As AADC inhibitors like carbidopa and benserazide do not cross the blood brain barrier, these adjunct therapies can be used to overcome peripheral side effects (Butcher & Engel, 1969). Additionally, COMT inhibitors like entacapone and tolcapone, which block L-DOPA degradation peripherally can be used to promote CNS delivery and prolong L-DOPA availability in the brain (Männistö & Kaakkola, 1989). Over the years, this "triple-therapy", L-DOPA together with the above mentioned enzyme inhibitors, has become the gold standard in PD management. Yet, chronic use of L-DOPA leads to response fluctuations, dyskinesias and in some cases the development of DAergic psychoses (Carey, Pinheiro-Carrera, Dai, Tomaz, & Huston, 1995; Voon et al., 2009).

Treatment using DA agonists (e.g. ropinirole, pramipexole and cabergoline) results in comparable clinical improvement to L-DOPA whilst providing a significant reduction in the development of L-DOPA-induced motor complications (Inzelberg, Schechtman, & Nisipeanu, 2003). Bibbiani and colleagues purport that DA agonists provide more continuous DA receptor stimulation than L-DOPA based therapy, reducing the incidence of dyskinesias (Bibbiani et al., 2005). Nevertheless, the majority of patients who receive DA agonist therapy still require eventual L-DOPA treatment, which in turn re-introduces the risk of motor complications (Rascol, Brooks, & Korczyn, 2000). Pharmacological interventions such as controlled release of L-DOPA, MAO-B inhibitors and the intravenous

delivery of L-DOPA have dominated the therapeutic landscape of late, however the efficacy and practicality of these alternate approaches compared to the gold standard triple therapy remains debatable (Ngwuluka et al., 2010).

Lamentably, none of these pharmacotherapies significantly retard or reverse the neurodegenerative process, thus a need remains to develop disease-altering interventions for PD.

1.3.2 Physical intervention

Whereas pharmacotherapy for PD is implemented for patients with mild, moderate or advanced disease states, surgery is reserved for patients with both severe motor impairments and complications from PD pharmacotherapy. Deep brain stimulation (DBS) of either the GPi or STN improves the motor symptoms of PD patients (Trépanier, Kumar, Lozano, & Lang, 2000). DBS involves the implantation of a "brain pacemaker" that emits electrical signals, which modulates the activity of the basal ganglia (Olanow, Brin, & Obeso, 2000). Whilst little understanding surrounds the mechanisms by which DBS works, it has provided immense benefits in treating more resistant motor dysfunction in PD patients (Krack et al., 2003). Interestingly, DBS may however promote personality changes and behavioural problems, similar to L-DOPA and DA agonist treatment (Temel et al., 2006).

1.3.3 Gene therapy

Conventional PD therapy is aimed at restoring striatal DA levels either through the administration of L-DOPA, DA agonists, or via the inhibition of DA metabolism. These therapies, however, become less efficacious as PD progresses. Gene therapy has been suggested as an approach that can alter cellular biochemistry through the introduction of DA biosynthesis enzymes (Shen et al., 2000), neurotrophins (Azzouz et al., 2004;

Yoshimoto et al., 1995) or enzymes such as glutamic acid decarboxylase (GAD) to counteract the imbalance of striatal output (Luo, 2002). Although many more examples of the application of gene therapy for PD exist, a detailed discussion of these approaches beyond the scope of this review. For further information see (Hutchinson, 2011).

1.6.4 Cell replacement therapy

Cell replacement therapy in PD is based on the notion that implanted DA-releasing cells replace intrinsic SNpc DA neurons and thus replenish striatal DA content. The cell replacement strategy has several critical issues associated with it: (1) the survival of the grafted cells, (2) the stability of the mbDA phenotype, (3) integration into the host circuitry and (4) the restoration of the damaged neuronal networks are but a few examples. Most studies have relied on ectopic engraftment into the striatum, an approach with demonstrated behavioural improvements in both animal models and PD patients. In the past both neuronal and non-neuronal sources have been used as cell sources for grafting (Backlund et al., 1985; Freed et al., 1981; Ganat et al., 2012; Guillot & Miller, 2009; Jönsson et al., 2009; Kriks et al., 2011; Pezzoli, Fahn, Dwork, & Truong, 1988). Neuronal cell sources that regulate DA release at synaptic sites via impulse-dependent mechanisms, as opposed to cell sources that secrete dopamine constitutively in a diffuse and non-synaptic manner (either neuronal or non-neuronal) are now recognised as a requirement for correct integration and function in the nigrostriatal circuitry, and avoidance of graft-induced dyskinesias. Generally grafting has proved to be a successful approach in a number of experimental models of PD, as well as in PD patients. These studies have used a variety of tissue and cell types for engraftment as discussed in subsequent sections.

1.6.4.a Dopaminergic grafting sources derived from fetal ventral midbrain tissue

A myriad of experimental studies have demonstrated functional improvement following ectopic grafting of embryonic ventral mesencephalic (VM) tissue into the striatum, of various animal models of PD (Bjorklund et al., 1983; Bjorklund & Stenevi, 1979; Bjorklund, Dunnett, Stenevi, Lewis, & Iversen, 1980a; Bjorklund, Schmidt, & Stenevi, 1980b; Bjorklund et al., 2002; Jönsson et al., 2009; Kim et al., 2002; Nikkhah et al., 1994; Thompson et al., 2009).

Human fetal grafting trials in PD patients began in Sweden in the 1980s (Lindvall et al., 1990; 1989; 1992), followed by similar studies in England (Henderson, Clough, Hughes, Hitchcock, & Kenny, 1991), Spain (López-Lozano, Bravo, Abascal, & de Hierro Neural Transplantation Group, 1991), Mexico (Madrazo et al., 1990), France (Peschanski et al., 1994) and Belgium (Levivier et al., 1997). Investigators in the USA also began trials around this time, and subsequently published three studies demonstrating positive results (Freed et al., 1992; Spencer et al., 1992; Widner et al., 1992). Interestingly these three clinical trials have been suggested to be the catalyst that overturned a ban on federal funding for fetal tissue research, which had been instigated some years earlier (Lindvall & Björklund, 2011; Barker, Barrett, Mason, & Bjorklund, 2013). Moreover, it has been speculated that they also provided impetus for the National Institutes of Health to provide funding (Barker, Barrett, Mason, & Bjorklund, 2013) for two-placebo controlled studies on the benefit of fetal transplantation in PD patients (Freed et al., 2001; Olanow et al., 2003).

In the first of these double-blind neurosurgical trials (Freed et al., 2001), both sham or fetal mesencephalic tissue transplantation surgeries were conducted. Although both survival and growth of the graft was confirmed via 18F-fluorodopa positron emission tomography (PET) scans and post-mortem analysis, no differences were observed between

sham and grafted patients in the "global rating scale" (GRS), a subjective patient measure of symptom (Freed et al., 2001). A recently published evaluation of this work, performed by some of the authors of the original clinical trial, outlined problems associated the GRS used in their study, in addition the authors went as far as to suggest that it "proved to be a meaningless measure" (Freed, Zhou, & Breeze, 2011). This suggestion was exemplified by the fact that when patients were shown a video of how they appeared preoperatively, their "perceived improvement" using the "global rating scale" was very different (Freed, Zhou, & Breeze, 2011). The second of these trials also stratified patients between a placebo and treatment group (Olanow et al., 2003). Again, despite evidence of graft survival and reinnervation of the striatum, the primary endpoint (significant difference between treatment groups in the change in off state Unified Parkinson's Disease Rating Scale [UPDRS] score between baseline and 24 months post surgery) of this study was not met (Olanow et al., 2003).

In an effort to understand what contributed to the outcome of these transplantation studies and others, Barker et al., (2013) performed a systematic review based on data from the numerous clinical trials that have been conducted using fetal tissue. The authors assert that the biggest effect in the change of UPDRS results from age at time of transplantation, with the effect of age being positive in most studies, such that UPDRS scores worsen by a greater amount in older patients (Barker, Barrett, Mason, & Bjorklund, 2013). For other variables investigated, such as sex, the numbers of donors that contributed to each graft, the duration of PD at the time of grafting and the grafting co-ordinates the results were inconclusive (Barker, Barrett, Mason, & Bjorklund, 2013).

In summary, the clinical trials performed to date have produced highly variable results. Unfortunately for the PD grafting community there seems to be no consensus as to

the reasons why. It could be argued the some of the expectations born out of the early animal studies were unfounded as current models of PD do not recapitulate the human disease, and that investigators were able to control variables more easily in animal models that is possible in human PD patients for (see section 1.5.1 on the 6-OHDA and pre selection of animals based on behaviour). This inability to control patient associated variables may be especially pertinent when considering the type and stage of PD patient to treat with grafts. For example in some clinical trials, younger patients (Freed et al., 2001) or patients suffering from a less advanced PD (Olanlow et al., 2003) responded better to grafts.

1.6.4.b Dopaminergic grafting sources derived from stem cells

Regardless of their performance, the use of fetal VM tissue as a cell source for CRT has raised significant bioethical and logistical issues for the field. One concern is that its use in large-scale clinical applications may create a demand for tissue and thus encourage abortions. Additionally, the lack of standardisation of fetal VM sources is believed to contribute high degree of variability in symptomatic relief (Goya et al., 2007).

In an attempt to address the technical and ethical limitations of fetal cell sources, investigators turned to the use of ESC sources for CRT. As ESCs self-renew indefinitely, they provide an unlimited cell source for both animal studies and potentially human CRT. Additionally, the benefit of using ESCs is their amenability to genetic engineering, which permits the isolation and functional analysis of specific cell types, addressing the lack of standardisation. Since the initial explorations into the feasibility of ESC-derived cell sources for CRT (Bjorklund et al., 2002; Kim et al., 2002; Lee et al., 2000) a multitude of studies have been conducted using both mouse and human ESCs (Ben-Hur et al., 2004; Brederlau et al., 2006; Cai et al., 2009; Chiba et al., 2008; Cho et al., 2011; Cho et al., 2008;

Chung et al., 2006; Fukuda et al., 2005; Kawasaki et al., 2000; Martinat et al., 2006; Nishimura et al., 2003; Rodriguez-Gomez et al., 2007; Sonntag et al., 2007; Yang et al., 2008). Whereas mESCs-derived DA cells have shown efficacy in numerous mouse models, hESC-derived DA cells have demonstrated a lack of *in vivo* performance (reviewed in Lindvall & Kokaia, 2010), which has been attributed to a deficiency in the generation of functional bonafide hESC-derived mbDA cells (Kriks et al., 2011).

The protocols used to generate mbDA cells from both mESCs and hESCs result in low yields of mbDA cells and contain cells of unwanted phenotypes. These unwanted cell types raise substantial safety concerns due to the potential of neural overgrowth or teratoma formation following engraftment (Brederlau et al., 2006; Chung et al., 2006; Elkabetz et al., 2008; Roy et al., 2006; Schulz et al., 2004; Sonntag et al., 2007). Thus for CRT to move forward, studies need to be undertaken which definitively delineate the cell source (differentiation conditions/protocol) that provide the best functional recovery in animal models of PD, whilst avoiding the presence of tumorigenic contaminants or other unwanted neuronal cell types.

1.7 Aims

The differentiation of ESCs to a highly pure population of mbDA neurons is currently hampered by the inherent heterogeneity of existing differentiation protocols. Over recent years, mouse *in vitro* studies have extensively characterised the transcriptional cascades that drive mbDA differentiation. The transcription factor *LMX1A*, has a prominent role in the early specification of mbDA neurons. In this thesis, human and mouse *LMX1A* reporter stem cell lines are used to investigate the phenotypic potential of isolated *LMX1A* reporter positive progenitor cells. In addition, a PITX3 reporter cell line will be used for

the optimisation of conditions required for the derivation of functional, *bona fide* mbDA neurons.

Thus, the aims of this project are to:

- Isolate and characterise *LMX1A* reporter positive cells isolated from mouse ESC-mdDA differentiating cultures (CDML and PA6 derived).
- Create a MPTP mouse model of Parkinson's disease. Implant *Lmx1a* reporter positive isolated cells into the MPTP model and ascertain their survivability, integration and ultimate fate in the striatal circuitry.
- Isolate and characterise *LMX1A* reporter positive cells from human ESC-mdDA differentiating cultures (PA6 derived).
- Investigate the phenotypic potential of isolated *LMX1A* reporter positive cells from both human ESCs to produce enriched yields of mbDA neurons in terminally differentiated cultures.
- Optimise *in vitro* differentiation conditions for the derivation of functional mbDA neurons under CDML conditions.

Chapter Two: General Methods

2.1 Cell Lines

2.1.1 Mouse ESC lines

E14-tg2a, a sub clone of the E14 mouse ES cell line was derived from the 129/Ola mouse strain (Hooper et al., 1987). The m*Lmx1a*-AIG reporter cell line was genetically engineered on an E14 ES cell background in our lab by Stewart Fabb using an m*Lmx1a*-AMP-IRES-eGFP-^{F}Neo^{F} targeting vector (Nefzger et al., 2012). The vector was engineered to replace exon one of the endogenous *Lmx1a* locus with the coding sequences (CDS) for *AMP* (β-lactamase) and *eGFP* separated by an internal ribosome entry site (*IRES*) followed by neomycin (*Neo*). Neo was flanked by flippase recognition target (FRT) sites to allow excision following recombination (Fig. 2.1A).

Following the excision of Neo from correctly targeted m*Lmx1a*-AIG clones, a dual reporter (m*Lmx1a*-AIG/Rosa26-mCherry) cell line was engineered by designing a vector targeting exon one of the *Rosa26* locus (Soriano et al., 1999) with the CDS for mCherry (Fig 2.21B).

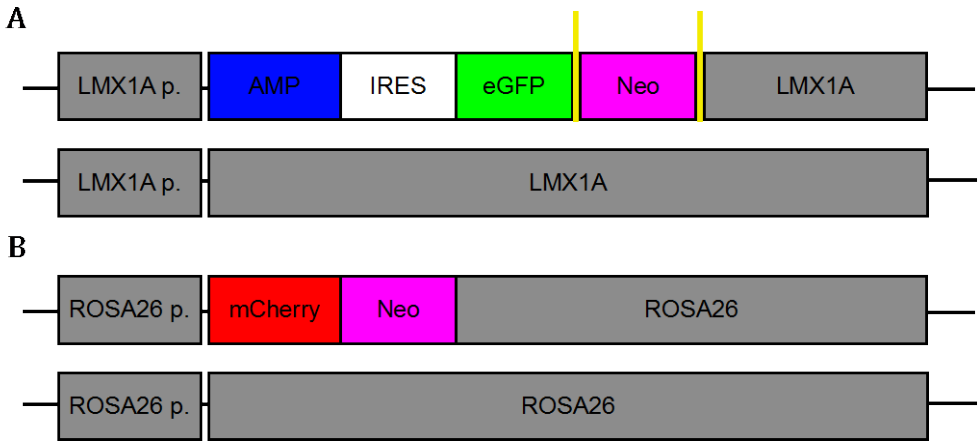

Figure 2.1. Schematic of correctly targeted genetic loci following homologous recombination. (**A**) Open reading frames targeted to exon1 of the endogenous *LMX1A* locus for *AMP* (blue) and *EGFP* (green) separated by an *IRES* sequence (white). Followed by the CDS for *Neo* (pink) flanked by FRT sites (yellow bars). (**B**) Dual reporter. Open reading frame for *mCherry* (red) followed by *Neo* (pink) targeted to exon 1 of the *ROSA26* genetic locus.

2.1.2 Human ESC lines

The hESC line, h9 derived by Thomson and colleagues was used in this thesis (Thomson et al., 1998). Two hESC reporter cell lines, h*LMX1A*-AMP-IRES-eGFP (h*LMX1A*-AiG) and hPITX3-EGFP were used in this thesis, for details see Section 4.2.2 (h*LMX1A*-AiG) and Section 5.2.3 (hPITX3-EGFP).

2.2 Cell maintenance

All cells were maintained at 37°C in a humidified 5% CO_2-in-air atmosphere (Thermo Scientific, Rochester, USA).

2.2.1 Feeder and stromal cell lines

Primary mouse embryonic feeder (MEF) cells and MEF-NeoR (Neomycin resistant MEFs)(both, Globalstem, U.S.A) were expanded in MEF media: Dulbecco's Modified Essential Medium (DMEM) containing 10% heat inactivated fetal bovine serum (HI-FBS) and penicillin 25U mL^{-1}, streptomycin 25 μg mL^{-1} (all from Life Technologies, Australia).

PA6 stromal cells (Riken Cell Bank, Japan) were expanded in Modified Essential Medium, Alpha (αMEM, Life Technologies) containing 10% HI-FBS and penicillin 25 U mL^{-1}, streptomycin 25 μg mL^{-1}. Following expansion cells were mitotically inactivated with mitomycin C (MitC, 10 μg mL^{-1}, Sigma, Australia), enzymatically dissociated using TryPLE™ Express (Life Technologies), aliquoted and stored in liquid nitrogen.

2.2.1.i MEF conditioned media (MEF-CM)

MEFs were thawed and plated at 4 x 10^5 cells cm^{-2} in MEF media (see section 2.2.1). The next day, the media was aspirated and the cells washed twice with 0.1M phosphate buffered saline (pH 7.4, PBS, Sigma) and hESC (see Section 2.2.3) media was

added. After 24 hrs, the MEF-CM was collected and replaced with fresh hESC media. This was repeated for up to 12 days. Before use, the MEF-CM was filter sterilised using a 0.22 μm filter and supplemented with 10 ng mL^{-1} recombinant human fibroblast growth factor 2 (FGF2, R&D Systems, U.S.A).

2.2.2 Mouse ES cells

All mESC lines were routinely cultured at 2.5 x 10^4 cells cm^{-2} in mESC media: DMEM with 15% FBS, 1 mM sodium pyruvate, 0.1 mM MEM non-essential amino acids (NEAA), 0.1 mM β-mercaptoethanol, 2 mM GlutaMAX™-I (all from Life Technologies) supplemented with 1000 U mL^{-1} recombinant mouse leukaemia inhibitory factor (LIF, Millipore, Australia). Cells were supplemented with fresh medium every 48 hrs until confluent, then sub cultured.

2.2.3 Human ES cells

Human embryonic stem cell lines (h9, h*LMX1A*-AIG [see Section 4.2.2] and hPITX3-EGFP [see Section 5.2.2]; passages 35-45) were cultured on MEFs (4 x 10^5 cells cm^{-2}) in hESC media: Dulbecco's Modified Eagle Medium: Nutrient Mixture F-12 (DMEM/F12 1:1, Life Technologies), 20% KnockOut™ Serum Replacement (KSR, Life Technologies), 1% NEAA, 2mM GlutaMAX™-I, penicillin 25 U mL^{-1}, streptomycin 25 μg mL^{-1}, 0.1 mM β-mercaptoethanol and 6 ng mL^{-1} rhFGF-2. Media was changed daily. Human embryonic stem cell cultures were manually groomed to remove differentiated colonies. Fragments (approximately 0.5mm^2 diameter) were manually passaged every 5-7 days onto freshly prepared MEFs.

2.3 Differentiation of ESCs

For details of differentiation protocols see Section 3.2.3 (mESCs), Section 4.2.1 (hESC PA6 neural induction and dopaminergic differentiation) and Section 5.2.1 (hESC chemically defined monolayer neural induction and dopaminergic differentiation).

2.4 Microscopy and immunocytochemistry

2.4.1 Sample preparation

All methods were performed at 4°C unless otherwise described. Cells were washed twice with PBS, fixed using 4% (wt/vol) paraformaldehyde in PBS at room temperature (PFA; Sigma) for 15 min and washed again with PBS (3 x 5 min). Following fixation cells were permeablised and blocked using 0.5% (vol/vol) Triton X (Sigma) in PBS containing 1% (wt/vol) BSA (Sigma) (PBS/BSA-T100X) for 30 min. Primary antibodies were diluted in PBS/BSA-T100X. Fixed and permeablised cultures were incubated with the primary antibody over night (see Table 2.1 for details).

The following day, cells were washed with PBS/BSA-T100X (3 x 5 min) then incubated for 2.5 hrs with an appropriate secondary antibody (see Table 2.1) diluted in PBS/BSA-T100X. For double immuno-labeling with primary antibodies from the same species, the first primary and secondary antibodies were added overnight as above. Unbound secondary antibody was then washed with PBS/BSA-T100X (3 x 5 min). Samples were then re-blocked in PBS/BSA-T100X for 30 mins. The second primary antibody was then added overnight as above. After incubation, cells were washed with PBS/BSA-T100X (3 x 5 min) then incubated with the second secondary antibody overnight and washed PBS/BSA-T100X (3 x 5 min).

The nuclear counter stains 4',6-diamidino-2-phenylindole (DAPI, 0.5 μg mL^{-1}, Life Technologies) or TO-PRO®-3 Iodide (0.5μM, Life Technologies) in 0.2% (w/v) were dissolved in sodium azide (Sigma) in PBS and added prior to confocal imaging. For secondary only control wells, cultures were incubated with the secondary antibody only.

Primary Antibodies

Antibody	Dilution	Source	Catalogue No.
Tyrosine Hydroxylase	1:1000	ImmunoStar	22941
Tyrosine Hydroxylase	1:200	Millipore	Ab152
β-III tubulin (TUJ1)	1:1000	Covance	MMS-435P/MRB-435P
FoxA2 (mouse)	1:4000	DSHB	4C7
FoxA2 (human)	1:100	Santa Cruz	sc-6554
Lmx-1	1:1000	Millipore	ab10533
Nestin (human)	1:100	Millipore	AB5922
Nestin (mouse)	1:40	DSHB	Rat-401
GABA	1:2000	Sigma	A2052
Serotonin (5-HT)	1:2000	Sigma	S5545
Corin	1:100	L. Thompson	(Jönsson et al., 2009)
NR4A2	1:30-1:1000	Santa Cruz	Sc-990
Forse-1	1:50	DSHB	FORSE-1
GAD67	1:1000	Millipore	AB5992
SATB2	1:40	Abcam	ab51502
Pitx3 (human)	1:50-1:1000	Millipore	AB5722
Otx2	1:100	Abcam	ab21990
Pax6	1:30	DSHB	PAX6
Pax7	1:30	DSHB	PAX67
GFAP	1:250	Millipore	04-1062

Oct4	1:400	Abcam	ab109884
I.C. Mouse IgM	1:100	Abcam	ab91545
I.C Mouse IgG	1:100	Abcam	ab37355
I.C Rabbit IgG	1:100	Abcam	ab125938

Secondary Antibodies

Antibody	**Dilution**	**Catalogue No.**
DαM-AF488	1:200-1000	A-21202
DαR-AF488	1:200-1000	A21206
DαG-AF488	1:200-1000	A11055
GαM-AF594	1:200-1000	A11005
DαR-AF594	1:200-1000	A21207
DαG-AF594	1:200-1000	A11058
DαM-AF647	1:200-1000	A31571
DαR-AF647	1:200-1000	A31573
DαG-AF647	1:200-1000	A21447
GαC-AF647	1:200-1000	A21449

Table 2.1 List of all antibodies used in this thesis. All secondary antibodies were sourced from Life Technologies. Abbreviations: DSHB, developmental studies hybridoma bank; I.C, isotype control, DαM, donkey anti-mouse; DαR, donkey anti-rabbit; GαM, goat anti-mouse; GαC, Goat anti-chicken; AF488, Alexa Flour 488; AF568, Alexa Flour 568 and AF647, Alexa Flour 647.

2.4.2 Image acquisition, analysis and quantitation

Immunofluorescent images were taken with a Nikon A1R confocal microscope (Nikon, Japan). For quantitation, laser power, gain and look up table parameters were set based on secondary antibody only labeled controls. Immuno-reactive cells were manually counted in 9 (3 technical replicates from 3 biological replicates) random fields of view (10x or 20x magnification, using Z-stacks of a maximum of 13 μm optical sections.

In order to assess deficiencies in a commitment to a neural phenotype (see Section 4.3.8) cells were labeled with TUJ1 with an appropriate AF647 secondary antibody and scanned with the Odyssey infrared imaging system (LI-COR Biosciences, U.S.A). Emission values of each well were standardised to control wells providing a background value to subtract.

2.5 Flow cytometry

2.5.1 Sample preparation

Media was aspirated and cultures were washed with 1 x Hank's Buffered Salt Solution (HBSS) for 5 min. Cells were harvested using either accutase (Life Technologies, CDML cultures) or collagenase/dispase (700 μg mL^{-1}, Roche, Vic, Australia; PA6 cultures) containing DNAse I (50 μg mL^{-1}, Sigma). To dilute enzyme DMEM/F12 containing 20% (vol/vol) KSR was added and the dissociated cells were centrifuged (200*g* 5 min). The dilute enzyme solution was aspirated, and the cells were washed again in DMEM/F12-20% KSR and centrifuged (200*g*, 5 min) to remove any residual enzyme.

2.5.1a Live cell FACS analysis

DMEM/F12-20% KSR was aspirated and the cells resuspended at 5 x 10^6 cells per mL in FACS live/dead cell buffer (HBSS containing 2 μg mL^{-1} Propidium Iodide, PI, Sigma

or 5 nM SYTOX® Red or Blue dead cell dye, Life Technologies). For β-lactamase expression analysis cells were loaded with the LiveBLAzer™-FRET B/G Loading Kit (Life Technologies) according to manufacturer's specifications and then resuspended in FACS live/dead cell buffer for analysis. Following 15 min incubation in FACS live/dead cell buffer samples were filtered through a 40 μm strainer cap (BD Biosciences, Australia) to remove cell aggregates. Data was collected using a FACS Canto II (BD Biosciences) and analysed as per Section 2.5.3.

2.5.1b Immunofluorescence FACS analysis

DMEM/F12-20% KSR was aspirated and the cells were treated as detailed in (i) for cell surface or (ii) for intracellular markers.

(i) For cell surface markers

Cells were resuspended in 1% (wt/vol) PBS-BSA at 2 x 10^6 cells per mL, filtered with a 40 μm strainer and incubated at 4°C for 30 mins. Two hundred microliters of vortexed cell suspension was then distributed into round bottom FACS tubes (BD Biosciences) and the primary antibody (see Table 2.1) was added for 30 mins at 4°C. Cells were washed thrice with chilled 1% PBS-BSA (200*g*, 5min) and resuspended in 1% PBS-BSA containing an appropriate secondary antibody (see Table 2.1) at a 1:1000 dilution. Following 30 min incubation at 4°C cells were again washed with 1% PBS-BSA (3x, 200*g*, 5min) then resuspended in FACS live/dead cell buffer (see Section 2.5.1a) and filtered.

(ii) For intracellular markers

Cells were filtered with a 40 μm strainer, resuspended in 4% PFA for 10 mins then washed with PBS twice (200*g*, 5mins). Following the second wash cells were

resuspended at 2 x 10^6 cells per mL in PBS/BSA-T100X and incubated for 30 mins 4°C. Four hundred microliters of vortexed cell suspension was then distributed into round bottom FACS tubes (BD Biosciences) and the primary antibody (see Table 2.1) was added at 4°C overnight. Cells were washed thrice with chilled PBS/BSA-T100X (200*g*, 5min), resuspended in an appropriate secondary antibody (see Table 2.1) and incubated for a minimum of 4 hrs at 4°C. Cells were again washed with PBS/BSA-T100X (3x, 200*g*, 5 min) resuspended in HBSS and filtered.

2.5.2 Fluorescence-activated cell sorting

Cell samples were prepared as above (Section 2.5.1). Cell sorting was performed on a MoFlo Astrios running Summit Software (v4.3, Beckman Coulter, U.S.A) using a 100 μm nozzle at 20 pounds per square inch (psi). Cells were collected into a 1:1 mixture of conditioned/fresh media, centrifuged (200g, 5 min), resuspended in 1:1 mixture of conditioned/fresh media supplemented with fresh growth factors and replated at different densities (see Section 4.3.9).

2.5.3 FACS gating strategies and analysis

All data for analysis was collected using a FACS Canto II (BD Biosciences). The cell populations of interest excluding debris, dead cells and doublets was identified by forward/side scatter gating and dead cell exclusion fluorescence. For live cell fluorescent detection naïve parental ESCs lines, E14-tg2a (mESC) and h9 (hESC) subjected to same differentiation conditions and staining procedures were used as negative controls. For immunofluorescence, isotype controls were used for cell surface markers analysis and secondary only controls were used for intracellular markers. All FACS experiments were repeated in triplicate from a minimum of three differentiations. Data analysis was performed using Tree Star FlowJo (v8.8.6).

2.6 Quantitative polymerase chain reaction

2.6.1 RNA extraction

Total RNA was extracted from ≥ 500 thousand cells using the RNeasy Micro Kit (Qiagen, Australia) following the manufacturers instructions. RNA quality and yields were quantified using the Nanodrop® ND-1000 (Thermo Scientific) spectrophotometer.

2.6.2 Quantitative polymerase chain reaction (qPCR)

Transcript analysis was carried out using a CFX96 real time machine using the iScript™ one-step RT-PCR kit for probes (both from Bio-Rad). Two microliters of RNA template (20 ng) was added to a PCR mix containing 9.45 µLs of nuclease free water, 0.75 µLs of 150 nM probe (Life Technologies) and 400 nM primer mix and 7.5 µLs of 2x RT-PCR mix. qPCR conditions were as follows, 50°C for 10 min, 95°C for 5 min followed by 45 cycles (95°C for 15 sec, 60°C for 30 sec). All probes used for hESC-derived cell qPCR are detailed in Table 2.3

Gene ID	Gene Name	Assay ID	Accession Number
HPRT	Hypoxanthine phosphoribosyl transferase	Hs99999909_m1	NM_000194
TBP	TATA box–binding protein	Hs99999910_m1	M34960
LMX1A	LIM homeobox transcription factor 1, alpha	Hs00892663_m1	NM_177398
FOXA2	forkhead box A2	Hs00232764_m1	NM_153675
CORIN	corin, serine peptidase	Hs00198141_m1	NM_006587
WNT1	wingless-type MMTV integration site family, member 1	Hs01011247_m1	NM_005430

FOXG1	forkhead box G1	Hs01850784_s1	NM_005249
EN1	engrailed homeobox 1	Hs00154977_m1	NM_001426
SIX3	SIX homeobox 3	Hs00193667_m1	NM_005413
NKX6.1	NK6 homeobox 1	Hs00232355_m1	NM_006168
TH	tyrosine hydroxylase	Hs00165941_m1	NM_199292
PITX3	paired-like homeodomain 3	Hs01013935_g1	NM_005029
NR4A2	nuclear receptor subfamily 4, group A, member 2	Hs00428691_m1	NM_006186
NTN1	netrin 1	Hs00924151_m1	NM_004822
NGN2	neurogenin 2	Hs00702774_s1	BC036847
SIX6	SIX homeobox 6	Hs00201310_m1	NM_007374
OTX2	orthodenticle homeobox 2	Hs00222238_m1	NM_021728
LHX2	LIM homeobox 2	Hs00180351_m1	NM_00478
PAX6	paired box 6	Hs00240871_m1	NM_001127612
DKK1	dickkopf 1 homolog (Xenopus laevis)	Hs00183740_m1	NM_012242

Table 2.3: Taqman Probes used for hESC qPCR assays

2.8.3 Data analysis

Data analyses was performed using the $2^{-\Delta\Delta CT}$ method (Livak, 2001). Relative quantification values were determined by standardising C_T values of each target gene to the averaged values of two house keeping genes (HPRT1 and TBP).

2.7 Statistical analysis

Results from all experiments are represented as the mean ± the standard error of the mean (S.E.M). Statistical analyses were performed in Prism v5.00 (Graphpad Software, USA). In all representations $p<0.05$ was considered statistically significant. Analysis was performed using Students t-test, one or two way analysis of variance (ANOVA) with post hoc Bartlett's test for equal variances, Bonferonni's or Dunnett's test.

Chapter Three: Implantation of mESC-derived *Lmx1a* positive neural progenitors in an MPTP Mouse Model of Parkinson's disease

3.1 Introduction

As outlined in section 1.6.4, there have been numerous investigations into the transplantation of tissue into Parkinsonian brains (both in human PD patients and animal models). These studies have used progenitor and neuronal cells derived from fetal tissue (see section 1.6.4). ESC-derived cells, including stem (Molcanyi et al., 2007), progenitor (Ben-Hur et al., 2004; Hovakimyan et al., 2006; 2008) and neuronal cells (Hedlund et al., 2008) have all been tested in animal transplantation models. Neural progenitor cells appear to have become the cell type choice, as they bring about the most robust functional outcome in commonly used PD animal model behavioural tests (Ben-Hur et al., 2004). An advantage of progenitor cells is that they have restricted self-renewal and phenotypic potential, reducing the likelihood of tumor formation (Chung et al., 2006; Roy et al., 2006; Yang et al., 2008).

In spite of this understanding the derivation of specific committed neuronal progenitors, in particular mbDA progenitors from ESCs at high purity is currently hampered by the heterogeneity of existing differentiation protocols (see section 1.3). The purification of committed mbDA progenitors may provide a way to address such caveats, as their proliferative potential makes subsequent expansion for *in vitro* and *in vivo* applications, such as CRT and *in vitro* PD modelling a possibility.

The engineering of ESC reporter cell lines provides the ability to isolate specific mitotic populations of progenitors by FACS (Chung et al., 2006; 2011). In recent investigations *Lmx1a* has gained distinction as a key transcription factor in the genesis of mbDA neurons (Andersson et al., 2006b; Deng et al., 2011). As discussed in Section 1.2.3.a, mbDA neurons arise *in vitro* from FoxA2+ ventral FP cells. In this context, Lmx1a

is purported to activate molecular determinants of mbDA phenotype, such as Msx1, Lmx1b, Wnt1 and other potential target genes (Andersson, et al., 2006b; Chung et al., 2009). Whilst important for mbDA differentiation, *Lmx1a* is also expressed in other neural developmental cascades, the cortical hem, a forebrain structure that gives rise to cortical neurons (Chizhikov et al., 2010; Desbordes & Studer, 2012; Mishima, Lindgren, Chizhikov, Johnson, & Millen, 2009), the roof plate of the developing cerebellum (G. Chen et al., 2011; Chizhikov & Millen, 2004; Millonig et al., 2000; Mishima et al., 2009) and the non-neurogenic roof plate of the neural tube (Chizhikov & Millen, 2004; Ganat & Studer, 2013; Khaira et al., 2011; Millonig et al., 2000; Raye et al., 2007). Thus, utilisation of an *Lmx1a*-reporter cell line requires a degree of caution.

In recent studies conducted in our laboratory we have shown that the CDML differentiation gives rise to heterogeneous populations of DA and GABAergic neurons (Kawasaki et al., 2000; Khaira et al., 2011; Raye et al., 2007). Using another protocol Kawasaki and co-workers show that ESC cultures differentiating on PA6 stromal cells also give rise to moderate proportions of mbDAergic neurons (Kawasaki et al., 2000; Lau et al., 1990).

3.1.1. Aims

This study therefore addresses whether a reporter cell line driven by *Lmx1a*-regulatory elements can be used to enrich for mbDA cells cultured using either CDML or PA6 conditions. The focus of this Chapter was to address a number of hypotheses. (1) The engraftment of *Lmx1a*-reporter positive cells would lead to better survival, integration and functional regeneration in a MPTP mouse model of PD, compared with *Lmx1a* negative or non-sorted cells. (2) The isolation of *Lmx1a*-reporter positive cells would lead to enrichment of mbDA neurons following terminal differentiation *in vitro*.

3.2 Methods

Unless outlined, all experimental methodologies are the same as described in Chapter 2: General Methods.

3.2.1 Animals

All methods utilising animals conformed to the Australian National Health and Medical Research Council published code of practice for the use of animal research and were approved by the Monash University Animal Ethics Committee. C57BL/6 wildtype mice were maintained on a 12 h light / dark cycle with constant temperature and humidity and food and water ad libitum.

3.2.2 Lesioning of the Substantia Nigra pars compacta

The Parkinsonian animal model was created by selectively lesioning mbDA SNpc neurons with the neurotoxin MPTP. Lesioning was conducted using a chronic or acute model.

3.2.2.a Chronic MPTP/probenecid treatment

In the chronic model (Lau et al., 1990), five or twelve month old mice were administered MPTP (25 mg kg^{-1}, dissolved in 0.9 % wt/vol saline, s.c.; Sigma-Aldrich) and probenecid (250 mg kg^{-1}, dissolved in DMSO, i.p; Sigma-Aldrich) or saline (0.9 % wt/vol, s.c.) and probenecid (250 mg kg^{-1}, i.p.). Ten doses were administered over a 5-week schedule, such that the injections were given with an interval of 3.5 days between consecutive doses. Probenecid was administered 30 min prior to MPTP and used to inhibit the rapid clearance and excretion of MPTP from the brain and kidney following each injection. Neither probenecid, nor DMSO at the above concentrations significantly affects striatal DA levels (Lau et al., 1990).

3.2.2.b Acute MPTP treatment

For the acute model (Tripanichkul et al., 2006), 5 month old mice were administered either MPTP (15 mg kg^{-1}, dissolved in 0.9% w/v saline; Sigma) or saline (0.9 % w/v) in a series of four intraperitoneal injections 2 h apart for a total of 60 mg $kg^{1.}$

3.2.3 Behavioural models of MPTP treated mice

Behavioural tests were performed 60 d post MPTP lesioning. All mice underwent handling every second day a week before testing in order to acclimatise them to handling, lighting conditions and environment..

3.2.3.a Rotarod test

To assess the motor effects of the bilateral lesion of the striatum caused by MPTP treatment, mice were subjected to a rotarod test (Li et al., 2001; Monville et al., 2006; Ogura et al., 2005). Mice were placed on a rotating rotarod (Panlab/Harvard Apparatus, Holliston, USA), spinning at 4RPM. When stabilised, mice were subjected to an incrementally increasing speed at a rate of 1 RPM for 30 sec. Three trials were conducted, in each, the length of time the animals could withstand walking on the rotarod and the speed when they fell off the rotarod was recorded. The average of the three trials was used for analysis.

3.2.3.b Pole test

The pole test has been used previously to asses rodent models of PD (Fernagut et al., 2003; Matsuura et al., 1997; Ogawa et al., 1985; Sedelis et al., 2001). Mice were placed a top a wooden pole (50 cm H and 1 cm W) that was painted in black paint containing sand to increase grip. The base of the pole was affixed to a thin wooden plank for stability (20cm L, 5cm W, 5cm H) and then placed in the animal's home cage. The time

taken to orient downward and descend the pole into the home cage was then recorded. Mice received two days of training (five trials each session). On the test day, the animals were tested over five trials, and the average of the five trials was calculated. If the mouse fell off the pole or was unable to climb down the pole in any given trial, the longest time from that animal's previous trial was recorded for the unsuccessful run.

3.2.3.c Challenging beam transversal test

Motor performance was also measured using a modified challenging beam transversal test (Fleming et al., 2004), adapted from a traditional beam walking test (Carter et al., 1999; Dluzen et al., 2001; Drucker-Colin & García-Hernández, 1991; Goldberg et al., 2003). The beam was constructed from wood (painted with black paint containing sand) and consisted of four sections (25 cm each, 1 m L), each section having a different width. The beam started with a width of 3.5 cm and narrowed by 1 cm increments to a final width of 0.5 cm and was covered in a black plastic mesh grid ($0.5cm^2$). Under hanging ledges (1.0 cm W) were placed 1.0cm below the beam. Animals were trained to transverse the length of the beam starting at the widest section and ending at the most narrowest. The narrow end of the beam was placed into animal's home cage so it was on a slope downward. Before testing animals received 2 d of training, without the grid. On the first day of training animals received two assisted trials, which consisted of orienting the animal in the correct position and positioning the home cage in close proximity to the animal. This encouraged the animal to move forward along the beam. After two assisted trials, the animals were usually able to transverse the entire length of the beam unassisted. Day one of training concluded when all animals were able to complete three full transversals unassisted. Day two of training required the animals to complete three unassisted transversals. On the day of trials, the mesh grid

was placed on top of the beam, leaving an approximate 1.0 cm space between the grid and the beam surface. The under hanging ledges were added as a support for the animal to use when a limb slipped on the grid, so that the mice did not need to use compensatory motor strategies to complete the task (Schallert & Woodlee, 2002).

Animals were videotaped while traversing the beam for a total of three trials. Video recordings were then viewed in slow motion playback and assessed for errors, number of steps made and total time to transverse the beam. An error was defined when a limb (either fore or hind limb) slipped through the grid and was visible between the grid and the beam. Each limb was scored individually, so that the severity of the error could be measured. An individual animal therefore was scored out of 4 for each step, 0 being no slips, 4 being all limbs slipping per step. Slips were not counted if the animal was not making a forward movement. Errors per step, time to transverse and number of steps were calculated for saline and MPTP treated mice and averaged across the three trials.

3.2.4 Neural induction and DA differentiation

3.2.4.a CDML differentiation

Chemically defined monolayer neural induction was achieved by seeding mESCs on 0.1% (wt/vol) gelatin coated wells at 3.5 x 10^3 cells cm^{-2} in mESC media (see Section 2.2.2). Cultures were incubated at 37°C in a humidified 5% CO_2-in-air atmosphere for at least 24 h. The culture medium was then replaced with N2B27 medium: a 1:1 mixture of DMEM/F-12 supplemented with 5 mL L^{-1} N2 additive, 50 μg mL^{-1} bovine albumin fraction V (all from Life Technologies), 25 μg mL^{-1} insulin (Sigma-Aldrich) and Neurobasal media supplemented with 10 mL L^{-1} B-27 serum-free additive (both Life Technologies). To induce mbDA patterning of differentiating mESCs, cells were treated from day 0 with 200

ng mL^{-1} recombinant mouse sonic hedgehog (Shh-N) and 100 ng mL^{-1} recombinant mouse fibroblast growth factor 8b (FGF8b, both R&D Systems). The culture medium was replaced three days later with an equal volume of the medium and supplements, and every day there after. Shh-N and FGF8 were withdrawn at day 5. At day 11 the media was changed to maturation medium: N2B27 medium containing 200 μM L(+)-ascorbic acid (AA, Merck, Australia), 200 ng mL^{-1} BDNF and 20 ng mL^{-1} GDNF (both R&D Systems) to maintain the culture up to day 21, with media changes performed every second day.

3.2.4.b PA6 Differentiation

PA6 stromal cell based *in vitro* differentiation was induced by the PA6 co-culture method (Kawasaki et al., 2000). PA6 cells were thawed and plated 24 h prior to mESCs at 5 x 10^4 cells cm^{-2}. Mouse ESCs (100 cells cm^{-2}) were cultured to form colonies from a single cell suspension on a PA6 stromal cell feeder layer in PA6 induction media (PIM): GMEM supplemented with 15% KSR, 2mM GlutaMAX™-I, 0.1mM NEAA, 1mM sodium pyruvate, 0.1mM β-mercaptoethanol. Media changes were performed on days 3 and 5 post plating and every day thereafter. Mouse ESCs were cultured on PA6 cells for 8 days in above medium and then the media was changed to maturation medium (see section 3.2.3.a) and renewed daily.

3.2.5 Fluorescence activated cell sorting

Extraction of reporter positive and negative cells was conducted on a Cytopeia Influx Cell Sorter using the Spigot Operating Software Version 5.0.3.1 (Cytopeia) or a BD Aria I using FACS Diva Version 6.1.1. Software. Sample preparation, sort parameters and collection were performed as per Section 2.5.1.

3.2.6 Transplantation

Sixty days post MPTP lesion, mice were anaesthetised with isoflurane (induced at 4%, maintained on 1.5% in oxygen; VM Supplies, Australia), the skull disinfected and a parasagittal incision of skin and subcutaneous tissue (1 cm long) was performed above the midline. Using a stereotaxic frame, through a 0.9 mm diameter burr hole in the skull, a total of 4.0 x 10^5 cells in 2 μL of HBSS were injected into the striatum at different co-ordinates (see Section 3.3.6). The needle was left in place for 5 minutes to avoid cells running back up the injection tract. The skin was then reapproximated and sutured.

Mice were provided with drinking water containing 2% (vol/vol) ethanol and 200 μg mL^{-1} cyclosporine (CsA) A from 3 days prior to intracranial transplantation until they were sacrificed. This treatment has been shown to maintain CsA blood concentrations at 297 ± 81 ng/ml, a level comparable to that of patients undergoing liver transplantation at Kyoto University Hospital (Levy et al., 2002).

3.2.7 Tissue processing

Following a lethal dose of sodium pentobarbitone (50 mg kg^{-1}; Lethabarb, Provet, Australia) mice were transcardially perfused with PBS containing heparin (1 unit ml^{-1}, Sigma), followed by 10 mL of chilled 4% (wt/vol) PFA in PBS (4°C). The brains were then removed and post fixed with 4% PFA (4°C) overnight before being stored in 30% (wt/vol) sucrose in PBS also at 4°C for 2-5 days. At which time they were snap frozen using liquid nitrogen and stored at -80°C.

Brains were cut using a cryostat (Leica, Germany) after being embedded in O.C.T TissueTek compound (Sakura-Finetek, Netherlands). For striatal sections a 1:6 series was cut through the coronal plane with a section thickness of 30 μm. Sections were mounted directly onto slides coated with 0.1% (w/v) chromium potassium sulphate and

1% (w/v) gelatin in water and then stored at -80°C until required. Coronal sections (1:3 series, 30μm thick) were cut through the SNpc with one series being mounted onto chromium potassium sulphate/gelatintised slides for Neutral Red staining and alternate sections places in free floating in cryoprotectant (Watson, 1986) for immunocytochemistry.

3.2.8 Histology, estimation of SNpc lesion size, stereological cell counts and detection of grafted cells

Following 30 μm sectioning and neutral red staining the number of cell bodies within the lesioned SNpc was estimated using a fractionator sampling design (West & Gundersen, 1990; Finkelstein et al., 2000; Stanic et al., 2004). Counts were made at regular predetermined intervals (x 140 μm, y 140 μm). Systematic samples of the area occupied by the nuclei were made from a random starting point. An unbiased counting frame of known area (45 μm × 35 μm) was superimposed on the image of the tissue sections using MBF Bioscience Stereology Investigator 7 software using a Leica DMLB microscope. Using the Nikon A1R confocal, images of 30 μm sections in series were taken using a 561 nM laser to excited mCherry-expressing cells.

3.3 Results

3.3.1 The chronic MPTP/probenecid PD model in aged animals does not yield sufficient viable animals for transplantation studies

Initially the chronic MPTP/probenecid model (Section 3.2.2.1) was used to elicit degeneration of the nigrostriatal pathway in aged animals (12-month-old), to try and establish a rodent model that closely resembles idiosyncratic PD in aged humans. However, at the end of the 5-week treatment regime it was observed that the survival of animals following co-administration of MPTP and probenecid was very low (MPTP, 8.3% ± 5.9, n=61)(saline, 100.0% ± 0.00, n=18)(Table 3.1)(Fig 3.1A). SNpc lesions as determined by neutral red staining were pronounced in the MPTP/Probenecid treated animals (3648 ± 600.3 raw neutral red cell body counts, n=5)(Saline, 5994 ± 157.3 raw neutral red counts, n=18)(Fig 3.1C & D). When normalised, MPTP/Probenecid treated mice SNpc lesions were 65.5 % ± 10.5 of saline treated animal SNpc cell bodies (Table 3.1)(Fig 3.1D).

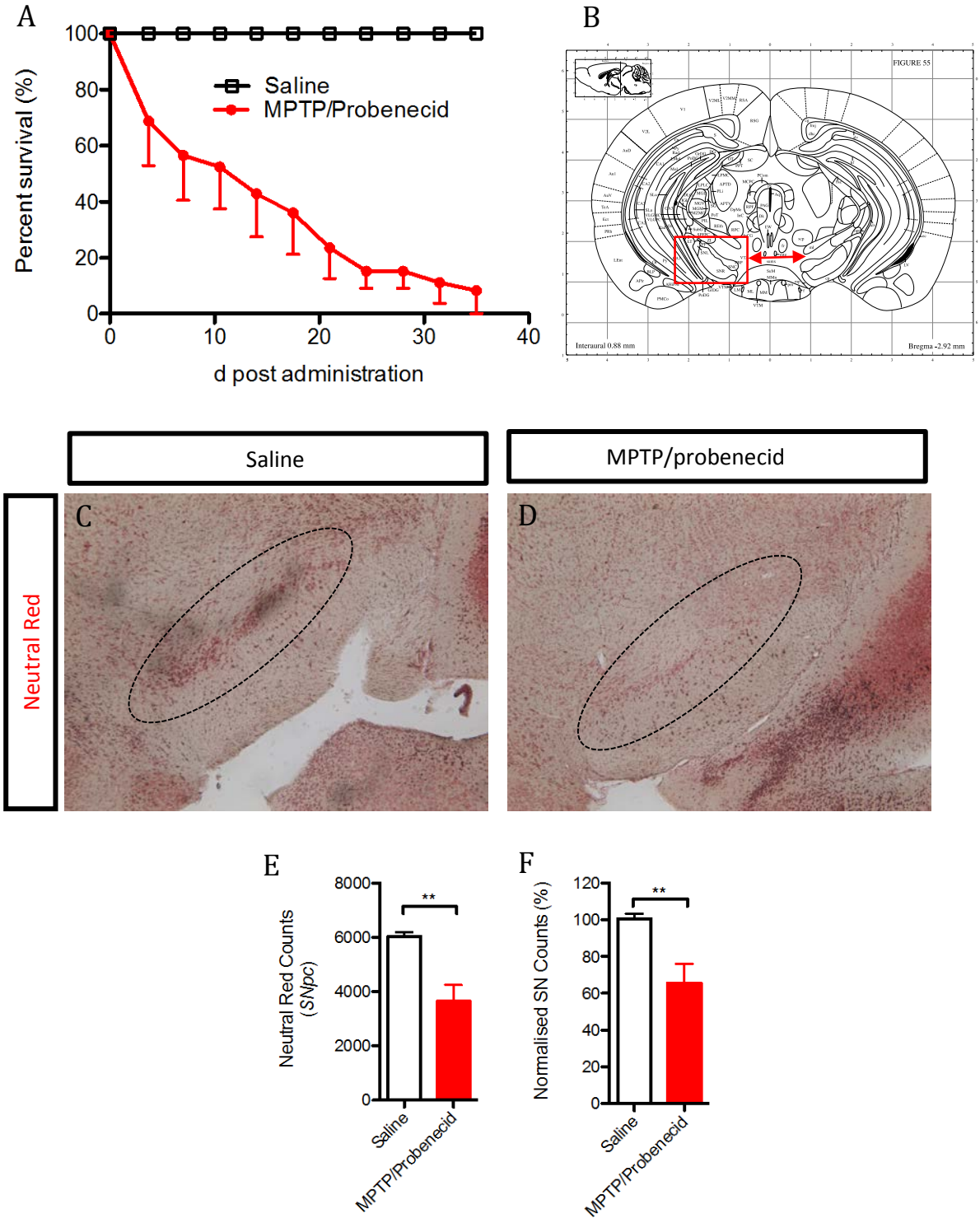

Figure 3.1 Chronic MPTP/Probenecid model in aged (12 m.o.) mice. (**A**) Survival of mice during chronic administration of MPTP/probenecid over 5-week period. (**B**) Schematic of mouse midbrain, red box and red arrows depicts SNpc regions (bregma, -2.62 mm). Quantification of the number of SNpc (black dashed ellipse) neurons following administration of (**C**) Saline and probenecid (white bar, n=16) or (**D**) MPTP/probenecid (red bar, n=5), represented as raw counts (**E**) or normalised counts (F). Data is presented as the mean ± S.E.M. Student's t-test was used to determine levels of significance. Asterisks indicate statistical significance in comparison to saline (**, $p < .01$).

3.3.2 The chronic MPTP/probenecid PD model in young animals does not yield sufficient viable animals for transplantation studies

It was hypothesized the low number of surviving animals following chronic MPTP/probenecid administration was due to their age. Thus, 5-month-old mice were assessed for their survivability following chronic MPTP/probenecid administration. At the end of the treatment regime, similar to the outcomes observed with 12-month-old mice, the survival of 5-month-old mice was low (27.8 % ± 16.9, n=36)(Fig. 3.3A)(Table 3.1). The number of neutral red positive SNpc cell bodies that remained was observed to be 54.2 % ± 5.1, n=10 of saline control treated animals (Table 3.1)(Fig 3.2B).

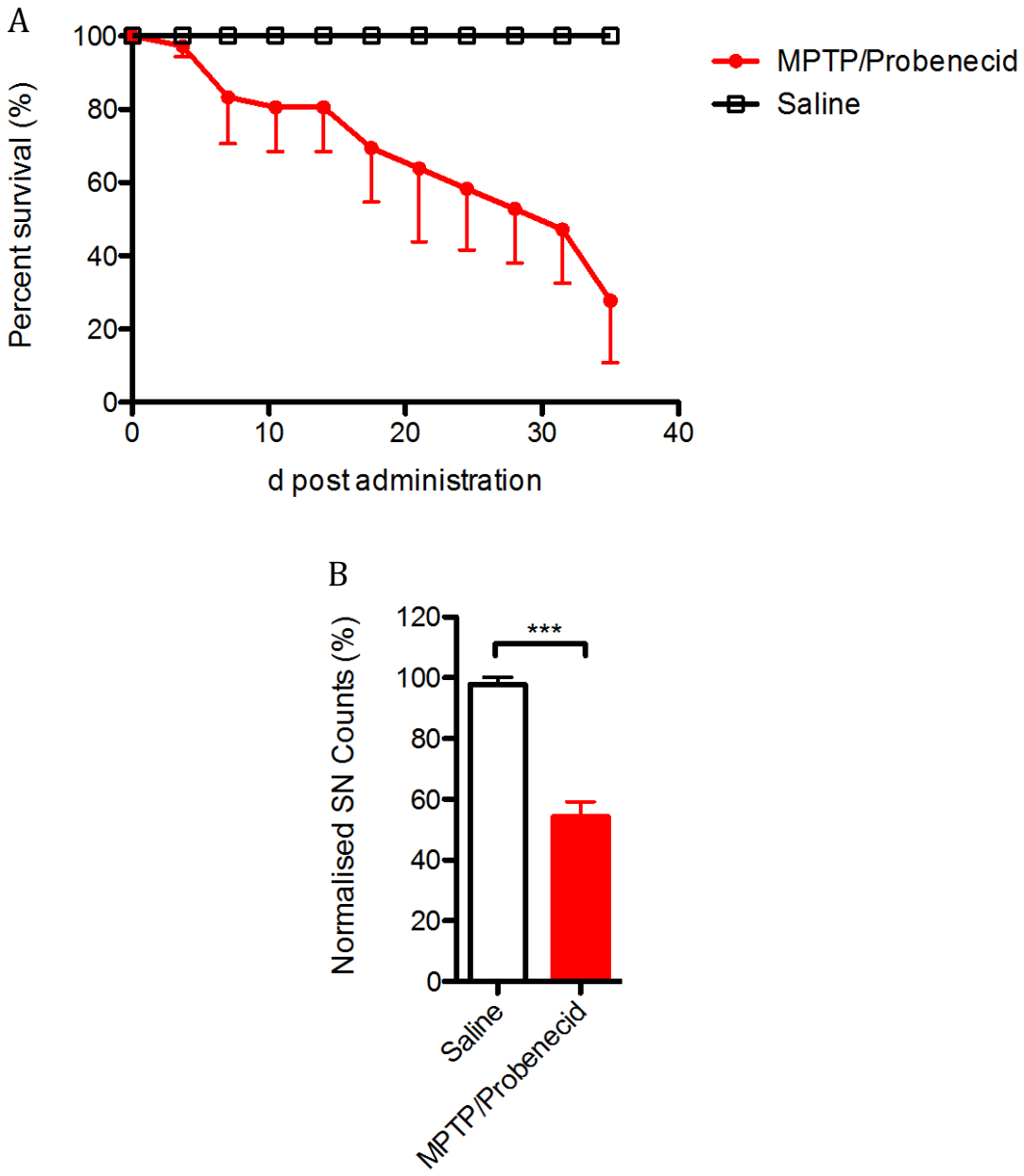

Figure 3.2 Chronic MPTP/Probenecid model in young (5 m.o.) mice. (**A**) Survival of 5 m.o. mice during chronic administration of MPTP/probenecid over 5-week period. (**B**) Quantification of the number of SNpc cell bodies following administration of saline (white bar, n=9) or MPTP/probenecid (red bar, n=10). Data is presented as the mean ± S.E.M. Student's t-test was used to determine levels of significance. Asterisks indicate statistical significance in comparison to saline (***, $p < .001$).

3.3.3 Acute MPTP model shows increased survival of animals

Following the observation that the chronic MPTP/probenecid model does not yield sufficient viable animals either in aged or young mice for transplantation studies, I decided to utilise the acute model of MPTP intoxication (see Section 3.2.2.2b). The administration of MPTP using the acute regime still resulted in death of over 50% of animals (47.2 % ± 5.6 survival, n=36)(Fig 3.3A)(Table 3.1). Importantly, acute intoxication with MPTP did not alter the number of remaining neutral red cell bodies in the SNpc compared with chronic MPTP treatment (55.8 % ± 7.7, n=17)(Fig 3.3B)(Table 3.1).

Following consultation with an investigator experienced with MPTP animal models of PD it was suggested that the death observed post MPTP administration was possibly due to toxin-induced hypothermia. The addition of heating pads and 50 mL tubes containing warm (~42°C) water directly to the cage following administration significantly increased the number of animals surviving acute MPTP administration (91.7 ± 4.8, n=36)(Fig 3.3B)(Table 3.1). The extent of SNpc lesion was determined to be 47.3 % ± 4.9, n=33 of saline treated animals (Fig 3.3D)(Table 3.1).

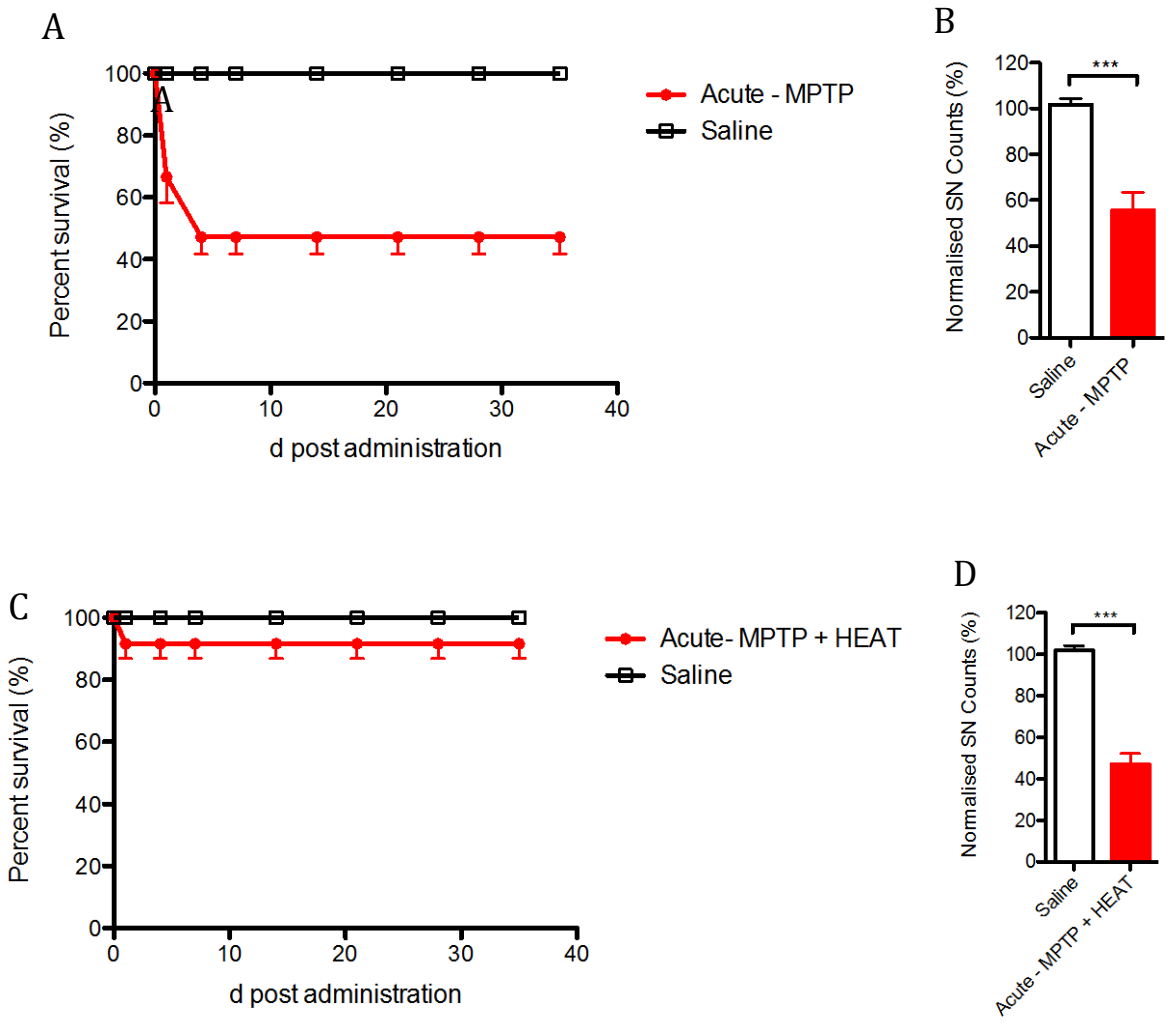

Figure 3.3 Acute MPTP model in young (5 m.o.) mice. (**A**) Survival of mice following acute administration of MPTP. (**B**) Quantification of the number of SNpc neurons following administration of saline (white bar, n=9) or acute MPTP (red bar, n= 17) (**C**) Survival of mice during chronic administration of MPTP following the addition of heating apparatus. (**D**) Quantification of the number of SNpc neurons following administration of saline (white bar, n=3) or acute MPTP with heating apparatus (red bar, n=12). Data is presented as the mean ± S.E.M. Student's t-test was used to determine levels of significance. Asterisks indicate statistical significance in comparison to saline (***, $p < .001$).

Dosing Regime	Survival of Animals	SNpc lesion size (% of normalised saline)
Chronic MPTP/probenecid (12 m.o)	8.3 % ± 5.9, n=61	65.5 % ± 10.5, n=5
Chronic MPTP/probenecid (5 m.o)	27.8 % ± 16.9, n=36	54.2 % ± 5.1, n=10
Acute MPTP (5 m.o.)	47.2 % ± 5.6, n=36	55.8 % ± 7.7, n=17
Acute MPTP (5 m.o.) + heating	91.7 ± 4.8, n=36	47.3 % ± 4.9, n=33

Table 3.1 Survival of animals and SNpc lesion size following treatment with different dosing regimes of MPTP. Data are presented as mean ± mean.

3.3.4 Behaviour deficits are not pronounced in mice following acute MPTP treatment

In order to evaluate the functional benefit in behavioural endpoints of grafted ESC-derived mbDA progenitors, it was necessary to first establish a baseline in motor deficits. To assess the effects of the bilateral lesion of the striatum caused by MPTP treatment mice were subjected to a number of classical motor tests.

3.3.4a Rotarod

Rotarod performance has been consistently associated with SNpc neuron loss in acute MPTP-treated mice (Ayton et al., 2012; Rozas et al., 1998; Sedelis et al., 2000). 60 d following acute MPTP lesioning five-month-old mice were compared with age matched saline treated controls for both rotarod measurement parameters, i.e. time at fall and speed at time of fall. No significant differences were observed for elapsed time at fall (MPTP, 25.9 ± 8.1 sec, n=21) vs. (saline, 24.2 ± 4.0 sec, n=9)(Student's t-test, $p > 0.05$)(Fig 3.4A) or speed of rotarod at the time of fall (MPTP, 7.9 ± 0.9 RPM, n=21) vs. (saline, 6.4 ± 1.3 RPM, n=9)(Student's t-test, $p > 0.05$)(Fig 3.4B).

3.3.4b Pole test

Time to orient down (down-t) and total time to transverse down (total-t) were assessed for both saline and MPTP-treated mice using a pole test. Mean score (seconds) for down-t were 1.2 ± 0.2 (saline, n=9) and 1.2 ± 0.3 (MPTP, n=21) demonstrating no significant difference (Student's t test, $p > .05$)(Fig 3.4C). For t-total, saline treated mice took 7.2 ± 0.5 seconds (n=9), and MPTP treated group took 7.4 ± 0.9 (n=21), again demonstrating no difference (Student's t test, $p > .05$)(Fig 3.4D).

3.3.4c Challenging beam transversal test

Saline and MPTP treated mice were tested for motor performance and co-ordination using a challenging beam transversal test. The parameters, errors per step, number of steps and time to transverse were recorded. A Student's t-test indicated no difference ($p > .05$) between saline (0.4 ± 0.1, $n=9$) and MPTP (0.5 ± 0.2, $n=21$) treated groups in the numbers of errors per step (Fig 3.4E). The number of steps taken for MPTP (13.7 ± 1.8, $n=21$) vs. saline (10.5 ± 1.6, $n=9$) treated animals was non-significant ($p > .05$; Student's t-test)(Fig 3.4F). A similar non-significant ($p > .05$, Student's t-test) result was observed for the total time to transverse the beam for MPTP (12.6 ± 2.7 $n=21$) vs. saline (10.6 ± 1.9, $n=9$) treated animals (Fig 3.4G).

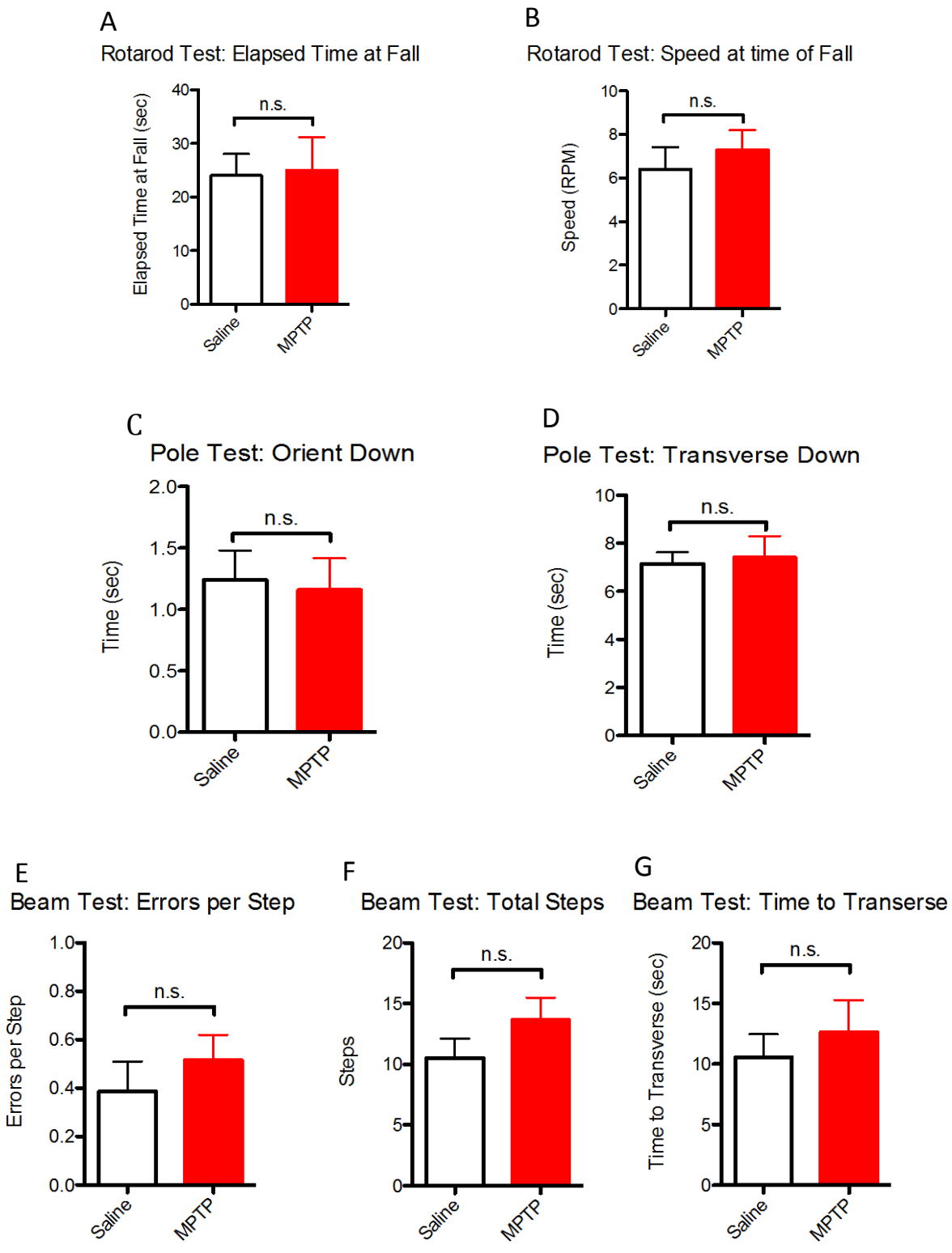

Figure 3.4 Motor performance and co-ordination tests in MPTP vs. saline treated mice 60 days post administration. Rotarod test, (A) elapsed time (sec) at fall and (**B**) speed (RPM) at fall. Pole Test, (**C**) time (sec) to orient down (down-t) and (**D**) total time (sec) to transverse down (total-t). Challenging beam transversal test, (**E**) number of errors per step, (**F**) total steps taken and (**G**) time (sec) to transverse the beam. Data presented as mean ± S.EM. of (saline, n=3; MPTP, n=21) Levels of significance calculated using Student's t test (n.s., non-significant, $p > .05$).

3.3.5 *Lmx1a*-promoter driven reporter expression during neural differentiation using CDML conditions

Previous work in our laboratory has demonstrated that CDML differentiation leads to efficient neural conversion of mESCs into *Sox1*-expressing neural progenitors. To examine the expression of *Lmx1a* during neural differentiation a m*Lmx1a*-AMP-IRES-eGFP (m*Lmx1a*-AIG, Fig. 2.1A) reporter cell line was engineered. Both the catalytic reporter β-lactamase (protein product of the ampicillin resistance gene, AMP) and eGFP were expressed under the control of the endogenous *Lmx1a*-promoter. *Lmx1a*-promoter driven reporter expression was ascertained at fixed time points during CDML differentiation. FACS analysis revealed no expression of either β-lactamase or eGFP at d0 (Fig 3.5A & D) or in the parental cell line, E14-tg2a (data not shown). At d6, 29.1 % ± 4.1 and 5.8 % ± 1.7 of cells expressed β-lactamase and eGFP respectively (Fig 3.5D). *Lmx1a*-promoter driven β-lactamase expression peaked at d8, with 37.6 % ± 4.4 of cells positive, while 18.3 % ± 4.0 expressed eGFP (Fig 3.5D). eGFP expression peaked two days later at d10 with 33.7 % ± 2.3 of cells positive, whilst β-lactamase expression was maintained at 34.3 % ± 2.4 of total cells (Fig 3.5B & D). From d12 to d20 both *Lmx1a*-promoter driven β-lactamase and eGFP expression appeared to be remain relatively stable (29.3 % ± 4.3 and 27.2 % ± 7.1, β-lactamase and eGFP respectively at d20, Fig 3.5C & D). Following fixation at d8, immunofluorescence labeling showed that eGFP positive cells co-labeled for the neural progenitor marker Nestin (Fig 3.5E), but not for the neuronal marker Tuj1 (3.5F).

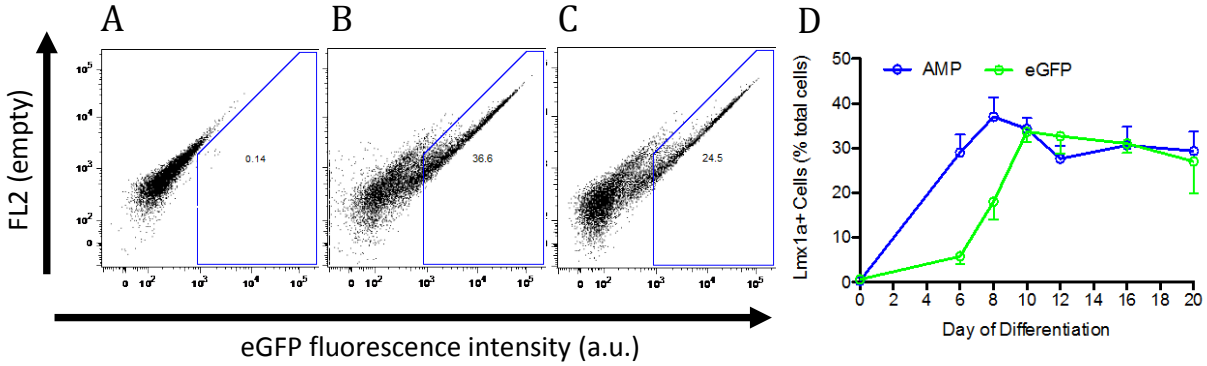

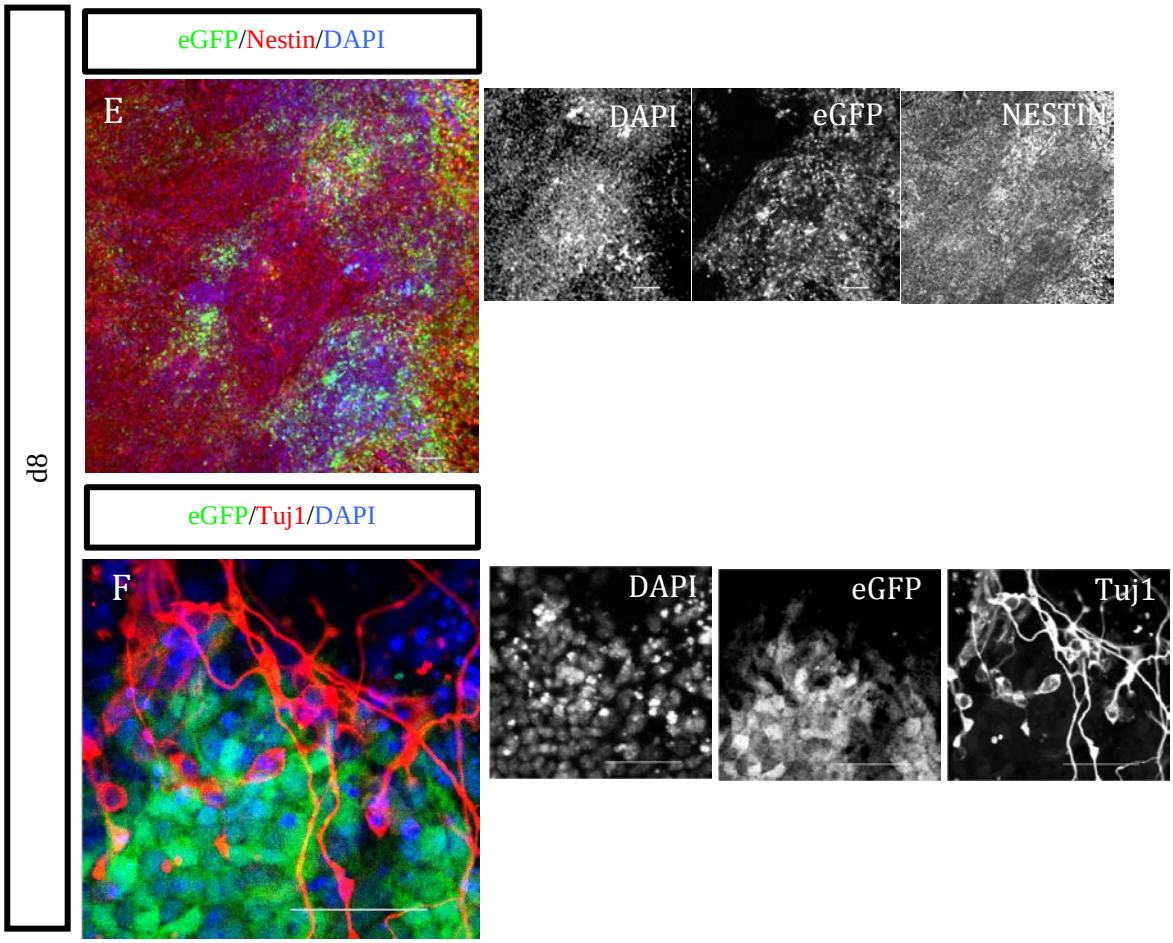

Figure 3.5 Expression of reporter genes driven by the *Lmx1α*-promoter under CDML conditions. Representative FACS plots of eGFP expression for (**A**) d0, (**B**) d10 and (**C**) d20 of differentiation. (**D**) Quantification of reporter gene expression for β-lactamase (blue line) and eGFP (green line) from d0 to d20 of differentiation Data presented as mean ± S.EM. Labeling of d8 EGFP (green) cultures for (**E**) Nestin (red), DAPI (blue) and (**F**) Tuj1 (red) and DAPI (blue). Scale bars, 100 µm.

3.3.6 *Lmx1a*-promoter driven reporter expression during neural differentiation using PA6 conditions

A well characterised differentiation protocol that generates mbDA neurons utilises a PA6 stromal cell layer (Kawasaki et al., 2000). This was used to characterise *Lmx1a*-promoter driven eGFP expression during differentiation. Similar to CDML conditions no reporter gene expression was observed at d0 of differentiation (Fig 3.6A & D). However, unlike CDML conditions eGFP expression did not transiently peak at d8 (Fig 3.6B & D), rather a gradual increase in the number of *Lmx1a* positive cells was observed up until d20 where ~ 20% of cells were positive detected as positive via FACS (Fig 3.6C & D). The majority of eGFP cells at d8 labeled for Nestin (Fig. 3.6E), although Tuj1/eGFP positive cells were observed at this point as well (Fig 3.6F).

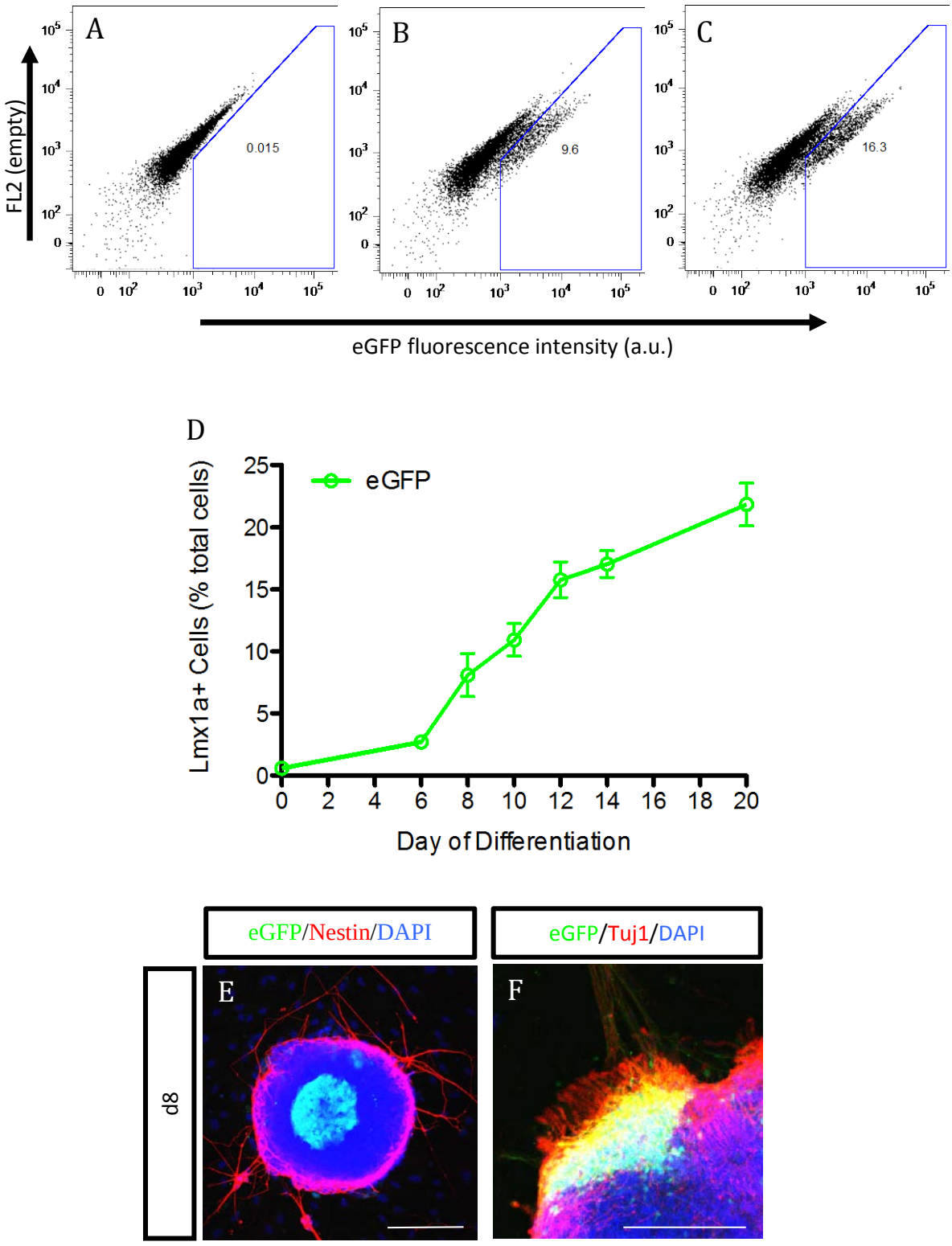

Figure 3.6. Expression of EGFP driven by the *Lmx1a*-promoter under PA6 conditions. Representative FACS plots for (**A**) d0, (**B**) d10 and (**C**) d20 of differentiation. (**D**) Quantification of EGFP expression (green line) from d0 to d20 of differentiation. Data presented as mean ± S.EM. Labeling of d8 EGFP (green) cultures for (**E**) Nestin (red), DAPI (blue) and (**F**) Tuj1 (red) and DAPI (blue). Scale bars, 100 µm.

3.3.7 Optimisation of grafting co-ordinates

Given that most grafting studies have been optimised in rats, which have a considerably large striatal volume than mice I initially used the m*Lmx1a*-AIG/R26-mCherry reporter cell line to optimise grafting striatal co-ordinates. Paxinos and Franklin co-ordinates (Paxinos & Franklin, 2003) for striatal targeting (R/C 0.00 mm, M/L 2.00mm and D/V 3.00mm) consistently placed grafts into the lateral ventricle subsequently mCherry positive cells were found in the cortex, most likely due to backflow into the injection tract (Fig. 3.7B and 3.8). Modification of co-ordinates (R/C 0.00 mm, M/L 2.20mm and D/V 3.00mm yielded grafts with correct placement in the dorsomedial striatum (Fig. 3.7C and 3.8).

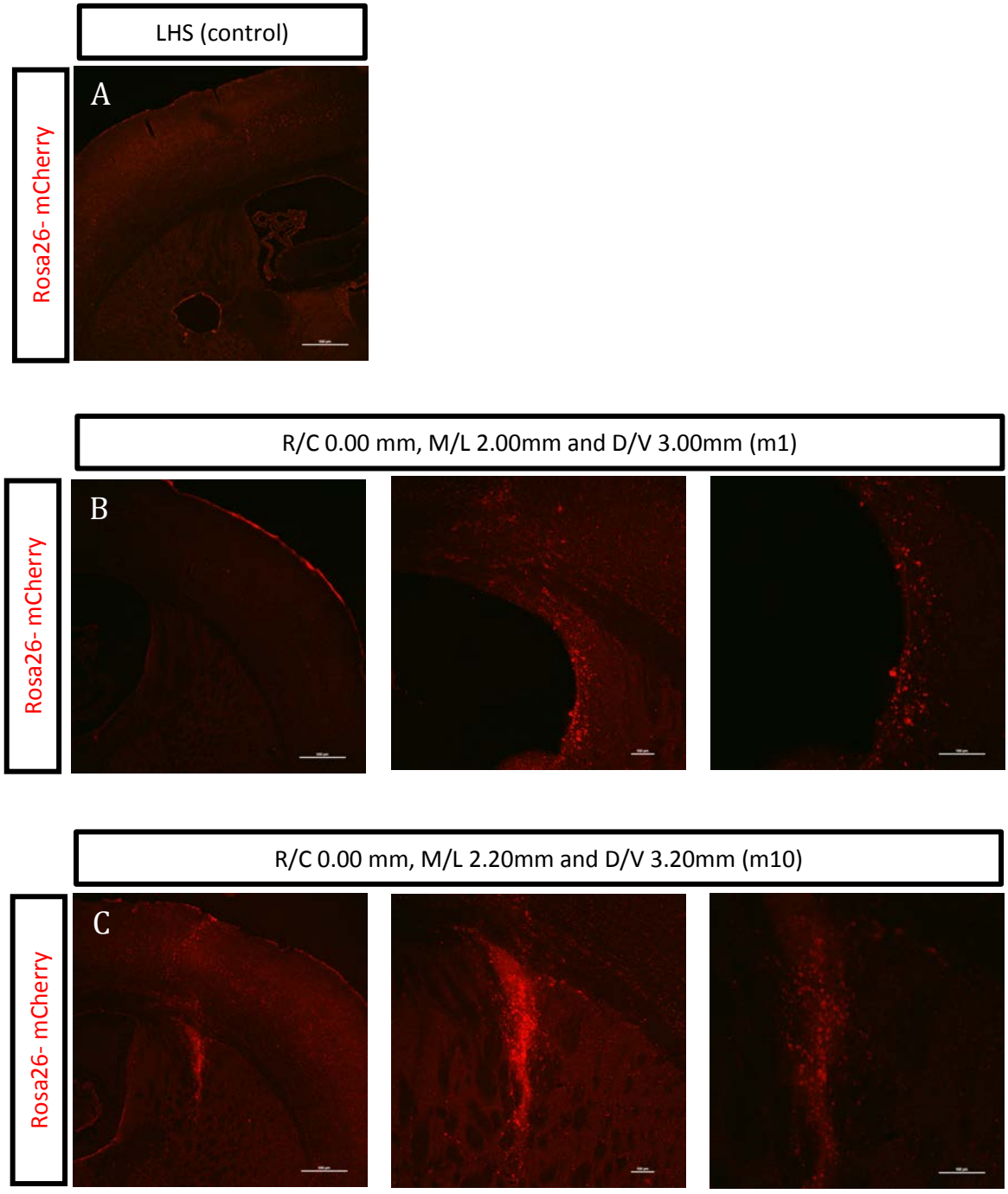

Figure 3.7 Optimisation of grafting co-ordinates (**A**) Left hand side control of striatum indicating background fluorescence detection after 561 nm excitation. mCherry positive cells following grafting using co-ordinates (**B**) R/C 0.00 mm, M/L 2.00mm and D/V 3.00mm (m1 – mouse 1) and (**C**) 0.00 mm, M/L 2.20mm and D/V 3.20mm (m10 – mouse 10).

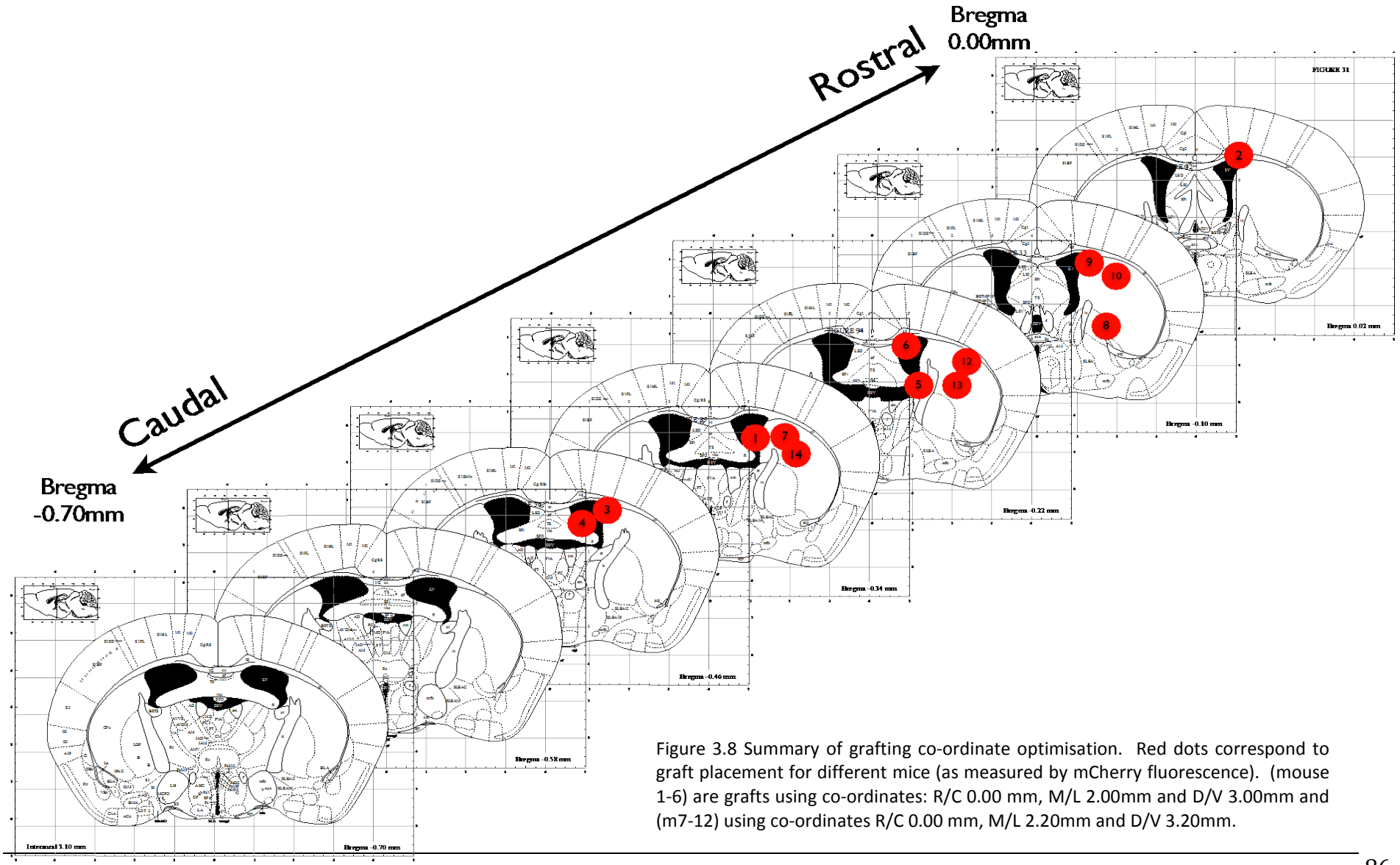

Figure 3.8 Summary of grafting co-ordinate optimisation. Red dots correspond to graft placement for different mice (as measured by mCherry fluorescence). (mouse 1-6) are grafts using co-ordinates: R/C 0.00 mm, M/L 2.00mm and D/V 3.00mm and (m7-12) using co-ordinates R/C 0.00 mm, M/L 2.20mm and D/V 3.20mm.

3.3.8 Grafting of sorted EGFP+ cells

Following optimisation of grafting co-ordinates, EGFP+ sorted cells from both CDML (d8) and PA6 (d8) differentiation conditions were grafted into the striatum. Only data from grafted d8 eGFP+ cells from PA6 differentiation is presented (as the outcomes were the same). There were initial concerns that grafts would contain proliferative progenitors or undifferentiated stem cells, which could lead to either neural overgrowths or teratomas. Immunofluorescent analysis revealed numerous mCherry grafted cells, however no Ki67 or SSEA1 positive cells were observed (Fig 3.9A and B). Additionally, mCherry positive cells were not found to co-localise with the neural progenitor marker Nestin (Fig 3.9C), the neuronal maker Tuj1 (Fig 3.9D) or the DAergic maker Th (Fig 3.9E). Moreover other makers (see Table 3.2) did not demonstrate any immunoreactivity, with the exception with GFAP (Fig 3.9F and F'). However this was never observed to co-localise with mCherry suggesting that GFAP+ cells were host derived.

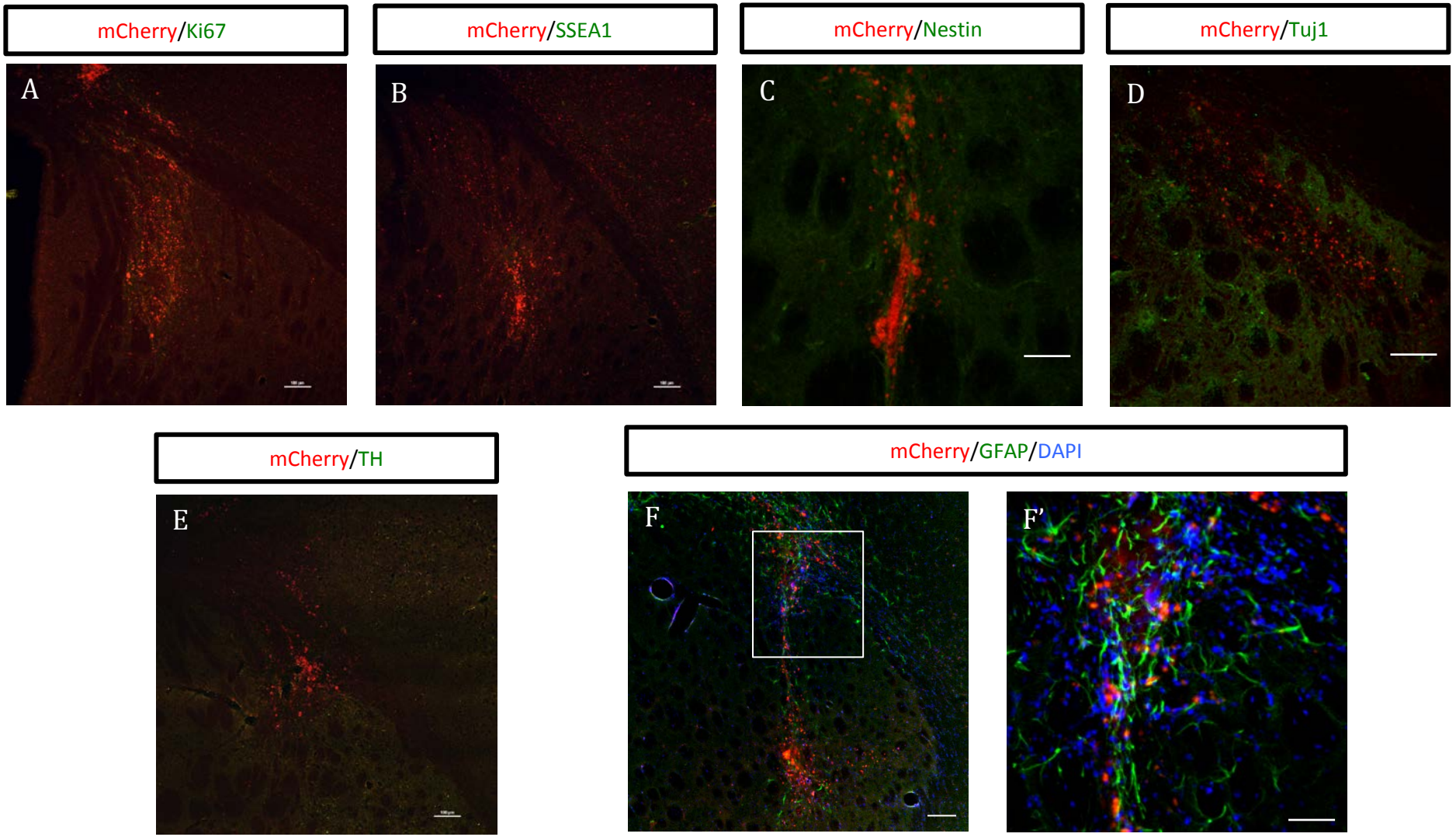

Figure 3.9 Immunofluorescence images of grafted striata of MPTP treated mice. mCherry (red) and (**A**) Ki67 (green), (**B**) SEEA (green), (**C**) Nestin (green), (**D**) Tuj1 (green), (**E**) Th (green) and (**F**) GFAP (green) and DAPI (blue) (**F'**) inset of F. Scale bars, 100 µm.

Antibody	**Reactivity (Graft/Host)**
Ki67	-/-
SSEA1	-/-
Nestin	-/+
Tuj1	-/+++
PSA-NCAM	-/-
MAP2	-/++
Th	-/++
GABA	-/+
GFAP	-/+++
Cd11b	-/-

Table 3.2 Summary of antibodies tried on striata of animals that received grafts of *Lmx1a* positive cells. (-, no staining, +, weak staining, ++, moderate staining, +++ strong staining).

3.3.9 *In vitro* phenotype of *Lmx1a*+ progenitors following terminal differentiation

As sorted *Lmx1a*+ cells did not seem to integrate or differentiate following engraftment into the MPTP-treated mouse striata, we were interested to see whether their development was also restricted under *in vitro* conditions. To study *Lmx1a*+ cells in more detail, *Lmx1a* negative and positive cells were FACS-isolated from d8 CDML cultures. Two days post sort, *Lmx1a*+ cells gave rise to relatively homogenous cultures with neural progenitor morphology demonstrated by robust Nestin immunoreactivity and the lack of Tuj1 labeling (Fig 3.10 A, B, E & F). Conversely, *Lmx1a*- cells produced heterogeneous cultures with significantly less cells immunoreactive for Nestin (Fig 3.10 C, D, E & F)(Student's t-test, n=3, $p<0.001$). Moreover, significantly more Tuj1 positive neurons were detected in the *Lmx1a* negative sorted cells (Fig 3.10 C, D & E)(Student's t-test, n=3, $p<0.05$).

Lmx1a positive cells were left to terminally differentiate for a further 12 d. At this time point the majority of d8 CDML *Lmx1a*+ sorted cells gave rise to GABA+/TUJ1+ neurons (Fig 3.11A), which also co-labeled for GAD67 (Fig 3.10B). In addition the GABA+ neurons frequently labeled for the upper layer cortical marker SatB2 (3.11C). Th+ cells were rarely detected amongst the vast majority of GABAergic neurons (Fig 3.11D).

Following terminal differentiation, d8 *Lmx1a*+ cells sorted from PA6 differentiation conditions gave rise to homogenous neuronal cultures that expressed Th at high frequency (Fig 3.11E). These Th+ neurons also co-expressed eGFP suggesting a mbDA phenotype (Fig 3.11F). GABA immunoreactive cells were detected infrequently (Fig 3.11G).

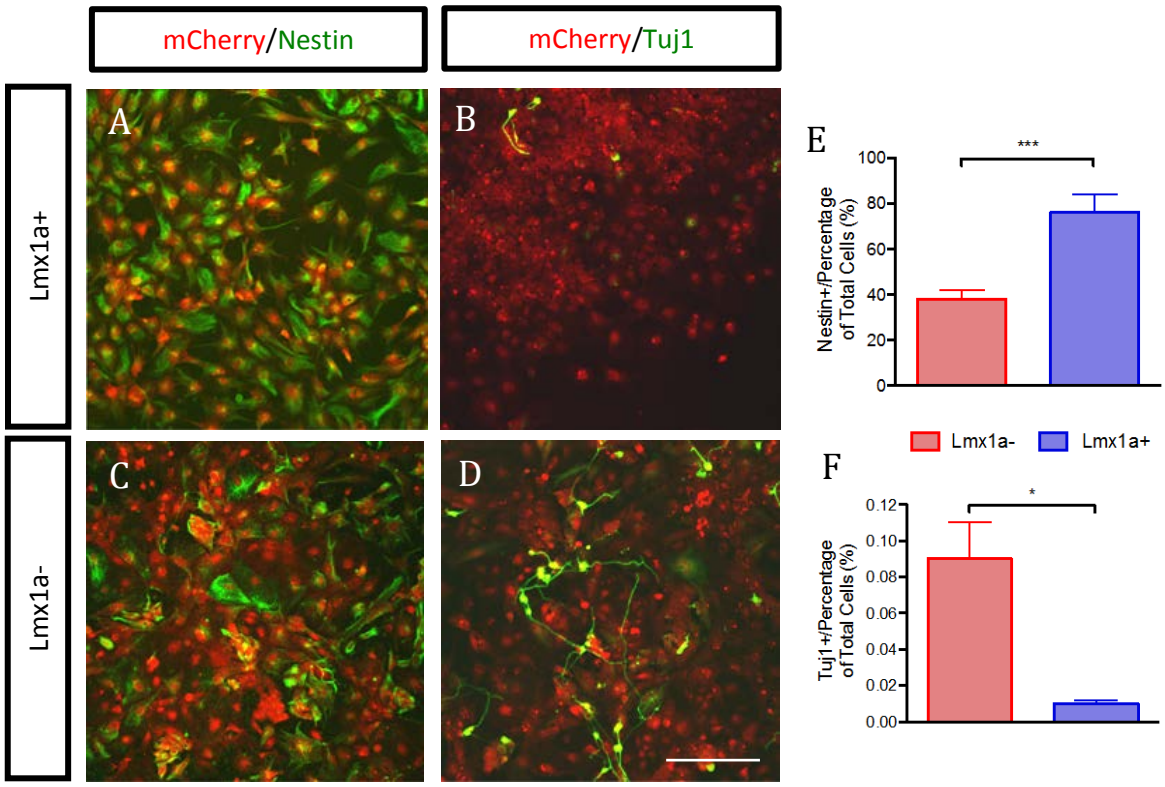

Figure 3.10 Post sort analysis (48 h post replating) Immunofluorescence images of *Lmx1a* positive (**A & B**) and negative (**C & D**) cultures labeled (**A**) Nestin (green), (**B**) Tuj1 (green), (**C**) Nestin (green) and (**D**) Tuj1 (green). (*, $p < .05$ and ***, $p < .001$) between *Lmx1a*+ and *Lmx1a*- cells with Student's t-test. Results are presented as the mean ± SEM of at least 3 independent experiments. Scale bar, 100 µm.

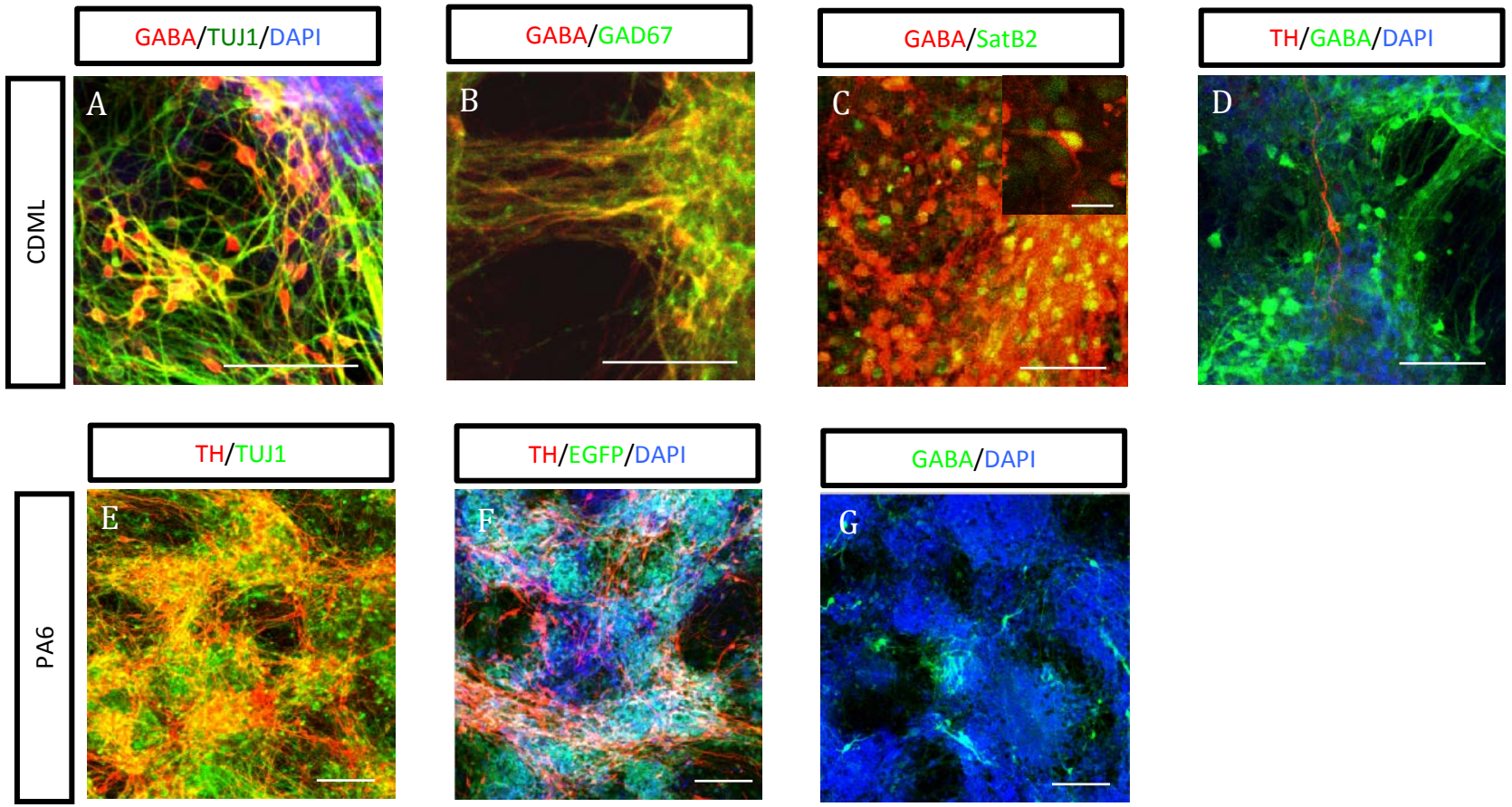

Figure 3.11 Immunofluorescence images of terminally differentiated *Lmx1a* positive cells FACS-isolated from (**A-D**) d8 CDML (12 d post sort) and (**E-G**) d10 PA6 (7d post sort). Labeled with (**A**) GABA (red), Tuj1 (green), (**B**) GABA (red), GAD67 (green), (**C**) GABA (red), SatB2 (green), (**D**) Th (red), GABA (green), (**E**) Th (red), Tuj1 (green) and (**F**) Th (red), eGFP (green) (**G**) GABA (green). Images (**A, D, F** and **G**) counterstained with DAPI. Scale bar, 100 µm (except for C', 20 µm).

3.4 Discussion

In this Chapter I attempted to create a MPTP mouse model of PD, which could be used to assess the survival, integration and function of mESC-derived *Lmx1a* positive FACS-isolated progenitors. In addition the *in vitro* fate of sorted m*Lmx1a* positive cells from CDML and PA6 differentiation conditions was assessed following terminal differentiation.

3.4.1 Animal model of PD

An animal model of PD was required in this study, in which the regenerative capacity of grafted *Lmx1a* reporter positive progenitors could be assessed. In the past 6-OHDA lesioned animals have been utilised to study the survival, integration and function of ventral midbrain and ESC derived grafts (Bjorklund et al., 1983; Bjorklund, Schmidt, & Stenevi, 1980b; Bjorklund et al., 2002; Chung et al., 2011; Hargus et al., 2010; Jönsson et al., 2009 Thompson et al., 2006; 2008; 2009). Although currently the gold standard in the evaluation of the functional regenerative capacity of ventral midbrain and ESC derived cells, due to its robust rotational asymmetry behavioural test, the unilateral 6-OHDA model does not resemble clinically presented PD (Meredith et al., 2008; Schober, 2004). The systemic administration of MPTP generates bilaterally lesioned animals, thus providing a model more reminiscent of PD (Meredith et al., 2008).

As the majority of PD cases arise in aged individuals (Dauer & Przedborski, 2003), aged mice (12 month old) were initially used in the study. Large cohorts of mice are usually required for transplantation studies; however, the chronic MPTP/probenecid model in 12-month-old mice did not yield sufficient surviving animals for grafting studies. The low survival of 12 month old mice following chronic MPTP administration in

my hands, is inconsistent with a wide body of publications demonstrating their use in other aspects of PD modelling (Andres-Mateos et al., 2007; Date et al., 1993; Irwin et al., 1993; Jackson-Lewis & Przedborski, 2007; Przedborski et al., 2001). Moreover, the use of younger mice (5-month-old) did not increase the survivability of MPTP-intoxicated animals. Together these observations suggested that age was most likely not the attributing factor in the survivability of mice that received chronic administration of MPTP/Probenecid.

Different MPTP dosing regimes have been shown to exhibit differential, undesirable consequences including acute death following administration (Jackson-Lewis & Przedborski, 2007; Przedborski et al., 2001). I speculated that the use of an acute MPTP model might decrease treatment lethality. Although a decrease in the frequency of mortality was observed following intoxication in the acute MPTP model, only 50% of animals survived to the end of the intoxication period. David Finkelstien, (Florey Neurosciences Institute) suggested that the high mortality rate might be due to toxin-induced hypothermia or dehydration. Since, the intake of water was not altered in MPTP-treated animals, I speculated that the cause of death in acute MPTP treated animals was most likely due hypothermia. The addition of heating mats and "hot water bottles" in the form of 50mL tubes filled with 60° C water decreased mortality following administration of MPTP in the acute model confirming this hypothesis, but this observation was not extended into the chronic MPTP/probenecid model. This finding fits with reports demonstrating hypothermia following administration of either MPTP or MPP+ analogues (Freyaldenhoven, Ali, & Hart, 1995; Satoh, Yonezawa, Tadano, Kisara, & Arai, 1987a; 1987b; Tadano, Satoh, Oyama, Kisara, & Arai, 1991).

Acute administration of MPTP to 5-month-old mice elicited degeneration of SNpc neurons to a similar extent as published (Tripanichkul et al., 2006), indicating that in my hands, the acute treatment of mice with MPTP provides a reliable animal model of PD, through the degeneration of SNpc neurons.

3.4.2 Behavioural phenotype of MPTP treated Mice

Conflicting reports exist regarding the behavioural phenotypes of MPTP treated mice. Generally, the behavioural deficits seem to be dependent on the type of MPTP model used to create the nigrostriatal lesion (reviewed in Sedelis et al., 2001). With respect to the acute MPTP mouse model, acute behavioural effects have been observed, such as alterations in locomotion, rearing behaviour and time spent in the central annuli of the open field test (Hofele et al., 2001). However, due to the paucity of long term behavioural changes following acute MPTP intoxication indicates no substantial behavioural deficits, with the exception of rotarod performance (Ayton et al., 2012; Rozas et al., 1998; Sedelis et al., 2001; Sundstrom et al., 1990). Thus, given the extent of their lesion, it is surprising to note no differences in rotarod performance of MPTP treated mice compared to aged matched saline treated controls. In summation the acute mouse model of MPTP intoxication did not produce a reliable platform to assess the behavioural changes following grafting of mESC-derived *Lmx1a*+ progenitors.

3.4.3 *Lmx1a* promoter-driven reporter expression during neural differentiation

In my hands, the acute intoxication with MPTP did not generate sufficient behavioural deficits in which the regenerative capacity of *Lmx1a* positive isolated progenitors could be assessed. Nonetheless, substantial degeneration of SNpc neurons was observed, indicating that the acute model could still be used to assess the survival and integration of grafted *Lmx1a*+ progenitors in a PD-like environment.

Initially, m*Lmx1a*-AIG mESCs were differentiated under CDML conditions to avoid difficulties associated with EBs and the undefined nature of animal serum or SDIA from stromal cell lines such as PA6. As transcription factors have been demonstrated to be expressed at extremely low levels, it was not clear that *Lmx1a*-promoter driven eGFP expression would be detectable by FACS (Aurell et al., 2007; Zlokarnik et al., 1998). Thus the catalytic reporter β-lactamase together with a fluorogenic substrate was initially used to determine levels of *Lmx1a* expression (Zlokarnik et al., 1998). Subsequently, EGFP expression was shown to be detectable by FACS, however, a lag was observed between the appearance of cells positive for β-lactamase compared with eGFP. This is not unexpected, for two reasons; (1) the β-lactamase reporter system is an enzyme based assay and will amplify the signal and (2) the detection of the eGFP by flow cytometry requires 3 orders of magnitude more molecules of eGFP per cell than the β-lactamase reporter (Zlokarnik et al., 1998). At d8, eGFP+ positive cells co-expressed the neural progenitor marker Nestin, but not the neuronal marker TUJ1, indicating at this time point the majority of *Lmx1a* positive cells are progenitors and meet the criteria of a progenitor cell type required for grafting.

As CDML conditions have not been consistently demonstrated to give rise to mbDA neurons, whereas PA6 based differentiation has (Kawasaki et al., 2000; Parmar & Li, 2007), m*Lmx1a*-AIG mESCs were also differentiated under PA6 conditions. Under PA6 conditions, eGFP was detected in fewer cells and was observed to consistently increase over the differentiation period, demonstrating different *Lmx1a* expression kinetics of compared to CDML conditions. Although the majority of d8 eGFP+ cells under PA6 conditions also co-labeled for Nestin, suggesting a neural progenitor identity, the incidence of Tuj1/eGFP positive cells was higher, suggesting accelerated neural

commitment and differentiation. This is consistent with published observations that demonstrate the presence of Tuj1+ neurons under PA6 conditions at earlier time points in comparison with CDML differentiation conditions (Parmar & Li, 2007). Thus, d8 represents an ideal time point in both CDML and PA6 differentiation conditions, to isolate *Lmx1a* positive progenitors, as they are highest in number.

3.4.4 Isolation and assessment of grafted *Lmx1a* positive cells

In the past mESC and ventral midbrain derived DA progenitors and neurons have been grafted into rat hosts, which allows subsequent detection of grafted cells using antigens, such as M2M6, that are only expressed on mouse cells (Thompson et al., 2008). As I was using a mouse MPTP model this approach could not be used to identify grafted mESC-derived neural progenitors and/or neurons. Thus the m*Lmx1a*-AIG reporter cell line was targeted with a vector, which delivered the mCherry ORF to exon 1 of the *Rosa26* locus (see 2.1.1). As *Rosa26* is ubiquitously expressed, mCherry fluorescence could be used to identify grafted cells over host tissue.

For grafting studies *Lmx1a* positive progenitors were isolated based on eGFP expression rather than β-lactamase activity. CCF2-AM uses a lipophilic acetoxymethyl ester (AM) to enter the cell; this group is cleaved by cytoplasmic esterases following cytoplasmic entry and remains in the cell. The de-esterification of acetoxymethyl ester liberates formaldehyde as hydrolysis product (Pawley, 2006). This, together with preparation and loading times (> 3hr for CCF2-AM assay) raised concerns that cell viability would be worse off than using freshly prepared cells for eGFP sorting.

Sixty days post grafting, eGFP could not be detected in FACS-isolated grafted *Lmx1a* positive progenitors. This indicated that eGFP and thus *Lmx1a* expression had

been down regulated. Nonetheless, due to the ubiquitous expression of Rosa26, grafted cells could be identified based on mCherry expression 60 d post grafting. Extensive immunofluorescent analysis did not reveal any Rosa26-mCherry cells that co-expressed either the neural progenitor marker Nestin, the neuronal maker, Tuj1, the proliferative marker, Ki67, the DA marker, Th or any other markers tested (Table 3.2). These markers were selected based on data showing that following isolation, replating and terminal differentiation of *Lmx1a* reporter positive cells maintain a neural phenotype and subsequently differentiate into either GABA+ (CDML) or Th+ (PA6) neurons (Nefzger et al,. 2012). As *Lmx1a* reporter positive cells give rise to neurons as well as GFAP+ cells (presumably glia or glial progenitors)(Nefzger et al., 2012) non-neural cells would have also been grafted into the MPTP treated animal. However GFAP immunofluorescent staining did not reveal any GFAP+/mCherry+ cells in MPTP treated striata post grafting suggesting that they either did not survive grafting or differentiate into GFAP immunofluorescent positive cells. It is entirely probable the environment (MPTP treated SNpc denervated striatum) in which these progenitors were grafted, may not have been permissive to subsequent differentiation, either towards a neural or astrocytic lineage. In the future, if I were to repeat this study I would assay for markers of different lineages, in order to assess whether the observed mCherry positive cells committed to different lineages.

Robust labeling of GFAP was observed in proximity to the graft site, delineated by mCherry expression, however GFAP immunoreactivity was not observed to co-localise with mCherry expressing cells. This indicated that GFAP positive cells were host derived, and most likely a local response to tissue damage or the presence of foreign cell type(s), which has been demonstrated in the past (Coyne et al., 2006). On the whole, these

observations indicate that although *Lmx1a* positive cells isolated from differentiating mESCs cultures appear to survive, following FACS and grafting, they do not differentiate or integrate in the host striatal circuitry. Such observations are challenging to interrupt as to date only two investigations have used reporter cell lines to extract cells from differentiating mESC cultures. One investigation utilised a Pitx3 reporter cell line, which marks mature mbDA neurons as opposed to progenitors. In this study investigators observed robust survival and integration in host striata, even following FACS of "mature" neurons (Hedlund et al., 2008). Thus, the lack of engraftment observed in this study may be a result of the maturity of the *Lmx1a* positive sorted cells. However this suggestion seems improbable as a study using a Sox1-eGFP reporter cell line which marks neural progenitors, which maybe less mature or at the same stage of development demonstrate grafts with robust Th+ staining, indicating that sorted progenitors survive, differentiate and integrate (Fukuda et al., 2006). As Sox1-eGFP cells would presumably contain both *Lmx1a* positive and negative cells, another possible explanation maybe that cells in the *Lmx1a* negative fraction support the survival and integration of *Lmx1a* positive cells and thus their separation may affect this. Alternatively, the mouse MPTP model of PD may not support the growth and differentiation of grafted progenitors, because of inappropriate differentiation, guidance or maintenance cues. As mentioned, very few studies have utilised the MPTP model for grafting of ESC-derived cells thus it is difficult to put the findings in this study into context. To begin to assess the role of cell-specific vs. model-specific issues in engraftment, it would be necessary to assess engraftment of control populations, including *Lmx1a* negative or non-sorted cell populations. Due to concerns of the local ethics committee, specifically the presence of cells with an undifferentiated phenotype, which may lead to the presence of teratomas, in *Lmx1a*

negative or un-sorted populations, I was unable to perform these experiments. It is worth noting however, that the most successful grafting experiment to date used mbDA cells that were of an immature neuronal phenotype rather than a neural progenitor phenotype (Kriks et al., 2011). Although this study utilised mbDA cells derived whole cultures, which would contain cell types at different stages of maturity, thus it is difficult to compare with work presented in this chapter.

3.3.5 *In vitro* phenotype of *Lmx1a* positive progenitors following sorting and terminal differentiation

FACS was used to isolate eGFP positive cells, to test the hypothesis that *Lmx1a+* cells could give rise to enriched cultures of mbDA neurons. *Lmx1a* positive cells demonstrated pronounced Nestin immunoreactivity compared with the negative fraction, indicating that d8 isolated eGFP positive cells were of a neural progenitor phenotype, confirming previous immunofluorescence data. Upon terminal differentiation of eGFP positive cells, Th+ cells were rarely observed, whereas GABA immunoreactive cells were abundant. This observation clearly refuted my hypothesis, that *Lmx1a* positive cells give rise to mbDA neurons. Further characterisation revealed that the GABA positive neurons were also immunoreactive for GAD67 and SatB2, a marker of upper layer cortical identity (Alcamo et al., 2008). These findings from our laboratory are the first to link *Lmx1a* expression to GABAergic neuron development. Furthermore, extensive work, outlined in Nefzger et al., (2012) demonstrates that eGFP positive cells by the time of isolation at d8, are already committed to a GABAergic fate as the addition of patterning cues cannot specify other neural phenotypes (Nefzger et al., 2012). This observation fits with other work, as patterning of ESCs occurs very early in the differentiation process (Fasano et al., 2010; Kirkeby et al., 2012; Kriks et al., 2011). Although these SatB2/GABAergic neurons

are functional (Nefzger et al., 2012), their physiological relevance is questionable as SatB2 positive neurons in the cortex are not GABAergic (Alcamo et al., 2008). SatB2/GABAergic positive interneurons have been reported in the developing mammalian retina (Kay et al., 2011), however no studies demonstrate a relationship between *Lmx1a* expression and eye development. We postulate that the SatB2/GABAergic marker profile in terminally differentiated *Lmx1a* positive isolated cells from CDML conditions may be an artifact of the *in vitro* differentiation process (Nefzger et al., 2012). Until such speculation has been fully explored it is unknown whether there is a direct *in vitro* equivalent of CDML derived *Lmx1a* positive cells.

In contrast to CDML cultures, *Lmx1a* positive cells isolated from PA6 differentiation conditions were able to give rise to functional mbDA neurons at high frequency following FACS isolation and terminal differentiation. These findings are in line with published work that demonstrates PA6 differentiation conditions give rise to numerous mbDA neurons. Moreover, as demonstrated in (Nefzger et al., 2012) the expression of *Lmx1a* in immature colonies was consistent with appearance of numerous Th+ positive cells in mature colonies. This is one of the first investigations demonstrating a predictive link between *Lmx1a* expression in progenitors and subsequent derivation of mbDA neurons.

3.5 Conclusion

Work presented in this chapter demonstrates that the use of an *Lmx1a* reporter cell line to isolate mbDA progenitors from differentiating mESCs is context dependent. Following terminal differentiation of *Lmx1a* positive cells isolated from CDML conditions, very few Th+ cells were detected. In contrast GABAergic neurons, which co-expressed GAD67 and upper the layer cortical marker SatB2 were frequently observed (Fig 3.13). The isolation and subsequent terminal differentiation of *Lmx1a* positive cells from PA6 conditions gave rise to high yields of mbDA neurons (Fig 3.13).

The acute MPTP mouse model of PD could not be used to ascertain the functional benefits of grafted *Lmx1a* positive progenitors due to the lack of behavioural deficits. Nonetheless, the extent of the SNpc lesion, which has been shown in other studies to be associated with significant DA depletion, provided a PD-like environment in which the survival, integration and differentiation of isolated progenitors could be examined. When either of these progenitor populations, either from CDML or PA6 conditions, was grafted into an acute MPTP mouse model, mCherry positive cells were detected, but specific immunoreactivity to a panel of antibodies was not observed. Thus their fate remains unknown.

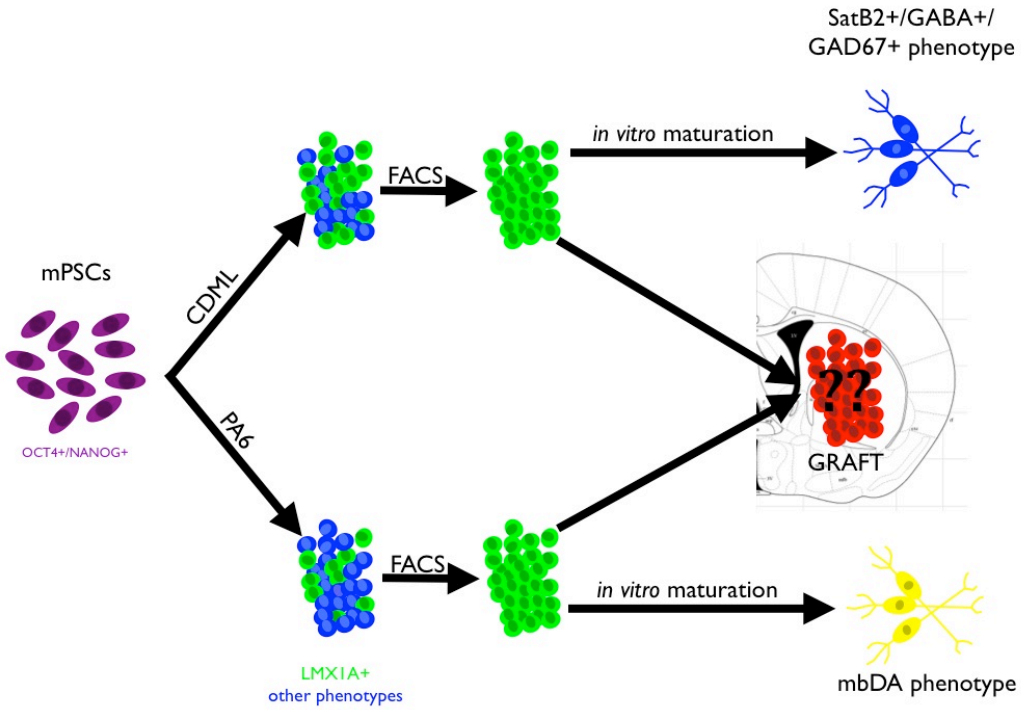

Figure 3.13 Differentiation and sorting model of mESCs. Neural induction and progenitor specification is achieved by CDML (top) or PA6 (bottom) conditions. CDML differentiation results in high numbers of *Lmx1a*+ cells (green), where as PA6 differentiation gives rise to lower numbers of *Lmx1a*+ cells. Following isolation and grafting into a MPTP mouse model, surviving mCherry positive cells (red) are observed but their fate is unknown. The terminal differentiation of *Lmx1a*+ cells FACS-isolated from CDML conditions gives rise to neurons with a SatB2+/GABA+/GAD67+ phenotype (blue neurons), where as neurons with a mbDA phenotype (yellow) are observed following terminal differentiation of *Lmx1a* positive cells isolated from PA6 conditions.

Chapter Four: The isolation of mbDA progenitors using a human *LMX1A* reporter cell line under PA6 conditions

4.1 Introduction

A new model system for studying human neural development (Carpenter et al., 2001), cell fate commitment (Li et al., 2005), and neural disease mechanisms (Di Giorgio, Carrasco, Siao, & Maniatis, 2007) has been enabled by the successful derivation of hESCs (Thomson et al., 1998). The derivation of human mbDA neurons from hESCs may provide a source of material for CRT (Lindvall & Björklund, 2011). In addition mbDA derivation from hESCs may provide a more suitable platform for *in vitro* PD modeling and subsequent large scale screening of disease altering pharmacotherapies (Desbordes & Studer, 2012), than current animal models or mESC-derived cells which are prone to species differences in neurochemistry and function (Cragg et al., 1997; Jakel & Schneider, 2004; Patel et al., 1993). However, as outlined in Section 1.1.2, the current knowledge of hESC differentiation is considerably inferior to that of mESCs. Directed differentiation of hESCs to physiologically relevant cell types has been demonstrated for multiple phenotypes including both neural (Chambers et al., 2009; Lee, Chambers, Tomishima, & Studer, 2010), cardiomyogenic (Kehat et al., 2001; Laflamme et al., 2007; Lev et al., 2005), hepatic (Cai et al., 2007; Rambhatla, Chiu, Kundu, Peng, & Carpenter, 2003), pancreatic (Kroon et al., 2008; Zhang et al., 2009) and skeletal muscle (Barberi et al., 2007; Darabi et al., 2012) lineages. For the neural lineage, derivation of motor neurons (Li et al., 2005) cholinergic neurons (Bissonnette et al., 2011), neural crest cells (Lee et al., 2010) and astrocytes (Emdad et al., 2012) have all been described.

While several research groups have reported the derivation of mbDA neurons from hESCs (Perrier et al., 2004; Roy et al., 2006; Yang et al., 2008), none of the current methods produce post-mitotic cultures with high yields of mbDA neurons. In addition the hESC-derived mbDA cells that have been generated using these methods and

transplanted into animal models of PD function poorly (reviewed in Lindvall & Björklund, 2011), indicating that these mbDA neurons are still lacking either some crucial developmental conditions or the correct phenotype to integrate and function into the host striatal neurocircuitry.

To date, most studies published on the derivation of mbDA neurons from hESCs focus on the post mitotic neuronal phenotypes generated following terminal differentiation, with very few examining the regional specification of progenitors. A recent publication has shown the importance of patterning early during differentiation (Fasano et al., 2010), demonstrating that modulating the phenotypic specification of progenitors in response to morphogens may provide higher yields of mbDA neurons in terminal cultures.

As described in Chapter 3, reporter cell lines enable the enrichment of mbDA neurons in terminal cultures via the extraction of committed mbDA progenitors. However the generation of reporter cell lines by homologous recombination is extremely inefficient for hESCs (Collin & Lako, 2011), and thus has only been documented in a hand full of cases (Costa et al., 2007; Davis et al., 2008; Di Domenico, Christodoulou, Pells, McWhir, & Thomson, 2008; Irion et al., 2007; Ruby & Zheng, 2009; Urbach et al., 2004; Zwaka & Thomson, 2003). The work in both Chapter 3 and (Nefzger et al., 2012) outlines the value of a reporter cell line driven by *Lmx1a*-regulatory elements in the isolation of mouse mbDA progenitors to enable the subsequent high yield of functional mbDA neurons following terminal differentiation. A key question, however, is whether this can also be achieved using a hESC- *LMX1A* reporter cell line.

4.1.1 Aims:

Based on work presented in Chapter 3, it was of interest to address whether early specification of mbDA progenitors could be achieved via known caudalising agents and whether *LMX1A* positive cells isolated from hESCs differentiating under PA6 conditions also result in high yields of terminally differentiated mbDA neurons. Thus the aim of this chapter was (1) to study the early specification of mbDA progenitors in response to known caudalising agents, (2) to engineer a hESC reporter cell driven by regulatory elements of *LMX1A* locus, (3) differentiate the hESC reporter cell line to a mbDA fate using a PA6 co-culture system, (4) isolate *LMX1A* positive cells and analyse their gene expression and fate upon terminal differentiation.

4.2 Methods

All experimental methodologies are the same as described in Chapter 2: General Methods, unless indicated.

4.2.1 PA6 neural induction and dopaminergic differentiation

For PA6 co-culture experiments, hESCs colonies were dissected into 0.5mm^2 fragments and transferred to dishes pre-plated with PA6 cells (5 x 10^4 cells cm^{-2}) in medium containing GMEM supplemented with 8% KSR, 1% NEAA, 2 mM GlutaMAX™-I, 1 mM sodium pyruvate, 0.1 mM β-mercaptoethanol, penicillin 25 U mL^{-1}, streptomycin 25 μg ml^{-1}. To inhibit commitment to other lineages, such as trophectoderm, mesendoderm and non-neural ectoderm (Chambers et al., 2009) hPSC fragments were differentiated in the presence of a selective inhibitor of TGFβ superfamily type I activin receptor-like kinase (ALK) receptor, SB431542 (10 μM; 4-[4-(1,3-benzodioxol-5-yl)-5-(2-pyridinyl)-1H-imidazol-2-yl]benzamide; Axon Medchem)(Chambers et al., 2009), noggin, a protein that binds endogenous TGFβ proteins and inhibits TGFβ signal transduction (500 ng mL^{-1})(Chambers et al., 2009) or various concentrations of a selective inhibitor of bone morphogenetic protein (BMP) type I receptors ALK2 and ALK3, LDN193189 (LDN; 3, 10, 30, 100, 300 nM; 4-[6-[4-(1-Piperazinyl)phenyl]pyrazolo[1,5-a]pyrimidin-3-yl]-quinoline dihydrochloride; Axon Medchem)(Kriks et al., 2011) for the first 12 days cells. PBS containing 1 mg mL^{-1} BSA and 0.1 % DMSO was used a vehicle control. From d2 to d12 cells were treated with recombinant N-terminal SHH (SHH-N; 200, 400, 600, 800 and 1000 ng mL^{-1}, R&D Systems)(Elkabetz et al.,, 2008) smoothened agonist, a small molecule agonist of the smoothened receptor (SAG; N-Methyl-N′-(3-pyridinylbenzyl)-N′-(3-chlorobenzo[b]thiophene-2-carbonyl)-1,4-diaminocyclohexane; 10, 30, 100, 300 and 1000 nM; Santa Cruz Biotechnology)(Denham et al., 2012), a recently modified version of

recombinant SHH, where SHH is tethered to two isoleucines, which more closely mimics the potency of endogenous mammalian SHH (SHH-C25II; 200 ng mL^{-1}, R&D Systems)(Fasano et al., 2010) or cyclopamine, a hedgehog signaling pathway inhibitor (1 μM, (3β,23R)-17,23-Epoxyveratraman-3-ol; Sigma)(Denham et al., 2010; Nefzger et al., 2012). For caudalisation studies, FGF8b (100 ng mL^{-1}, R&D Systems)(Elkabetz et al., 2008) and WNT1 (100 ng mL^{-1}, Peprotech, U.S.A)(Elkabetz et al., 2008) were added at different time points (d2, 4 and 6). At day 20 of differentiation media was changed to N2B27 media supplemented with 20 ng mL^{-1} BDNF, 20 ng mL^{-1} GDNF, 0.2 mM, AA, 1 ng mL^{-1} TGFβ3 and 0.5 mM db-cAMP, a media containing neurotrophins commonly used to mature mbDA neurons (Chambers et al., 2009; Kriks et al., 2011).

4.2.2 Engineering of the human LMX1A-AMP-IRES-EGFP reporter cell line

A h*LMX1A*-AMP-IRES-EGFP-FneoF vector was constructed for homologous recombination by Janet Rientjes (see Fig. 2.1A). Following dissociation with accutase and two consecutive washes with hESC media (see Section 2.2.3, 200g, 5 min), hESCs were plated on 0.1 % (vol/vol) gelatin coated dishes in hESC media containing ROCK inhibitor (10μM; Y-27632; (1R,4r)-4-((R)-1-aminoethyl)-N-(pyridin-4-yl)cyclohexanecarboxamide; Cellagen Technology, CA, U.S.A)(Watanabe et al., 2007) at 37°C in a humidified 5% CO_2-in-air atmosphere. Following 30 min incubation the non-adherent hESCs were collected, centrifuged (200g, 5 min), resuspended (7.5 x 10^6 cells) in 800 μL of 0.22 μm filtered ice cold PBS and transferred to a 0.4 cm electroporation cuvette (BioRad). Forty micrograms of linearized hLMX1A-AMP-IRES-EGFP-FneoF vector was added and the cell/DNA mixture incubated on ice for 5 min. The vector was then introduced into h9 hESCs by electroporation with a GenePulser XCell™ instrument (250V 500μF, BioRad). Following electroporation cells were transferred to prewarmed hESC

media, centrifuged (200*g*, 5 min), resuspended in hESC media containing 10μM Y-27632 and plated onto three 100 mm dishes preplated with MEFs-NeoR (40 x 10^5 cells cm^2). Fresh hESC media was added daily with 10μM Y-27632 added for the first two days post plating. On day 4, 50 μg mL^{-1} G418 (Life Technologies) was added to begin antibiotic selection. Fourteen to seventeen days following selection colonies approximately 2 mm in diameter were dissected into 0.5mm^2 fragments. One third of the dissected colony was transferred to a 48 well plate pre plated with MEFs (40 x 10^5 cells cm^{-2}) and the other two thirds to a 96 well pre coated with Matrigel® containing MEF-CM. This was repeated for a 150 individual colonies. Following 5-7 days of growth the 96 well plate was used for DNA preparation. Neomycin-positive colonies were first screened for correct targeting by PCR and subsequently confirmed by southern blot analysis (Stewart Fabb, see Appendix IV). Colonies that contained correct insertion of the transgene (confirmed via PCR and southern blot) were then expanded from the 48 well plate and sub-cloned as follows: cultures were digested with accutase to render colonies single cells, treated as above (gelatin replating feeder removal step including ROCK inhibition) and replated at low density (6 x 10^4 cells per 60mm dish). Fourteen to seventeen days later colonies approximately 2 mm in diameter were dissected into 0.5mm^2 fragments. One third of the dissected colony was transferred to a 48 well plate pre plated with MEFs (40 x 10^5 cells cm^{-2}) and the other two thirds to a 96 well pre coated with Matrigel® containing MEF-CM. This was repeated for 6 individual clones. Following 5-7 days of growth the 96 well plate was used for DNA preparation rescreened via PCR expanded and frozen if positive.

4.2.3 Fluorescence-activated cell sorting and analysis

Cell samples were prepared by first manually dissecting the hESCs colonies from the PA6 stromal layer, prior to digestion, to limit contamination by PA6 cells. All subsequent procedures were performed as detailed in Section 2.6.2.

4.3 Results

4.3.1. The small molecule BMP receptor inhibitor, LDN193189 is a Noggin mimetic

Unlike mESC differentiation PA6 directed neural induction is not as robust for hESCs (Chambers et al., 2009). Noggin together with SB431542 (NSB) is typically used to augment PA6 neural induction of hESCs (Sonntag et al., 2007; Denham et al., 2010).. However noggin, being a recombinant protein has a number of issues associated with its use in large-scale cell culture (see Section 4.4.1). Thus a small molecule BMP receptor inhibitor, LDN193189 (LDN) was assayed for its neural induction properties. Under vehicle conditions, 35.8 % ± 2.6 and 22.7 % ± 6.1 of all cells were positive for the neuroepithelial markers NESTIN and PAX6, respectively (Fig 4.1A, B and J). While 16.8% ± 3.9 of cells were positive for the pluripotency marker OCT4 (Fig 4.1C and J). NSB significantly altered the fate of differentiating cells, observed by a decrease in OCT4 (2.7 % ± 0.6)(Dunnett's test, n=4, $p < 0.01$) and an increase in NESTIN (71.5 % ± 2.9)(Dunnett's test, n=5, $p < 0.001$) and PAX6 (60.5 % ± 9.3)(Dunnett's test, n=7, $p < 0.001$) labeling (Fig 4.1D, E, F and J). Addition of LDN at concentrations above 100 nM also increased the presence of NESTIN (69.0 % ± 2.8)(Dunnett's test, n=5, $p < 0.001$) and PAX6 (58.9 % ± 11.0)(Dunnett's test, n=7, $p < 0.01$) positive cells (Fig 4.1 G, H and I) while concomitantly decreasing the presence OCT4 labeled cells (3.6 % ± 0.8, Fig 4.1I and J)(Dunnett's test, n=4, $p < 0.01$).

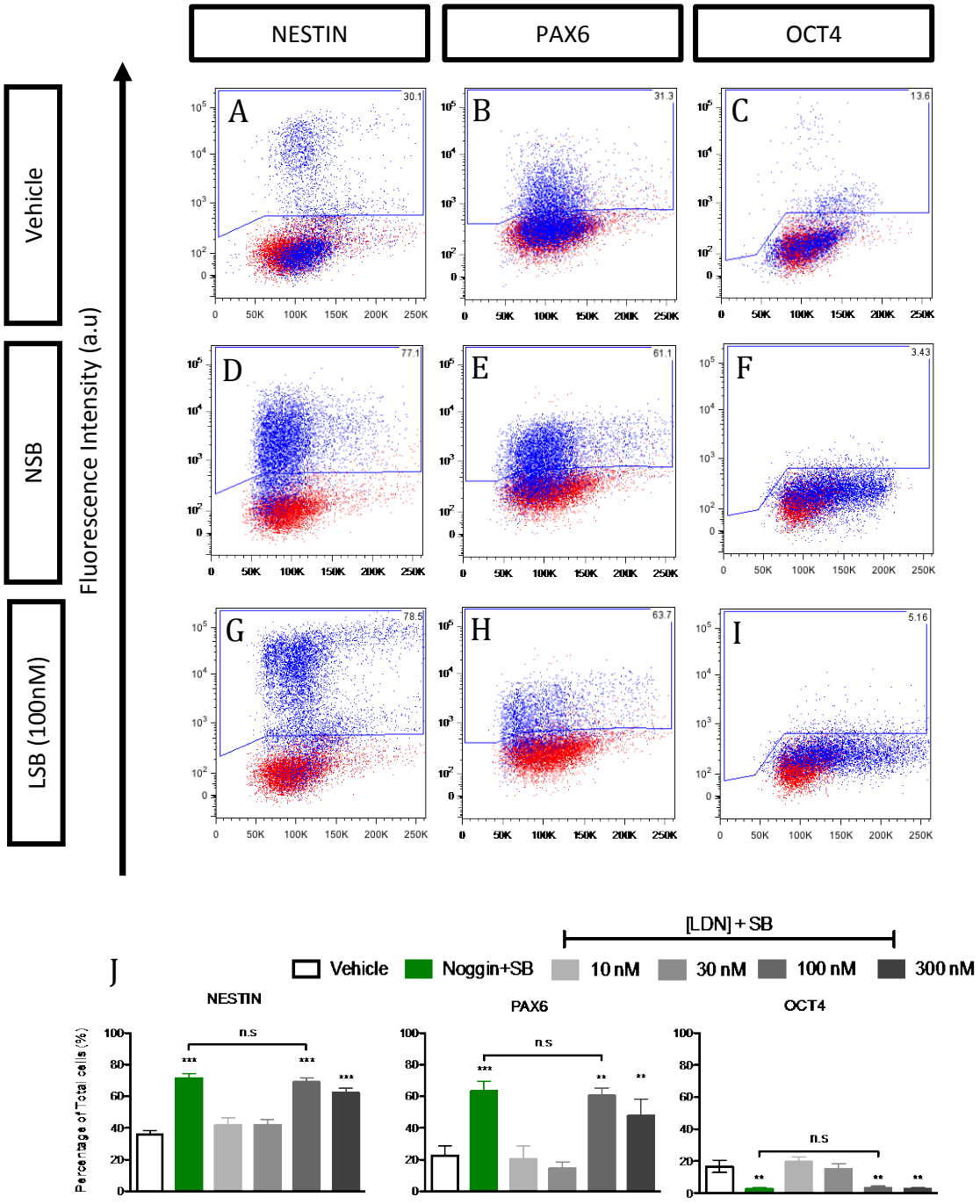

Figure 4.1: Intracellular FACS analysis of hESCs on PA6 stromal cells under inhibition of BMP (Noggin or various concentrations of LDN193189) and activin/nodal (SB431542) signals. FACS analysis of cells expressing NESTIN (**A, D & G**), PAX6 (**B, E &H**) and OCT4 (**C, F & I**), when treated with either vehicle (**A-C**), NSB (**D-F**) or LSB 100 nM (**G-I**). Controls are shown in red. Antibody of interest is shown in blue. (**J**) Quantification of intracellular flow cytometry analysis. The percentage of cells positive for NESTIN, PAX6 and OCT4 are shown for vehicle (white bar), Noggin + SB431542 (NSB) (green bar) and LDN193189 + SB431542 (LSB) concentrations (scales of grey). Data are presented as mean ± S.E.M of 3-7 experiments. Bonferonni's Multiple comparisons test was used to determine levels of significance. Asterisks indicate statistical significance in comparison to vehicle (**, $p < .01$; ***, $p < .001$ and n.s., non-significant NSB in comparison to LSB 100 nM).

4.3.2 Differentiation of hESCs using a PA6 co-culture protocol results in mixed precursor phenotypes

Following neural induction in the presence of 100 nM LDN and SB (herein referred to as LSB) d15 progenitor cultures were assessed for regional marker expression. Very few CORIN immunoreactive cells were detected (1.6 % ± 0.3; Fig. 4.2A,D and G). In contrast, robust expression of OTX2 and FORSE1 was observed (71.3 % ± 3.8) and (39.4 % ± 3.5) of cells respectively (Fig. 4.2B, C, E and G).

Since OTX2 expression is restricted to the fore and midbrain, the observation that FORSE-1 positive forebrain cells only made up ~40% of OTX2 positive cells suggested the presence of one or more other cell type(s). This prompted me to further examine the phenotypes present in PA6-derived LSB treated cells. When assessed for dorsoventral markers progenitor cultures demonstrated strong PAX7 (54.9 % ± 6.4, Fig 4.3A and J) and very little detectable NKX6.1 (0.7% ± 0.4, Fig 4.3B and J) or FOXA2 (3.3% ± 1.0 Fig. 4.3C and J) expression. These data indicate that hESC cultures differentiating under PA6/LSB conditions contain a mix of rostral and dorsal midbrain cell types.

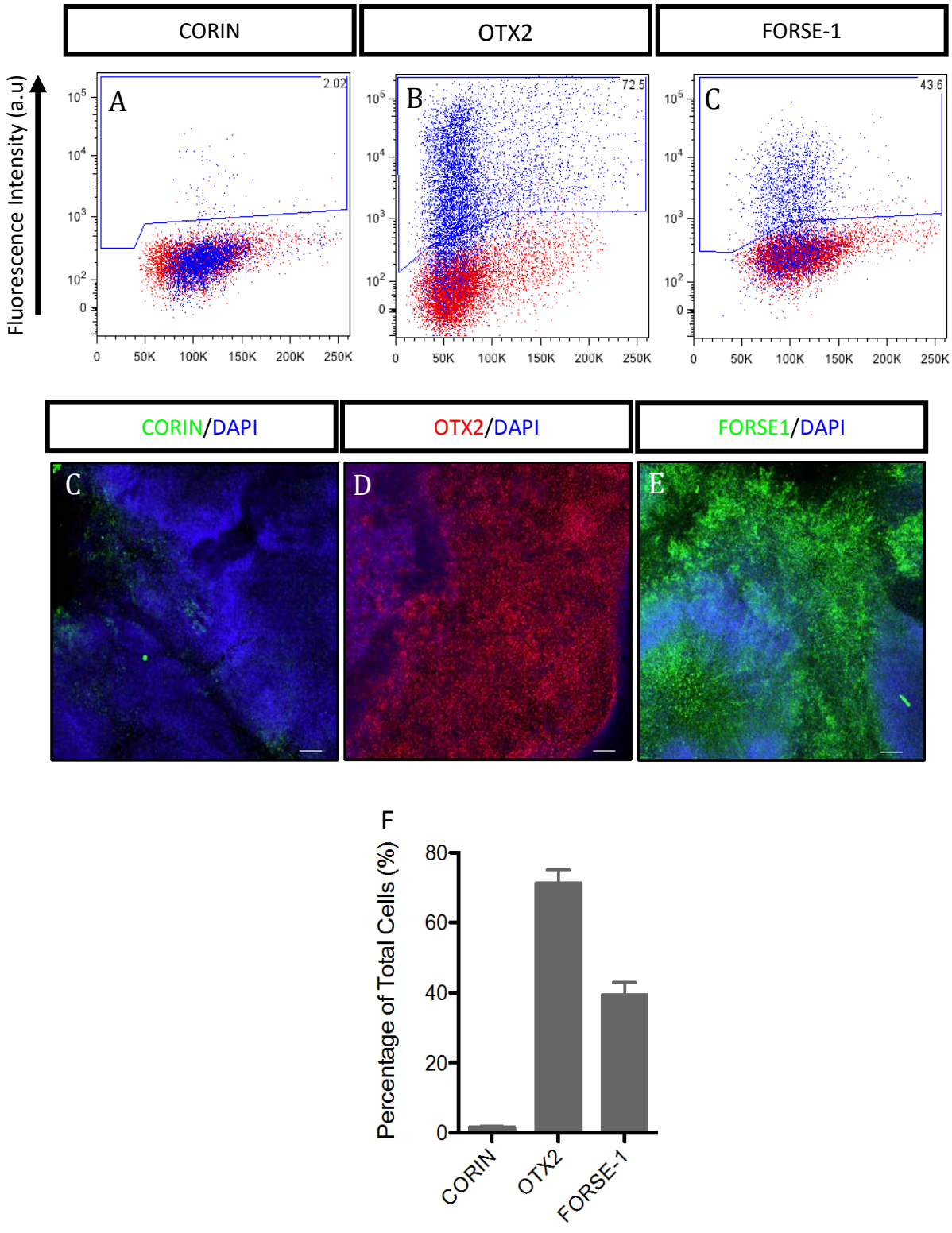

Figure 4.2: Rostrocaudal phenotype analysis of hESCs differentiating under PA6/LSB conditions. Flow cytometry analysis of cells positive for CORIN (**A**), OTX2 (**B**), FORSE-1 (**C**). Controls are shown in red. Antibody of interest is shown in blue. Representative immunofluorescence images of CORIN (**D**), OTX2 (**E**), FORSE1 (**F**) antibody labeling. (**G**) Quantification FACS data. Data are presented as mean ± S.E.M of 3-6 experiments. Scale bars, 50 µm (D-F).

4.3.3 Recombinant SHH-N does not induce a ventral phenotype in PA6/LSB culture conditions

Recombinant N-terminal SHH (SHH-N) has been used in numerous differentiation protocols of mESCs and hESCs to specify a ventral phenotype. SHH-N was assessed for its ability to induce a ventral phenotype under PA6/LSB conditions. In my hands, the addition of SHH-N at a 200 ng mL^{-1} did not significantly alter the number of cells positive for PAX7 (37.6% ± 7.6; Fig. 4.3D and J), NKX6.1 (2.4 % ± 0.8 % Fig. 4.4E and J) or FOXA2 (1.9 % ± 0.4 %; Fig 4.3F and J)(Dunnett's test, n=7, $p > 0.05$). When a concentration-response of SHH-N up to 1000 ng mL^{-1} was conducted, significant decreases were observed in PAX7 expression above 600 ng mL^{-1} (Dunnett's test, n=7, $p < 0.05$), however NKX6.1 or FOXA2 expression were not significantly altered at any concentration (Fig. 4.3J)(Dunnett's test, n=7, $p > 0.05$). Conversely, when the SHH-receptor antagonist, cyclopamine was administered FOXA2 expressing cells were significantly decreased (0.3 % ± 0.1 %, Fig. 4.3J).

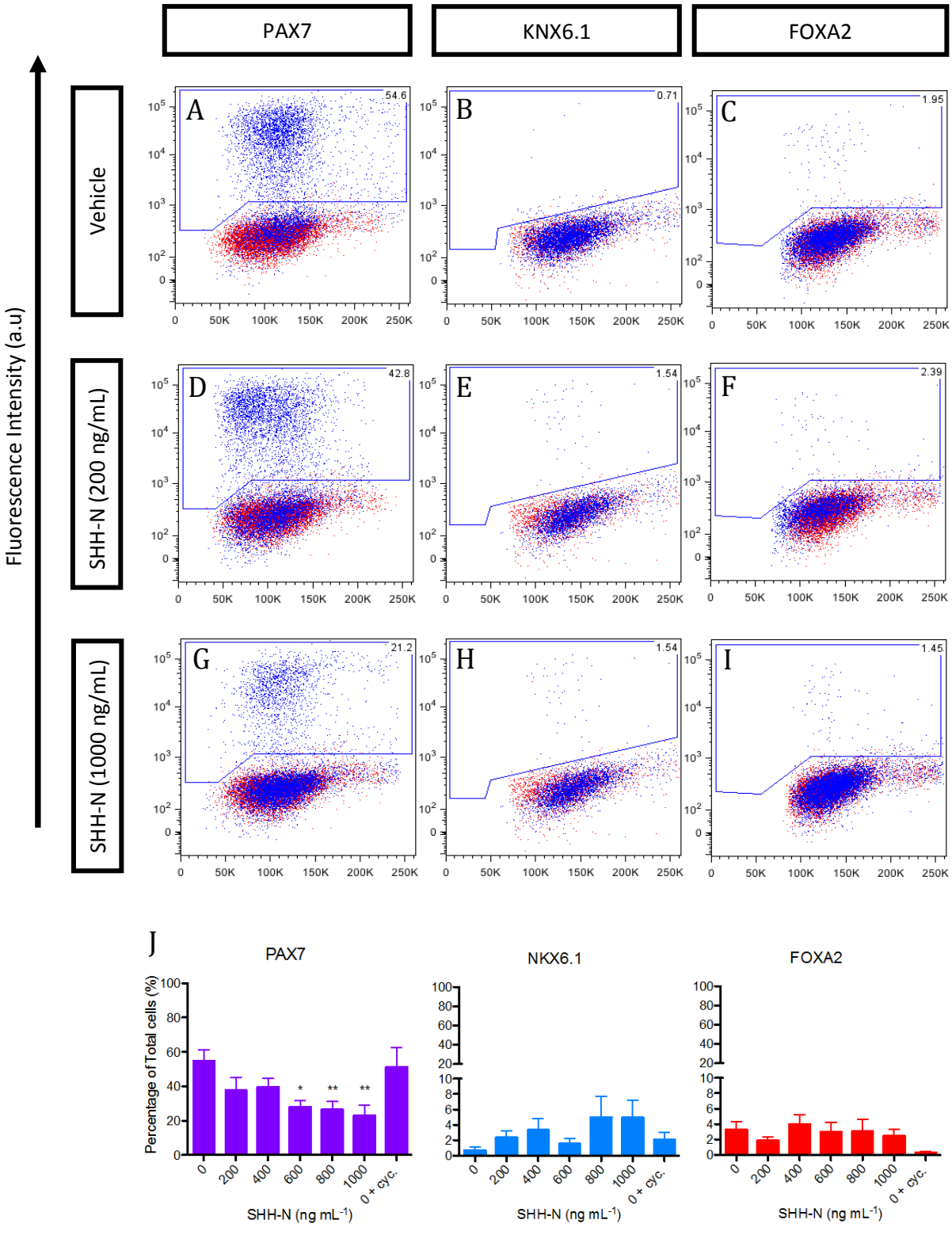

Figure 4.3: Dorsoventral phenotype analysis of hESCs differentiating under PA6/LSB conditions in response to differing concentrations of SHH-N. Flow cytometry analysis of cells positive for PAX7 (**A, D & G**), NKX6.1 (**B, E & H**) and FOXA2 (**C, F & I**). Controls are shown in red. Antibody of interest staining is shown blue. (**J**) Quantification FACS data. Data are presented as mean ± S.E.M of 7-9 experiments. Bonferonni's Multiple comparisons test was used to determine levels of significance. Asterisks indicate statistical significance in comparison to vehicle (*, $p < .05$ and ** $p < .0.01$)

4.3.4 The small molecule smoothened agonist, SAG is able to ventralise cells differentiating under PA6/LSB conditions

The lack of SHH-N potency provided impetus to search for a small molecule SHH signalling alternative. Numerous small molecule agonists of the SHH receptor, Smoothened, have been reported. One of these molecules, smoothened agonist (SAG), was assayed for its ability to induce FOXA2+ cells under PA6/LSB conditions. SAG was added to from days 2 to 12 at various concentrations to determine a dose response of *FOXA2*, *NKX6.1* and *CORIN* expression. The recently modified version of SHH, SHH-C25II (see section 4.2.1.) was added as a positive control. At low SAG concentrations no increases in either *FOXA2* or *CORIN* transcript were detected, increases in *NKX6.1* were observed however (Fig. 4.4F). Addition of SAG at 300 nM and 1000 nM significantly increased the number of FOXA2 positive cells to (49.8% ± 4.3, Fig 4.4C and E, Dunnett's test, n=6, $p < 0.001$) and (49.9 % ± 3.1 SEM, Fig 4.4E, Dunnett's test, n=6, $p < 0.001$) respectively. The increase in FOXA2 protein positive cells was also verified at the level of FOXA2 mRNA (Fig 4.4F). CORIN transcript levels also significantly increased following addition of SAG above 300 nM (Fig 4.4F)(Dunnett's test, n=5, $p < 0.05$).

LMX1A

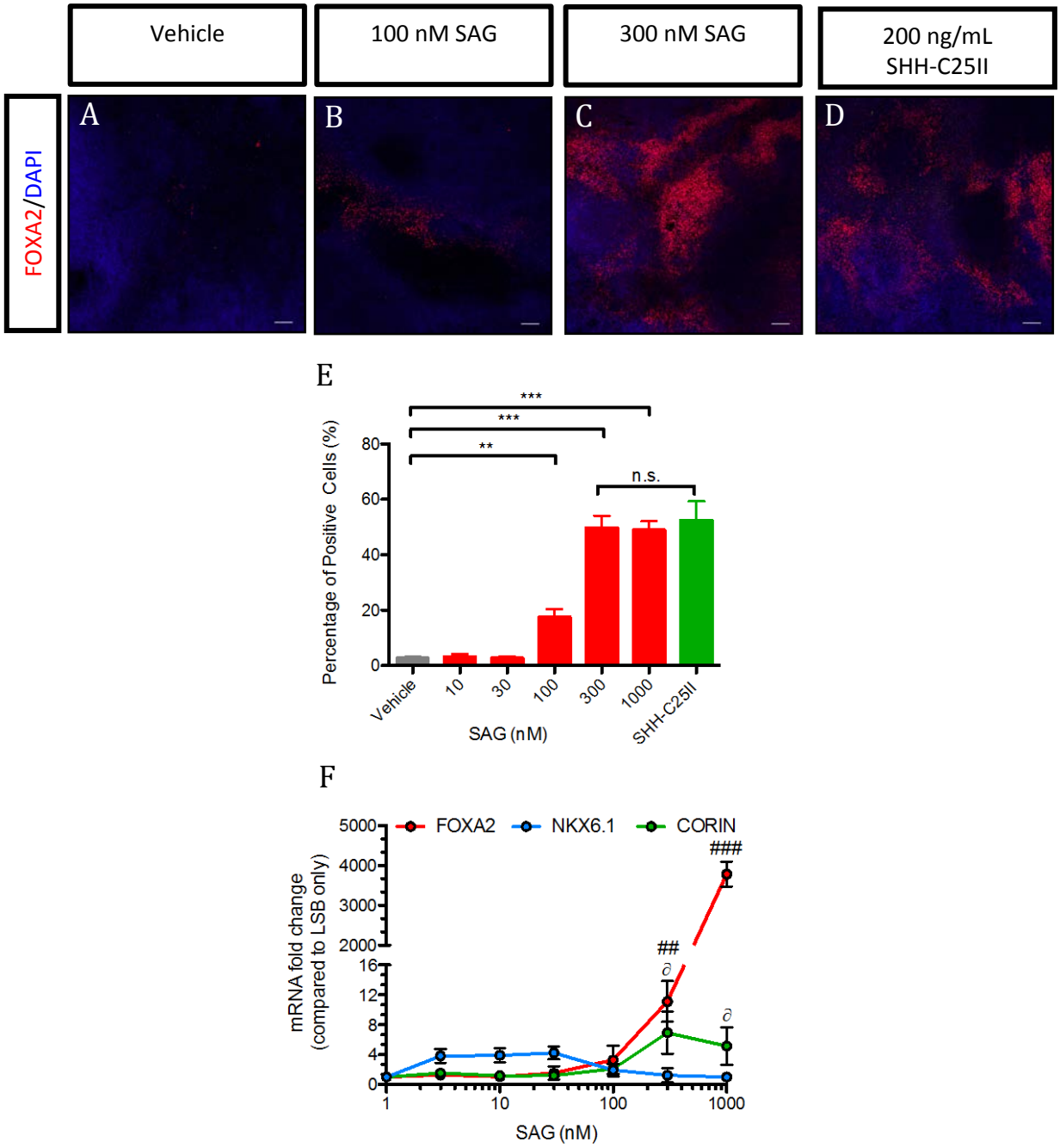

Figure 4.4. Smoothened agonist (SAG) can mimic SHH-C25II activity in PA6/LSB cultures. (**A-D**) Immunofluorescence micrographs of cultures labeled with FOXA2 (red) following treatment with various concentrations of SAG. (**A**) No SAG, (**B**) 100 nM SAG, (**C**) 300nM SAG and (**D**) 200 ng mL^{-1} SHH-C25II. Counterstained with DAPI. Scale bar, 50 µm. (**E**) Concentration response of FOXA2 protein positive cells in response to various concentrations of SAG determined via intracellular FACS analysis, grey bar (Vehicle), red bars (various SAG concentrations), green bar (200 ng mL^{-1} SHH-C25II). (**F**) qPCR dose response examining the induction of the *FOXA2*, *CORIN* and *NKX6.1*. Data is presented as the mean ± S.E.M of 3-6 experiments. Dunnett's test was used to determine levels of significance following one-way ANOVA. Statistical significance (**, $p < .01$; ***, $p < .001$, compared to vehicle and n.s., non-significant, 300 nM SAG vs SHH-C25II for E), (∂, $p < 0.05$, compared to 0 nM SAG for CORIN - F)(##, $p < .01$ and ### $p < .001$ compared to 0 nM SAG for FOXA2 - F).

4.3.5 SAG treatment induces a midbrain phenotype in cultures under PA6/LSB conditions

Although the activation of SHH signalling induces FP cells in the PA6/LSB system, the question of whether these cultures generate mbDA precursors remained unknown. To test this, cultures were treated with 300 nM SAG and assayed for mbDA marker expression. At day 15, the number of cells positive for the FP marker, FOXA2 significantly increased in response to 300 nM SAG (Fig 4.5A & B)(Dunnett's test, n=8, $p < 0.001$). The number of immunoreactive cells for anti-LMX-1 (the only commercially available antibody that exhibits LMX1A immuno reactivity - Personal communication A. Kirkeby) did not differ between cultures incubated with (0.9% ± 0.3) or with out 300 nM SAG (3.2 % ± 1.2)(Fig 4.5A and B). The number of double positive FOXA2/LMX-1 cells differed significantly when 300 nM SAG was administered, 1.4% ± 0.2 vs. 11.3 % ± 2.0 SEM (Fig 4.5A and B)(Dunnett's test, n=8, $p < 0.05$). However as anti-LMX-1 recognises both LMX1A and LMX1B, qPCR data was used to confirm induction of *LMX1A* following SAG addition (Fig 4.5E).

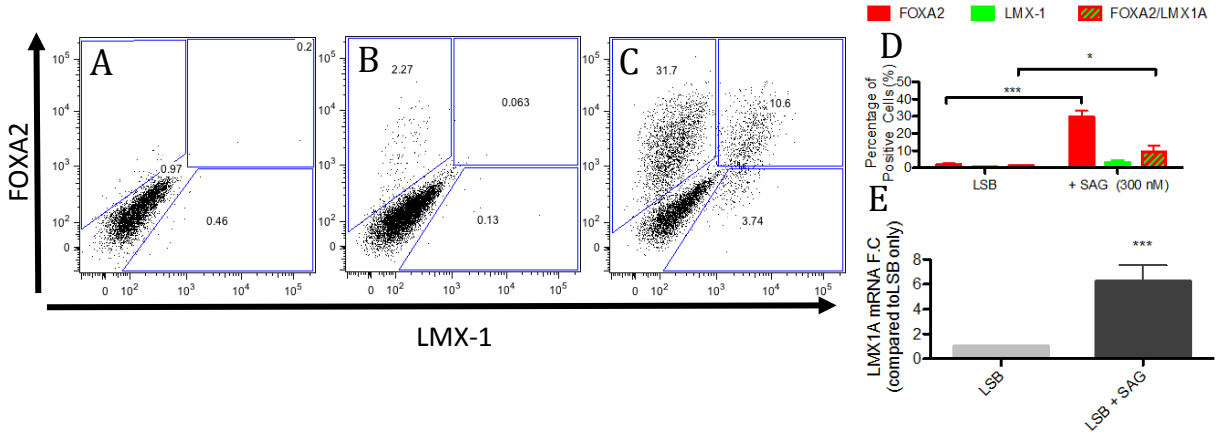

Figure 4.5 SAG treatment can alter the rostrocaudal phenotype of hESCs differentiating under PA6/LSB conditions. FACS analysis of FOXA2 and LMX-1 positive cells when treated with either (**A**) Vehicle or (**B**) LSB or (**C**) LSB + SAG 300nM. (**D**) Quantification of FACS analysis, red bars (FOXA2), green bars (LMX-1), red and green striped bars (FOXA2/LMX-1 double positive cells). (**E**) qPCR comparing *LMX1A* transcript levels before (light grey) and after (dark grey) 300 nM SAG addition. Data is represent at the mean ± S.E.M of 8 (D) and 5 (E) experiments. Asterisks indicate statistical significance in comparison to LSB only (*, $p < .01$, ***, $p < .001$), (D) one-way ANOVA with post-hoc Dunnett's test and (E) Student's t-test.

4.3.6 Caudalisation of cultures under PA6/LSB/SAG conditions

Two reported caudalising agents, FGF8b and WNT1, were tested for their ability to induce FP (*FOXA2* and *NTN1*), mbFP (*CORIN*), mbDA progenitor (*LMX1A*, *EN1* and *NGN2*), or retard rostral (*FOXG1*) makers under PA6/LSB/SAG conditions at different time points.

FGF8b did not alter the expression of FP genes, *FOXA2* and *NTN1* (Fig 4.6A). CORIN transcript was significantly increased following addition of FGF8b at day 4 (Fig 4.6A)(Bonferroni's test, $p < 0.05$, n=4). Increases in the expression of *EN1* and *LMX1A* were observed following FGF8b addition at d2 (Fig 4.6A)(Bonferroni's test, $p < 0.001$, n=4). Decrease in *FOXG1* transcript abundance was observed following d4 FGF8b addition (Fig 4.6A)(Bonferroni's test, $p < 0.01$, n=4).

WNT1 at d2, d4 or d6 did not alter the expression of either of *FOXA2*, *NTN1*, *CORIN*, *LMX1A*, *EN1*, *NGN2* or *FOXG1* (Fig 4.6B). These findings suggest that in the presence of SAG, PA6/LSB treated cultures represent a heterogeneous mixture of cells with a FP, mbFP, mbDA progenitor and rostral phenotype. The addition of FGF8b can alter the rostrocaudal phenotype of the cultures, but does not result in a significant increase in expression of all mbDA progenitor related genes.

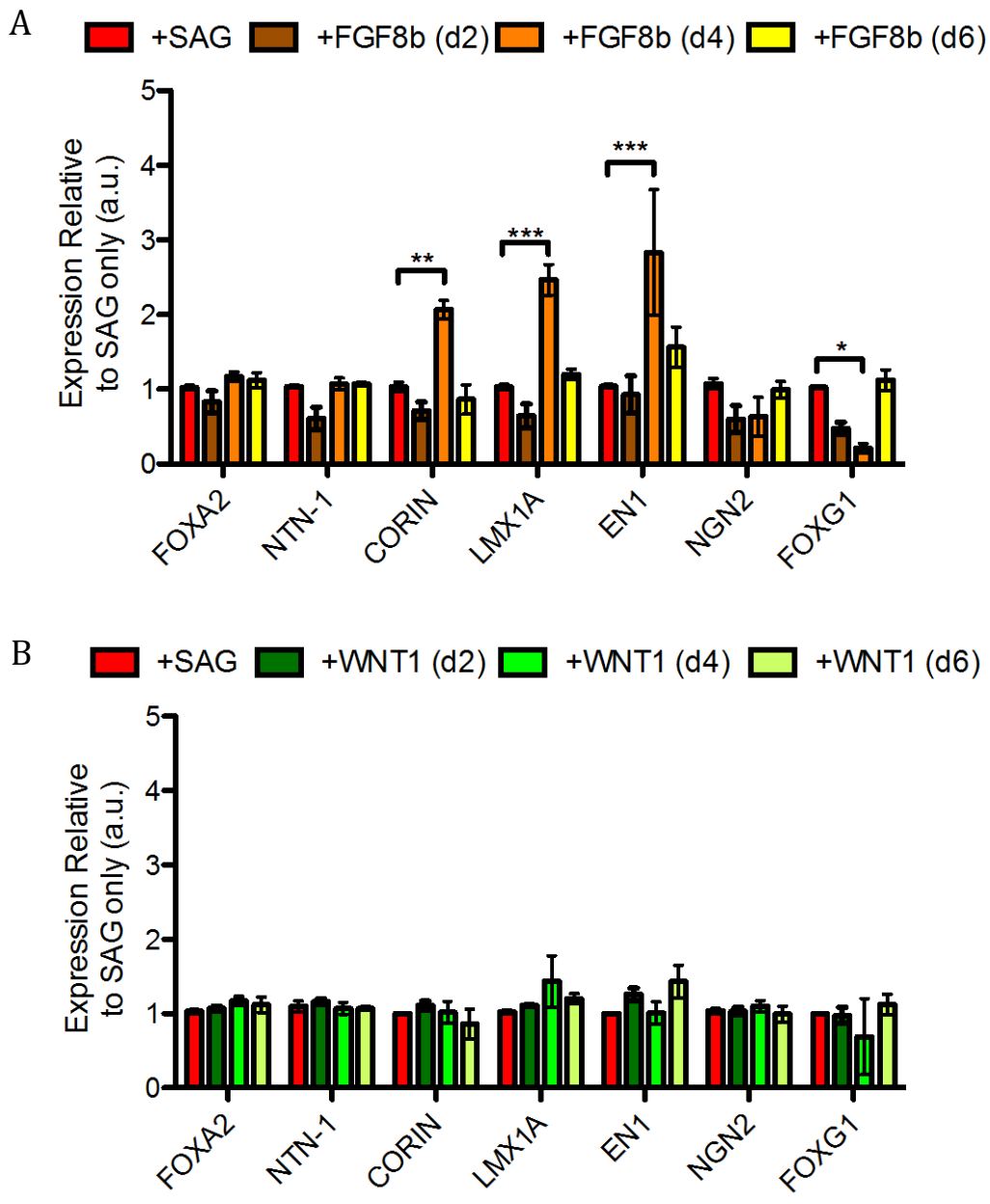

Figure 4.6. The rostrocaudal phenotype of hESCs differentiating under PA6/LSB/SAG conditions can be altered by caudalising factors. qPCR analysis consisting of a panel probes for FP, mb, mbFP, mbDA and rostral genes in response to (**A**) FGF8b (red bars represent SAG only addition, dark orange bars represent GF addition at d2, light orange bars at day 4 and yellow at day 6) or (**B**) WNT (red bars represent SAG only addition, dark green bars represent WNT addition at d2, light green bars at day 4 and lime green at day). Data are presented as mean ± S.E.M. of 4 (FGF8b) and 6 (WNT1) experiments. Asterisks indicate statistical significance in comparison to SHH only (*, $p < .05$; **, $p < .01$; and ***, $p < .001$), two-way ANOVA with post-hoc Bonferroni's test.

4.3.7 Targeting EGFP to the *LMX1A* locus of human embryonic stem cells.

Five *Neo* positive hLMX1A-AMP-IRES-EGFP targeted colonies were correctly targeted to exon 1 of *LMX1A*. Three correctly targeted clones were sub-cloned. All sub-clones were positive and maintained expression of pluripotency markers and proper growth characteristics. Subclone #1.4 was chosen for further experimentation.

4.3.8 Generation and characterisation of the hLMX1A-AIG reporter cell line

Similar to the mouse Lmx1a-AIG reporter system, the first exon was replaced with the coding sequence for the AMP and EGFP genes separated by an IRES sequence to ensure high fidelity reporting of *LMX1A* transcription (see Section 4.2.2 and 4.3.1). In order to be confident that EGFP expression was indicative of endogenous LMX1A expression the colocalisation of EGFP together with LMX-1 immunoreactivity was determined by immunofluorescence. EGFP co-localised with LMX-1 positive cells (Fig 4.7A). Some cells were found to be EGFP-/LMX-1+, as well as EGFP+/LMX-1-. However, as indicated above, the LMX antibody recognises both LMX1A and LMX1B protein. Thus qPCR was used confirm FACS data. *LMX1A* transcript was found to be upregulated 32 fold following qPCR analysis of FACs isolated EGFP+ cells (compared with EGFP- cells)(Fig. 4.11). EGFP colocalisation was carried out in conjunction with FOXA2 and NESTIN labeling to ensure EGFP+ were of FP origin. EGFP positive cells co-labeled with both FOXA2 (Fig 4.7B) and NESTIN (Fig 4.7C).

The ability of the targeted h*LMX1A*-AIG reporter cell line to differentiate into NESTIN+/PAX6+ neural precursors (Fig. 4.7D) and TUJ1+ neurons (Fig. 4.7E, F, G, H and I) was not affected. In addition, no differences were observed in the specification of either a GABAergic or DAergic neurotransmitter phenotype (Figure 4.7 D, E, F G, H and I).

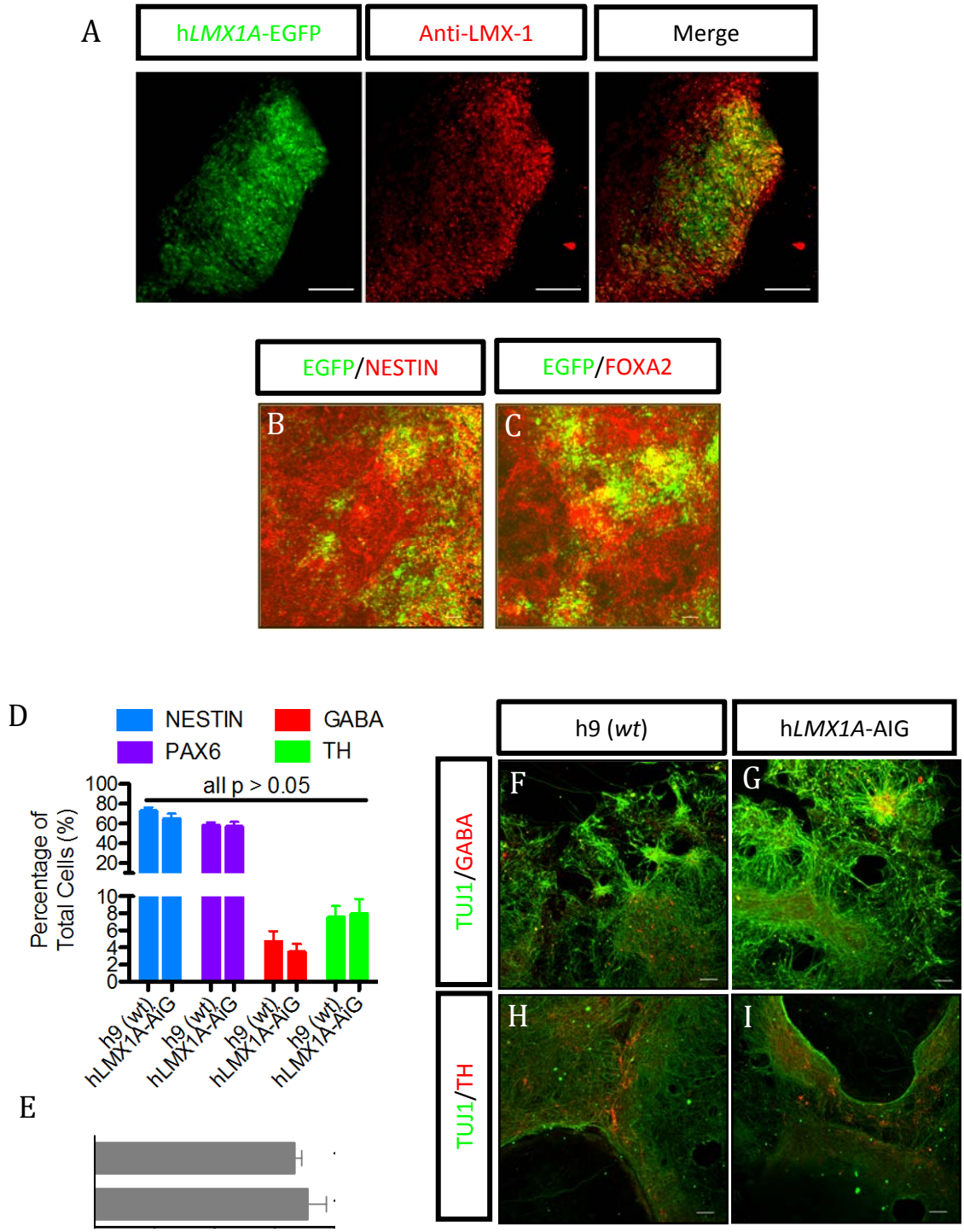

Figure 4.7 Characterisation of the h*LMX1A*-AIG reporter cell line. Immunofluorescent images demonstrating EGFP co-localisation with (**A**) LMX-1, (**B**) NESTIN & (**C**) FOXA2. (**D**) Percentage of cells positive for NESTIN (blue), PAX6 (purple), GABA (red) and TH (green) for both h9 (*wt*) and h*LMX1A*-AIG. (**E**) TUJ1 fluorescence intensity for h9 (*wt*) and h*LMX1A*-AIG. Immunofluorescent images of d40 cultures for (**F & G**) TUJ1 (green) and GABA (red) and (**H & I**) TUJ1 (green) and TH (red). Scale bars, (A) µM and (B, C, E-H) 50 µM. Data is presented as the mean ± S.E.M of 4-7 (D), and 3 (E) experiments. Student's t-test compared to h9 (*wt*).

4.3.9 *LMX1A*-promoter driven EGFP expression in caudalised cultures

The combination of LSB, SAG and FGF8 treatment in the PA6 co-culture system in my hands generates mbDA precursors, albeit in relatively low abundance. Thus I hypothesised that the isolation of mbDA precursors using a hLMX1A-AIG reporter cell line via FACS may allow enrichment of mbDA neurons in terminally differentiated cultures as observed with mESCs in Chapter 3. Thus *LMX1A*-promoter driven EGFP expression was ascertained via flow cytometry to understand the kinetics of *LMX1A* expression during differentiation. No EGFP expression was detected at days 0 and 5 (Fig 4.8A & D). At day 10, 3.9 % ± 0.8 of total live cells began to express EGFP (Fig 4.8D), with an increase to 6.1 % ± 1.5 at day 15 (Fig 4.8B & D). Enhanced GFP expression was detected in 10.3 % ± 1.5 and 14.7 % ± 2.1 of total cells at days 20 and 25 respectively (Fig 4.8C & D). At day 30 EGFP expression peak at 16.7 % ± 2.1 of total cells (Fig 4.8D). Expression then decreased to 16.7 % ± 2.1 and 13.5 % ± 2.9 on days 30 and 40 respectively (Fig 4.8D).

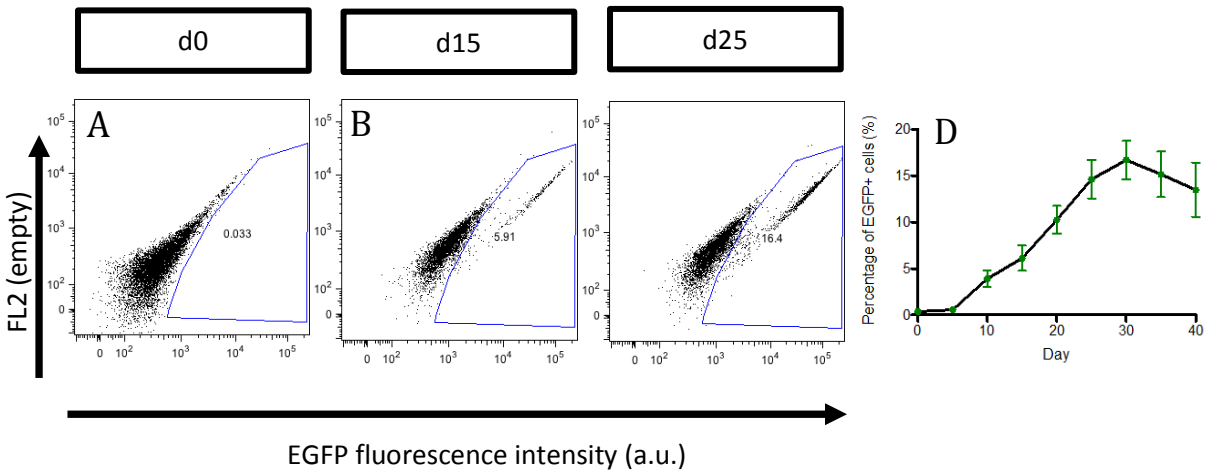

Figure 4.8 *LMX1A*-promoter driven EGFP expression during differentiation of hESCs under PA6/LSB/SHH/FGF8 conditions for d0 (**A**), d15 (**B**) and d25 (**C**) of differentiation. **(D)** Time course of EGFP expression from day 0-40. Data are presented as the mean ± S.E.M of 4 experiments.

4.3.10 Proliferation of h*LMX1A*-EGFP+ progenitors

To determine whether cells expressing EGFP represent a mitotic progenitor population, differentiating cultures were subjected to KI67/EGFP FACS analysis at various time points. The number of KI67/EGFP double positive cells gradually increased during differentiation peaking at day 25, where 11.6 % ± 1.2 of total cells co-expressed EGFP and KI67 (Fig. 4.9B and D). Very few EGFP+/KI67- cells were observed at this time point (Fig. 4.9B and D). There was a decrease in the number of KI67+/EGFP+ cells up until d45 of differentiation, where only 6.4 % ± 1.0 of total cells were detected as KI67 positive proliferative EGFP+ cells (Fig. 4.9C and D).

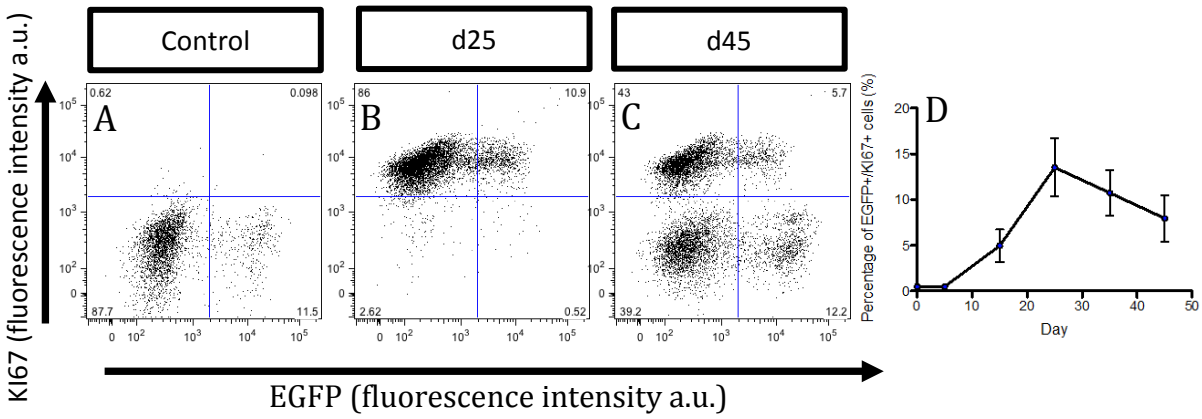

Figure 4.9 Mitotic analysis of EGFP+ cells during differentiation. FACS plots for antibody controls (**A**), d25 (**B**) and d45 (**C**) of differentiation. **(D)** Time course of KI67/EGFP positive cells from day 0-45. Data are presented as the mean ± S.E.M from 6 experiments.

4.3.11 Enrichment of mbDA precursors using a h*LMX1A*-AIG reporter cell line

Therefore it was hypothesised that day 25 would be the most ideal time to isolate EGFP positive cells as they are most numerous in proliferative state. To study EGFP+ cells in more detail and to investigate their potential to give rise to high yields of mbDA neurons EGFP positive and negative cells were isolated at day 25 via FACS (Fig 4.10).

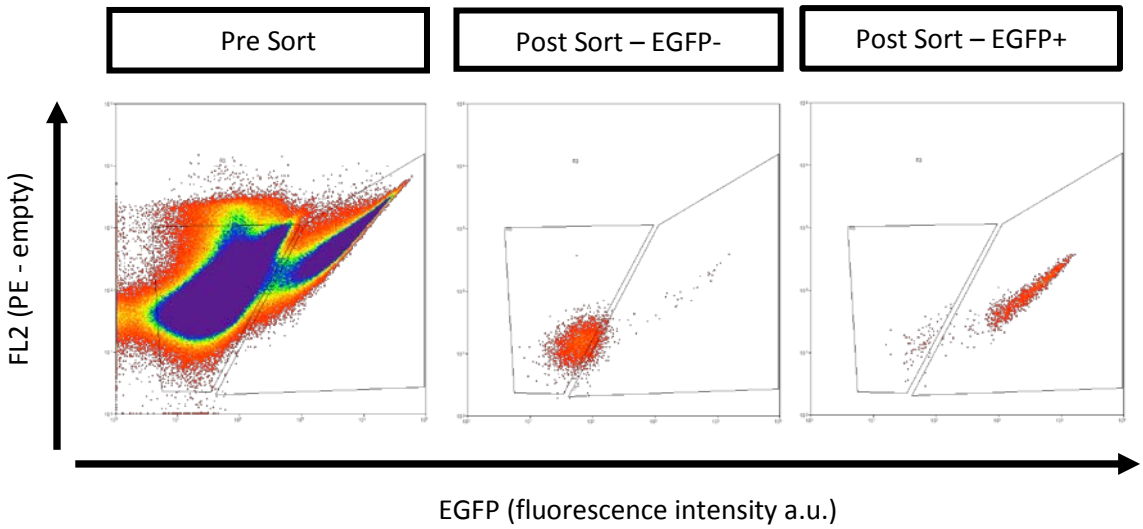

Figure 4.10 Gating Strategy for FACS. (**A**) Typical FACS dot blot demonstrating EGFP negative (left polygon) and positive gates (right polygon). Re-analysis of EGFP (**B**) negative and (**C**) positive collected fractions following sorting.

Quantitative PCR analysis of the EGFP positive and negative fractions (Fig 4.10) revealed that transcript levels of *LMX1A* were over 32 fold higher in the positive fraction when compared to the negative fraction (Fig 4.11). When analysed for downstream targets of *LMX1A*, the positive fraction demonstrated significant enrichment for transcripts of *MSX1*, *LMX1B*, and *NGN2* (Fig 4.11). The FP marker *FOXA2* was also highly enriched in the EGFP+ fraction. The EGFP negative fraction demonstrated a slight up-regulation of the rostral markers *FOXG1* and *LHX2* and the roofplate marker *GDF7* (Fig

4.11). Markers for mature mdDA neurons, *NR4A2*, *PITX3* and *TH* were present in the positive fraction (Fig 4.11), albeit at relatively low amounts. Together, these data demonstrate that EGFP+ cells isolated from colonies differentiating under PA6/LSB/SAG conditions represent mbDA progenitors.

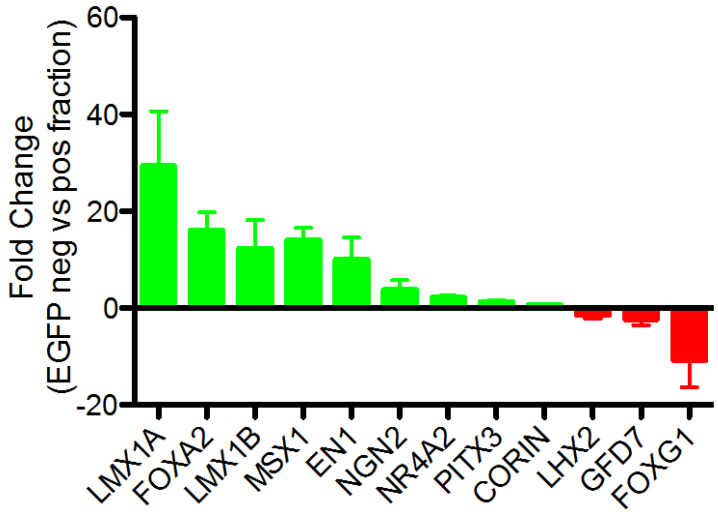

Figure 4.11 qPCR fold differences for a panel of genes representing mb, mbDA progenitor and neuron**,** forebrain and cerebellum markers. Green bars represent upregulation in the EGFP positive cells. Red bars represent upregulation in EGFP negative cells. Data are presented as the mean ± S.E.M of 4 individual sort experiments.

4.3.12 Optimisation of post sort conditions

As EGFP+ cells exhibited a transcriptional profile indicative of mbDA progenitors they were isolated via FACS and replated for *in vitro* maturation. Cells were initially seeded at a low density (0.3 x 10^5 cells cm^{-2}) to try and achieve a homogenous monolayer of neural precursors, however considerable cell death was observed. High cell plating densities (> 3 x 10^5 cells cm^{-2}) aided in cell survival, however variability in survival from well to well still remained. To test the possibility that survival factors released from the unsorted or negative population maybe absent from sorted populations, EGFP positive cells were seeded in conditioned media prepared from unsorted cells (diff-CM). Remarkably, the addition of diff-CM increased the survival of EGP+ cells following sorting (Fig 4.12A).

Using these optimised conditions, replating EGFP+ sorted cells produced homogenous cultures with morphology resembling neural progenitors (Fig 4.12A). This was supported by immunocytochemical FACS analysis showing that 94.7 % ± 2.7 % of cells labeled positive for nestin, while TUJ1+ cells were rarely found, 5.3 % ± 2.7 % (Fig 4.12B).

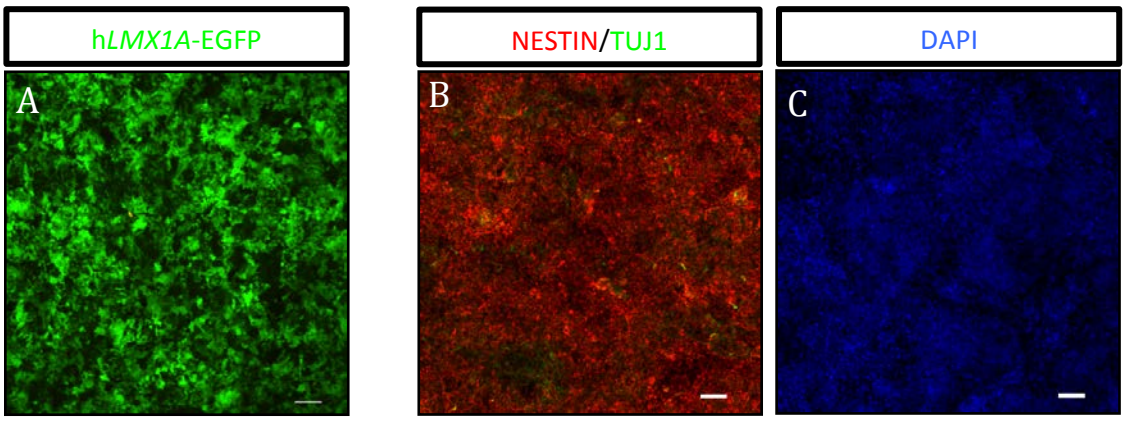

Figure 4.12. Replated EGFP+ cells two days post FACS extraction. (**A**) Live cell imaging. (**B**) NESTIN (red) and TUJ1 (green) labeling and (**C**) DAPI counterstain. Scale Bars (B &C) 50 µm.

4.3.13.EGFP+ cells give rise to mbDA neurons

Following 7-10 days of maturation, isolated cells migrated into large "web-like" structures (Fig 4.13A). Thereafter, over a 14-21 day period, the "web-like" structure would then migrate into cluster-like structures (Fig 4.13 B, C & D and Fig 4.14A). When left in culture, bundles of projection neurons were observed to protrude out of the clusters and form interconnections between others clusters as well project along PLO/LAM/FN coated surface of the well (Fig 4.13C & D). This suggested a global rearrangement of culture morphology, rather than large-scale cell death and was observed across numerous differentiations. These cell clusters were very fragile and difficult to work with, as even the slightest movement such as picking up the plate or changing the media could detach clusters from the surface of the well.

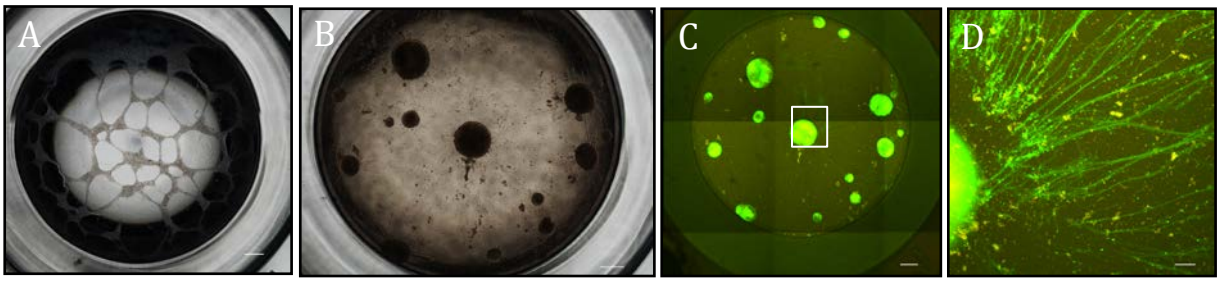

Figure 4.13. Migration of EGFP+ sorted cells. Brightfield of EGFP+ cells (**A**) d32 - 7 days post sort and (**B**) d50 – 25 days post sort. (**C**) Corresponding live cell image of d50 h*LMX1A*-EGFP positive cell clusters. (**D**) Inset of Image C. Scale bars, (**A-C**) 500 µm and (**D**) 100 µm

The fate of the EGFP positive cells was assessed via immunocytochemical analysis 7 days post sorting (d32) before migration. However, this was extremely difficult, as the addition of the fixation agent PFA, caused the "web-like" structure to detach from the coated surface of the well and roll up into a ball. Numerous modifications to fixation conditions were made, such as the concentration of PFA added, fixation time and temperature. The only modification that made a discernable difference was addition of 4% PFA straight to media, so that a final concentration of 2% (1:1 mix of 4% PFA and media, with out washing) was achieved. Nonetheless, cultures would still detach after numerous washes required for the immunocytochemistry, even when completed under a dissecting microscope. Thus immunolabeling was effectively carried out in suspension, using specific placement of the pipette tip to unravel the "web-like" ball structures following each wash.

Using these semi-optimised conditions d32 EGFP+ (7 days post sort) cells were found to express TH but only infrequently (Fig 4.14A, B and C). Most TH cells were found to co-express FOXA2 and EGFP (68.41 ± 17.42, Fig 4.14A,B and C) and OTX2 and EGFP

(72.29 ± 11.63, Fig 4.14D) indicating a mbDA phenotype. Very few cells labeled for GABA (Fig 4.14E) or 5-HT (Fig 4.14F).

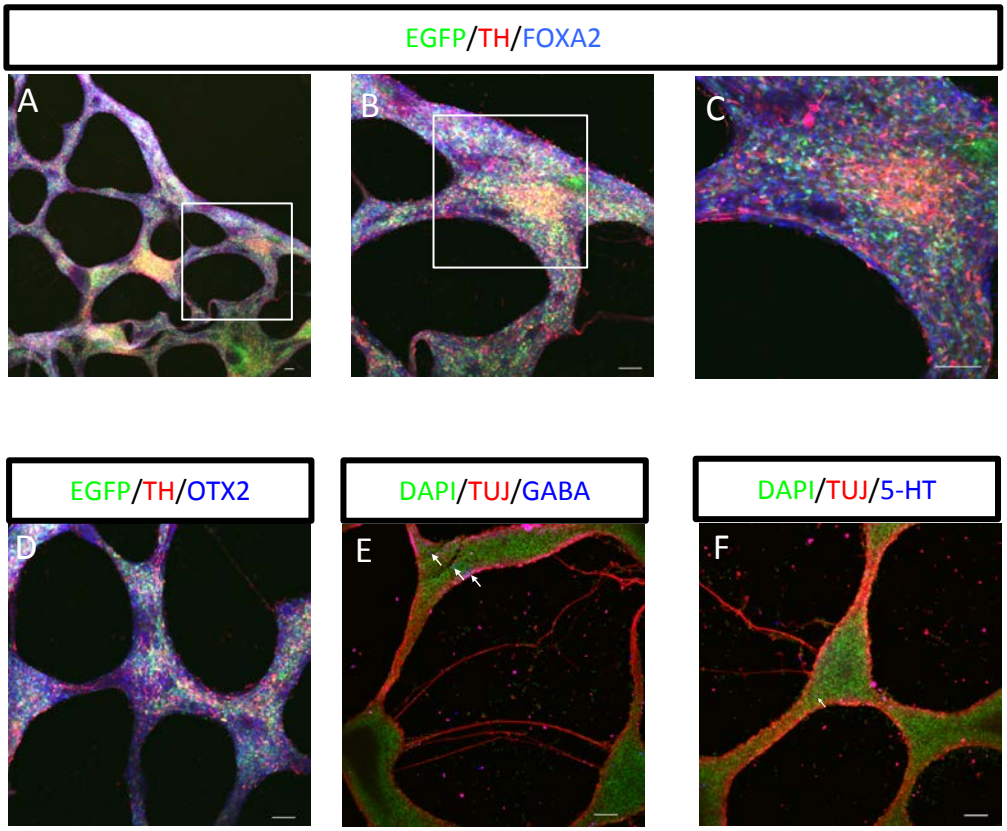

Figure 4.14 Immunocytochemical analysis of d32 EGFP+ sorted cells (7 days post sort). Antibody labeling is shown for (**A**) EGFP (green), TH (red) and FOXA2 (blue), (**B**) inset of A, (**C**) inset of B. (**D**) EGFP (green), TH (red) and OTX2 (blue). (**E**) TUJI (red), GABA (blue) and (**F**) TUJ1 (red) and 5-HT (blue). Arrows depict positive cells. Counterstained with DAPI (green) in E and F. Scale bar represents 50 µM.

Under these conditions it was possible that the lack of TH staining was related to the maturity of the sorted cells, thus cells were left to differentiate for a further 25 days. Immunofluorescent analysis of d50 cultures was also extremely difficulty due to issues with fixation and detachment of the cluster structures, from the well. In addition numerous washing steps would dislodge clusters and/or snap the fine projections between them. Due to the lack of antibody penetration and their three-dimensional

nature, these large clusters of cells were very difficult to image even using confocal microscopy.

Nonetheless, large cell clusters were observed to consist mainly of FOXA2+ (Fig 4.15A) and OTX2+ (data no shown) nuclei. Day 50 cultures exhibited robust TH staining, although it was very difficult to correctly quantify the amount of TH cells or their co-localisation with other markers in the cell body clusters. In the projections that ran along the surface of the well TH immunolabeling was found to co-localise with EGFP (Fig 4.15B). No immunoreactivity was observed for markers of other neural phenotypes such as GABA (Fig 4.15D) or 5-HT (Fig 4.15E) at this time point.

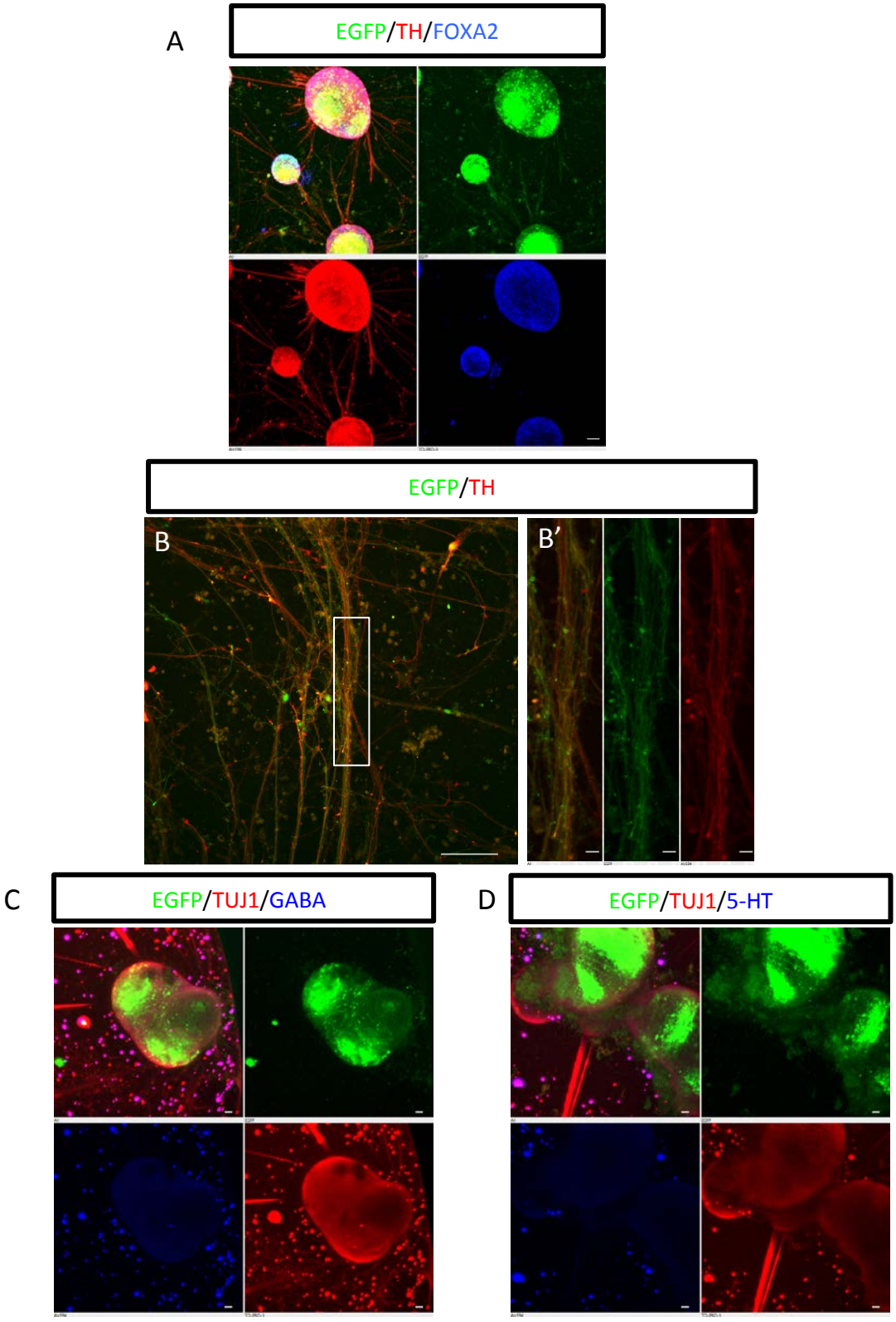

Figure 4.15 Immunocytochemical analysis of d50 EGFP+ sorted cells (25 days post sort). Antibody labeling is shown for (**A**) EGFP (green), TH (red) and FOXA2 (blue). (**B**) EGFP (green) and TH (red) (**B'**) inset of C. (**C**) EGFP (green), TUJI (red) and GABA (blue) and (**D**) EGFP (green), TUJ1 (red) and 5-HT (blue). Arrows depict positive cells. Counterstained with DAPI (green) in E and F. Scale bar, (A, B, C and D) 50 and (B') 10 µm.

4.4 Discussion

4.4.1 The small molecule BMP receptor inhibitor, LDN193189 is a Noggin mimetic

In the past, the BMP signalling antagonist noggin has been used to augment the neural induction of hESCs under PA6 conditions (Sonntag et al., 2007). However, noggin, being a recombinant protein is subject to batch variation and is also extremely costly. Thus, I initially wanted to address whether the cost effective small molecule BMP receptor inhibitors LDN (Cuny et al., 2008) or dorsomorphin (Hao et al., 2008; 2010) could substitute for noggin. As dorsomorphin has been shown to have significant "off-target" effects, of note vascular endothelial growth factor (VEGF) inhibition (Hao et al., 2010), a pathway important for mbDA differentiation (Swistowska et al., 2010) LDN was chosen as the most suitable candidate molecule for neural induction studies.

As previously reported, I demonstrated that noggin together with the TGFβ inhibitor SB431542 (NSB) addition altered the fate of differentiating cells towards a neuroepithelial phenotype (Chambers et al., 2009; Denham et al., 2010; Sonntag et al., 2007). The substitution of noggin with LDN was sufficient for neural induction. These observations are consistent with a previous publication that used LDN in place of noggin in the neural specification of progenitors prior to motor neuron specification (Boulting et al., 2011) and a more recent publication directing ESCs towards mbDA neurons (Kriks et al., 2011).

4.4.2 Differentiation of hESCs using a PA6 co-culture protocol results in low numbers of mbDA precursors

The use of the PA6 stromal cells to direct differentiation of hESCs toward a DAergic phenotype has been used in the past. However there are conflicting reports

regarding the yield of *bona fide* mbDA neurons in terminal cultures (Brederlau et al., 2006; Buytaert-Hoefen et al., 2004; Denham et al., 2010; Freed et al., 2008; Irioka et al., 2005; Yang et al., 2008; Zeng et al., 2004; 2006), with some investigators using TH labeling only as endpoint which, given the widespread expression of TH in the mammalian brain (Bjorklund & Dunnett, 2007), is not definitive of a mbDA neuron. In addition, the regional specification of the developing neural precursors has not been well characterised. It was thought that understanding the early regional specification of progenitors would help enrich the final composition of terminally differentiated cultures. My data demonstrated that the expression of CORIN, a ventral midline marker (Jönsson et al., 2009; Ono et al., 2007) was extremely rare, indicating that PA6 based differentiation protocols do not yield cells with a ventral mbDA phenotype (Denham et al., 2010).

The demonstration of PAX7 in the majority of progenitors, as well as FORSE-1 expression in a subset of progenitors was indicative of the presence of dorsal midbrain and rostral phenotypes, respectively (Denham et al., 2010; Fasano et al., 2010), further supporting the notion that PA6-directed differentiation of hESCs does not yield a mbDA phenotype. Although contrary to PA6-derived mESC cultures and other previously reported PA6 stromal derived hESCs studies (Yang et al., 2008; Han et al., 2009; Nefzger et al., 2012) these observations are in line with other published investigations (Denham et al., 2010; Irioka et al., 2005).

4.4.3 Recombinant SHH-N does not induce a ventral phenotype in PA6/LSB culture conditions

I postulated that the low number of mdDA neurons generated in the PA6/LSB conditions resulted from a lack of cues to specify a correct regional identity. Indeed, my data demonstrated that treatment with SHH-N during neural induction was able to

repress commitment to a dorsal neural tube fate in PA6/LSB differentiating cultures. Despite this shift from a dorsal fate, SHH-N was unable to increase FOXA2 expression even a high concentrations, indicating a lack of ventral specification. Such observations have been previously reported (Denham et al., 2010; Fasano et al., 2010). Nonetheless SHH signalling appeared necessary for FOXA2 induction under PA6 conditions as, cyclopamine, a Smoothened receptor antagonist (Incardona et al., 2000) completely abolished the presence of FOXA2 positive cells, presumably induced though endogenous SHH activity of stromal cells (Barberi et al., 2003; Okada et al., 2004; Perrier et al., 2004).

PA6 stromal cells have been suggested to not allow high levels of SHH signalling to occur, through the excretion of other signalling pathways modulators such as DKK1 (Denham et al., 2010). Certainly, the addition of DKK1 to differentiating cultures has been shown to retard the induction of FOXA2 positive cells (Fasano et al., 2010).

It is now apparent that commercially available SHH-N lacks posttranslational modifications, such as the addition of a cholesterol group to the C-terminus and a palmitoyl group to the N-terminus (Fasano et al., 2010). These lipid modifications are known to affect the range and potency of SHH activity (Burke et al., 1999; Chen et al., 2004). Although i*n vivo* work has demonstrated that secreted N-terminal SHH can partially rescue a phenotype in *SHH* knockout mice, deficits in the generation of ventral cell types in the neural tube are still observed (Huang et al., 2007). Thus, the inability of SHH-N to induce ventral phenotypes in differentiating PA6/LSB cultures may be due to the lack of SHH-N protein activity and that endogenous SHH signalling via SDIA is not potent enough to direct hESCs toward a ventral fate.

4.4.4 The small molecule smoothened agonist, SAG is able to ventralise cells differentiating under PA6/LSB conditions

Small molecule modulators of cellular biochemistry are revolutionising ESC differentiation protocols (Ding et al., 2003a; Ding & Schultz, 2004; Zhu et al., 2010). I postulated that high activity of the SHH signalling pathway could be attained via the use of small molecule smoothened receptor activators (Chen et al., 2002; Sinha & Chen, 2006; Wichterle et al., 2002). I demonstrated that smoothened agonist (SAG) was able to induce FOXA2 both at the level of transcript and protein. Additionally SAG treatment was able to induce ventral midline characteristic gene expression (CORIN) in developing neuroepithelia. In line with recent reports (Denham et al., 2012; Mak et al., 2012; Sommer et al., 2010) these data indicate that the substitution of SAG is sufficient for mimicking high activity SHH protein signalling, providing further evidence that fate of differentiating cells can be controlled by small molecules and that hESCs cultures differentiating under LSB conditions only do not contain ventral midbrain cell types. The induction of FOXA2 via SAG was not different from treatment with SHH-C25II a recently described highly potent modified version of recombinant mouse SHH (Fasano et al., 2010).

4.4.5 SAG treatment induces a midbrain phenotype in cultures under PA6/LSB conditions, albeit at a low frequency

As LMX1A and FOXA2 expression domains outside the midbrain do not overlap their co-expression was used to define mbDA progenitors (Failli et al., 2002; Kittappa et al., 2007; Ono et al., 2007). I demonstrated that SAG treatment increased the number of cells that co-labeled for FOXA2 and LMX-1 antibodies via FACS. Although used in publications to date (Baron et al., 2012; Brown et al., 2011; Kirkeby et al., 2012; Kriks et

al., 2011) as a marker of *LMX1A*, the LMX-1 antibody recognises both LMX1A and LMX1B, due to high sequence similarity. As the expression domain of LMX1B in the developing neural tube is less restricted than LMX1A (Cheng et al., 2003; Ding et al., 2003b; 2004; Nefzger et al., 2011) an LMX-1/FOXA2 antibody marker profile may not be indicative of mbDA progenitors. However subsequent qPCR analysis confirmed the induction of *LMX1A* following SAG addition. These data indicate that SAG is able to induce FP characteristics, however due the frequency of mbDA progenitor induction it appears that additional factors maybe involved.

4.4.6 Caudalisation of cultures under PA6/LSB/SAG conditions

The frequency of mbDA precursors that arise under PA6/LSB/SAG differentiation conditions is low, perhaps due to due to incorrect rostrocaudal regional specification of cultures during neural induction. Morphogens such as FGF8 and WNT1 have been demonstrated to play a role in the specification of midbrain (Ye et al., 1998; Martinez et al., 1998; Yamauchi et al., 2009; Prakash et al., 2006; Joksimovic et al., 2009; Tang et al., 2010).

The importance of FGF8 to the specification of mbDA neurons has been demonstrated convincingly in numerous mouse models (Chi et al., 2003; Lee et al., 1997; Martinez et al., 1999). Importantly, exogenous FGF8b enhances commitment to a mbDA fate in human and mouse ESCs (Cooper et al., 2010; Lee et al., 2000; Yang et al., 2008) and Nr4a2 over expressing mouse NSCs (Kim et al., 2003). When added to PA6/LSB conditions FGF8b upregulated the expression of *CORIN*, *LMX1A* and *EN1*. However this was observed to be dependent of the day of addition, suggesting a temporal requirement for caudalisation signals, as addition at either d2 or d6 did not alter transcript levels

when compared to d4. The observation that FGF8b decreased *FOXG1* mRNA provided more evidence of caudalising ability.

The palmitoylated glycoprotein WNT1 is secreted in numerous brain regions, such as the basal plate of the cephalic flexure (Prakash et al., 2006; Roelink & Nusse, 1991), the roofplate (Chizhikov & Millen, 2004; Hollyday & McMahon, 1995; Megason & McMahon, 2002; Roelink & Nusse, 1991) and floor plate of midbrain (Joksimovic et al., 2009; Tang et al., 2010). The latter expression of WNT1 has been shown to coincide with the region where mbDA first arise in the mouse midbrain (Prakash et al., 2006) providing evidence for its role in the patterning of mbDA precursors. In contrast WNT3a and WNT5a are more important in the expansion of the established progenitor pool of mbDA precursors (Castelo-Branco et al., 2003; Parish et al., 2008).

In vitro studies have demonstrated that WNT1 forms an auto regulatory loop with LMX1A that cooperates with the SHH-FOXA2 loop to regulate mbDA neuron development (Chung et al., 2009). Given this information, it is interesting to note that WNT1 addition at d2, d4 or d6 did not alter the expression either FP, mbDA precursor or rostral genes in developing neuroepithelia under PA6/LSB conditions. Similar to the lack of post translation modification of SHH-N discussed above it is not unreasonable to suggest that recombinant WNT1 may lack the glycosylation or palmitoylation required for full morphogenic activity (Galli et al., 2007). Conversely, WNT1 signalling may not be potent enough to over come the inhibition caused by DKK1 expression, which, as discussed above has been demonstrated in cultures containing rostral cellular phenotypes (Fasano et al., 2010).

4.4.7 Targeting EGFP to the *LMX1A* locus of human embryonic stem cells

As demonstrated in Chapter 3, homologous recombination of mESCs is efficient, with a calculated hit rate of one in 10^3 cells (Thomas et al., 1986). However, since the first account of gene targeting in hESCs by Jamie Thomson's group only a few reports using this technique have been published (Costa et al., 2007; Davis et al., 2008; Di Domenico et al., 2008; Irion et al., 2007; Ruby & Zheng, 2009; Urbach et al., 2004; Zwaka & Thomson, 2003). These publications also demonstrate technical difficulties involved, often resulting in targeting efficiencies of less than 1 in 10^6 cells (Collin & Lako, 2011). Surprisingly, the targeting of the h*LMX1A*-AIG reporter cell line was not as inefficient as other reported hESC targeted cell lines (Ruby & Zheng, 2009; Urbach et al., 2004) with a frequency of 5 per 10^6 input cells. It has been suggested that the frequency of homologous recombination is a function of the genetic locus being targeted (Costa et al., 2007; Deng & Capecchi, 1992; Hasty et al., 1994). Data presented in this chapter indicates that the *LMX1A* locus is easier to target than other targeted genes. Although not investigated in this thesis, this could be due to a relaxed chromatin state or lack of epigenetic insulation around the *LMX1A* locus (Gaszner & Felsenfeld, 2006; Müller, 1999; Zou et al., 2009).

4.4.8 Generation and characterisation of the h*LMX1A*-AIG reporter cell line

To date no commercially available extracellular antibodies that definitively mark hESC-derived mbDA progenitors exist. Although CORIN has been used in the past to isolate mbDA progenitors (Jönsson et al., 2009), its expression domain extends into the FP of the spinal cord (Ono et al., 2007). Clearly an isolation technique not dependent on extracellular antibody binding, such as a genetic reporter cell line would be advantageous for the extraction of mbDAergic progenitors.

A useful hESC reporter cell line needs to meet certain criteria, such as the faithful reproduction of endogenous patterns of expression and lack of haploinsufficiency. We chose to use the most robust method of genome editing, homologous recombination, to ensure high fidelity reporting, as viral based approaches are subject to silencing (Laker et al., 1998) and bacterial artificial chromosome (BAC) reporters insert randomly into the genome and do not contain all the upstream genetic elements that maybe be important for the regulation of gene expression (Chin et al., 1994; Min et al., 1994; Thameem et al., 2002).

The loss of one allele for some genes has been reported to result in haploinsufficiency (Amizuka & Karaplis, 1996; Kwabi-Addo et al., 2001; Song et al., 1999); this is especially an issue for genes involved in development (Kalinichenko et al., 2002; Mahlapuu et al., 2001). For the hLMX1A-AIG cell line this did not seem to be the case, as targeting the reporter construct to replace exon 1 of a single allele of *LMX1A* did not alter the ability of the reporter cell line to differentiate into neurons or distinct neurotransmitter phenotypes. This is not surprising, as deficits for mbDA neurogenesis at least, are not observed until both alleles of *LMX1A* have been removed/altered (Deng et al., 2011).

Immunofluorescence labeling revealed co-expression of EGFP with LMX1A protein. This indicated that cells expressing *LMX1A*-promoter driven EGFP also expressed LMX1A protein. EGFP positive cells also co-expressed FOXA2 and NESTIN demonstrating that they were of a mbFP plate origin (Ono et al., 2007). Quantitative-PCR data comparing EGFP positive and negative fractions isolated via FACS (presented in section 4.3.11) demonstrated upregulation of mbDA progenitor transcripts in the EGFP positive fraction (Kriks et al., 2011; Kirkeby et al., 2012), whilst transcripts important in

the development of other brain regions such as the telencephalon (FOXG1)(Fasano et al., 2010), the cortical hem (LHX2)(Bulchand et al., 2001) and roof plate (GDF7)(Chizhikov et al., 2010) were all down regulated in the EGFP positive fraction. These data are consistent with the hypothesis that the h*LMX1A*-AIG reporter cell line enabled the isolation of a population of cells with a mbDA progenitor phenotype. However, in future studies it would be of extreme interest to isolate *LMX1A* positive cells and compare their gene expression data at a more exhaustive level, for example comparing their gene expression profile to human fetal midbrain tissue, similar to work by Kirkeby et al., (2012) or to other differentiation protocols which give rise to bonafide mbDA progenitors and neurons (Kriks et al., 2011).

4.4.9 *LMX1A*-promoter driven EGFP expression in caudalised cultures

EGFP expression could be detected at low levels in PA6/LSB/SAG/FGF8 treated cultures following 10 days of differentiation. Peak EGFP expression was observed at d30 of differentiation indicating that expansion of mbDA progenitors occurs between d10 and d30. Interestingly the percentage of EGFP cells decreased there after. This could be explained by decreases in mbDA progenitor expansion rates, either induced by unknown PA6 factor(s) or by constituents of maturation media. Another plausible explanation may be continued or increased expansion of EGFP negative cells. Although not conducted in this study, it would be interesting to determine if EGFP expression is indicative of cells exhibiting a mbDA neuronal phenotype following terminal differentiation by using Cre-recombinase fate mapping techniques (Zhang et al., 2010). This data would definitively link *LMX1A* expression in progenitors with a mbDA phenotype in terminal differentiated neurons.

4.4.10 Proliferation of h*LMX1A*-EGFP+ progenitors

The concept of isolating committed progenitors is attractive as their proliferative potential allows subsequent expansion for downstream use (Nefzger et al., 2012). Data demonstrated that EGFP positive cells remain in a highly proliferative state up until d25 of differentiation. Thereafter proliferation begins to decrease, presumably due to cell cycle exit either induced by exposure to maturation media (see Section 4.2.1), or by undefined factors associated with PA6s. Nonetheless, even at d45 of differentiation a subset of mitotic mbDA progenitors could still be detected. The presence of these mitotic cells may explain neural over growths observed in some animals following grafting of DA cells derived from ESCs (Ferrari et al., 2006; Roy et al., 2006). It would be interesting to test if N-[N-(3,5-Difluorophenacetyl)-L-alanyl]-S-phenylglycine t-butyl ester (DAPT), a pharmacological inhibitor of the notch pathway (Louvi & Artavanis-Tsakonas, 2006), which has been shown to induce maturation of neuronal progenitors (Kirkeby et al., 2012; Kriks et al., 2011) could promote cell cycle exit of progenitors. To this end, recent reports have demonstrated that following treatment with DAPT no neural overgrowths were observed in animals grafted with mbDA progenitors derived from hESCs (Kirkeby et al., 2012; Kriks et al., 2011).

4.4.11 Enrichment of mbDA precursors using a hLMX1A-AIG reporter cell line

It was necessary to confirm enrichment of genes associated with a mbDA phenotype following extraction of EGFP+ cells. Quantitative PCR revealed that transcript levels of *LMX1A* in the positive fraction were over 32 fold higher when compared to EGFP negative fraction. Providing further evidence that the hLMX1A-AIG reporter cell line provided robust separation of *LMX1A* expressing cells. Although *LMX1A* transcript was still present in the negative fraction this was most likely due to cells that were below the level of EGFP detection via FACS, but still expressed *LMX1A*.

Expression of *FOXA2* in the EGFP positive fraction confirmed that EGFP positive cells were of a mbDA phenotype. Interestingly, no difference in the expression of the ventral midline marker CORIN was detected between EGFP positive and negative cells. In addition the normalised expression data of CORIN showed transcript levels to be very low. This result is perplexing and requires further investigation as data presented in both (Section 4.3.4 and 4.3.6) demonstrates up regulation of CORIN following the addition of both SAG and FGF8b. However a d25 time point maybe too late to detect CORIN expression, given its transient expression in mbDA precursors (Jönsson et al., 2009; Ono et al., 2007) .

Engrailed 1 and *NGN2* are midbrain markers and have been shown to regulate the transcriptional network associated with mbDA progenitors (Alavian et al., 2008; Ang, 2006; Kele et al., 2006; Simon et al., 2001; 2004; Thompson et al., 2006). Concurrent with EGFP+ cells being of mbDA phenotype the expression of *NGN2* and *EN1* was observed to upregulated in the positive fraction following sorting.

The expression of *TH*, *NURR1* and *PITX3* is surprising, as these genes are not induced until later in the life of mbDA neurons (Alavian et al., 2008; Ang, 2006; Kim et al., 2007). This indicated that although d25 EGFP+ cells appear to represent a progenitor cell type, genes that are involved in the mature mbDA neurons are expressed at this time point. For *PITX3* at least, this is observation is most likely explained by the fact that *PITX3* transcript is expressed early and its expression is mediated my microRNA feedback loops (Kim et al., 2007). Interestingly, in contrast to *NURR1* and *PITX3*, *TH* expression was also detected in the negative fraction, providing further evidence that *TH* is not a reliable marker of mbDA neurons.

Both *LHX2* (Bulchand et al., 2001; Mangale et al., 2008) and *FOXG1* transcript were detected in the negative fraction. These observations suggest that cells with a rostral phenotype were present in the negative fraction. This data is not surprising as earlier work in this chapter (section 4.3.2) demonstrates that PA6/LSB differentiation yields cells with a rostral phenotype.

4.4.12 Isolation of EGFP+ cells from PA6/LSB/SHH conditions give rise to high yields of mbDA neurons

Although d25 EGFP+ sorted cells exhibited a transcriptional profile that was indicative of mbDA progenitors; the question of whether these cells become *bona fide* mbDA neurons remained to be addressed. During differentiation EGFP positive cells consistently formed large spherical clusters of cell bodies. Such observations have not been reported to date and are difficult to explain given the paucity of high-resolution brain development imaging studies in humans. Initially this observation was interpreted to be a result of wide spread cell migration, as mouse developmental studies show that between E11 and E16 waves of migration are observed as cells first migrate ventrally and subsequently laterally and rostrally towards the definitive site in the SNpc (Kawano et al., 1995; Maxwell et al., 2005 and see Fig 1.3). Interestingly, following FACS of *Lmx1a*-reporter positive progenitors derived from differentiating mPSCs these migration events were not observed indicating that this may be a characteristic of hPSC-derived cultures. However, it is also entirely probable that the formation of large spherical cell body clusters was due to changes in cell substrate or cell adhesion requirements during maturation of these cultures as opposed to migration events.

Mature d50 cultures demonstrated robust staining of TH, FOXA2 and OTX2 in combination with EGFP. This is in contrast to cultures assessed at d32, suggesting at d32,

cultures have not undergone appropriate differentiation to a "mature" phenotype. Taken together these data indicate that hESC-derived *LMX1A*-reporter positive cells FACS isolated from PA6 cells following ventralisation and caudalisation represent an efficient methodology to generate high yields of neurons that exhibit a mbDA phenotype.

4.5 Conclusion

In comparison to mESC differentiation, PA6 differentiation of hESCs does not yield neural or mbDA precursors to the same extent. Nonetheless, efficient neuralisation could be achieved by the use of small molecule modulators of BMP and TGFβ signalling. In the absence of external regionalisation cues, neuroepithelial progenitors default to a mixed culture containing cells with rostral and dorsal midbrain phenotypes. The dorsoventral phenotype of cells could be altered by the addition of a small molecule modulator of smoothened, but this did not induce widespread mbDA progenitor differentiation suggesting a requirement of caudalisation signals. Fibroblast factor 8b, a known caudalising agent could slightly upregulate the expression of mbDA progenitor genes, and thus was used in the directed differentiation of neural precursors before FACS isolation. Quantitative PCR following FACS isolation of *LMX1A*-promoter driven EGFP positive cells demonstrated a transcriptional profile indicative of mbDA progenitors. Following protracted maturation in defined medium, high yields of mbDA neurons were observed. The dependency on PA6 stromal cells is not ideal however, especially for CRT given their non-xenofree nature. In addition, the use of PA6 cells provides no clues to the signals that are required for the directed differentiation of hESCs to a midbrain phenotype. Thus in order for either CRT or *in vitro* PD modelling to become a reality, a purely chemically defined protocol will be required.

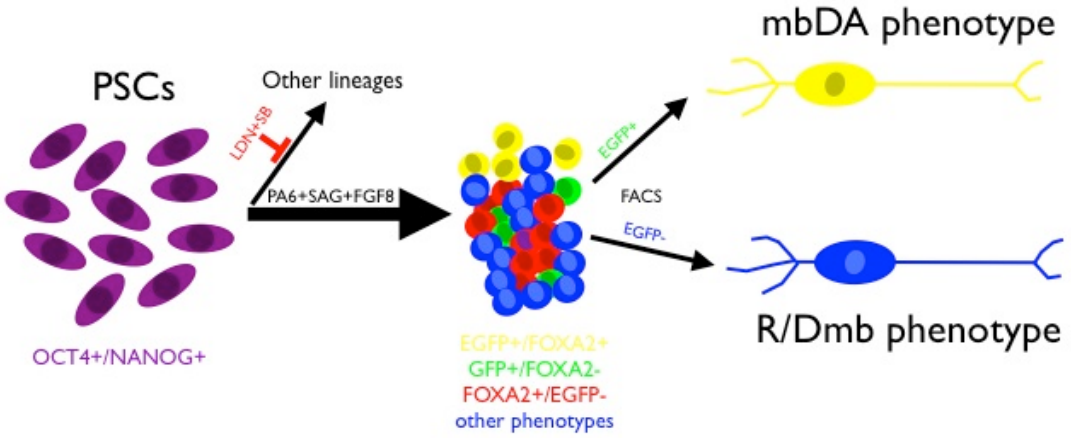

Figure 4.15 hESC- PA6 differentiation and EGFP+ sorting model. Neural induction is achieved by LSB inhibition of BMP and TGFβ signalling. Addition of SAG and FGF8 supplementation yields a subset of cells with a mbDA phenotype (yellow). EGFP+ cells (yellow and green) and then isolated via FACS and subsequently become mbDA neurons following maturation.

Chapter Five: Chemically defined monolayer conditions for the derivation of mbDA cells from hESCs

5.1 Introduction

The reliance on SDIA via cell lines such as PA6 and MS5s in the neuralisation and directed differentiation of mbDA neurons is not ideal, as their non xeno-free nature may elicit an immune reaction in patients receiving hESC-derived grafts. The use of stromal cell lines, also, provide no clues as to the molecular determinants required for directed differentiation of hESCs to mbDA neurons, as well as potentially skewing cellular behaviour in *in vitro* models. The heterogeneous nature of EB differentiation protocols (Bain, Kitchens, Yao, Huettner, & Gottlieb, 1995) together with the poor yields obtained following selection of neural precursors using 5 stage protocols (Lee et al., 2000) render these approaches impractical. Thus, to realise the potential of hESCs for either CRT or *in vitro* PD modelling a chemically defined monolayer protocol is required.

The discovery that ROCK inhibition promotes the survival of single cell hESCs following dissociation (Watanabe et al., 2007) has facilitated the use of CDML cultures in directed differentiation protocols (Chambers et al., 2009, 2012; Fasano et al., 2010; Kirks et al., 2011). Moreover, a recent advance in the neuralisation of hESCs via the inhibition of BMP and activin/nodal signals (dual SMAD inhibition) under CDML conditions has also resulted in an improved differentiation protocol, which yields more efficient and synchronised neural progenitors cultures (Chambers et al., 2009). However, to date, there has been limited investigation into the early-directed regional specification of neural progenitors, and their subsequent differentiation into specific neuronal phenotypes from hESCs under CDML conditions. Previous studies have documented the directed differentiation of mESCs to regional specific progenitors and neurons (Gaspard et al., 2008; Watanabe et al., 2005; Wichterle et al., 2002) following the addition of patterning factors that specify R/C and D/V CNS identities.

Following neuralisation, hESCs differentiating under CDML/dual SMAD inhibition generate a rostral phenotype marked by the expression of FOXG1 and OTX2 (Chambers et al., 2009; Fasano et al., 2010; Kriks et al., 2011). Recent work by Fasano et al., (2010) has, however, demonstrated that early exposure to high activity SHH signalling promotes conversion of PAX6+/NESTIN+ neuroepithelial cells into FOXA2+/NETRIN1+/F-SPONDIN+ FP cells under dual SAMD conditions. Others have also demonstrated that early forced expression of the SHH signal transducing transcription factor GLI1 during differentiation under CDML conditions can generate FP cells (Denham et al., 2010). These studies demonstrate that hESCs cultures following neural induction can be directed away from their "default" anterior neuroectoderm identity towards a FP identity.

The FP extends along the midline of the ventral neural tube (Jessell et al., 1989), thus although high activity SHH signalling can specify a FP phenotype along the D/V axis in developing neuroepithelia under CDML conditions, there is still a requirement for the correct specification along the R/C axis in order to generate regional specific cell types, such as mbDA neurons.

5.1.1 Aims

In Chapter 4, I show the utility of reporter cell lines as tools for isolating mbDA neural precursors from cultures differentiating under PA6/LSB/SAG/FGF8 conditions; it was hypothesised that they could also be used as a screening tool to search for factors that enrich for a mbDA phenotype.

Thus the aims of this chapter are (1) to understand the conditions required in a CDML context to generate regionally specified neural progenitors and subsequent mbDA

neurons using two hESC reporter cell lines, h*LMX1A*-AIG and hPITX3-EGFP, and (2) to test whether CDML generated mbDA neurons posses a functional capacity to respond to neurotransmitter stimulation.

5.2 Methods

Unless outlined all experimental methodologies are the same as described in Chapter 2.

5.2.1 Chemically defined monolayer neural induction and differentiation

Chemically defined monolayer neural induction and mbDA differentiation were performed using a modification of published protocols (Chambers et al., 2009; Fasano et al., 2010; Kriks et al., 2011). To remove MEFS, cells, dissociated with accutase were resuspended in hESC medium containing 10μM Y-27632, were plated on 0.1% (wt/vol) gelatin-coated dishes for 30 min. The non-adherent hESCs were washed (200g, 5 min) with hESC media and plated on Matrigel™ coated dishes in MEF-CM supplemented with 10μM Y-27632 at 10 x 10^5 – 13 x 10^5 cells cm^{-2}. Media was renewed every day. One to two days post plating, when cells were confluent, d0 of differentiation; the media was changed to hESC differentiation media 1, (HDM1): KnockOut™-DMEM (Life Technologies), 15% KSR, 1% NEAA, 2 mM GlutaMAX™-I, penicillin 25 U mL^{-1}, streptomycin 25 μg mL^{-1} and 0.1 mM β-mercaptoethanol. For neural induction studies, noggin (500 ng mL^{-1}) or LDN (100 or 300 nM) were added together with SB431542 (10 μM), d0-11. PBS containing 1 mg mL^{-1} BSA and 0.1 % DMSO was used a vehicle control. At d5 increasing amounts of hESC differentiation media 2 (HDM2)(25%, 50%, 75%,) was added to HD1 media every two days. For ventralisation studies 100, 300 and 1000 nM SAG or 100 ng mL^{-1}, SHH-C25II together with a different smoothened small molecule agonist Purmorphamine (2 μM; 9- cyclohexyl- N- [4- (morpholinyl)phenyl]- 2- (1-naphthalenyloxy)- 9H- purin- 6- amine; Santa Cruz)(Purmorphamine was used instead of SAG to keep consistent with the Kriks et al., 2011 protocol) was added from d1 to d7. For caudalisation studies, FGF8b (100ng mL^{-1}), WNT1 (100 ng mL^{-1}), SPIE factors (IGF2 (100

ng mL^{-1}), IGFBP4 (500 ng mL^{-1}), SDF-1 (100 ng mL^{-1}), PTN (100 ng mL^{-1}) and EFNB1 (200 ng mL^{-1})(Vazin et al., 2009) were added from d2, 4 or 6 till day 14. CHIR99021, a small molecule GSK3β inhibitor, which mimics canonical WNT signalling (CHIR; 0.7 μM, 1.4 μM, 3.0 μM or 6.0 μM; 6- [[2- [[4- (2, 4- dichlorophenyl)- 5- (5- methyl- 1H- imidazol- 2- yl)- 2- pyrimidinyl]amino]ethyl]amino]- 3- pyridinecarbonitrile; Axon Medchem) was added from d3 to 13. On d11 media was changed to Neurobasal media containing 2 mM GlutaMAX™-I and 10 mL L^{-1} B-27 serum-free additive (NBM/B27/gMAX) supplemented 20 ng ml−1 BDNF, 20 ng ml−1 GDNF, 0.2 mM AA, 1 ng ml−1 TGFβ3, 0.5 mM db-cAMP and DAPT (10 nM; N- [2S- (3, 5- difluorophenyl)acetyl]- L- alanyl- 2- phenyl- 1, 1- dimethylethyl ester- glycine; Axon Medcem). Cells were dissociated with accutase and replated at high density (5 x 10^5 cells cm^{-2}) in supplemented NBM/B27/gMAX media onto PLO/LAM/FN pre-coated wells at d20-25 to induce mbDA neuronal maturation.

5.2.2 Engineering of the human PITX3-EGFP reporter cell line

To engineer a hPITX3-EGFP reporter cell line, a previously described EGFP targeting vector (Hockemeyer et al., 2009) which targets the first exon of the PITX3 endogenous locus was used (Addgene, U.S.A). Forty micrograms of EGFP targeting vector was co-electroporated with 10 μg of custom designed ZFN pairs (Sigma Aldrich) following conditions outlined in Section 4.2.2. Individual colonies were picked and expanded following puromycin selection (0.5 μg mL^{-1}, Life Technologies), 10–14 d after electroporation. See appendix V for representative southern blot of positive clones.

5.2.3 Calcium imaging

Following regions of interest (ROI) determination by EGFP expression, differentiated cells were loaded with Fluo-4AM (Fluo4, 2.5 μM, Life Technologies) for 30 min at 37°C in a humidified 5% CO_2-in-air atmosphere incubator. Cells were then washed

twice with PBS and incubated with supplemented NBM/B27/gMAX (see Section 5.2.1) for a further 30 min at 37°C in a humidified 5% CO_2-in-air atmosphere incubator. Calcium flux was monitored using a Nikon A1 confocal microscope. Fluo4 was excited at 488 nm and emission was recorded at 515 nm. Fluorescent intensities were captured with NIS-elements-AR software. To monitor stimulation, basal Fluo4 fluorescence was recorded for 30 sec, and then GABA (Sigma-Aldrich) was added to the differentiation medium to give a final concentration of 30 μM. □Calcium

per second (15 fps). At the completion of each experiment KCl (60 mM, Sigma) was added as second stimulation to ensure only viable neural cells were included in subsequent analyses. Following data collection, ROIs segmentation was determined using intensity and event size thresholding (Nikon Elements v4.0). Calcium flux was determined by subtracting the mean basal intensity from the max intensity post stimulation for each ROI that demonstrated a response to KCl.

5.3 Results

5.3.1 Neural Induction using LSB under chemically defined monolayer conditions

I wanted to ensure that sufficient neural induction was achieved under CDML conditions using the LDN concentrations optimised for SDIA augmented neural induction. NSB significantly altered the number of NESTIN (72.6% ± 4.1) and PAX6 (74.9% ± 1.3) positive cells (Fig 5.1A & B)(Dunnett's test, n=4, $p < 0.001$), whilst reducing the presence of OCT4+ cells (Fig. 5.1C). SB together with 100 nM LDN significantly enhanced the number of NESTIN (69.1% ± 3.1%)(Dunnett's test, n=4, $p < 0.001$) and PAX6 (78.9% ± 1.3%)(Dunnett's test, n=4, $p < 0.001$) cells (Fig 5.1A & B) and also abrogated the presence OCT4+ cells (Fig 5.1C). Increasing LDN to 300 nM had no additional effect (Fig 5.1A, B & C). These data demonstrate the small molecule LDN provides adequate BMP inhibition under CDML conditions.

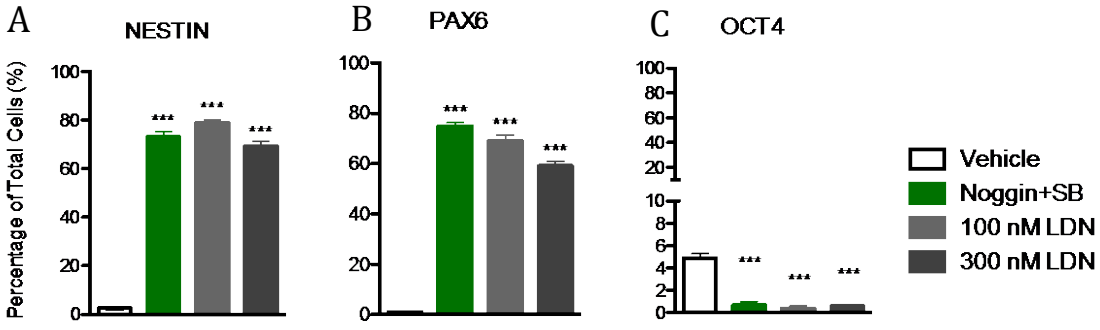

Figure 5.1 Intracellular FACS analysis of hESCs under CDML conditions together with inhibition of BMP (noggin or various concentrations of LDN193189) and activin/nodal (SB431542) signals. FACS analysis of d12 cells expressing NESTIN (A), PAX6 (B) and OCT4 (C), when treated with either vehicle (white bar), NSB (green bar) or different concentrations of LDN193189 + 10 µM SB (grey bars). Data are presented as mean ± S.E.M of 4 experiments. Dunnett's post hoc test was used to determine levels of significance following one-way ANOVA. Asterisks indicate statistical significance in comparison to vehicle (***, $p < .001$).

5.3.2 Differentiation of hESCs under CDML LSB conditions results in cultures with a rostral phenotype.

I next sought to characterise cultures for regional specific markers to understand what cellular phenotypes arose from differentiation under CDML/LSB conditions. Total RNA was extracted for qPCR, or cultures were used for immunofluorescence analysis, at d15. The expression of *FOXA2*, *EN1*, *NGN2* and *CORIN* transcripts at d15 was not different from d1 cultures (Fig 5.2A). Consistent with this finding, both FOXA2 (0.7 % ± 0.2)(Fig 5.2C & H) and CORIN (0.4 % ± 0.2)(Fig 5.2E & H) positive cells were rarely detected. Increases in *OTX2* transcript levels were observed in d15 cultures when compared to d1 LSB cultures (Fig 5.2A). Extensive immunoreactivity was observed for OTX2 (67.1% ± 3.7)(Fig 5.2B & H) and FORSE-1 (62.8% ± 7.1)(Fig 5.2D & H). The immunofluorescent labeling of FORSE-1 was also corroborated by an ~18 fold up regulation of the rostral marker *FOXG1* (Fig 5.2A). *LMX1A* transcript abundance was also observed to be increased in d15 LSB treated cultures (Fig 5.2A). This was confirmed by microscopy, which revealed numerous EGFP positive cells associated with rosettes (Fig 5.2F). These observations indicate that the majority of hESC-derived neural progenitors that arise from CDML/LSB differentiation conditions represent cells with a rostral phenotype, of which a proportion express *LMX1A*.

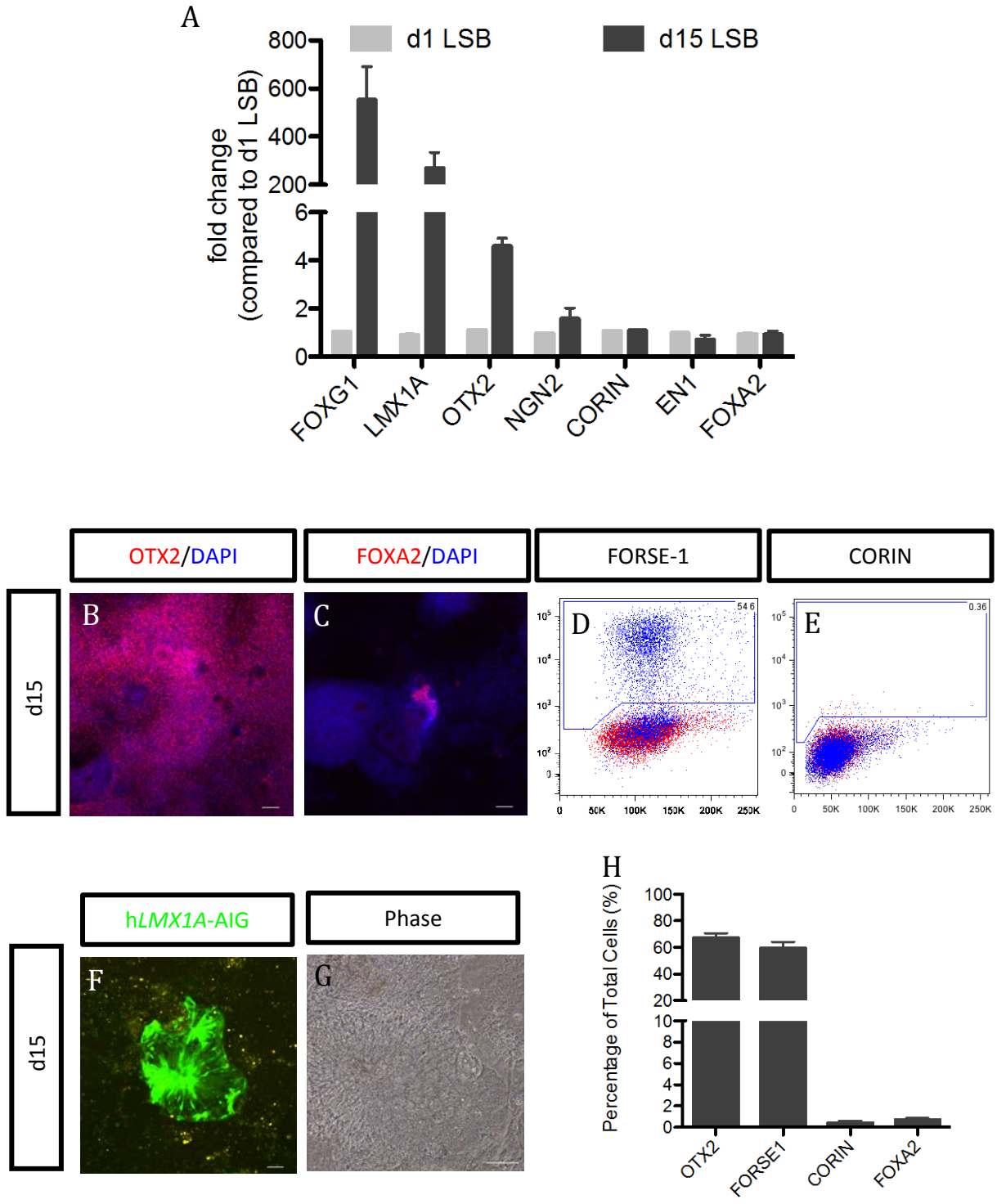

Figure 5.2 Phenotype analysis of CDML/LSB cultures at d15. (**A**) Quantitative PCR for a panel of probes. Immunofluorescent images for (**B**) OTX2 and (**C**) FOXA2, both counterstained with DAPI. FACS dot plots for (**D**) FORSE-1 and (**E**) CORIN. (**F**) Live cell imaging of h*LMX1A*-AIG (**G**) Phase contrast image of EGFP rosette from (**F**). (**H**) Quantification of (B-E). Scale bars, (B, C, F & G) 50 µM. Data is presented as the mean ± S.E.M of 4-7 (A), 4 (B & C) and 5 (D & E) experiments.

5.3.3 Generation of floor plate cells under CDML conditions

Different concentrations of SAG (30, 100, 300 and 1000 nM) or the positive control SHH-C25II + Purmorphamine (Kriks et al., 2011) were added to CDML/LSB cultures from d1-11, cultures were fixed subsequently fixed on d13 for FACS analysis. At low concentrations of SAG no FOXA2+ cells were detected (Fig 5.3B and E). Very few FOXA2+ cells were observed following treatment with 30 or 100 nM SAG (Fig 5.3E). Concentrations of SAG above 300 nM were able to increase the number of cells immunoreactive for FOXA2, however this was only significant when cells were treated with 1000 nM SAG (Fig 5.3B, C and E)(Bonferonni's test, n=4, $p < 0.001$). Nonetheless, 1000 nM SAG was not able to induce FOXA2 positive cells as consistently as the positive control, (SHH-C25II + Purmorphamine treatment)(see error bars, Fig 5.3E). These data indicate that although SAG is able to induce FOXA2+ cells in hESC-derived developing neuroepithelium under CDML/LSB conditions it is not as consistent as SHH-C25II + Purmorphamine treatment. Thus SHH was used in all experiments going forward.

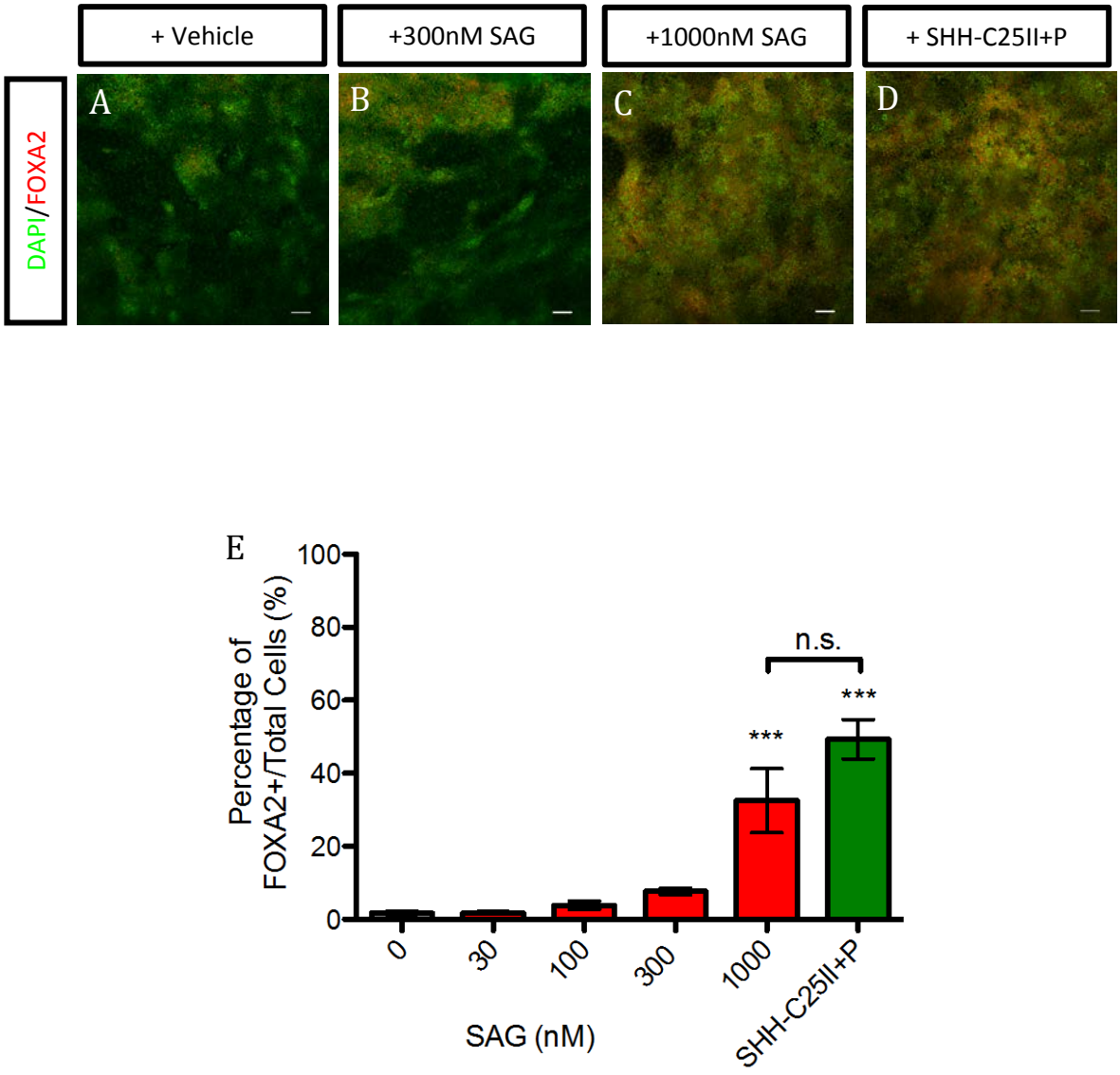

Figure 5.3 FOXA2 induction under CDML/LSB conditions. Immunofluorescence images of cells labeled with FOXA2 (red) following treatment with various concentrations of SAG or SHH-C25II + Purmorphamine (Kriks et al., 2011) used as control. . (**A**) Vehicle, (**B**) 300 nM SAG, (**C**) 1000 nM SAG and (**D**) 200 ng mL^{-1} SHH-C25II + 2 µM Purmorphamine (SHH-C25II+P). Counterstained with DAPI (green). Scale bars, 50 µm. (**E**) The number of FOXA2+ cells detected via intracellular FACS. Grey bar (Vehicle), red bars (various SAG concentrations) and green bar (SHH). Data is presented as the mean ± S.E.M of 6 experiments. Bonferonni's post hoc test was used to determine levels of significance following one-way ANOVA. Asterisks indicate statistical significance in comparison to vehicle (**, p <

5.3.4 Using h*LMX1A*-EGFP as screening tool

FGF8b, WNT1 and a combination of proteins known as SPIE (see Section 1.3.1) were added to cultures differentiating under CDML/LSB/SHH conditions at d2, d4, or d6 and assessed for their ability to upregulate EGFP expression. Total RNA was also extracted from d15 cultures and analysed for the expression of a panel probes for FP (*FOXA2, NTN-1*), mb (*EN1, NGN2*) mbFP (*CORIN*), mbDA (*LMX1A*) and rostral (*FOXG1*) genes. The addition of FGF8b at d2 or d4 did not alter the number of EGFP+ cells (Fig. 5.4B & E). FGF8b added at d6 significantly upregulated expression of EN1 (Bonferroni's test, n=4, $p < 0.01$). Changes in the levels of other transcripts were not observed (Fig 5.4F).

Although WNT1 did not alter the number of EGFP+ cells at d15 (Fig 5.4G), it did increase both *LMX1A* (Bonferroni's test, n=5, $p < 0.001$) and *EN1* (Bonferroni's test, n=5, $p < 0.001$) transcript following addition d2 (Fig 5.4H).

SPIE factors at d2 or d4 significantly increased the number of EGFP+ cells to 13.9 % ± 2.2 and 7.8 % ± 1.1 respectively at d15 (Fig 5.4I). *FOXA2* (Bonferroni's test, $p < 0.05$, n=4) and *CORIN* (Bonferroni's test, $p < 0.01$, n=4) transcript increased following addition of SPIE d2 and d4 (Bonferroni's test, $p < 0.01$, n=4) (Fig 5.4J). *LMX1A* and *EN1* mRNA increased significantly in response to addition of SPIE at d2 (Fig 5.4J)(Bonferroni's test, $p < 0.01$, n=4). Day 4 addition of SPIE factors also increased *EN1* expression (Fig 5.4J)(Bonferroni's test, $p < 0.001$, n=4). *FOXG1* decreased following d2 addition of SPIE (Fig 5.4J) (Bonferroni's test, $p < 0.001$, n=4).

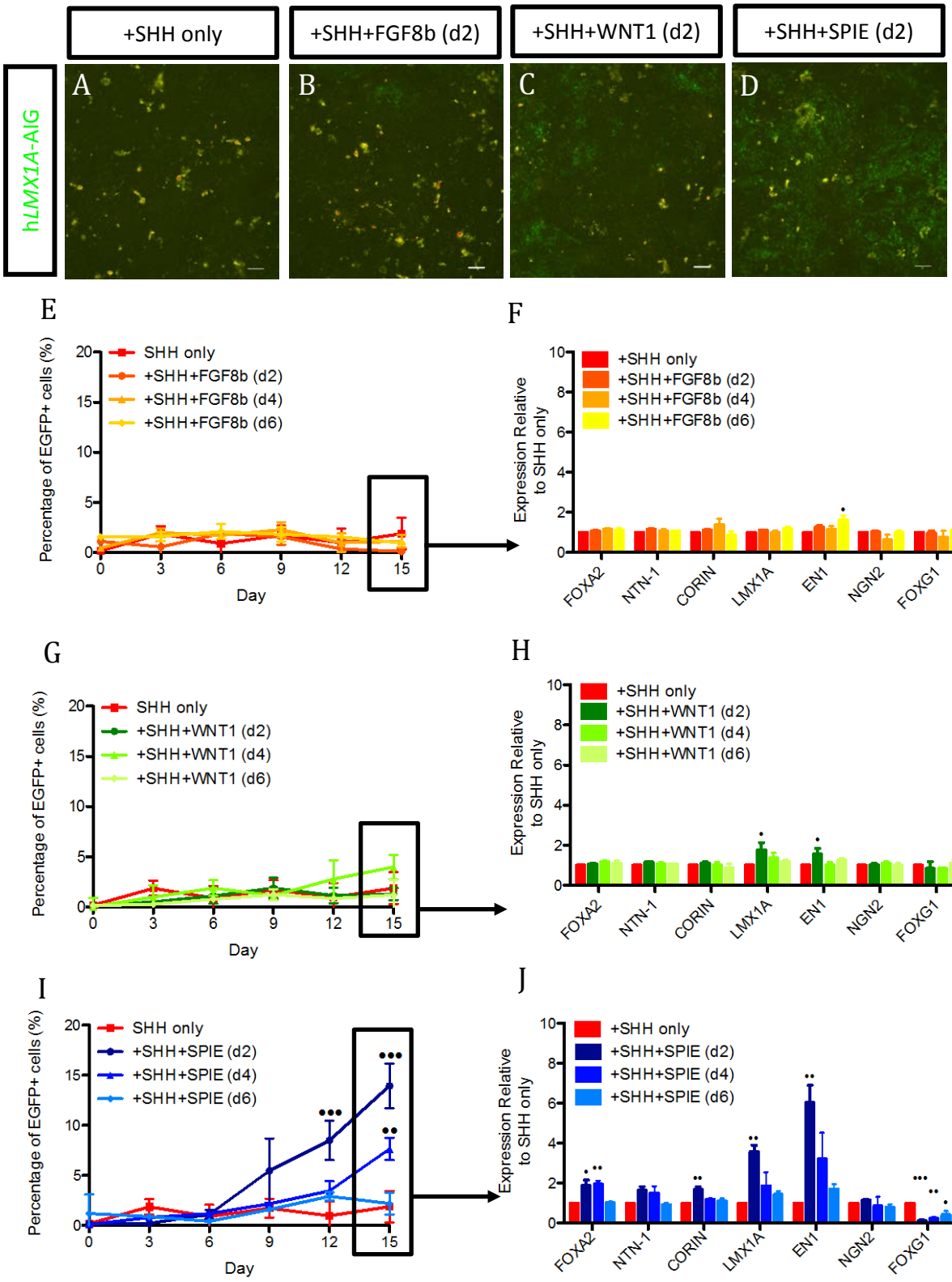
+SHH only
+SHH+FGF8b (d2)
+SHH+WNT1 (d2)
+SHH+SPIE (d2)
hLMX1A-AIG
A
B
C
D
E
F
Percentage of EGFP+ cells (%)
SHH only
+SHH+FGF8b (d2)
+SHH+FGF8b (d4)
+SHH+FGF8b (d6)
Day
Expression Relative to SHH only
FOXA2
NTN-1
CORIN
LMX1A
EN1
NGN2
FOXG1
G
H
+SHH+WNT1 (d2)
+SHH+WNT1 (d4)
+SHH+WNT1 (d6)
I
J
+SHH+SPIE (d2)
+SHH+SPIE (d4)
+SHH+SPIE (d6)

Figure 5.4 The rostrocaudal phenotype of h*LMX1A*-AIG hESCs differentiating under CDML/LSB/SHH conditions can be altered by SPIE factors. Live cell EGFP imaging of d15 cultures following incubation with (**A**) SHH only (**B**) SHH+FGF8b (d2), (**C**) SHH+WNT1 (d2) and (**D**) SHH+SPIE (d2). Scale bars, 50 µm. Time course (d0-d15) of *LMX1A* driven-EGFP expression for (**E**) FGF8b - SHH only (red square), FGF8b addition at d2 (dark orange circles), d4 (light orange triangles), d6 (yellow diamonds). (**G**) WNT1 - SHH only (red squares), WNT1 addition at d2 (dark green circles), d4 (light green triangles), d6 (lime diamonds). (**I**) SPIE factors - SHH only (red squares), SPIE addition at d2 (dark blue circles), d4 (light blue triangles), d6 (azure diamonds). qPCR analysis consisting of a panel probes for FP, mb, mbFP, mbDA and rostral genes in response to (**F**) FGF8b - red bars represent SHH only, dark orange bars (d2 addition), light orange bars (d4 addition) and yellow bars (d6 addition). (**H**) WNT1 - red bars represent SHH only, dark green bars (d2 addition), light green bars (d4 addition) and lime bars (d6 addition) or SPIE (**J**) red bars represent SHH only, dark blue bars (d2 addition), light blue bars (d4 addition) and azure bars (d6 addition). Data are presented as mean ± S.E.M. of FGF8b 4 (FACS) 4 (qPCR), WNT1 4 (FACS) 5 (qPCR) and SPIE 3 (FACS), 4 (qPCR) experiments. Dunnett's multiple comparison test was used to levels of significance following one-way ANOVA (qPCR). Circles indicate statistical significance in comparison to SHH only for qPCR analysis (•, $p < .05$; ••, $p < .01$; and •••, $p < .001$). Bonferonni's post hoc test was used to determine levels of significance following two-way ANOVA (FACS). Circles indicate statistical significance in comparison to d0 (••, $p < .01$; and •••, $p < .001$).

5.3.5 SPIE factor treatment inefficiently induces mbDA neurons

As d2 appeared to be the time point when differentiating cells responded most to caudalising factors, h*LMX1A*-AIG hESCs were differentiated with either FGF8b, WNT1 or SPIE added at d2 under CDML/LSB/SHH conditions and analysed for mbDA neural markers at d25. When FGF8b was added, no EGFP+/FOXA2+ progenitors or EGFP+/TH+/FOXA2+ neurons were observed (Fig 5.5B & F). The addition of WNT1 resulted in very few EGFP+/FOXA2+ progenitors and EGFP+/TH+/FOXA2+ neurons (1.2 % ± 0.9)(Fig 5.5C & F). SPIE factors increased the number FOXA2+/EGFP+ cells were observed. This was also corroborated by the presence of 21.6 % ± 9.1 EGFP+/FOXA2+/TH+ mbDA neurons (Fig. 5.5D, E and F).

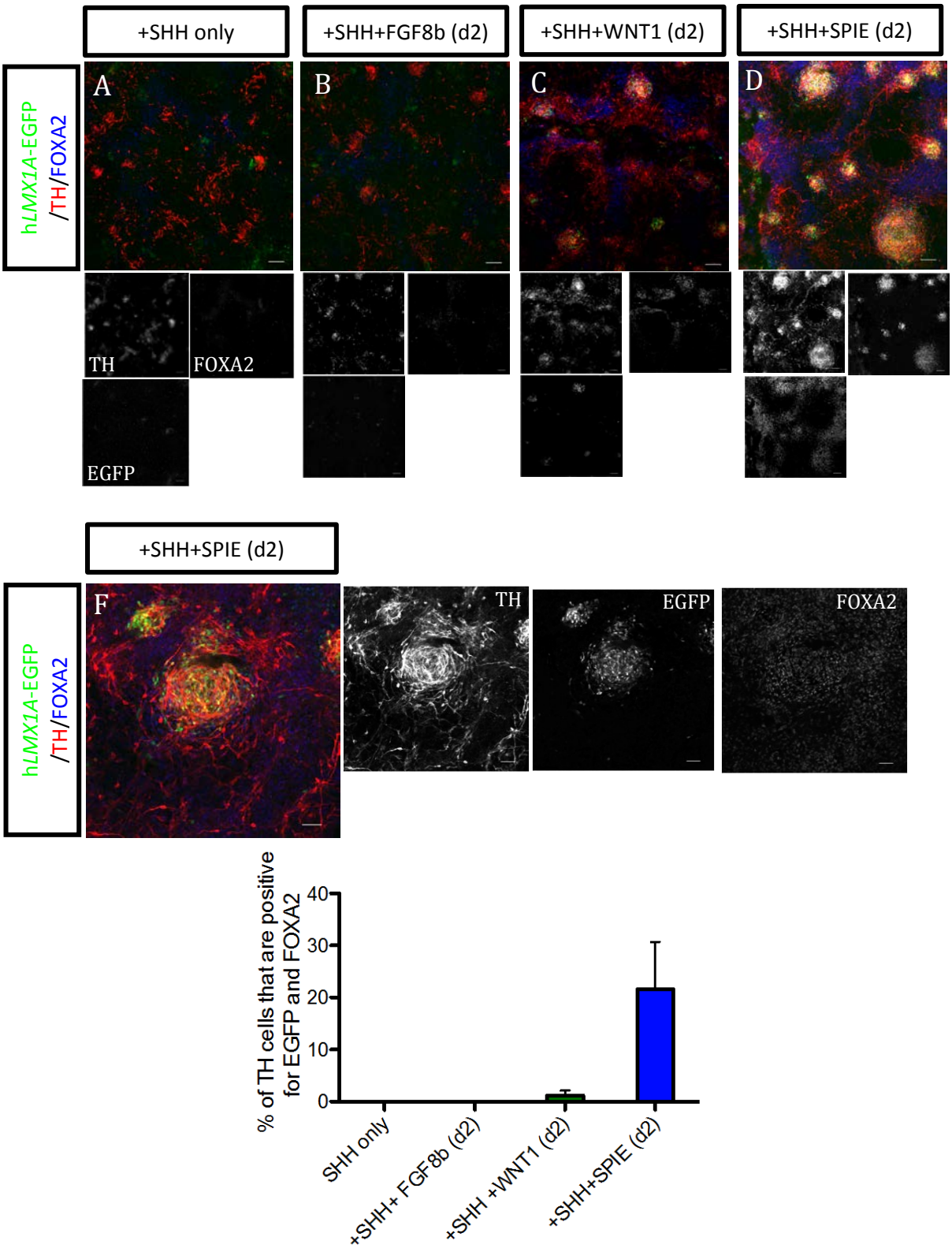

Figure 5.5 SPIE factors inefficiently induce mbDA neurons. Immunofluorescence images of d25 cells labeled with EGFP (green), TH (red) and FOXA2 (blue) following the addition of (**A**) SHH only, (**B**) SHH+FGF8b (d2), (**C**) SHH+WNT1 (d2) and (**D**) SHH+SPIE (d2). (**E**) inset of D. Scale bars, (**A-D**) 50 and (**E**) 100 µm. (**F**) Quantification of immunofluorescence data. Data are presented as mean ± S.E.M. of 4 experiments.

5.3.6 CHIR99021 caudalises progenitors differentiating under CDML/LSB/SHH conditions.

I hypothesized that extraction of EGFP+ cells from h*LMX1A*-AIG differentiating cultures under CDML/LSB/SHH/SPIE would allow enrichment of mbDA neurons in terminally differentiating cultures (as observed in Chapter 4). However, during the time that I was setting up these experiments, publications from three independent groups (Kirkeby et al., 2012; Kriks et al., 2011; Xi et al., 2012) demonstrated that the addition of a small molecule GSK3β inhibitor, CHIR99021 (CHIR), which mimics canonical WNT signalling, could robustly induce the expression of *LMX1A* and other related mbDA genes. However, these reports used different CHIR concentrations, thus CHIR was assayed for its ability to induce EGFP expression as a surrogate measure of commitment to mbDA progenitor phenotype. In the absence of CHIR, 1.9 % ± 0.4 of cells expressed EGFP (Fig 5.6 A, E and I). The addition of 0.7 μM CHIR resulted in 4.1 % ± 0.6 of cells expressing EGFP from the *LMX1A* locus (Fig 5.6 B, F and I). Significant increases in EGFP cell numbers were observed following 1.4 μM CHIR addition (17.0 % 4.0, Fig 5.6 C, G and I)(Dunnett's test, $p < 0.01$, n=3). The most robust increase in EGFP+ cells was observed following 3.0 μM CHIR (62.5% ± 6.2, Fig 5.6 D, H and I). High concentrations of CHIR completely abolished the presence of EGFP+ cells (Fig 5.6 I). EGFP was also co-localised with FOXA2 and NESTIN following 3 μM CHIR addition confirming a correct mbFP progenitor identity (Fig 5.6J).

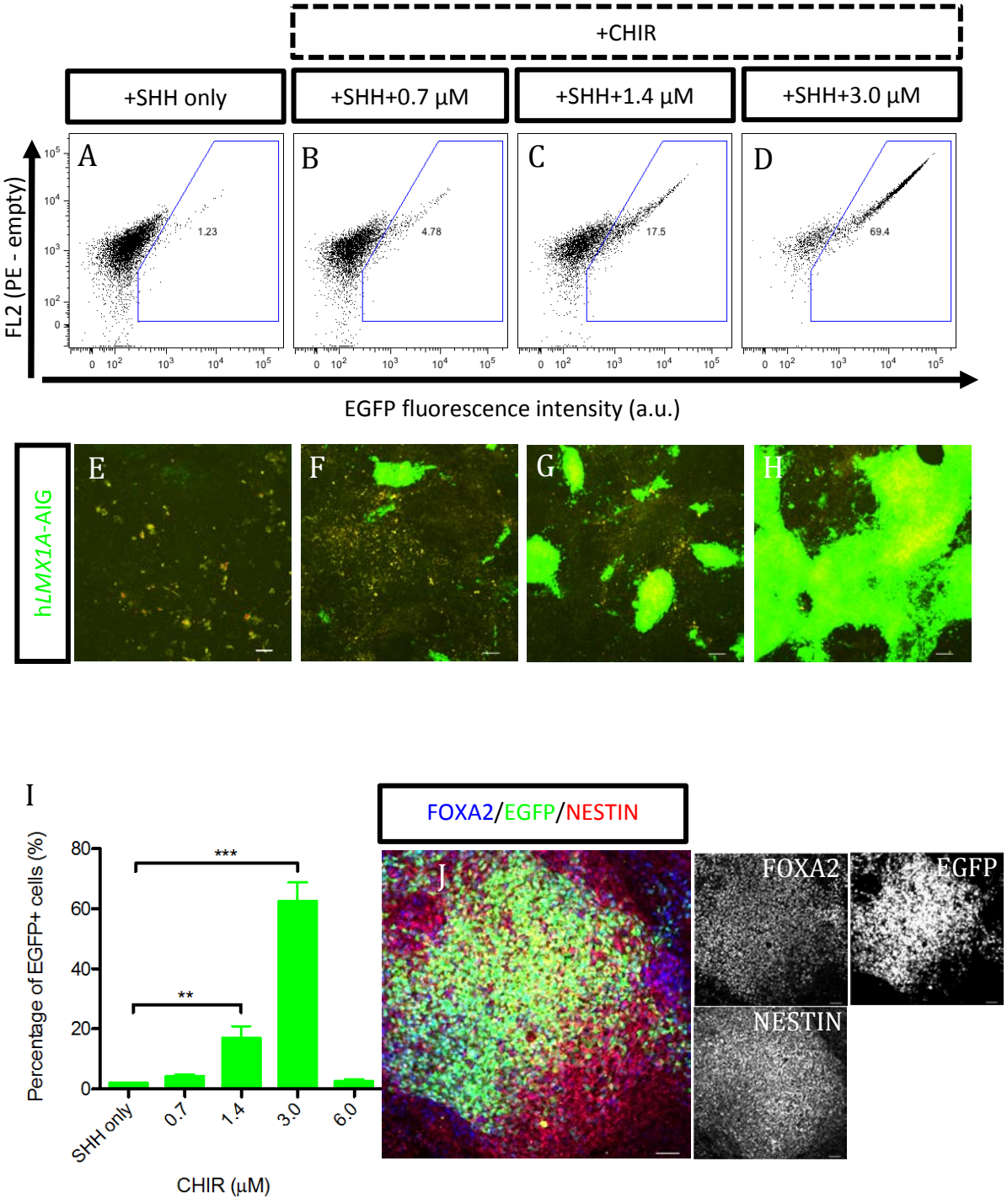

Figure 5.6 CHIR99021 efficiently induces EGFP from h*LMX1A*-AIG cells. FACS dot plots of EGFP expression following treatment with (**A**) Vehicle, (**B**) 0.7, (**C**) 1.4 and (**D**) 3.0 µM CHIR. Day 15 live cell EGFP imaging following treatment with (**E**) Vehicle, (**F**) 0.7, (**G**) 1.4 and (**H**) 3.0 µM CHIR. (**I**) Quantification of FACS data. **(J)** Immunofluorescent image of EGFP (green), NESTIN (red) and FOXA2 (blue). Scale bars, (E-H) 50 µm. Data are presented as mean ± S.E.M. of 3 experiments. Dunnett's post hoc test was used to determine levels of significance following one-way ANOVA. Asterisks indicate statistical significance in comparison to SHH only (**, $p < .01$ and ***, $p < .001$).

5.3.7 GSK3β inhibition least to robust induction of mbDA from CDML/LSB/SHH cultures

To confirm that the expression of EGFP driven by *LMX1A*-promoter was indicative of mbDA phenotype commitment, a hPITX3-EGFP reporter cell line was engineered (see Section 5.2.3). Co-electroporation of the donor plasmid together with custom designed ZFN pairs resulted in correctly targeted puromycin resistant clones with an efficiency of 18.7 % as determined by PCR and Southern blot analysis (data not shown).

Initially, to ensure that EGP expression was denotative of PITX3 expression, hPITX3-EGFP cells were differentiated under PA6/LSB/SAG/FGF8 conditions (see Chapter 4) and assessed immunocytochemically for the co-expression of EGFP with other mbDA neuron markers. 66.3 % ± 5.7 of EGFP+ cells co-localised with FOXA2 (Fig. 5.7A & D), while TH was found co-labeled with 43.1 % ± 15.9 of EGFP positive cells (Fig. 5.7B & D). Interestingly numerous TH+/EGFP- and TH-/EGFP+ cells were also observed (Fig. 5.7B). The PITX3 antibody used in Chapter 4 did not demonstrate immunoreactivity (data not shown). No colocalisation of EGFP with GABA immunoreactive neurons was observed (Fig. 5.7C & D).

Next, hPITX3-EGFP hESCs were differentiated under CDML/LSB/SHH conditions supplemented with 3.0 μM CHIR and assessed at d25 via immunofluorescence. Numerous EGFP cells with neuronal morphology were observed following differentiation under CDML/LSB/SHH conditions together with 3 μM CHIR (Fig. 5.8 A and B). Terminally differentiated cultures were efficient in the generation of EGFP+/FOXA2+ cells (73.1 % ± 4.2; Fig 5.8 A, B & E). 57.1 % ± 4.9 (Fig 5.8 A, B & E) of EGFP+ cells co-expressed FOXA2 and TH. Of the EGFP+/TH+ double positive cells 27.2 % ± 5.7 (Fig 5.8 C, D & E) co-expressed OTX2. Interestingly numerous EGFP+/FOXA2+/TH- and EGFP+/OTX2+/TH- (Fig. 5.7 A, B, C and D) cells were observed. Importantly, very few 5-HT+ or GABA+

immunoreactive cells were detected in d25 LSB/SHH/CHIR treated cultures and none were found to co-localise with EGFP (Fig 5.8 F & G). As observed above the PITX3 antibody did not demonstrate any labeling under CDML/LSB/SHH/CHIR conditions.

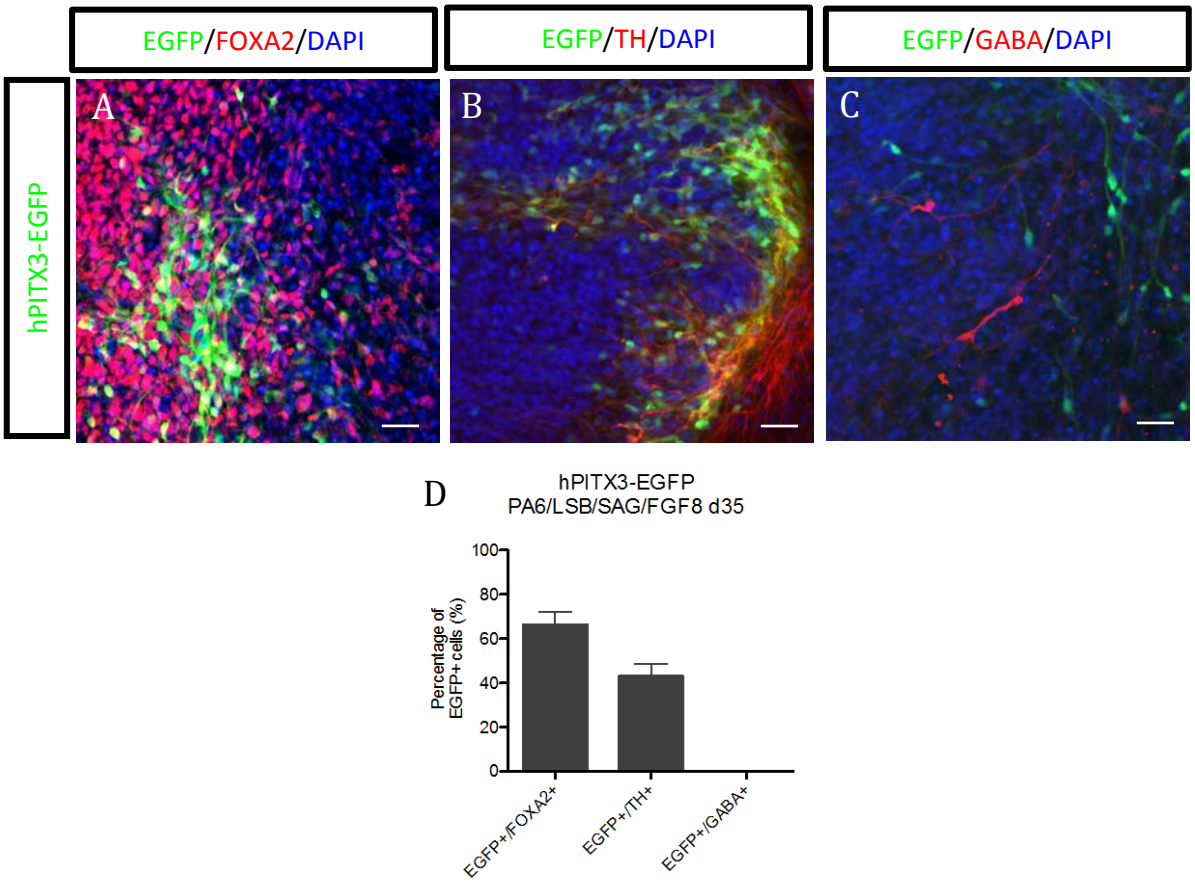

Figure 5.7 d35 hPITX3-EGFP hESCs differentiated under PA6/LSB/SAG/FGF8 conditions. Immunofluorescent images of EGFP labeled with (**A**) FOXA2 (red), (**B**) TH (red) and (**C**) GABA (red). Counterstained with DAPI (blue). Scales bars, 50 µm. (D) Quantification of double positive cells. Data are presented as mean ± S.E.M. of 3 experiments.

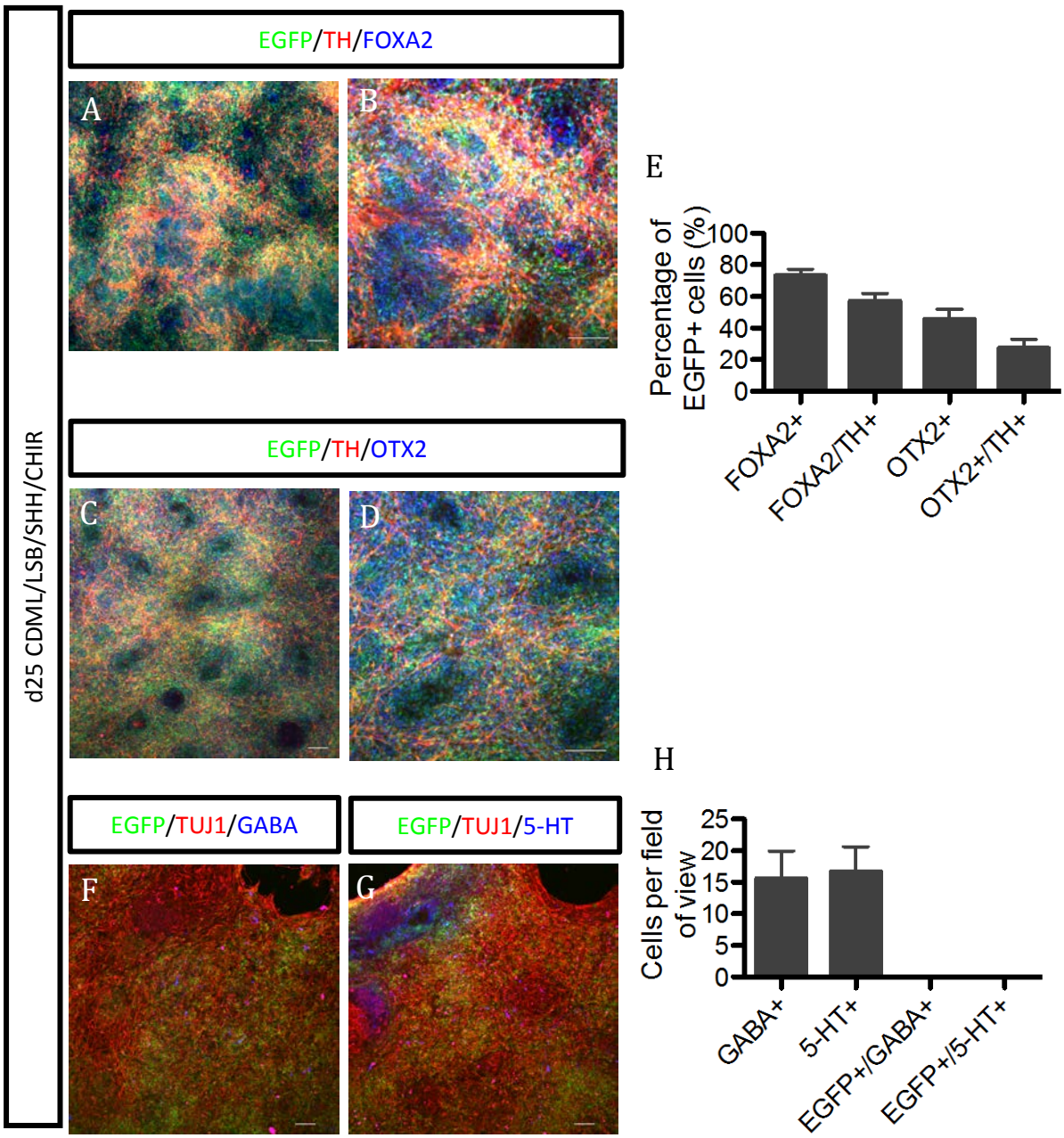

Figure 5.8 CHIR efficiently induces mbDA neurons. Immunofluorescent images of d25 CDML/LSB/SHH/CHIR cultures labeled with (**A & B**), EGFP (green), TH (red) and FOXA2 (blue). (**C & D**) EGFP (green), TH (red) and OTX2 (blue). (**E**) Quantification of A-D. (**F**) EGFP (green), TUJ1 (red) and GABA (blue) and (**G**) EGFP (green), TUJ1 (red) and 5-HT (blue). (**H**) Quantification of F & G. Scale bars, 50 µm. Data are presented as mean ± S.E.M. of 3 experiments.

5.3.8 Functional response of PITX3-EGFP positive cells

Although PITX3-EGFP positive cells present a protein profile indicative of mbDA neurons whether they are functional remained to be established. GABA (30 μM) was added to d25 cultures and assed for its ability to alter intracellular calcium levels ($[Ca^{2+}]_i$). When added to d25 cultures, both increases and decreases in $[Ca^{2+}]_i$ following GABA addition (Fig 5.9A and B) were observed. I hypothesized that the observed increase in $[Ca^{2+}]_i$ following GABA addition was due to "immaturity" of the EGFP+ cells. However after d30 of differentiation cultures would begin to detach from the matrigel coated well in sheets. It has been reported (Kriks et al., 2011) that cells require replating following prolonged culturing due to the their different substrate requirements during differentiation.

Following replating, cells migrated into large clusters, with many projections emanating from them (Fig 5.19C). At d50, GABA frequently decreased $[Ca^{2+}]_i$ (Fig 5.9B). Interestingly during the recording of baseline $[Ca^{2+}]_i$ for some regions of the well, slow spontaneous synchronous calcium oscillations were observed (Fig 5.9C and D).

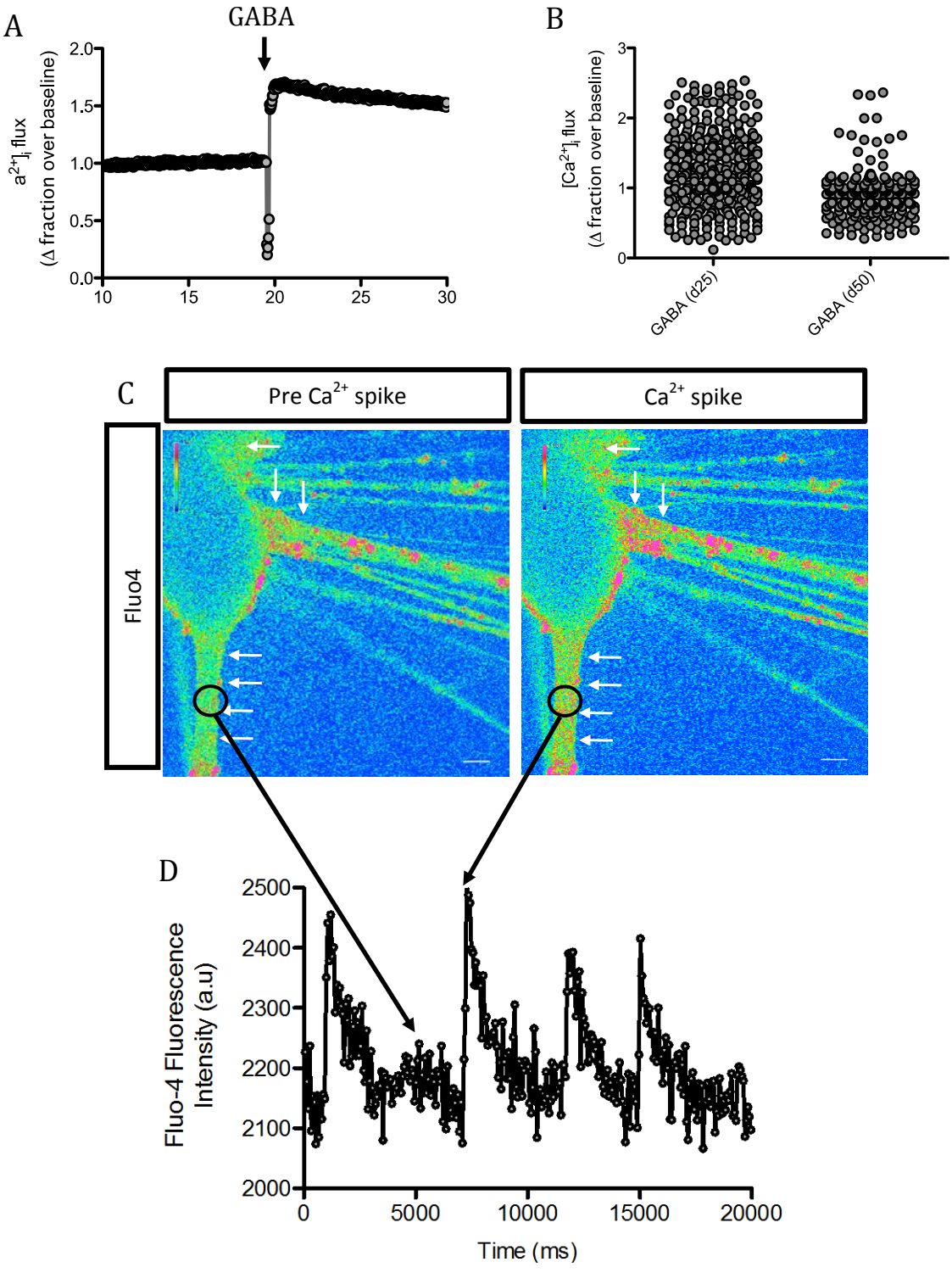

Figure 5.9 Functional activity of CDML/LSB/SHH/CHIR treated cells. (**A**) Trace showing increased $[Ca2^+]_i$ following the addition of GABA at d25. (**B**) $[Ca2^+]_i$ fluxes in response to GABA addition either at d25 (left column) or d50 (right column). (**C**) Spontaneous $[Ca2^+]_i$ oscillations in d50 cultures. Left image, Pre Ca^{2+} spike, right image, during Ca^{2+} spike. White arrows indicated ROIs with increased $[Ca2^+]_i$. (**D**) Spontaneous Ca^{2+} activity from ROI depicted in C (black circle). Scale bars, 50 µm

5.4 Discussion

5.3.1 Neural Induction under LSB chemically defined monolayer conditions

The concentration of LDN that provides the most robust neural induction under PA6 conditions was more efficient at inducing a neuroepithelial phenotype under CDML conditions. This phenomenon is most likely explained by the fact that the establishment of a homogenous single cell monolayer of cells provides more effective BMP and activin/nodal inhibition (Chambers et al., 2009), as opposed to clumps used in PA6 differentiation conditions. As there is a necessity for cost effective, recombinant protein free conditions that induce rapid and almost complete neural conversion, LSB treatment may represent such a protocol for use in the future.

5.4.2 Differentiation of hESCs under CDML/LSB conditions results in cultures with an rostral phenotype

It has been demonstrated that ESC cells differentiated under CDML/neural induction cues only, predominantly exhibit a rostral phenotype (Gaspard and Vanderhaeghen, 2006; Fasano et al., 2010; Kriks et al., 2011). This is also true for a subset of progenitors differentiated under PA6/LSB conditions as demonstrated in Chapter 4. Chemically defined monolayer conditions have previously been shown to result in a rostral phenotype (Chambers et al., 2009; Fasano et al., 2010; Kriks et al., 2011). My data is consistent with these publications, confirming that the ”default” phenotype of ESCs following neural induction is towards a rostral phenotype. One explanation for this, maybe that BMP and activin/nodal inhibition may activate signalling pathways that bias differentiating neural progenitors towards a rostral phenotype, alternatively, endogenous factors such as DKK1, produced by cells during early differentiation may result in such a bias. Data showing that induced neurons consistently

exhibit characteristics of an rostral phenotype (Lujan et al., 2012; Pang et al., 2011; Vierbuchen et al., 2010; Yang et al., 2011), unless transcription factors known to be involved in other regional specific cell types are forced expressed (Caiazzo et al., 2011; Pfisterer et al., 2011), supports the notion that a rostral phenotype maybe the default pathway of neural progenitors generated from hESCs.

5.4.3 Generation of FOXA2+ cells under CDML conditions

In contrast to cells differentiated under PA6/LSB/SAG conditions (Chapter 4), small molecule activation of smoothened with SAG did not induce FOXA2 positive cells as consistently as recombinant SHH-C25II protein together with Purmorphamine (see error bars Fig 5.3). This could be explained by the fact that PA6 cells provide endogenous SHH signalling (see Section 4.3.3), which may be initially required; and subsequently augmented by the addition of SAG. In, support of this idea, the expression of *SHH*, or its mediators *PTCH1*, *GLI1* and *GLI2* is almost completely absent under CDML conditions with neural induction cues only (Fasano et al., 2010). It is interesting to note that in a recent publication, the small molecule smoothened agonist Purmorphamine was able to induce robust FOXA2 expression (Kriks et al., 2011). The authors however only present immunofluorescent data, without quantification, thus it is difficult to ascertain whether similar levels of FOXA2+ cells are obtained using Purmorphamine in comparison to SHH-C25II. Moreover, the investigators used a combination of SHH-C25II and Purmorphamine in their final differentiation protocol. Although not explained as to why, it suggests that SHH protein signalling as discussed above may be required in addition to small molecule modulation of smoothened.

My data, showing an elevation of FOXA2 positive cell numbers in response to SHH-C25II + Purmorphamine addition was not at levels consistent with recently published

data (49.33% ± 16.11 vs. ~82%) (Kriks et al., 2011). However this publication quantified the number of FOXA2+ cells following the addition of CHIR, suggesting a requirement of canonical WNT signalling to induce proper FP conversion during differentiation. Indeed qPCR data from Kirkeby and colleagues (2012) demonstrates robust induction of FOXA2 transcript only after treatment with both CHIR and SHH. Nonetheless, there seems to be a contradiction in literature, as an earlier paper from Lorenz Studer's group, demonstrates that 80% of cells express FOXA2 following SHH-C25II addition in the absence of CHIR (Fasano et al., 2010), but the latter paper (Kriks et al., 2011), shows only a ~30% FOXA2+ population following the activation of SHH signalling in the absence of CHIR. However, as discussed above, the latter study used a combination of both SHH-C25II protein and Purmorphamine, suggesting that in the absence of CHIR, SHH protein and small molecule addition is not as potent as high concentration SHH-C25II protein alone.

5.4.4 Using h*LMX1A*-EGFP as screening tool

Work in Chapter 4 illustrates the utility of the h*LMX1A*-AIG reporter cell line as a tool for isolating mbDA neural progenitors from cultures differentiating under PA6/LSB/SAG/FGF8 conditions using FACS. I hypothesised that it could also be used a screening tool to search for factors that enrich for a mbDA phenotype, as *LMX1A*-promoter driven EGFP expression would only be observed in mbDA precursors following FP commitment induced by SHH treatment (see Ono et al., 2007; Kriks et al., 2011).

The addition of FGF8b, in contrast to SDIA/LSB/SAG conditions (Chapter 4) was only able to alter the expression of *EN1*. This observation is interesting, as a recent paper has suggested that the addition of FGF8b to CDML/LSB/SHH cultures results in cells with a hypothalamic precursor identity (Kriks et al., 2011) marked by increases in *RAX*, *SIX3*

and *SIX6* and not *EN1* (VanDunk et al., 2011). Kriks and colleagues did not report changes in *EN1* expression via their microarray analysis, making it difficult to draw conclusions regarding *EN1* expression changes in this context. As the expression domain of *EN1* is tightly regulated around the MHB (Lee et al., 1997; Simon et al., 2001), the observation that other mb, FP and mbFP genes are not altered in response to FGF8b may simply be an artifact of differentiation. Once again this is pure conjecture and would require more in-depth analysis to resolve.

The addition of WNT1 at d2 increased the expression of both *LMX1A* and *EN1*, however, this was not accompanied by decreases in *FOXG1* transcript or changes in levels other markers, *FOXA2*, *NTN1*, *CORIN* or *NGN2*. As WNT1 has been reported to be involved in an auto regulatory loop with *LMX1A* (Chung et al., 2009), canonical WNT signalling activation by exogenous WNT1 maybe sufficient to induce expression of *LMX1A* and *EN1* following high activity SHH (the use of SHH-C25II instead of SHH-N) signalling (Fasano et al., 2010; Kriks et al., 2011) in a CDML context, but not the induction of other mbDA genes. Kriks and colleagues report the investigation of WNT1 in the caudalisation of progenitors under CDML/LSB conditions, but do not provide any data as to it effects on gene expression or the induction of *LMX1A*, thus once again its difficult to draw conclusions regarding the changes in gene expression in response to the addition of WNT1 in a CDML context.

My data showed that, for hESCs differentiating under CDML/LSB/SHH conditions, the SPIE factor combination altered the rostrocaudal regionalisation a subset of cells toward a mbDA progenitor phenotype. This finding is consistent with data published by Vazin and co-workers (2009) who demonstrated an up regulation of mbDA markers following SPIE addition. Together these data confirm that SPIE factors alter

differentiating hESCs, pushing them towards a mbDA progenitor phenotype. As these changes are only observed following the addition of SPIE factors at d2, it is clear that a temporal requirement for the induction of mbDA neurons exists. Similar temporal requirements have been observed for SHH specification of the FP under CDML conditions (Fasano et al., 2010), and more recently the addition of CHIR in the induction of *LMX1A* (Kriks et al., 2011).

5.4.5 SPIE factor treatment results in the production of mbDA neurons

As outlined above, markers of a mbDA progenitor fate were observed following the addition of SPIE factors at d2. Neurons with a mbDA phenotype were also observed following differentiation to d25. It should be noted, however, that the efficiency of the SPIE factor treatment was very low, with only ~20% of TH positive cells demonstrating an immunocytochemical profile indicative of a mbDA neuron, which was consistent with my EGFP FACS data. As Vazin and co-authors (2009) did not quantify the number of mbDA neurons following SPIE treatment in their study, putting the efficiency observed in this investigation into context of previously published work is difficult.

The screening investigation performed by Vazin and colleagues (2009) identified 288 genes that were differentially regulated in cultures that exhibit SDIA activity. The SPIE factors were selected based on their CNS development and regulatory roles, as well as the fact that they are known secreted molecules. However, other work has demonstrated that membrane bound proteins synergize with secreted proteins to induce mbDA neurons from ESCs under SDIA conditions (Kawasaki et al., 2000; Yamazoe et al., 2005). Thus, the selection criteria used by Vazin and colleagues may have excluded other factors that are important in the generation of mbDA neurons via SDIA. Nonetheless, the

lack of commercial availability of a number of these known proteins makes it difficult to search for candidate factors that may enhance a commitment to a mbDA fate.

The addition of FGF8b did not result in the production of neurons with a mbDA phenotype. This was not unexpected, as mbDA progenitor screening did not demonstrate induction of either EGFP or many of the genes associated with mbDA phenotype. WNT1 addition was able to induce mbDA neurons in d25 cultures, albeit inefficiently. This is interesting given the fact that with the exception of *LMX1A*, midbrain specific transcripts were not upregulated following WNT1 incubation. Again this is difficult to put into context, as the only study that examines WNT1 addition under CDML conditions does not provide any data as to its ability to induce mbDA neurons (Kriks et al., 2011).

5.4.6 GSK3β inhibition caudalises progenitors differentiating under CDML/SHH conditions.

The addition of SPIE factors, at d2, to cultures differentiating under CDML/LSB/SHH conditions resulted in the biggest increases in expression of EGFP. Moreover, SPIE treatment induced mbDA progenitor genes and a immunocytochemical profile indicative of mbDA neurons, consistent with previous work (Vazin et al., 2009). It was hypothesized that extraction of EGFP+ cells from h*LMX1A*-EGFP hESCs differentiating under CDML/LSB/SHH/SPIE conditions may allow enrichment of mbDA neurons in terminally differentiating cultures, as observed in Chapter 4. However, during the time that I was setting up these experiments, publications from (Kirkeby et al., 2012; Kriks et al., Xi et al., 2012) demonstrated that the addition of a small molecule GSK3β inhibitor, CHIR99021 (CHIR), which mimics canonical WNT signalling (Lyashenko et al., 2011), could robustly induce the expression of *LMX1A* and other related mbDA genes. Thus CHIR was assayed in my hands for its ability to induce a mbDA progenitor

phenotype. The addition of CHIR, generated hESC-derived neural progenitors with an immunocytochemical and transcriptional profile similar to mbDA progenitors (Kirkeby et al., 2012; Kriks et al., 2011). Three micromolar CHIR was the optimal concentration for the induction mbDA progenitors as determined by EGFP expression and FOXA2 co-localisation. This finding is consistent with the demonstration of mbDA neuron induction using CHIR (Kriks et al., 2011) but is in contrast to latter studies (Kirkeby et al., 2012; Xi et al., 2012). I speculate that this difference is a result the timing of CHIR-mediated canonical WNT signalling as both the Kirkeby and Xi studies added CHIR from d0 (Kirkeby et al., 2012; Xi et al., 2012). However, the use of EBs in the Kirkeby study may also contribute to the differential level of GSKβ inhibition necessary for mbDA neurogenesis, as endogenous WNTs have previously been shown in EBs (Berge et al., 2008).

5.4.7 GSK3β inhibition least to induction of mbDA neurons from CDML/LSB/SHH cultures

To further confirm the identity of cells differentiated under CDML conditions supplemented with LSB/SHH/CHIR, a hPITX3-EGFP reporter cell line was engineered. The restricted expression of PITX3 in the ventral midbrain of the developing CNS and adult brain (Smidt et al., 1997) makes it an ideal candidate as a genetic reporter of mbDA neuron fate commitment. This approach is exemplified by a publication that used a mESC PITX3 reporter cell line to purify mbDA neurons, which were subsequently shown to maintain a functional mbDA phenotype following grafting into a 6-OHDA model of PD (Hedlund et al., 2008).

Although the generation of a hESC PITX3 reporter cell line has already been described (Hockemeyer et al., 2009), its differentiation has not. This is presumably due to the lack of a protocol that could reliably generate *PITX3* expressing cells at the time.

Currently, only one publication has investigated the expression of *PITX3* transcript in a CDML context (Kriks et al., 2011). As the authors reported very low levels of *PITX3* induction it was initially not known if *PITX3*-promoter driven EGFP expression could be detected under CDML/LSB/SHH/CHIR conditions. This, together with the uncertainty regarding mbDA neuron induction under CDML/LSB/SHH/CHIR conditions provided impetus for me to initially differentiate the hPITX3 reporter cell line using PA6/LSB/SAG/FGF8 conditions (see Chapter 4). EGFP was observed by d35, confirming that EGFP was detectable under the control of *PITX3* regulatory elements. Moreover, EGFP co-localised with both FOXA2 and TH, but never with GABA confirming specific expression of EGFP in mbDA neurons. Consistent with the work of Kriks and co-workers, I found that the addition of CHIR together with high activity SHH signalling under CDML induced widespread expression of EGFP driven by *PITX3* regulatory elements. EGFP co-localised with TH, FOXA2 and OTX2, demonstrating that timed exposure to CHIR could indeed induce mbDA neurons. At d25 I observed numerous EGFP+/FOXA2+/TH- cells which may reflect the SNpc vs. VTA phenotypic component of cultures, as in the SNpc, expression of PITX3 occurs before TH (Maxwell et al., 2005). Although this is pure speculation and is difficult to interpret such data as it is confounded by experimental issues such as EGFP maturation time, protein half life and immunofluorescent detection limits of TH expression (Li et al., 1998). Nonetheless recent work has demonstrated that the expression of OTX2 is restricted to VTA mbDA neurons (Di Salvio et al., 2010). This together with the observation that not all EGFP+ or TH+ cells coexpress OTX2 under CDML/LSB/SHH/CHIR gives some weight to this notion.

5.4.8 Functional response in hPITX3-EGFP positive cells

Primary input into the SNpc is provided by GABAergic neurons (Lee & Tepper, 2009). My data showed that after d25 of differentiation, EGFP+ cells responded to GABA. Although, both increases and decreases of $[Ca^{2+}]_i$ were observed, this was probably indicative of cells at different stages of maturity. Certainly, data from mESC-derived DA neurons (Watmuff et al., 2012) has demonstrated that immature neurons will depolarize in response to GABA as a result of high levels of intracellular Cl^- (Ben-Ari et al., 2007). This also corroborated by the fact that the majority of neurons in more "mature" d50 cultures that respond to GABA show decreases in $[Ca^{2+}]_i$.

Adult DAergic neurons of the SNpc show electrophysiological characteristics that distinguish them from other neurons in the brain. For example they demonstrate slow spontaneous pacemaking activity accompanied by a slow, sub-threshold oscillatory profile (Guzman et al., 2010). Protracted *in vitro* differentiation resulted in similar physiological characteristics such as spontaneous pacemaking in the absence of neurotransmitters, suggesting that d50 cultures contain cells of a mature mbDA phenotype, of particular a SNpc phenotype, which is consistent with a previous publication (Kriks et al., 2011). This, to an extent, gives weight to the earlier suggestion that CDML/LSB/SHH/CHIR cultures contain a mix of VTA and SNpc neurons (see Section 5.4.8). Although not conducted in this study it would be necessary to show abrogation of spontaneous Ca^{2+} activity using a L-type calcium channel blocker, to confirm their true SNpc nature, as has been demonstrated for *ex vivo* mbDA preparations (Guzman et al., 2010).

Although these data demonstrate that hESCs differentiated under CDML/LSB/SHH/CHIR conditions possess functional capacity, especially following protracted differentiation; as well as activity concomitant with SNpc pacemaking activity,

further studies will be required to ascertain whether all physiological features of SNpc neurons are recapitulated. Recent work has shown that cells differentiated under CDML/LSB/SHH/CHIR conditions and engrafted into animal models of PD reverse motor symptoms and posses the ability to re-innervate striatal compartments (Kriks et al., 2011), indicating they have the capacity to function like *bona fide* mbDA neurons.

5.5 Conclusion

The use of ESC-derived mbDA cells for CRT, *in vitro* modelling and drug screening is dependent on producing *bona fide* functional mbDA neurons in a chemically defined, xenofree system. In my hands efficient neuralisation of CDML cultures could be achieved using two small molecule inhibitors of BMP and TGFβ signalling. Similar to CDML differentiation of mESC, hESCs defaulted to a rostral phenotype, which could be altered by the addition of either a small molecule or by protein modulation of SHH signalling; although small molecule activation of smoothened via SAG was not as consistent as it was with SHH-C25II recombinant protein together with Purmorphamine. Previous reported caudalising agents such as FGF8b and WNT1 could not efficiently direct differentiating ventralised neuroepithelia towards a mbDA fate. The addition of four recombinant proteins, the SPIE factors, previously identified as factors secreted by PA6s, altered the rostrocaudal specification of differentiating cells, but only to a very limited extent. A recently described, GSK3β inhibitor, CHIR, which mimics canonical WNT signalling, robustly induced both mbDA progenitors and neurons. Following *in vitro* maturation of CDML/LSB/SHH/CHIR treated cultures, functional response to GABA the predominant neurotransmitter input into the SNpc was observed. More over, cultures demonstrated spontaneous activity indicative of *bona fide* SNpc neurons. These data demonstrate that following stepwise timed exposure to morphogens mimicking the environment in which

mbDA neurons develop *in vitro*, *bona fide* functional mbDA neurons can be generated from hESCs in a chemically defined monolayer context.

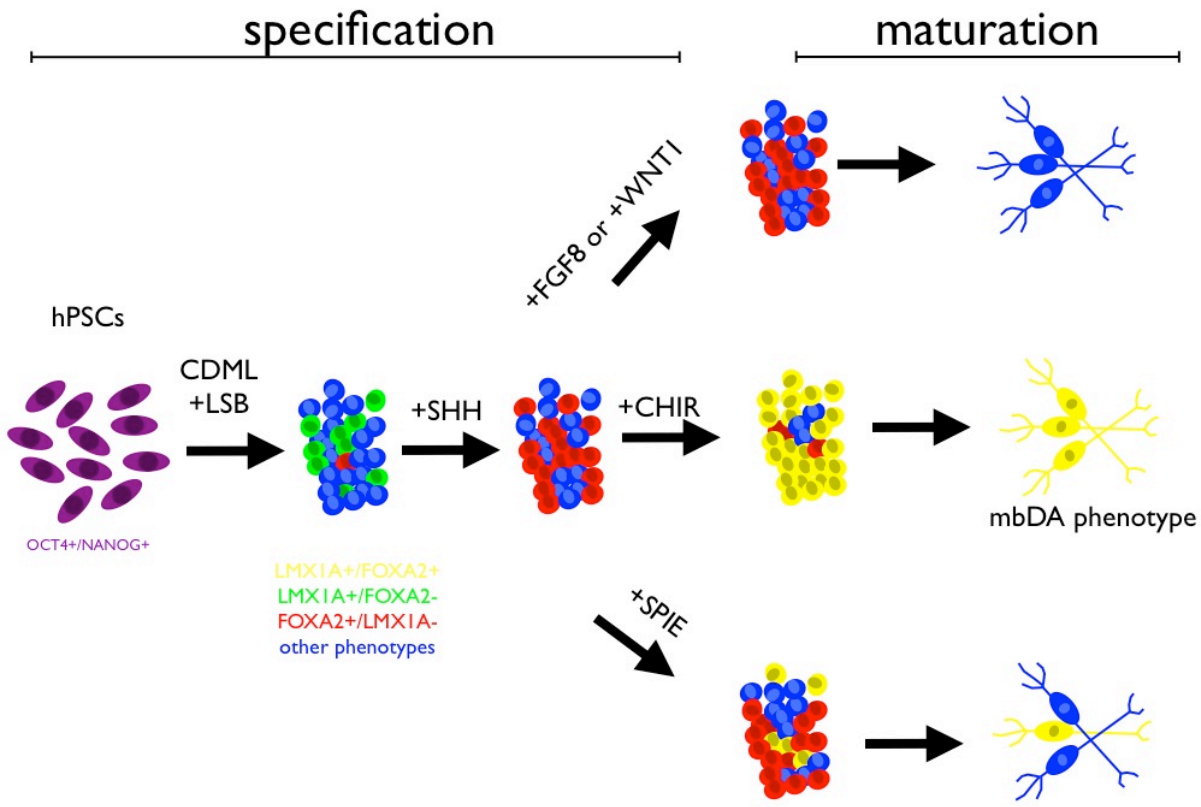

Figure 5.10 CDML differentiation and specification model. Neural induction is achieved by LSB inhibition of BMP and TGFβ signalling. Numerous EGFP+ (*LMX1A*+, green) cells are observed following LSB treatment. The addition of SHH + Purmorphamine robustly induces the number of cells positive for FOXA2 (red) while concomitantly abolishing EGFP+ (*LMX1A*+, green) cells. The addition of FGF8b or WNT1 does not affect the R/C specification of neurons. SPIE factor addition slightly increases the number of mbDA neurons (yellow). CHIR robustly increased the number of mbDA neurons following maturation.

Chapter Six: General Discussion

The generation of somatic cell types from ESCs has motivated scientists to interrogate questions of human development, disease processes and even attempt to replace degenerate, malfunctioning or dead cells in the body. These experimental concepts are all, however, dependent on the ability to generate *bona fide* functional cellular phenotypes. Although on the face of it, these appear to be rather ambitious goals, considerable advancements have already been described (Urbach et al., 2004; Wang et al., 2013).

The derivation of cells with a mbDA phenotype from ESCs may pave the way for CRT, for PD patients whose disease is refractory to current pharmacotherapy or physical interventions such as DBS. Moreover, the derivation of functional *bona fide* mbDA neurons may also help interrogate the molecular processes that underlie pathogenesis of PD, through *in vitro* PD modelling. Work in this thesis examined the hypothesis that ESC-reporter lines, driven by the *Lmx1a*-endogenous promoter would allow the enrichment, following FACS, of mbDA neurons in terminally differentiated cultures. The survival, integration and regenerative capacity of grafted *Lmx1a* positive precursors in a MPTP mouse model of PD were also examined. Finally it was hypothesised that both the human *LMX1A* and PITX3 reporter cell lines would provide screening tools, to search for factors that would help delineate the chemically defined monolayer conditions required for the generation of mbDA from hESCs.

Findings presented in this thesis demonstrate that the MPTP mouse model of PD is not suitable to assess the functional regenerative capacity of grafted *Lmx1a* positive precursors. In addition to the demonstration that *Lmx1a* is a context specific marker of mbDA progenitors in both mouse and human ESCs; it was also shown that the isolation and subsequent grafting of *Lmx1a* positive progenitors did not result in differentiation or

integration into the host striatal circuitry of MPTP treated mice. Finally, it was demonstrated that, following stepwise exposure to morphogens that approximate *in vitro* mbDA neuron developmental conditions, functional mbDA neurons could be derived from hESCs.

Accurate assessment of the translational potential of ESC-derived cell sources for human CRT requires selection of an animal model that reflects the neurochemical, pathophysiological and behavioural changes of PD. The 6-OHDA rat and mouse model has been the most widely used in transplantation studies (Cai et al., 2010; Chung et al., 2011; Kirkeby et al., 2012; Kriks et al., 2011; Parish et al., 2008; Zhu et al., 2009). The unilateral lesion induced by 6-OHDA may be assessed by the rotational asymmetry behavioural assay to give a robust measure of the functional regenerative capacity of grafted cells (Thompson et al., 2005). In contrast, the MPTP model is more clinically reminiscent of PD than the lesion induced by 6-OHDA treatment and thus has proved extremely valuable in testing neuroprotective and neurorestorative strategies (Araki, Kumagai, Tanaka, Matsubara, & Kato, 2001; Delgado & Ganea, 2003; Geng, Song, Pu, & Tu, 2004; Lu, Ko, Chen, & Huang, 2008; Zhang et al., 2004; Tripanichkul et al, 2006; Ayton et al., 2012). However, to date only one investigation has utilised the MPTP mouse model in the evaluation of ESC-derived grafts (Fukuda et al., 2006).

In this study *Lmx1a* positive progenitors did not integrate or differentiate following engraftment into MPTP treated mice. Lack of engraftment may result because *Lmx1a* positive precursors are not a suitable cell source for grafting. Alternatively, the MPTP model of PD may not support the growth and differentiation of grafted progenitors, possibly because of the lack of appropriate differentiation, guidance or maintenance cues. To begin to assess the role of cell-specific vs. model-specific issues in engraftment, I

proposed to assess engraftment of control populations, including *Lmx1a* negative or non-sorted cell populations. However, due to concerns of the local ethics committee, I was not permitted to assess the fate of appropriate control cell populations. Specifically, their concerns included that the presence of contaminating undifferentiated cells in *Lmx1a* negative or non-sorted cell populations might result in teratoma formation. While additional insights maybe gained from studying the contributions of such specific cell populations, mouse or rat models are of limited usefulness due to differences in neurochemistry, anatomy and behaviour compared to humans. To address these caveats, recent studies have employed a more clinically relevant model of PD through the use of MPTP-treated monkeys (Muramatsu et al., 2009; Takahashi et al., 2009; Kriks et al., 2011). Although limited, the information that is available to date suggests that human hESC-derived mbDAergic neurons successfully engraft in this model (Kriks et al., 2011).

Although a substantial body of work outlines progress towards the generation of mbDA neurons from hESCs (Zeng et al., 2004; Yan et al., 2005; Sonntag et al., 2007; Kriks et al., 2011; Kirkeby et al., 2012; Denham et al., 2010; 2012), significant obstacles remain in moving this technology from the bench to the clinic. Chapter 3 demonstrated that the isolation of mbDA progenitors from differentiating mESCs using a *Lmx1a* reporter cell line is context specific. However, due to differences in neurochemistry and function, mESC-derived mbDA neurons are not suitable candidates for CRT in PD patients, or for *in vitro* based PD modelling and high throughput new chemical entity (NCE) screening. Thus, for clinical and industrial translation to become a reality, there is a need to derive mbDA cells from human ESCs. Work presented in Chapter 4, demonstrated that following the inhibition of commitment to other lineages such as trophectoderm, mesendoderm and non-neural ectoderm by the use of inhibitors of TFGβ superfamily receptors, e.g.

ALKs (Chambers et al., 2009) and after correct regional specification through the use of small molecules, mbDA neurons could be generated from hESCs, demonstrating proof of principle of hESC technology. However, this was achieved in the presence of stromal cells following FACS isolation of *Lmx1a* positive cells. The use of stromal cell lines in the directed differentiation of hESCs is not suitable for CRT or mbDA cell based PD modelling and NCE screening because GMP compliance will require full characterisation of culture components as well as xenofree derivation conditions. Accordingly, the focus of the last experimental chapter was to define stromal free conditions required for the generation of regionally specified DA precursors and neurons *in vitro*. Following timed exposure to morphogens that approximate *in vitro* mbDA neuron developmental conditions (SHH and WNT signalling), functional DA neurons with a protein profile indicative of a midbrain phenotype could be derived. However, due the use of KnockOut™ Serum Replacement and Matrigel™, which are undefined and contain animal derived components, this current approach is not GMP compliant and thus not suitable for clinical applications. A recent study has addressed this issue by the use of a fully chemically defined medium through the generation of EB cultures that are sub-cultured and subsequently plated onto defined substrates and matured to mbDA neurons. However, this protocol has many steps therefore it is questionable whether the Kirkeby et al., (2012) protocol can be scaled up to meet clinical and industrial needs. Thus, for translation of ESC-derived mbDA for CRT or PD cell based modelling and NCE screening to be realised, a fully characterised chemically defined robust, reproducible non-labour intensive protocol amenable to scaling up, e.g. suspension bioreactors will be required. Although the advent of recent tissue engineering technologies is beginning to provide a system in which large-scale differentiation can be undertaken, if neurons are to be used in assays, particularly of a

high throughput manner, a replating monolayer step will be required in order to provide an assay format that is compatible current technologies, such as plate readers or microscopes.

While genetically modified reporter ESC lines may not appropriate for transplantation in human patients due to concerns surrounding transgene activation of proto-oncogenes (Kaji & Leiden, 2001), reporter cell lines may help elucidate cellular mechanisms that will direct future clinical trials. For example reporter cell lines may help reveal the optimal stage of differentiation of the cell source for PD CRT. Only one study to date has investigated the optimal stage of differentiation. Kriks and colleagues show that d25 cells survive, differentiate and integrate in a monkey model of PD, and bring about substantial behavioural improvement in rat and mouse models (Kriks et al., 2011). The motivation for using d25 cells is that they avoid introducing proliferative progenitors from less mature cultures, which can cause neural overgrowths (Roy et al., 2006). However, both work presented in Chapter 6, and in Kriks et al., (2011) demonstrate, that d25 cultures contain a mixture of LMX1A+/FOXA2+/TH+ and LMX1A+/FOXA2+/TH- cells. Thus, it unknown whether the LMX1A+/FOXA2+/TH- neural progenitors or LMX1A+/FOXA2+/TH+ immature neurons or both populations are responsible for the behavioural reversals observed in PD modelled animals. As discussed in Section 1.2.3.a, the transcription factor NR4A2 is expressed by mbDA progenitors when they leave the cell cycle and subsequently express TH. Therefore, the isolation of cells based on the reporter expression driven by either the *NR4A2* or *TH* endogenous promoter may help address whether neural progenitors or immature neurons will result in a more successful cell source of transplantation.

The end goal of using hESC-derived mbDA cells in either CRT or *in vitro* modelling and NCE screening will require large numbers of cells. This raises issues, such as the cost of scaling up differentiation to meet patient and industry needs. Work presented in both Chapter 4 and 5 revealed that the use of cheap, highly potent, small molecule ligands such as canonical WNT signalling mimetics and inhibitors of BMP and TGFβ signalling efficiently directed the fate of differentiating hESCs in place of recombinant protein. In contrast, findings presented in this thesis suggest that the specification of FP cells appears more difficult than simply substituting currently available small molecule smoothened agonists for SHH protein. Despite this, small molecule ligands of smoothened could be used to augment exogenous SHH protein, thus helping to control large-scale derivation costs. Given that trophic factors such as GDNF, BDNF and TGFβ3 are required from d11 until terminal differentiation (> d50), for the maturation and survival of mbDA neurons, mimicking these recombinant proteins will also reduce large-scale derivation costs of mbDA neurons. However, the use of small molecules to mimic GDNF, BDNF and TGFβ3 may prove to be extremely difficult, as the activation of receptor tyrosine kinase signalling requires ligand mediated dimerization a process which requires the occupancy of large chemical space (Ibáñez et al., 1993; Wiesmann et al., 1999). This, however, could be overcome by modulating proteins in signalling pathways that are downstream of the receptor(s), similar to the effects induced by CHIR on WNT activation via the inhibition of GSK3β.

However it should be noted, that although the use of small molecules addresses issues such as cost and growth factor lot variation, there can also be downsides associated with their use. For example a recent study that investigated specificities of common small molecules used in the neural specification of hESCs, such as LDN and

SB431542 (compounds used in this thesis) substantial off target effects were demonstrated on a panel of protein kinases (Vogt, Traynor, & Sapkota, 2011). Given that the field is moving more and more towards the use of small molecules in differentiation, studies will need to be conducted to examine the off target effects of newly discovered small molecules.

The behaviour of cultures during *in vitro* maturation also raises significant issues for *in vitro* PD modelling and subsequent high throughput NCE screening. Work presented in Chapter 4 and 5 demonstrated that the protracted culturing of mbDA neurons leads to significant changes in the morphology of ESC-derived mbDA neuronal cultures. Specifically, the migration of cells into clusters with complex three-dimensional architecture poses a problem. These clusters are difficult to work with, as they tend to detach from the well and float in culture. Thus the amenability of mature mbDA neural cultures to high throughput NCE screening will prove difficult. Recent work has demonstrated that small peptide epitopes can be integrated into three dimensional scaffolds that are functionally active and provide differentiation and maturation cues for certain phenotypes (Levenberg et al., 2005). Whether this can be achieved for mbDA neural differentiation remains to be addressed, however scaffold biology and three-dimensional cultures will most likely play a major role in moving forward the PD *in vitro* modelling and NCE screening.

Numerous other difficulties exist in moving these discoveries from the bench to the clinic. Of note is the dependence of MEF layers on the maintenance of pluripotent hESC cultures. When maintained on MEFs, hESCs can incorporate molecules such as N-Glycolylneuraminic acid, a reactive sialic acid that renders hESC-derived cells subject to immune rejection in humans (Robinton & Daley, 2012). Although “partially” chemically

defined feeder free conditions have been developed for the maintenance of hESCs, including mTeSR™ and Matrigel™, feeders still remain the gold standard, as pluripotency is lost following numerous passages under "partial" chemically defined conditions (Desbordes & Studer, 2012). It will be interesting to see if the recent advances in a fully defined chemical culture system can address such issues (Chen et al., 2011).

Finally, although work presented in this thesis demonstrates the derivation of functional mbDA neurons following timed exposure to morphogens that mimic *in vitro* mbDA neuron developmental conditions, the efficiency of differentiation is still not even close to 100% (Kriks et al., 2011; Ganat & Studer, 2013). Moving forward to CRT, the presence of undefined cell types raises issues of translation of ESC-derived mbDA cells into a clinical setting. A recently approved patent from the Studer lab addressed this issue through the use of a cell surface antibody for the GUCY2C receptor, which was shown to be expressed exclusively on mbDA neurons of the SN (Ganat & Studer, 2013). The use of this antibody together with cell isolation techniques such as FACS and magnetic assisted cell sorting, would allow the preparation of pure mbDA neurons for grafting, of CRT for PD feasible.

While our understanding of the molecular mechanisms of neurodegeneration has improved since James Parkinson's initial description, disease-modifying pharmacotherapies remain elusive. With an ageing population, the management of PD is proving an increasingly important and challenging aspect for medical professionals and governments. The notion of CRT for PD, which began back in the late 1970s with seminal work using exogenous sources of DAergic cells prepared from fetal VM preparations, is becoming a reality with the pioneering work over the last two decades in the derivation of mbDA cells from ESCs. However, for the immediate future numerous hurdles, in both

scientific and regulatory issues still remain to be addressed before translation of hESC-based CRT from the laboratory into the clinic. A more immediate benefit that may arise from the ESC-derivation of mbDA cells is their use in disease modifying NCE discovery. As outlined, current pharmacotherapy and other disease management strategies address symptoms and do not alter the progression of the PD disease course. This is most likely due to the lack of understanding surrounding the molecular pathogenesis of PD due to the limitations of current methodologies available to study PD, such as non-human relevant animal and cell culture models. Additionally, characterisation of the conditions required for the derivation of ESCs into mbDA neurons will enhance our understanding of developmental neurobiology and may provide insights into the derivation of other neural phenotypes, providing a platform for the therapeutic intervention into other neurodegenerative disease.

References

Aberle, H., Bauer, A., Stappert, J., Kispert, A., & Kemler, R. (1997). beta-catenin is a target for the ubiquitin-proteasome pathway. *The EMBO Journal*, 16(13), 3797–3804. doi:10.1093/emboj/16.13.3797

Adams, K. A., Maida, J. M., Golden, J. A., & Riddle, R. D. (2000). The transcription factor Lmx1b maintains Wnt1 expression within the isthmic organizer. *Development*, 127(9), 1857–1867.

Alam, M., & Schmidt, W. (2002). Rotenone destroys dopaminergic neurons and induces parkinsonian symptoms in rats. *Behavioural brain research*, 136(1), 317–324.

Alavian, K., Scholz, C., & Simon, H. (2008). Transcriptional regulation of mesencephalic dopaminergic neurons: The full circle of life and death. *Movement Disorders*, 23(3), 319–328.

Albin, R., & Young, A. (1989). The functional anatomy of basal ganglia disorders. *Trends in Neurosciences*, 12(10), 366–375.

Alcamo, E. A., Chirivella, L., Dautzenberg, M., Dobreva, G., Fariñas, I., Grosschedl, R., & McConnell, S. K. (2008). Satb2 regulates callosal projection neuron identity in the developing cerebral cortex. *Neuron*, 57(3), 364–377. doi:10.1016/j.neuron.2007.12.012

Ambasudhan, R., Talantova, M., Coleman, R., Yuan, X., Zhu, S., Lipton, S. A., & Ding, S. (2011). Direct Reprogramming of Adult Human Fibroblasts to Functional Neurons under Defined Conditions. *Cell stem cell*, 9(2), 113–118. doi:10.1016/j.stem.2011.07.002

Amit, M., Shariki, C., & Margulets, V. (2004). Feeder layer-and serum-free culture of human embryonic stem cells. *Biology of Reproduction*

Amizuka, N., & Karaplis, A. C. (1996). Haploinsufficiency of parathyroid hormone-related peptide (PTHrP) results in abnormal postnatal bone development. *Developmental Biology* 175(1):166-76.

Andersson, E, Jensen, J., Parmar, M., Guillemot, F., & Bjorklund, A. (2006a). Development of the mesencephalic dopaminergic neuron system is compromised in the absence of neurogenin 2. *Development*, 133(3), 507–516.

Andersson, Elisabet, Tryggvason, U., Deng, Q., Friling, S., Alekseenko, Z., Robert, B., Perlmann, T., & Ericson, J. (2006b). Identification of Intrinsic Determinants of Midbrain Dopamine Neurons. *Cell*, 124(2), 393–405.

Andersson, Elisabet, Tryggvason, U., Deng, Q., Friling, S., Alekseenko, Z., Robert, B., Perlmann, T., & Ericson, J. (2006c). Identification of intrinsic determinants of midbrain dopamine neurons. *Cell*, 124(2), 393–405. doi:10.1016/j.cell.2005.10.037

Andres-Mateos, E., Perier, C., Zhang, L., Blanchard-Fillion, B., Greco, T. M., Thomas, B., et al. (2007). DJ-1 gene deletion reveals that DJ-1 is an atypical peroxiredoxin-like peroxidase. *Proceedings of the National Academy of Sciences*, 104(37), 14807–14812. doi:10.1073/pnas.0703219104

Ang, S. (2006). Transcriptional control of midbrain dopaminergic neuron development. *Development*, 133(18), 3499–3506.

Anokye-Danso, F., Trivedi, C. M., Juhr, D., Gupta, M., Cui, Z., Tian, Y., et al. (2011). Highly Efficient miRNA-Mediated Reprogramming of Mouse and Human Somatic Cells to Pluripotency. *Cell stem cell*, 8(4), 376–388. doi:10.1016/j.stem.2011.03.001

Arai, R., Karasawa, N., Geffard, M., & Nagatsu, T. (1994). Immunohistochemical evidence that central serotonin neurons produce dopamine from exogenousl-DOPA in the rat, with reference to the involvement of aromatic L- amino acid decarboxylase. *Brain research*, 667(2), 295–299.

Araki, T., Kumagai, T., Tanaka, K., Matsubara, M., & Kato, H. (2001). Neuroprotective effect of riluzole in MPTP-treated mice. *Brain research*. 918(1-2):176-181

Arsenijevic, Y., Villemure, J. G., Brunet, J. F., Bloch, J. J., Déglon, N., Kostic, C., et al. (2001). Isolation of multipotent neural precursors residing in the cortex of the adult human brain. *Experimental neurology*, 170(1), 48–62. doi:10.1006/exnr.2001.7691

Aurell, E., d'Hérouël, A. F., Malmnäs, C., & Vergassola, M. (2007). Transcription factor concentrations versus binding site affinities in the yeast S. cerevisiae. *Physical biology*, 4(2), 134–143. doi:10.1088/1478-3975/4/2/006

Ayton, S., Lei, P., Duce, J. A., Wong, B. X. W., Sedjahtera, A., Adlard, P. A., et al. (2012). Ceruloplasmin dysfunction and therapeutic potential for parkinson disease. *Ann Neurol*. doi:10.1002/ana.23817

Azzouz, M., Ralph, S., Wong, L., & Day, D. (2004). Neuroprotection in a rat Parkinson model by GDNF gene therapy using EIAV vector. *Neuroreport*.

Backlund, E. O., Granberg, P. O., Hamberger, B., Knutsson, E., Mårtensson, A., Sedvall, G., et al. (1985). Transplantation of adrenal medullary tissue to striatum in parkinsonism. First clinical trials. *J Neurosurg*, 62(2), 169–173. doi:10.3171/jns.1985.62.2.0169

Bain, G., Kitchens, D., Yao, M., Huettner, J. E., & Gottlieb, D. I. (1995). Embryonic stem cells express neuronal properties *in vitro*. *Developmental Biology*, 168(2), 342–357. doi:10.1006/dbio.1995.1085

Baker, J. C., Beddington, R. S., & Harland, R. M. (1999). Wnt signalling in Xenopus embryos inhibits bmp4 expression and activates neural development. *Genes & development*, 13(23), 3149–3159.

Barbeau, A. (1969). L-dopa therapy in Parkinson"s disease: a critical review of nine years" experience. *Canadian Medical Association journal*, 101(13), 59–68.

Barberi, T., Bradbury, M., Dincer, Z., Panagiotakos, G., Socci, N. D., & Studer, L. (2007). Derivation of engraftable skeletal myoblasts from human embryonic stem cells. Nature medicine, 13(5), 642–648. doi:10.1038/nm1533

Barberi, T., Klivenyi, P., Calingasan, N. Y., Lee, H., Kawamata, H., Loonam, K., et al. (2003). Neural subtype specification of fertilization and nuclear transfer embryonic stem cells and application in parkinsonian mice. *Nature biotechnology*, 21(10), 1200–1207. doi:10.1038/nbt870

Barker, R. A., Barrett, J., Mason, S. L., & Bjorklund, A. (2013). Fetal dopaminergic transplantation trials and the future of neural grafting in Parkinson's disease. The Lancet Neurology.12(1)84-91

Baron, O., Foerthmann, B., Lee, Y. W., & Terranova, C. (2012). Cooperation of nuclear FGFR1 and Nurr1 offers a new interactive mechanism in postmitotic development of mesencephalic dopaminergic neurons. *Journal of Biological Sciences*

Beal, M. F. (2001). Experimental models of Parkinson's disease. *Nature Reviews Neuroscience*, 2(5), 325–334. doi:10.1038/35072550

Beattie, G. M., Lopez, A. D., Bucay, N., Hinton, A., Firpo, M. T., King, C. C., & Hayek, A. (2005). Activin A Maintains Pluripotency of Human Embryonic Stem Cells in the Absence of Feeder Layers. *Stem cells (Dayton, Ohio)*, *23*(4), 489–495. doi:10.1634/stemcells.2004-0279

Behrens, J., Kries, von, J. P., Kühl, M., Bruhn, L., & Wedlich, D. (1996). Functional interaction of β-catenin with the transcription factor LEF-1. *Nature*.

Ben-Ari, Y., Gaiarsa, J.-L., Tyzio, R., & Khazipov, R. (2007). GABA: a pioneer transmitter that excites immature neurons and generates primitive oscillations. Physiological reviews, 87(4), 1215–1284. doi:10.1152/physrev.00017.2006

Ben-Hur, T., Idelson, M., Khaner, H., Pera, M., Reinhartz, E., Itzik, A., & Reubinoff, B. E. (2004). Transplantation of Human Embryonic Stem Cell-Derived Neural Progenitors Improves Behavioral Deficit in Parkinsonian Rats. *Stem cells*, 22(7), 1246–1255. doi:10.1634/stemcells.2004-0094

Bentivoglio, M., & Morelli, M. (2005). Chapter I The organization and circuits of mesencephalic dopaminergic neurons and the distribution of dopamine receptors in the brain. *Handbook of chemical neuroanatomy*.

Berge, ten, D., Koole, W., Fuerer, C., Fish, M., Eroglu, E., & Nusse, R. (2008). Wnt signalling mediates self-organization and axis formation in embryoid bodies. *Cell stem cell*, 3(5), 508–518. doi:10.1016/j.stem.2008.09.013

Bernheimer, H., Birkmayer, W., Hornykiewicz, O., Jellinger, K., & Seitelberger, F. (1973). Brain dopamine and the syndromes of Parkinson and Huntington. Clinical, morphological and neurochemical correlations. *Journal of the neurological sciences*, 20(4), 415–455.

Besson, M. J., Cheramy, A., Feltz, P., & Glowinski, J. (1969). Release of newly synthesized dopamine from dopamine-containing terminals in the striatum of the rat. *Proceedings of the National Academy of Sciences*, 62(3), 741–748.

Bezard, E., Gross, C. E., & Brotchie, J. M. (2003). Presymptomatic compensation in Parkinson's disease is not dopamine-mediated. *Trends in Neurosciences*, 26(4), 215–221.

Bezard, E., Gross, C., Fournier, M., Dovero, S., Bloch, B., & Jaber, M. (1999). Absence of MPTP-induced neuronal death in mice lacking the dopamine transporter. *Experimental neurology*, 155(2), 268–273.

Bhanot, P., Brink, M., Samos, C. H., Hsieh, J. C., Wang, Y., Macke, J. P., et al. (1996). A new member of the frizzled family from Drosophila functions as a Wingless receptor. *Nature*, 382(6588), 225–230. doi:10.1038/382225a0

Bibbiani, F., Costantini, L. C., Patel, R., & Chase, T. N. (2005). Continuous dopaminergic stimulation reduces risk of motor complications in parkinsonian primates. *Experimental neurology*, 192(1), 73–78. doi:10.1016/j.expneurol.2004.11.013

Biben, C., Stanley, E., Fabri, L., & Kotecha, S. (1998). Murine cerberus homologue mCer-1: a candidate anterior patterning molecule. *Developmental Biology*

Birkmayer, W., & Hornykiewicz, O. (1961). The L-3, 4-dioxyphenylalanine (DOPA)-effect in Parkinson-akinesia. Wiener klinische Wochenschrift.

Bissonnette, C. J., Lyass, L., Bhattacharyya, B. J., Belmadani, A., Miller, R. J., & Kessler, J. A. (2011). The controlled generation of functional basal forebrain cholinergic neurons from human embryonic stem cells. *Stem cells*, 29(5), 802–811. doi:10.1002/stem.626

Bjorklund, A., & Dunnett, S. B. (2007). Dopamine neuron systems in the brain: an update. *Trends in Neurosciences*, 30(5), 194–202.

Bjorklund, A., & Stenevi, U. (1979). Reconstruction of the nigrostriatal dopamine pathway by intracerebral nigral transplants. *Brain research*, 177(3), 555–560.

Bjorklund, A., Dunnett, S., Stenevi, U., Lewis, M., & Iversen, S. (1980a). Reinnervation of the denervated striatum by substantia nigra transplants: Functional consequences as revealed by pharmacological and sensorimotor testing. *Brain research*, 199(2), 307–333.

Bjorklund, A., Schmidt, R., & Stenevi, U. (1980b). Functional reinnervation of the neostriatum in the adult rat by use of intraparenchymal grafting of dissociated cell suspensions from the substantia nigra. *Cell and Tissue Research*, 212(1), 39–45.

Bjorklund, A., Stenevi, U., Schmidt, R., Dunnett, S., & Gage, F. (1983). Intracerebral grafting of neuronal cell suspensions. II. Survival and growth of nigral cell suspensions implanted in different brain sites. *Acta physiologica Scandinavica. Supplementum*, 522, 9.

Bjorklund, L. M., Sánchez-Pernaute, R., Chung, S., Andersson, T., Chen, I. Y. C., McNaught, K. S. P., et al. (2002). Embryonic stem cells develop into functional dopaminergic neurons after transplantation in a Parkinson rat model. *Proceedings of the National Academy of Sciences*, 99(4), 2344–2349. doi:10.1073/pnas.022438099

Boadle-Biber, M. C. (1993). Regulation of serotonin synthesis. *Progress in biophysics and molecular biology*, 60(1), 1–15.

Bonilla, S., Hall, A., Pinto, L., Attardo, A., Gotz, M., Huttner, W., & Arenas, E. (2008). Identification of midbrain floor plate radial glia-like cells as dopaminergic progenitors. *Glia*, 56(8), 809–820.

Boulting, G. L., Kiskinis, E., Croft, G. F., Amoroso, M. W., Oakley, D. H., Wainger, B. J., et al. (2011). A functionally characterized test set of human induced pluripotent stem cells. *Nature biotechnology*, 29(3), 279–286. doi:10.1038/nbt.1783

Bouwmeester, T., Kim, S., Sasai, Y., & Lu, B. (1996). Cerberus is a head-inducing secreted factor expressed in the anterior endoderm of Spemann's organizer. *Nature*.

Boyce, S., Kelly, E., Reavill, C., & Jenner, P. (1984). Repeated administration of N-methyl-4-phenyl 1, 2, 5, 6-tetrahydropyridine to rats is not toxic to striatal dopamine neurones. *Biochemical Pharmacology*

Boyer, L., Lee, T., Cole, M., & Johnstone, S. (2005). Core transcriptional regulatory circuitry in human embryonic stem cells. *Cell*.

Bradley, J. A., Bolton, E. M., & Pedersen, R. A. (2002). Stem cell medicine encounters the immune system. *Nature reviews. Immunology*, 2(11), 859–871. doi:10.1038/nri934

Bradley, L., Sun, B., Collins-Racie, L., LaVallie, E., McCoy, J., & Sive, H. (2000). Different activities of the frizzled-related proteins frzb2 and sizzled2 during Xenopus anteroposterior patterning. *Developmental Biology*, 227(1), 118–132. doi:10.1006/dbio.2000.9873

Brederlau, A., Correia, A., Anisimov, S., Elmi, M., Paul, G., Roybon, L., et al. (2006). Transplantation of Human Embryonic Stem Cell Derived Cells to a Rat Model of Parkinson's Disease: Effect of In vitro Differentiation on Graft Survival and Teratoma Formation. *Stem cells*, 24(6), 1433–1440.

Brimble, S. N., Zeng, X., Weiler, D. A., Luo, Y., Liu, Y., Lyons, I. G., et al. (2004). Karyotypic Stability, Genotyping, Differentiation, Feeder-Free Maintenance, and Gene Expression Sampling in Three Human Embryonic Stem Cell Lines Derived Prior to August 9, 2001. S*tem Cells Dev*, 13(6), 585–597. doi:10.1089/scd.2004.13.585

Briscoe, J., Pierani, A., Jessell, T. M., & Ericson, J. (2000). A homeodomain protein code specifies progenitor cell identity and neuronal fate in the ventral neural tube. *Cell*, 101(4), 435–445.

Brodski, C., Weisenhorn, D. M. V., Signore, M., Sillaber, I., Oesterheld, M., Broccoli, V., et al. (2003). Location and size of dopaminergic and serotonergic cell populations are controlled by the position of the midbrain-hindbrain organizer. *The Journal of neuroscience*, 23(10), 4199–4207.

Brons, I. G. M., Smithers, L. E., Trotter, M. W. B., Rugg-Gunn, P., Sun, B., Chuva de Sousa Lopes, S. M., et al. (2007). Derivation of pluripotent epiblast stem cells from mammalian embryos. *Nature*, 448(7150), 191–195. doi:10.1038/nature05950

Brott, B. (2002). Regulation of Wnt/LRP signalling by distinct domains of Dickkopf proteins. *Molecular and cellular biology*.

Brown, A., Machan, J. T., & Hayes, L. (2011). Molecular organization and timing of Wnt1 expression define cohorts of midbrain dopamine neuron progenitors *in vitro*. *The J Comp Neurol*. 15;519(15):2978-3000

Bulchand, S., Grove, E. A., Porter, F. D., & Tole, S. (2001). LIM-homeodomain gene Lhx2 regulates the formation of the cortical hem. *Mechanisms of Development.*

Burke, R., Nellen, D., Bellotto, M., Hafen, E., Senti, K. A., Dickson, B. J., & Basler, K. (1999). Dispatched, a novel sterol-sensing domain protein dedicated to the release of cholesterol-modified hedgehog from signalling cells. *Cell*, 99(7), 803–815.

Butcher, L. L., & Engel, J. (1969). Behavioral and biochemical effects of L-dopa after peripheral decarboxylase inhibition. *Brain research*, 15(1), 233–242.

Buytaert-Hoefen, K. A., Alvarez, E., & Freed, C. R. (2004). Generation of tyrosine hydroxylase positive neurons from human embryonic stem cells after coculture with cellular substrates and exposure to GDNF. *Stem cells*, 22(5), 669–674. doi:10.1634/stemcells.22-5-669

Cai, J., Donaldson, A., Yang, M., & German, M. (2009). The role of *Lmx1a* in the differentiation of human embryonic stem cells into midbrain dopamine neurons in culture and after transplantation into a Parkinson's disease Model *Stem Cells*

Cai, J., Yang, M., Poremsky, E., Kidd, S., Schneider, J. S., & Iacovitti, L. (2010). Dopaminergic neurons derived from human induced pluripotent stem cells survive and integrate into 6-OHDA-lesioned rats. *Stem Cells Dev*, 19(7), 1017–1023. doi:10.1089/scd.2009.0319

Cai, J., Zhao, Y., Liu, Y., Ye, F., Song, Z., Qin, H., et al. (2007). Directed differentiation of human embryonic stem cells into functional hepatic cells. *Hepatology*, 45(5), 1229–1239. doi:10.1002/hep.21582

Caiazzo, M., Dell'Anno, M. T., Dvoretskova, E., Lazarevic, D., Taverna, S., Leo, D., et al. (2011). Direct generation of functional dopaminergic neurons from mouse and human fibroblasts. *Nature*, (7359), 224–227. doi:10.1038/nature10284

Canet-Avilés, R., & Wilson, M. (2004). The Parkinson's disease protein DJ-1 is neuroprotective due to cysteine-sulfinic acid-driven mitochondrial localization. *Proceedings of the National Academy of Sciences*

Capdevila, J., Tabin, C., & Johnson, R. L. (1998). Control of dorsoventral somite patterning by Wnt-1 and beta-catenin. *Developmental Biology*, 193(2), 182–194. doi:10.1006/dbio.1997.8806

Carey, R. J., Pinheiro-Carrera, M., Dai, H., Tomaz, C., & Huston, J. P. (1995). L-DOPA and psychosis: evidence for L-DOPA-induced increases in prefrontal cortex dopamine and in serum corticosterone. *Biological psychiatry,* 38(10), 669–676. doi:10.1016/0006-3223(94)00378-5

Carlsson, T., Carta, M., Munoz, A., Mattsson, B., Winkler, C., Kirik, D., & Bjorklund, A. (2009). Impact of grafted serotonin and dopamine neurons on development of L-DOPA-

induced dyskinesias in parkinsonian rats is determined by the extent of dopamine neuron degeneration. *Brain*, 132(Pt 2), 319–335. doi:10.1093/brain/awn305

Carpenter, M. K., Inokuma, M. S., Denham, J., Mujtaba, T., Chiu, C. P., & Rao, M. S. (2001). Enrichment of neurons and neural precursors from human embryonic stem cells. *Experimental neurology*, 172(2), 383–397. doi:10.1006/exnr.2001.7832

Carta, M., Carlsson, T., Kirik, D., & Björklund, A. (2007). Dopamine released from 5-HT terminals is the cause of L-DOPA-induced dyskinesia in parkinsonian rats. *Brain*, 130(Pt 7), 1819–1833. doi:10.1093/brain/awm082

Carter, R. J., Lione, L. A., Humby, T., Mangiarini, L., Mahal, A., Bates, G. P., et al. (1999). Characterization of progressive motor deficits in mice transgenic for the human Huntington's disease mutation. *The Journal of Neuroscience*, 19(8), 3248–3257.

Castelo-Branco, G., Wagner, J., Rodriguez, F., Kele, J., Sousa, K., Rawal, N., et al. (2003). Differential regulation of midbrain dopaminergic neuron development by Wnt-1, Wnt-3a, and Wnt-5a. Proceedings of the National Academy of Sciences, 100(22), 12747–12752.

Cazorla, P., Smidt, M. P., O'Malley, K. L., & Burbach, J. P. (2000). A response element for the homeodomain transcription factor Ptx3 in the tyrosine hydroxylase gene promoter. *Journal of Neurochemistry*, 74(5), 1829–1837.

Celada, P., & Paladini, C. (1999). GABAergic control of rat substantia nigra dopaminergic neurons: role of globus pallidus and substantia nigra pars reticulata. *Neuroscience*.

Chamberlain, C. E., Jeong, J., Guo, C., Allen, B. L., & McMahon, A. P. (2008). Notochord-derived Shh concentrates in close association with the apically positioned basal body in neural target cells and forms a dynamic gradient during neural patterning. *Development*, 135(6), 1097–1106. doi:10.1242/dev.013086

Chambers, I. (2004). The molecular basis of pluripotency in mouse embryonic stem cells. Cloning and stem cells, 6(4), 386–391. doi:10.1089/clo.2004.6.386

Chambers, S. M., Fasano, C. A., Papapetrou, E. P., Tomishima, M., Sadelain, M., & Studer, L. (2009). Highly efficient neural conversion of human ES and iPS cells by dual inhibition of SMAD signalling. *Nature biotechnology*, 27(3), 275–280. doi:10.1038/nbt.1529

Chambers, S. M., Qi, Y., Mica, Y., Lee, G., Zhang, X.-J., Niu, L., et al. (2012). Combined small-molecule inhibition accelerates developmental timing and converts human pluripotent stem cells into nociceptors. *Nature biotechnology*. doi:10.1038/nbt.2249

Chan, P., DeLanney, L. E., Irwin, I., Langston, J. W., & Di Monte, D. (1991). Rapid ATP loss caused by 1-methyl-4-phenyl-1,2,3,6-tetrahydropyridine in mouse brain. *Journal of Neurochemistry*, 57(1), 348–351.

Chaudhuri, K. R., & Schapira, A. H. (2009). Non-motor symptoms of Parkinson's disease: dopaminergic pathophysiology and treatment. *Lancet neurology*.

Chen, G., Gulbranson, D. R., Hou, Z., Bolin, J. M., Ruotti, V., Probasco, M. D., et al. (2011). Chemically defined conditions for human iPSC derivation and culture. *Nature methods*, 8(5), 424–429. doi:10.1038/nmeth.1593

Chen, J. K., Taipale, J., Young, K. E., Maiti, T., & Beachy, P. A. (2002). Small molecule modulation of Smoothened activity. *Proceedings of the National Academy of Sciences*, 99(22), 14071–14076. doi:10.1073/pnas.182542899

Chen, M.-H., Li, Y.-J., Kawakami, T., Xu, S.-M., & Chuang, P.-T. (2004). Palmitoylation is required for the production of a soluble multimeric Hedgehog protein complex and long-range signalling in vertebrates. *Genes & development*, 18(6), 641–659. doi:10.1101/gad.1185804

Cheng, L., Chen, C.-L., Luo, P., Tan, M., Qiu, M., Johnson, R., & Ma, Q. (2003). Lmx1b, Pet-1, and Nkx2.2 coordinately specify serotonergic neurotransmitter phenotype. *The Journal of neuroscience*, 23(31), 9961–9967.

Chi, C. L., Martinez, S., Wurst, W., & Martin, G. R. (2003). The isthmic organizer signal FGF8 is required for cell survival in the prospective midbrain and cerebellum. *Development*, 130(12), 2633–2644.

Chiang, C., Litingtung, Y., Lee, E., Young, K. E., Corden, J. L., Westphal, H., & Beachy, P. A. (1996). Cyclopia and defective axial patterning in mice lacking Sonic hedgehog gene function. *Nature*, 383(6599), 407–413. doi:10.1038/383407a0

Chiba, S. (2006). Concise review: Notch signalling in stem cell systems. *Stem cells*.

Chiba, S., Lee, Y., Zhou, W., & Freed, C. (2008). Noggin enhances dopamine neuron production from human embryonic stem cells and improves behavioral outcome after transplantation into Parkinsonian rats. *Stem cells*, 26(11), 2810–2820.

Chin, L. S., Li, L., & Greengard, P. (1994). Neuron-specific expression of the synapsin II gene is directed by a specific core promoter and upstream regulatory elements. *Journal of Biological Chemistry*.

Chin, M., Mason, M., Xie, W., Volinia, S., & Singer, M. (2009). Induced pluripotent stem cells and embryonic stem cells are distinguished by gene expression signatures. *Cell stem cell*.

Chizhikov, V. V., & Millen, K. J. (2004). Control of roof plate formation by *Lmx1a* in the developing spinal cord. *Development*, 131(11), 2693–2705. doi:10.1242/dev.01139

Chizhikov, V. V., Lindgren, A. G., Mishima, Y., Roberts, R. W., Aldinger, K. A., Miesegaes, G. R., et al. (2010). *Lmx1a* regulates fates and location of cells originating from the cerebellar rhombic lip and telencephalic cortical hem. *Proceedings of the National Academy of Sciences of the United States of America*, 107(23), 10725–10730. doi:10.1073/pnas.0910786107

Cho, E.-G., Zaremba, J. D., McKercher, S. R., Talantova, M., Tu, S., Masliah, E., et al. (2011). MEF2C enhances dopaminergic neuron differentiation of human embryonic stem cells in a parkinsonian rat model. *PLoS ONE*, 6(8), e24027. doi:10.1371/journal.pone.0024027

Cho, H.-J., Lee, C.-S., Kwon, Y.-W., Paek, J. S., Lee, S.-H., Hur, J., et al. (2010). Induction of pluripotent stem cells from adult somatic cells by protein-based reprogramming without genetic manipulation. *Blood*, 116(3), 386–395. doi:10.1182/blood-2010-02-269589

Cho, M. S., Lee, Y.-E., Kim, J. Y., Chung, S., Cho, Y. H., Kim, D.-S., et al. (2008). Highly efficient and large-scale generation of functional dopamine neurons from human embryonic stem cells. *Proceedings of the National Academy of Sciences of the United States of America*, 105(9), 3392–3397. doi:10.1073/pnas.0712359105

Choi, W., Yoon, S., Oh, T., & Choi, E. (1999). Two distinct mechanisms are involved in 6-hydroxydopamine-and MPP^+-induced dopaminergic neuronal cell death: role of caspases, ROS, and JNK. Journal of Neuroscience Research

Choi, W.-S., Palmiter, R. D., & Xia, Z. (2011). Loss of mitochondrial complex I activity potentiates dopamine neuron death induced by microtubule dysfunction in a Parkinson‚Äôs disease model. *The Journal of Cell Biology*, 192(5), 873–882. doi:10.1083/jcb.201009132

Chung, S., Leung, A., Han, B.-S., Chang, M.-Y., Moon, J.-I., Kim, C.-H., et al. (2009). Wnt1-lmx1a forms a novel autoregulatory loop and controls midbrain dopaminergic differentiation synergistically with the SHH-FoxA2 pathway. *Cell stem cell*, 5(6), 646–658. doi:10.1016/j.stem.2009.09.015

Chung, S., Moon, J.-I., Leung, A., Aldrich, D., Lukianov, S., Kitayama, Y., et al. (2011). ES cell-derived renewable and functional midbrain dopaminergic progenitors. *Proceedings of the National Academy of Sciences of the United States of America*, 108(23), 9703–9708. doi:10.1073/pnas.1016443108

Chung, S., Shin, B., & Hedlund, E. (2006). Genetic selection of sox1GFP-expressing neural precursors removes residual tumorigenic pluripotent stem cells and attenuates tumor formation after transplantation. Journal of Neurochemistry

Clark, I. E., Dodson, M. W., Jiang, C., Cao, J. H., Huh, J. R., Seol, J. H., et al. (2006). Drosophila pink1 is required for mitochondrial function and interacts genetically with parkin. *Nature*, 441(7097), 1162–1166. doi:10.1038/nature04779

Cleeter, M., Cooper, J., & Schapira, A. (1992). Irreversible inhibition of mitochondrial complex I by 1-methyl-4-phenylpyridinium: evidence for free radical involvement. *Journal of Neurochemistry*, 58(2), 786–789.

Cliffe, A., Hamada, F., & Bienz, M. (2003). A role of Dishevelled in relocating Axin to the plasma membrane during wingless signalling. *Current biology* : CB, 13(11), 960–966.

Collin, J., & Lako, M. (2011). Concise review: putting a finger on stem cell biology: zinc finger nuclease-driven targeted genetic editing in human pluripotent stem cells. *Stem cells*, 29(7), 1021–1033. doi:10.1002/stem.658

Cooper, O., Hargus, G., Deleidi, M., Blak, A., Osborn, T., Marlow, E., et al. (2010). Differentiation of human ES and Parkinson's disease iPS cells into ventral midbrain dopaminergic neurons requires a high activity form of SHH, FGF8a and specific regionalization by retinoic acid. *Molecular and Cellular Neuroscience*, 45(3), 258–266.

Costa, M., Dottori, M., Sourris, K., Jamshidi, P., Hatzistavrou, T., Davis, R., et al. (2007). A method for genetic modification of human embryonic stem cells using electroporation. *Nature protocols*, 2(4), 792–796. doi:10.1038/nprot.2007.105

Coyne, T. M., Marcus, A. J., Woodbury, D., & Black, I. B. (2006). Marrow stromal cells transplanted to the adult brain are rejected by an inflammatory response and transfer donor labels to host neurons and glia. *Stem cells*, 24(11), 2483–2492. doi:10.1634/stemcells.2006-0174

Cragg, S. J., Hawkey, C. R., & Greenfield, S. A. (1997). Comparison of serotonin and dopamine release in substantia nigra and ventral tegmental area: region and species differences. *Journal of Neurochemistry*, 69(6), 2378–2386.

Cuny, G. D., Yu, P. B., Laha, J. K., Xing, X., & Liu, J. F. (2008). Structure–activity relationship study of bone morphogenetic protein (BMP) signalling inhibitors. Bioorganic & medicinal chemistry letters

Czlonkowska, A., & Kohutnicka, M. (1996). Microglial reaction in MPTP (1-methyl-4-phenyl-1, 2, 3, 6-tetrahydropyridine) induced Parkinson's disease mice model. Neurodegeneration.

Dahéron, L., Opitz, S. L., Zaehres, H., Lensch, M. W., Lensch, W. M., Andrews, P. W., et al. (2004). LIF/STAT3 signalling fails to maintain self-renewal of human embryonic stem cells. *Stem cells*, 22(5), 770–778. doi:10.1634/stemcells.22-5-770

Danielian, P., & McMahon, A. (1996). Engrailed-1 as a target of the Wnt-1 signalling pathway in vertebrate midbrain development. *Nature*, 383(6598), 332–334.

Darabi, R., Arpke, R. W., Irion, S., Dimos, J. T., Grskovic, M., Kyba, M., & Perlingeiro, R. C. R. (2012). Human ES- and iPS-derived myogenic progenitors restore dystrophin and improve contractility upon transplantation in dystrophic mice. *Cell stem cell*, 10(5), 610–619. doi:10.1016/j.stem.2012.02.015

Date, I., Yoshimoto, Y., Imaoka, T., Miyoshi, Y., Gohda, Y., Furuta, T., et al. (1993). Enhanced recovery of the nigrostriatal dopaminergic system in MPTP-treated mice following intrastriatal injection of basic fibroblast growth factor in relation to aging. *Brain research*, 621(1), 150–154.

Dauer, W., & Przedborski, S. (2003). Parkinson's disease mechanisms and models. *Neuron*, 39(6), 889–909.

Davey, G. P., & Clark, J. B. (1996). Threshold effects and control of oxidative phosphorylation in nonsynaptic rat brain mitochondria. *Journal of Neurochemistry*, 66(4), 1617–1624.

Davis, R. P., Ng, E. S., Costa, M., Mossman, A. K., Sourris, K., Elefanty, A. G., & Stanley, E. G. (2008). Targeting a GFP reporter gene to the MIXL1 locus of human embryonic stem cells identifies human primitive streak-like cells and enables isolation of primitive hematopoietic precursors. *Blood*, 111(4), 1876–1884. doi:10.1182/blood-2007-06-093609

Dawson, T., & Ko, H. (2010). Genetic animal models of Parkinson's disease. *Neuron*. DOI 10.1016/j.neuron.2010.04.034

de Lau, L. (2006). Epidemiology of Parkinson's disease. *The Lancet Neurology*. 5(6):525–535 http://dx.doi.org/10.1016/S1474-4422(06)70471-9

del Barco Barrantes, I., Davidson, G., Gröne, H.-J., Westphal, H., & Niehrs, C. (2003). Dkk1 and noggin cooperate in mammalian head induction. *Genes & development*, 17(18), 2239–2244. doi:10.1101/gad.269103

Delgado, M., & Ganea, D. (2003). Neuroprotective effect of vasoactive intestinal peptide (VIP) in a mouse model of Parkinson's disease by blocking microglial activation. *The FASEB journal*. 17(8):944-946 10.1096/fj.02-0799fje

Deng, C., & Capecchi, M. R. (1992). Reexamination of gene targeting frequency as a function of the extent of homology between the targeting vector and the target locus. *Molecular and cellular biology*, 12(8), 3365–3371.

Deng, Q., Andersson, E., Hedlund, E., Alekseenko, Z., Coppola, E., Panman, L., et al. (2011). Specific and integrated roles of *Lmx1a*, Lmx1b and Phox2a in ventral midbrain development. *Development*, 138(16), 3399–3408. doi:10.1242/dev.065482

Denham, M., Bye, C., Leung, J., Conley, B. J., Thompson, L. H., & Dottori, M. (2012). GSK3β and Activin/Nodal Inhibition in Human Embryonic Stem Cells Induces a Pre-Neuroepithelial State that is Required for Specification to a Floor Plate Cell Lineage. *Stem cells*. doi:10.1002/stem.1204

Denham, M., Thompson, L. H., Leung, J., Pébay, A., Björklund, A., & Dottori, M. (2010). Gli1 is an inducing factor in generating floor plate progenitor cells from human embryonic stem cells. *Stem cells*, 28(10), 1805–1815. doi:10.1002/stem.510

Dennis, S., Aikawa, M., & Szeto, W. (1999). A secreted frizzled related protein, FrzA, selectively associates with Wnt-1 protein and regulates wnt-1 signalling. Journal of cell Science

Desbordes, S. C., & Studer, L. (2012). Adapting human pluripotent stem cells to high-throughput and high-content screening. *Nature protocols*, 8(1), 111–130. doi:10.1038/nprot.2012.139

Di Domenico, A. I., Christodoulou, I., Pells, S. C., McWhir, J., & Thomson, A. J. (2008). Sequential genetic modification of the hprt locus in human ESCs combining gene targeting and recombinase-mediated cassette exchange. *Cloning and stem cells*, 10(2), 217–230. doi:10.1089/clo.2008.0016

Di Giorgio, F. P., Carrasco, M. A., Siao, M. C., & Maniatis, T. (2007). Non–cell autonomous effect of glia on motor neurons in an embryonic stem cell–based ALS model. *Nature*.

Di Salvio, M., Di Giovannantonio, L., Acampora, D., Prosperi, R., Omodei, D., Prakash, N., et al. (2010). Otx2 controls neuron subtype identity in ventral tegmental area and antagonizes vulnerability to MPTP. *Nature neuroscience*, 13(12), 1481–1488.

Diecke, S., Quiroga-Negreira, A., Redmer, T., & Besser, D. (2008). FGF2 signaling in mouse embryonic fibroblasts is crucial for self-renewal of embryonic stem cells. *Cells Tissues Organs*, *188*(1-2), 52–61. doi:10.1159/000121282

Diep, D. B., Hoen, N., Backman, M., Machon, O., & Krauss, S. (2004). Characterisation of the Wnt antagonists and their response to conditionally activated Wnt signalling in the developing mouse forebrain. *Brain research. Developmental brain research*, 153(2), 261–270. doi:10.1016/j.devbrainres.2004.09.008

Dimos, J., Rodolfa, K., Niakan, K., & Weisenthal, L. (2008). Induced pluripotent stem cells generated from patients with ALS can be differentiated into motor neurons. *Science*.

Ding, S., & Schultz, P. G. (2004). A role for chemistry in stem cell biology. *Nature biotechnology*, 22(7), 833–840. doi:10.1038/nbt987

Ding, S., Wu, T. Y. H., Brinker, A., Peters, E. C., Hur, W., Gray, N. S., & Schultz, P. G. (2003a). Synthetic small molecules that control stem cell fate. *Proceedings of the National Academy of Sciences*, 100(13), 7632–7637. doi:10.1073/pnas.0732087100

Ding, Y.-Q., Marklund, U., Yuan, W., Yin, J., Wegman, L., Ericson, J., et al. (2003b). Lmx1b is essential for the development of serotonergic neurons. *Nature neuroscience*, 6(9), 933–938. doi:10.1038/nn1104

Ding, Y.-Q., Yin, J., Kania, A., Zhao, Z.-Q., Johnson, R. L., & Chen, Z.-F. (2004). Lmx1b controls the differentiation and migration of the superficial dorsal horn neurons of the spinal cord. *Development*, 131(15), 3693–3703. doi:10.1242/dev.01250

Dluzen, D. E., Gao, X., Story, G. M., Anderson, L. I., Kucera, J., & Walro, J. M. (2001). Evaluation of nigrostriatal dopaminergic function in adult +/+ and +/- BDNF mutant mice. *Experimental neurology*, 170(1), 121–128. doi:10.1006/exnr.2001.7698

Donkelaar, H. (2006). Overview of the development of the human brain and spinal cord. Clinical *Neuroembryology*.

Donovan, D. M., Miner, L. L., Perry, M. P., Revay, R. S., Sharpe, L. G., Przedborski, S., et al. (1999). Cocaine reward and MPTP toxicity: alteration by regional variant dopamine transporter overexpression. *Molecular Brain Research*, 73(1-2), 37–49.

Drucker-Colin, R., & García-Hernández, F. (1991). A new motor test sensitive to aging and dopaminergic function. *Journal of Neuroscience Methods*, 39(2), 153–161.

Dunnett, S., & Bjorklund, A. (1999). Prospects for new restorative and neuroprotective treatments in Parkinson's disease. *Nature*, 32–39.

Echelard, Y., Epstein, D., St-Jacques, B., & Shen, L. (1993). Sonic hedgehog, a member of a family of putative signalling molecules, is implicated in the regulation of CNS polarity. *Cell*.

Efe, J. A., Hilcove, S., Kim, J., Zhou, H., Ouyang, K., Wang, G., et al. (2011). Conversion of mouse fibroblasts into cardiomyocytes using a direct reprogramming strategy. *Nature cell biology*, 13(3), 215–222. doi:10.1038/ncb2164

Eiselleova, L., Matulka, K., Kriz, V., & Kunova, M. (2009). A Complex Role for FGF-2 in Self-Renewal, Survival, and Adhesion of Human Embryonic Stem Cells. *Stem …*.

Elkabetz, Y., Panagiotakos, G., Al-Shamy, G., Socci, N. D., Tabar, V., & Studer, L. (2008). Human ES cell-derived neural rosettes reveal a functionally distinct early neural stem cell stage. *Genes & development*, 22(2), 152.

Emdad, L., D'Souza, S. L., Kothari, H. P., Qadeer, Z. A., & Germano, I. M. (2012). Efficient differentiation of human embryonic and induced pluripotent stem cells into functional astrocytes. *Stem Cells Dev*, 21(3), 404–410. doi:10.1089/scd.2010.0560

Ericson, J., Briscoe, J., Rashbass, P., van Heyningen, V., & Jessell, T. M. (1997). Graded sonic hedgehog signalling and the specification of cell fate in the ventral neural tube. *Cold Spring Harbor symposia on quantitative biology*, 62, 451–466.

Evans, M., & Kaufman, M. (1981). Establishment in culture of pluripotential cells from mouse embryos. *Nature*.

Exner, N., Lutz, A. K., Haass, C., & Winklhofer, K. F. (2012). Mitochondrial dysfunction in Parkinson's disease: molecular mechanisms and pathophysiological consequences. The EMBO Journal, 31(14), 3038–3062. doi:10.1038/emboj.2012.170

Exner, N., Treske, B., Paquet, D., Holmström, K., Schiesling, C., Gispert, S., et al. (2007). Loss-of-function of human PINK1 results in mitochondrial pathology and can be rescued by parkin. *The Journal of neuroscience*, 27(45), 12413–12418. doi:10.1523/JNEUROSCI.0719-07.2007

Failli, V., Bachy, I., & RÈtaux, S. (2002). Expression of the LIM-homeodomain gene *Lmx1a* (dreher) during development of the mouse nervous system. *Mechanisms of Development*, 118(1-2), 225–228.

Fasano, C. A., Chambers, S. M., Lee, G., Tomishima, M. J., & Studer, L. (2010). Efficient derivation of functional floor plate tissue from human embryonic stem cells. *Cell stem cell*, 6(4), 336–347. doi:10.1016/j.stem.2010.03.001

Fearnley, J. M., & Lees, A. J. (1991). Ageing and Parkinson's disease: substantia nigra regional selectivity. *Brain*, 114 (Pt 5), 2283–2301.

Fernagut, P.-O., Chalon, S., Diguet, E., Guilloteau, D., Tison, F., & Jaber, M. (2003). Motor behaviour deficits and their histopathological and functional correlates in the nigrostriatal system of dopamine transporter knockout mice. *Neuroscience*, 116(4), 1123–1130.

Ferrari, D., Sanchez-Pernaute, R., Lee, H., Studer, L., & Isacson, O. (2006). Transplanted dopamine neurons derived from primate ES cells preferentially innervate DARPP-32 striatal progenitors within the graft. T*he European journal of neuroscience*, 24(7), 1885.

Finch, P. W., He, X., Kelley, M. J., Uren, A., Schaudies, R. P., Popescu, N. C., et al. (1997). Purification and molecular cloning of a secreted, Frizzled-related antagonist of Wnt action. *Proceedings of the National Academy of Sciences*, 94(13), 6770–6775.

Finkelstein, D. I., Stanic, D., Parish, C. L., Tomas, D., Dickson, K., & Horne, M. K. (2000). Axonal sprouting following lesions of the rat substantia nigra. *Neuroscience*, 97(1), 99–112.

Fitzpatrick, P. (1991). Studies of the rate-limiting step in the tyrosine hydroxylase reaction: alternate substrates, solvent isotope effects, and transition-state analogs. *Biochemistry*.

Fleming, S. M., Salcedo, J., Fernagut, P.-O., Rockenstein, E., Masliah, E., Levine, M. S., & Chesselet, M.-F. (2004). Early and Progressive Sensorimotor Anomalies in Mice Overexpressing Wild-Type Human {alpha}-Synuclein. *The Journal of neuroscience* 24(42), 9434–9440. doi:10.1523/JNEUROSCI.3080-04.2004

Freed, C. R., Breeze, R. E., Rosenberg, N. L., Schneck, S. A., Wells, T. H., Barrett, J. N., et al. (1990a). Transplantation of human fetal dopamine cells for Parkinson's disease. Results at 1 year. *Arch Neurol*, 47(5), 505–512.

Freed, C., Breeze, R., & Rosenberg, N. (1990b). Therapeutic effects of human fetal dopamine cells transplanted in a patient with Parkinson's disease. Progress in Brain Research

Freed, W. J., Chen, J., Bäckman, C. M., Schwartz, C. M., Vazin, T., Cai, J., et al. (2008). Gene expression profile of neuronal progenitor cells derived from hESCs: activation of chromosome 11p15.5 and comparison to human dopaminergic neurons. *PLoS ONE*, 3(1), e1422. doi:10.1371/journal.pone.0001422

Freed, W. J., Morihisa, J. M., Spoor, E., Hoffer, B. J., Olson, L., Seiger, Å., & Wyatt, R. J. (1981). Transplanted adrenal chromaffin cells in rat brain reduce lesion-induced rotational behaviour. *Nature*, 292(5821), 351–352.

Freed, C. R., Zhou, W., & Breeze, R. E. (2011). Dopamine cell transplantation for Parkinson's disease: the importance of controlled clinical trials. Neurotherapeutics : the journal of the American Society for Experimental NeuroTherapeutics 8(4) 549-561.

Freyaldenhoven, T. E., Ali, S. F., & Hart, R. W. (1995). MPTP-and MPP+-induced effects on body temperature exhibit age-and strain-dependence in mice. Brain research. Volume 688, Issues 1–2, 7 August 1995, Pages 161–170

Friling, S., Andersson, E., Thompson, L. H., Jönsson, M. E., Hebsgaard, J. B., Nanou, E., et al. (2009). Efficient production of mesencephalic dopamine neurons by *Lmx1a* expression in embryonic stem cells. *Proceedings of the National Academy of Sciences of the United States of America*, 106(18), 7613–7618. doi:10.1073/pnas.0902396106

Fukuda, H., Takahashi, J., & Watanabe, K. (2006). Fluorescence-Activated Cell Sorting–Based Purification of Embryonic Stem Cell–Derived Neural Precursors Averts Tumor Formation after Transplantation. Stem Cells

Fukuda, H., Takahashi, J., Watanabe, K., Hayashi, H., Morizane, A., Koyanagi, M., et al. (2005). Fluorescence-activated cell sorting-based purification of embryonic stem cell-derived neural precursors averts tumor formation after transplantation. *Stem cells*, 24(3), 763–771.

Galli, L. M., Barnes, T. L., Secrest, S. S., Kadowaki, T., & Burrus, L. W. (2007). Porcupine-mediated lipid-modification regulates the activity and distribution of Wnt proteins in the chick neural tube. *Development*, 134(18), 3339–3348. doi:10.1242/dev.02881

Ganat, Y. M., Calder, E. L., Kriks, S., Nelander, J., Tu, E. Y., Jia, F., et al. (2012). Identification of embryonic stem cell-derived midbrain dopaminergic neurons for engraftment. *The Journal of Clinical Investigation*, 122(8), 2928–2939. doi:10.1172/JCI58767

Ganat, Y., & Studer, L. (2013). Diagnosis and Treatment of Parkinson's Disease. WO Patent 2,013,016,662.

Gaspard, N., & Vanderhaeghen, P. (2010). Mechanisms of neural specification from embryonic stem cells. *Current Opinion in Neurobiology*.

Gaspard, N., Bouschet, T., Hourez, R., Dimidschstein, J., Naeije, G., van den Ameele, J., et al. (2008). An intrinsic mechanism of corticogenesis from embryonic stem cells. *Nature*, 455, 351–357.

Gaszner, M., & Felsenfeld, G. (2006). Insulators: exploiting transcriptional and epigenetic mechanisms. *Nature Reviews Genetics*, 7(9), 703–713. doi:10.1038/nrg1925

Geng, X., Song, L., Pu, X., & Tu, P. (2004). Neuroprotective effects of phenylethanoid glycosides from Cistanches salsa against 1-methyl-4-phenyl-1, 2, 3, 6-tetrahydropyridine (MPTP)-induced dopaminergic toxicity in C57 Mice *Biological and Pharmaceutical Bulletin*. 27 (6):797-801 http://dx.doi.org/10.1248/bpb.27.797

Gerhard, A., Pavese, N., Hotton, G., & Turkheimer, F. (2006). In vivo imaging of microglial activation with [11 C](R)-PK11195 PET in idiopathic Parkinson's disease. Neurobiology of disease. 21 (2) 404-412

German, D., Manaye, K., & White, C., III. (1992). Disease-specific patterns of locus coeruleus cell loss. *Annals of Neurology* 32 (5) 667-676

Gibb, W. R., & Lees, A. J. (1988). The relevance of the Lewy body to the pathogenesis of idiopathic Parkinson's disease. *Journal of neurology, neurosurgery, and psychiatry*, 51(6), 745–752.

Ginis, I., Luo, Y., Miura, T., Thies, S., Brandenberger, R., Gerecht-Nir, S., et al. (2004). Differences between human and mouse embryonic stem cells. *Developmental Biology*, 269(2), 360–380. doi:10.1016/j.ydbio.2003.12.034

Glinka, A., Wu, W., Delius, H., Monaghan, A. P., Blumenstock, C., & Niehrs, C. (1998). Dickkopf-1 is a member of a new family of secreted proteins and functions in head induction. *Nature*, 391(6665), 357–362. doi:10.1038/34848

Goldberg, M., Fleming, S., Palacino, J., Cepeda, C., Lam, H., Bhatnagar, A., et al. (2003). Parkin-deficient Mice Exhibit Nigrostriatal Deficits but Not Loss of Dopaminergic Neurons. *Journal of Biological Chemistry*, 278(44), 43628–43635. Retrieved from http://www.jbc.org/content/278/44/43628.short

Gorell, J. M., Johnson, C. C., Rybicki, B. A., Peterson, E. L., & Richardson, R. J. (1998). The risk of Parkinson's disease with exposure to pesticides, farming, well water, and rural living. *Neurology*, 50(5), 1346–1350.

Graham, V., Khudyakov, J., Ellis, P., & Pevny, L. (2003). SOX2 functions to maintain neural progenitor identity. *Neuron*, 39(5), 749–765.

Gray, P. C., Greenwald, J., Blount, A. L., Kunitake, K. S., Donaldson, C. J., Choe, S., & Vale, W. (2000). Identification of a binding site on the type II activin receptor for activin and inhibin. *J Biol Chem*, *275*(5), 3206–3212.

Greber, B., Lehrach, H., & Adjaye, J. (2007). Fibroblast growth factor 2 modulates transforming growth factor beta signaling in mouse embryonic fibroblasts and human ESCs (hESCs) to support hESC self-renewal. *Stem cells (Dayton, Ohio)*, *25*(2), 455–464. doi:10.1634/stemcells.2006-0476

Greber, B., Wu, G., Bernemann, C., Joo, J. Y., Han, D. W., & Ko, K. (2010). Conserved and divergent roles of FGF signaling in mouse epiblast stem cells and human embryonic stem cells. *Cell stem cell*.

Guenther, M. G., Frampton, G. M., Soldner, F., Hockemeyer, D., Mitalipova, M., Jaenisch, R., & Young, R. A. (2010). Chromatin structure and gene expression programs of human embryonic and induced pluripotent stem cells. *Cell stem cell*, 7(2), 249–257. doi:10.1016/j.stem.2010.06.015

Guillot, T. S., & Miller, G. W. (2009). Protective actions of the vesicular monoamine transporter 2 (VMAT2) in monoaminergic neurons. *Molecular neurobiology*, 39(2), 149–170. doi:10.1007/s12035-009-8059-y

Guzman, J. N., Sanchez-Padilla, J., Wokosin, D., Kondapalli, J., Ilijic, E., Schumacker, P. T., & Surmeier, D. J. (2010). Oxidant stress evoked by pacemaking in dopaminergic neurons is attenuated by DJ-1. *Nature*, 468(7324), 696–700. doi:10.1038/nature09536

Habas, R., Kato, Y., & He, X. (2001). Wnt/Frizzled activation of Rho regulates vertebrate gastrulation and requires a novel Formin homology protein Daam1. *Cell*, 107(7), 843–854.

Hall, P. A., & Watt, F. M. (1989). Stem cells: the generation and maintenance of cellular diversity. *Development*, 106(4), 619–633.

Halliday, G., Blumbergs, P., & Cotton, R. (1990). Loss of brainstem serotonin-and substance P-containing neurons in Parkinson's disease. *Brain research*. 510 (1) 104–107

Han, D. W., Tapia, N., Hermann, A., Hemmer, K., Höing, S., Araúzo-Bravo, M. J., et al. (2012). Direct Reprogramming of Fibroblasts into Neural Stem Cells by Defined Factors. *Cell stem cell*. doi:10.1016/j.stem.2012.02.021

Han, Y., Miller, A., Mangada, J., Liu, Y., Swistowski, A., Zhan, M., et al. (2009). Identification by Automated Screening of a Small Molecule that Selectively Eliminates Neural Stem Cells Derived from hESCs but Not Dopamine Neurons. *PLoS ONE*, 4(9), e7155. doi:10.1371/journal.pone.0007155

Hao, J., Daleo, M. A., Murphy, C. K., Yu, P. B., Ho, J. N., Hu, J., et al. (2008). Dorsomorphin, a selective small molecule inhibitor of BMP signalling, promotes cardiomyogenesis in embryonic stem cells. *PLoS ONE*, 3(8), e2904. doi:10.1371/journal.pone.0002904

Hao, J., Ho, J. N., Lewis, J. A., & Karim, K. A. (2010). In Vivo Structure– Activity Relationship Study of Dorsomorphin Analogues Identifies Selective VEGF and BMP Inhibitors. ACS chemical biology 2010, *5* (2), pp 245–253, DOI: 10.1021/cb9002865

Hargus, G., Cooper, O., Deleidi, M., Levy, A., Lee, K., Marlow, E., et al. (2010). Differentiated Parkinson patient-derived induced pluripotent stem cells grow in the adult rodent brain and reduce motor asymmetry in Parkinsonian rats. *Proceedings of the National Academy of Sciences of the United States of America*, 107(36), 15921–15926. doi:10.1073/pnas.1010209107

Hart, M. J., de los Santos, R., Albert, I. N., & Rubinfeld, B. (1998). Downregulation of β-catenin by human Axin and its association with the APC tumor suppressor, β-catenin and GSK3β. *Current Biology*. 8 (10) 573-581

Hashimoto, H., Itoh, M., Yamanaka, Y., Yamashita, S., Shimizu, T., Solnica-Krezel, L., et al. (2000). Zebrafish Dkk1 functions in forebrain specification and axial mesendoderm formation. *Developmental Biology*, 217(1), 138–152. doi:10.1006/dbio.1999.9537

Hasty, P., Crist, M., Grompe, M., & Bradley, A. (1994). Efficiency of insertion versus replacement vector targeting varies at different chromosomal loci. *Molecular and cellular biology*, 14(12), 8385–8390.

Hawley, S., & Wünnenberg-Stapleton, K. (1995). Disruption of BMP signals in embryonic Xenopus ectoderm leads to direct neural induction. Genes & Development 9:2923-2935

Hedlund, E., Pruszak, J., Lardaro, T., Ludwig, W., Vinuela, A., Kim, K.-S., & Isacson, O. (2008). Embryonic Stem Cell-Derived Pitx3-Enhanced Green Fluorescent Protein Midbrain Dopamine Neurons Survive Enrichment by Fluorescence-Activated Cell Sorting and Function in an Animal Model of Parkinson's Disease. *Stem cells*, 26(6), 1526–1536. doi:10.1634/stemcells.2007-0996

Heeg-Truesdell, E., & LaBonne, C. (2006). Neural induction in Xenopus requires inhibition of Wnt-β-catenin signalling. Developmental Biology. 298:71-86

Hemmati-Brivanlou, A., Kelly, O. G., & Melton, D. A. (1994). Follistatin, an antagonist of activin, is expressed in the Spemann organizer and displays direct neuralizing activity. *Cell*, 77(2), 283–295.

Hermann, A., Maisel, M., Wegner, F., Liebau, S., Kim, D., Gerlach, M., et al. (2006). Multipotent Neural Stem Cells from the Adult Tegmentum with Dopaminergic Potential Develop Essential Properties of Functional Neurons. *Stem cells* 24, 949–964.

Hirsch, E., Graybiel, A. M., & Agid, Y. A. (1988). Melanized dopaminergic neurons are differentially susceptible to degeneration in Parkinson's disease. *Nature*, 334(6180), 345–348. doi:10.1038/334345a0

Hockemeyer, D., Soldner, F., Beard, C., Gao, Q., Mitalipova, M., DeKelver, R., et al. (2009). Efficient targeting of expressed and silent genes in human ESCs and iPSCs using zinc-finger nucleases. *Nature biotechnology*, 27(9), 851–857.

Hoehn, M. M., & Yahr, M. D. (1998). Parkinsonism: onset, progression, and mortality. *Neurology*. 17(5):427-442

Hofele, K., Sedelis, M., Auburger, G. W., & Morgan, S. (2001). Evidence for a dissociation between MPTP toxicity and tyrosinase activity based on congenic mouse strain susceptibility. *Experimental Neurology*. 168(1):116-122

Hoffman, L. M., Hall, L., Batten, J. L., Young, H., Pardasani, D., Baetge, E. E., et al. (2005). X-inactivation status varies in human embryonic stem cell lines. *Stem cells (Dayton, Ohio)*, *23*(10), 1468–1478. doi:10.1634/stemcells.2004-0371

Hollyday, M., & McMahon, J. (1995). Wnt expression patterns in chick embryo nervous system. *Mechanisms of Development*.

Hooper, M., Hardy, K., Handyside, A., Hunter, S., & Monk, M. (1987). HPRT-deficient (Lesch-Nyhan) mouse embryos derived from germline colonization by cultured cells. *Nature*, 326(6110), 292–295. doi:10.1038/326292a0

Horiguchi, S., Takahashi, J., Kishi, Y., Morizane, A., Okamoto, Y., Koyanagi, M., et al. (2004). Neural precursor cells derived from human embryonic brain retain regional specificity. *Journal of Neuroscience Research*, 75(6), 817–824. doi:10.1002/jnr.20046

Hsu, L. J., Sagara, Y., Arroyo, A., Rockenstein, E., Sisk, A., Mallory, M., et al. (2000). alpha-synuclein promotes mitochondrial deficit and oxidative stress. *The American journal of pathology*, 157(2), 401–410.

Huang, X., Litingtung, Y., & Chiang, C. (2007). Region-specific requirement for cholesterol modification of sonic hedgehog in patterning the telencephalon and spinal cord. *Development*, 134(11), 2095–2105. doi:10.1242/dev.000729

Huangfu, D., Maehr, R., Guo, W., Eijkelenboom, A., Snitow, M., Chen, A. E., & Melton, D. A. (2008). Induction of pluripotent stem cells by defined factors is greatly improved by small-molecule compounds. *Nature biotechnology*, 26(7), 795–797. doi:10.1038/nbt1418

Ibáñez, C. F., Ilag, L. L., Murray-Rust, J., & Persson, H. (1993). An extended surface of binding to Trk tyrosine kinase receptors in NGF and BDNF allows the engineering of a multifunctional pan-neurotrophin. *The EMBO Journal*, 12(6), 2281–2293.

Ikeya, M., & Takada, S. (1998). Wnt signalling from the dorsal neural tube is required for the formation of the medial dermomyotome. *Development*, 125(24), 4969–4976.

Incardona, J. P., Gaffield, W., Lange, Y., & Cooney, A. (2000). Cyclopamine inhibition of Sonic hedgehog signal transduction is not mediated through effects on cholesterol transport. Developmental Biology

Ingham, P. W., & McMahon, A. P. (2001). Hedgehog signalling in animal development: paradigms and principles. *Genes & development*, 15(23), 3059–3087. doi:10.1101/gad.938601

Inzelberg, R., Schechtman, E., & Nisipeanu, P. (2003). Cabergoline, pramipexole and ropinirole used as monotherapy in early Parkinson's disease: an evidence-based comparison. *Drugs & aging*, 20(11), 847–855.

Iravani, M., Kashefi, K., Mander, P., & Rose, S. (2002). Involvement of inducible nitric oxide synthase in inflammation-induced dopaminergic neurodegeneration. *Neuroscience*.

Irioka, T., Watanabe, K., Mizusawa, H., Mizuseki, K., & Sasai, Y. (2005). Distinct effects of caudalizing factors on regional specification of embryonic stem cell-derived neural precursors. *Brain research. Developmental brain research*, 154(1), 63–70. doi:10.1016/j.devbrainres.2004.10.004

Irion, S., Luche, H., Gadue, P., Fehling, H. J., Kennedy, M., & Keller, G. (2007). Identification and targeting of the ROSA26 locus in human embryonic stem cells. *Nature* biotechnology, 25(12), 1477–1482. doi:10.1038/nbt1362

Irrcher, I., Aleyasin, H., Seifert, E. L., Hewitt, S. J., Chhabra, S., Phillips, M., et al. (2010). Loss of the Parkinson's disease-linked gene DJ-1 perturbs mitochondrial dynamics. *Human Molecular Genetics*, 19(19), 3734–3746. doi:10.1093/hmg/ddq288

Irwin, I., DeLanney, L., & Langston, J. (1993). MPTP and aging: studies in the C 57 BL/6 mouse. *Advances in neurology*, 60, 197–206.

Ischiropoulos, H., Al-Mehdi, AB. (1995). Peroxynitrite-mediated oxidative protein modifications. *FEBS Letters*, 364(3), 279–282.

Itier, J.-M., Ibanez, P., Mena, M. A., Abbas, N., Cohen-Salmon, C., Bohme, G. A., et al. (2003). Parkin gene inactivation alters behaviour and dopamine neurotransmission in the mouse. *Human Molecular Genetics*, 12(18), 2277–2291. doi:10.1093/hmg/ddg239

Jackson-Lewis, V., & Przedborski, S. (2007). Protocol for the MPTP mouse model of Parkinson's disease. *Nature protocols*, 2(1), 141–151.

Jackson-Lewis, V., Jakowec, M., Burke, R., & Przedborski, S. (1995). Time course and morphology of dopaminergic neuronal death caused by the neurotoxin 1-methyl-4-phenyl-1, 2, 3, 6-tetrahydropyridine. *Neurodegeneration*, 4(3), 257–269.

Jakel, R., & Schneider, B. (2004). Using human neural stem cells to model neurological disease. *Nature Reviews Genetics*.

James, D., Levine, A. J., Besser, D., & Hemmati-Brivanlou, A. (2005). TGFbeta/activin/nodal signalling is necessary for the maintenance of pluripotency in human embryonic stem cells. *Development*, 132(6), 1273–1282. doi:10.1242/dev.01706

Javitch, J., D'Amato, R., Strittmatter, S., & Snyder, S. (1985). Parkinsonism-inducing neurotoxin, N-methyl-4-phenyl-1, 2, 3, 6-tetrahydropyridine: uptake of the metabolite N-

methyl-4-phenylpyridine by dopamine neurons explains selective toxicity. *Proceedings of the National Academy of Sciences*, 82(7), 2173–2177.

Javoy, F., Sotelo, C., Herbet, A., & Agid, Y. (1976). Specificity of dopaminergic neuronal degeneration induced by intracerebral injection of 6-hydroxydopamine in the nigrostriatal dopamine system. *Brain research*, 102(2), 201.

Jenner, P., & Marsden, C. D. (1986). The actions of 1-methyl-4-phenyl-1, 2, 3, 6-tetrahydropyridine in animals as a model of Parkinson's disease. J*ournal of neural transmission*.

Jeon, B. S., Jackson-Lewis, V., & Burke, R. E. (1995). 6-Hydroxydopamine lesion of the rat substantia nigra: time course and morphology of cell death. *Neurodegeneration*, 4(2), 131–137.

Jessell, T. M., Bovolenta, P., Placzek, M., Tessier-Lavigne, M., & Dodd, J. (1989). Polarity and patterning in the neural tube: the origin and function of the floor plate. *Ciba Foundation symposium*, 144, 255–76– discussion 276–80– 290–5.

Jiang, H., Jackson-Lewis, V., Muthane, U., Dollison, A., Ferreira, M., Espinosa, A., et al. (1993). Adenosine receptor antagonists potentiate dopamine receptor agonist-induced rotational behavior in 6-hydroxydopamine-lesioned rats. *Brain research*, 613(2), 347–351.

Jiménez, F. J., & Mateo, D. (1992). Exposure to well water and pesticides in Parkinson's disease: A case-control study in the madrid area. *Movement Disorders*

Johnson, M. M., Michelhaugh, S. K., Bouhamdan, M., Schmidt, C. J., & Bannon, M. J. (2011). The Transcription Factor NURR1 Exerts Concentration-Dependent Effects on Target Genes Mediating Distinct Biological Processes. *Frontiers in neuroscience*, 5, 135. doi:10.3389/fnins.2011.00135

Joksimovic, M., Yun, B., Kittappa, R., Anderegg, A., Chang, W., Taketo, M., et al. (2009). Wnt antagonism of Shh facilitates midbrain floor plate neurogenesis. *Nature neuroscience*, 12, 125–131.

Jonsson, G. (1983). Chemical lesioning techniques: monoamine neurotoxins. *Handbook of chemical neuroanatomy*, 1, 463–507.

Joseph, B., Wallén-Mackenzie, A., Benoit, G., Murata, T., Joodmardi, E., Okret, S., & Perlmann, T. (2003). p57(Kip2) cooperates with Nurr1 in developing dopamine cells. *Proceedings of the National Academy of Sciences*, 100(26), 15619–15624. doi:10.1073/pnas.2635658100

Joyner, A., & Liu, A. (2000). Otx2, Gbx2 and Fgf8 interact to position and maintain a mid–hindbrain organizer. *Current opinion in cell biology*.

Jönsson, M. E., Ono, Y., Björklund, A., & Thompson, L. H. (2009). Identification of transplantable dopamine neuron precursors at different stages of midbrain neurogenesis. *Experimental neurology*, 219(1), 341–354. doi:10.1016/j.expneurol.2009.06.006

Kaji, E. H., & Leiden, J. M. (2001). Gene and stem cell therapies. *JAMA: the journal of the American Medical Association* 285(5):545-550. doi:10.1001/jama.285.5.545.

Kalinichenko, V. V., Zhou, Y., & Bhattacharyya, D. (2002). Haploinsufficiency of the mouse Forkhead Box f1 gene causes defects in gall bladder development. *Journal of Biological Chemistry* 277(14):12369-12374

Kattman, S. J., Witty, A. D., Gagliardi, M., Dubois, N. C., Niapour, M., Hotta, A., et al. (2011). Stage-specific optimization of activin/nodal and BMP signalling promotes cardiac differentiation of mouse and human pluripotent stem cell lines. *Cell stem cell*, 8(2), 228–240. doi:10.1016/j.stem.2010.12.008

Kawano, H., Ohyama, K., Kawamura, K., & Nagatsu, I. (1995). Migration of dopaminergic neurons in the embryonic mesencephalon of mice. *Brain research. Developmental brain research*, 86(1-2), 101–113.

Kawasaki, H., Mizuseki, K., Nishikawa, S., Kaneko, S., Kuwana, Y., Nakanishi, S., et al. (2000). Induction of midbrain dopaminergic neurons from ES cells by stromal cell–derived inducing activity. *Neuron*, 28(1), 31–40.

Kawasaki, H., Suemori, H., Mizuseki, K., Watanabe, K., Urano, F., Ichinose, H., et al. (2002). Generation of dopaminergic neurons and pigmented epithelia from primate ES cells by stromal cell-derived inducing activity. *Proceedings of the National Academy of Sciences of the United States of America*, 99(3), 1580.

Kay, J. N., Voinescu, P. E., Chu, M. W., & Sanes, J. R. (2011). Neurod6 expression defines new retinal amacrine cell subtypes and regulates their fate. *Nature neuroscience*, 14(8), 965–972. doi:10.1038/nn.2859

Kehat, I., Kenyagin-Karsenti, D., Snir, M., Segev, H., Amit, M., Gepstein, A., et al. (2001). Human embryonic stem cells can differentiate into myocytes with structural and functional properties of cardiomyocytes. *The Journal of Clinical Investigation*, 108(3), 407–414. doi:10.1172/JCI12131

Kele, J., Simplicio, N., Ferri, A. L. M., Mira, H., Guillemot, F., Arenas, E., & Ang, S.-L. (2006). Neurogenin 2 is required for the development of ventral midbrain dopaminergic neurons. *Development*, 133(3), 495–505. doi:10.1242/dev.02223

Khaira, S. K., Nefzger, C. M., Beh, S. J., Pouton, C. W., & Haynes, J. M. (2011). Midbrain and forebrain patterning delivers immunocytochemically and functionally similar populations of neuropeptide Y containing GABAergic neurons. *Neurochemistry international*, 59(3), 413–420. doi:10.1016/j.neuint.2011.02.016

Kiecker, C., & Niehrs, C. (2001). A morphogen gradient of Wnt/beta-catenin signalling regulates anteroposterior neural patterning in Xenopus. *Development*, 128(21), 4189–4201.

Kim, A., & Lowenstein, D. (2001). Wnt receptors and Wnt inhibitors are expressed in gradients in the developing telencephalon. *Mechanisms of Development*.

Kim, D., Kim, C., Moon, J., & Chung, Y. (2009). Generation of human induced pluripotent stem cells by direct delivery of reprogramming proteins. *Cell Stem Cell*

Kim, H., Lee, G., Ganat, Y., Papapetrou, E. P., Lipchina, I., Socci, N. D., et al. (2011a). miR-371-3 expression predicts neural differentiation propensity in human pluripotent stem cells. *Cell stem cell*, 8(6), 695–706. doi:10.1016/j.stem.2011.04.002

Kim, JH, Auerbach, J., Rodríguez-Gómez, J., Velasco, I., Gavin, D., Lumelsky, N., et al. (2002). Dopamine neurons derived from embryonic stem cells function in an animal model of Parkinson's disease. *Nature*, 418, 50–56.

Kim, Jongpil, Inoue, K., Ishii, J., Vanti, W. B., Voronov, S. V., Murchison, E., et al. (2007). A MicroRNA feedback circuit in midbrain dopamine neurons. *Science*, 317(5842), 1220–1224. doi:10.1126/science.1140481

Kim, Jongpil, Su, S. C., Wang, H., Cheng, A. W., Cassady, J. P., Lodato, M. A., et al. (2011b). Functional integration of dopaminergic neurons directly converted from mouse fibroblasts. *Cell stem cell*, 9(5), 413–419. doi:10.1016/j.stem.2011.09.011

Kim, K., Kim, C., Hwang, D., & Seo, H. (2003). Orphan nuclear receptor Nurr1 directly transactivates the promoter activity of the tyrosine hydroxylase gene in a cell-specific manner. Journal of Neurochemistry 85(3):622-634

Kim, T. K., Sul, J.-Y., Peternko, N. B., Lee, J. H., Lee, M., Patel, V. V., et al. (2011c). Transcriptome transfer provides a model for understanding the phenotype of cardiomyocytes. *Proceedings of the National Academy of Sciences of the United States of America*, 108(29), 11918–11923. doi:10.1073/pnas.1101223108

Kirkeby, A., & Parmar, M. (2012). Building authentic midbrain dopaminergic neurons from stem cells-lessons from development. *Translational Neuroscience*.

Kirkeby, A., Grealish, S., Wolf, D. A., Nelander, J., Wood, J., Lundblad, M., et al. (2012). Generation of Regionally Specified Neural Progenitors and Functional Neurons from Human Embryonic Stem Cells under Defined Conditions. *Cell Reports*, 1(6), 703–714. doi:10.1016/j.celrep.2012.04.009

Kirschenbaum, B., Nedergaard, M., Preuss, A., Barami, K., Fraser, R. A., & Goldman, S. A. (1994). In vitro neuronal production and differentiation by precursor cells derived from the adult human forebrain. *Cerebral cortex*, 4(6), 576–589.

Kishida, S., Yamamoto, H., Ikeda, S., Kishida, M., Sakamoto, I., Koyama, S., & Kikuchi, A. (1998). Axin, a negative regulator of the wnt signalling pathway, directly interacts with adenomatous polyposis coli and regulates the stabilization of beta-catenin. *Journal of Biological Chemistry*, 273(18), 10823–10826.

Kittappa, R., Chang, W., Awatramani, R., & McKay, R. (2007). The foxa2 gene controls the birth and spontaneous degeneration of dopamine neurons in old age. P*LoS Biol*, 5(12), e325.

Klaidman, L., Adams, J., Jr, Leung, A., Kim, S., & Cadenas, E. (1993). Redox cycling of MPP+: evidence for a new mechanism involving hydride transfer with xanthine oxidase, aldehyde dehydrogenase, and lipoamide dehydrogenase. *Free Radical Biology and Medicine,* 15(2), 169.

Klivenyi, P., Siwek, D., Gardian, G., Yang, L., Starkov, A., Cleren, C., et al. (2006). Mice lacking alpha-synuclein are resistant to mitochondrial toxins. *Neurobiology of disease*, 21(3), 541–548. doi:10.1016/j.nbd.2005.08.018

Kohn, A. D., & Moon, R. T. (2005). Wnt and calcium signalling: beta-catenin-independent pathways. *Cell calcium*, 38(3-4), 439–446. doi:10.1016/j.ceca.2005.06.022

Kohutnicka, M., Lewandowska, E., & Czlonkowski, A. (1998). Microglial and astrocytic involvement in a murine model of Parkinson's disease induced by 1-methyl-4-phenyl-1,2,3,6-tetrahydropyridine (MPTP). Immunopharmacology. 39(3):167-180

Kozlowski, D. A., Connor, B., Tillerson, J. L., Schallert, T., & Bohn, M. C. (2000). Delivery of a GDNF gene into the substantia nigra after a progressive 6-OHDA lesion maintains functional nigrostriatal connections. *Experimental neurology*, 166(1), 1–15. doi:10.1006/exnr.2000.7463

Krack, P., Batir, A., Van Blercom, N., Chabardes, S., Fraix, V., Ardouin, C., et al. (2003). Five-year follow-up of bilateral stimulation of the subthalamic nucleus in advanced Parkinson's disease. *N Engl J Med*, 349(20), 1925–1934. doi:10.1056/NEJMoa035275

Kriks, S., Shim, J.-W., Piao, J., Ganat, Y. M., Wakeman, D. R., Xie, Z., et al. (2011). Dopamine neurons derived from human ES cells efficiently engraft in animal models of Parkinson's disease. *Nature*. doi:10.1038/nature10648

Kroon, E., Martinson, L. A., Kadoya, K., Bang, A. G., Kelly, O. G., Eliazer, S., et al. (2008). Pancreatic endoderm derived from human embryonic stem cells generates glucose-responsive insulin-secreting cells *in vitro*. *Nature biotechnology*, 26(4), 443–452. doi:10.1038/nbt1393

Kukekov, V. G., Laywell, E. D., Suslov, O., Davies, K., Scheffler, B., Thomas, L. B., et al. (1999). Multipotent stem/progenitor cells with similar properties arise from two neurogenic regions of adult human brain. *Experimental neurology*, 156(2), 333–344. doi:10.1006/exnr.1999.7028

Kulich, S. M., & Chu, C. T. (2003). Role of reactive oxygen species in extracellular signal-regulated protein kinase phosphorylation and 6-hydroxydopamine cytotoxicity. *Journal of biosciences*, 28(1), 83–89.

Kwabi-Addo, B., Giri, D., & Schmidt, K. (2001). Haploinsufficiency of the Pten tumor suppressor gene promotes prostate cancer progression. *Proceedings of the National Academy of Sciences* 98(20):11563-11568

Laflamme, M. A., Chen, K. Y., Naumova, A. V., Muskheli, V., Fugate, J. A., Dupras, S. K., et al. (2007). Cardiomyocytes derived from human embryonic stem cells in pro-survival factors enhance function of infarcted rat hearts. *Nature biotechnology*, 25(9), 1015–1024. doi:10.1038/nbt1327

Lagarkova, M. A., Shutova, M. V., Bogomazova, A. N., Vassina, E. M., Glazov, E. A., Zhang, P., et al. (2010). Induction of pluripotency in human endothelial cells resets epigenetic profile on genome scale. *Cell cycle*, 9(5), 937–946.

Laguna Goya, R., Kuan, W.-L., & Barker, R. A. (2007). The future of cell therapies in the treatment of Parkinson's disease. *Expert opinion on biological therapy*, 7(10), 1487–1498. doi:10.1517/14712598.7.10.1487

Laker, C., Meyer, J., Schopen, A., Friel, J., Heberlein, C., Ostertag, W., & Stocking, C. (1998). Host cis-mediated extinction of a retrovirus permissive for expression in embryonal stem cells during differentiation. *Journal of virology*, 72(1), 339–348.

Lamb, T., Knecht, A., Smith, W., & Stachel, S. (1993). Neural induction by the secreted polypeptide noggin. *Science*.

Landry, D. W., & Zucker, H. A. (2004). Embryonic death and the creation of human embryonic stem cells. *The Journal of Clinical Investigation*, 114(9), 1184–1186. doi:10.1172/JCI23065

Langston, J. W., Forno, L. S., Tetrud, J., Reeves, A. G., Kaplan, J. A., & Karluk, D. (1999). Evidence of active nerve cell degeneration in the substantia nigra of humans years after 1-methyl-4-phenyl-1,2,3,6-tetrahydropyridine exposure. *Ann Neuro*l, 46(4), 598–605.

Langston, J., Ballard, P., Tetrud, J., & Irwin, I. (1983). Chronic parkinsonism in humans due to a product of meperidine-analog synthesis. *Science*, 219(4587), 979–980.

Lau, Y. S., Trobough, K. L., Crampton, J. M., & Wilson, J. A. (1990). Effects of probenecid on striatal dopamine depletion in acute and long-term 1-methyl-4-phenyl-1, 2, 3, 6-tetrahydropyridine (MPTP)-treated mice. *General pharmacology*, 21(2), 181–187.

Lau, Y.-S., Novikova, L., & Roels, C. (2005). MPTP treatment in mice does not transmit and cause Parkinsonian neurotoxicity in non-treated cagemates through close contact. *Neuroscience research*, 52(4), 371–378.

Laurent, L. C., Ulitsky, I., Slavin, I., Tran, H., Schork, A., Morey, R., et al. (2011). Dynamic changes in the copy number of pluripotency and cell proliferation genes in human ESCs and iPSCs during reprogramming and time in culture. *Cell stem cell*, 8(1), 106–118. doi:10.1016/j.stem.2010.12.003

Lebel, M., Gauthier, Y., & Moreau, A. (2001). Pitx3 activates mouse tyrosine hydroxylase promoter via a high-affinity binding site. Journal of Neurochemistry 77(2):558-567

Lee, C. R., & Tepper, J. M. (2009). Basal ganglia control of substantia nigra dopaminergic neurons. *Journal of neural transmission. Supplementum*, (73), 71–90.

Lee, G., Chambers, S. M., Tomishima, M. J., & Studer, L. (2010). Derivation of neural crest cells from human pluripotent stem cells. *Nature protocols*, 5(4), 688–701. doi:10.1038/nprot.2010.35

Lee, G., Papapetrou, E. P., Kim, H., Chambers, S. M., Tomishima, M. J., Fasano, C. A., et al. (2009). Modelling pathogenesis and treatment of familial dysautonomia using patient-specific iPSCs. *Nature*, 461(7262), 402–406. doi:10.1038/nature08320

Lee, G., Ramirez, C. N., Kim, H., Zeltner, N., Liu, B., Radu, C., et al. (2012). Large-scale screening using familial dysautonomia induced pluripotent stem cells identifies compounds that rescue IKBKAP expression. *Nature biotechnology*, 30(12), 1244–1248. doi:10.1038/nbt.2435

Lee, S. H., Lumelsky, N., Studer, L., Auerbach, J. M., & McKay, R. D. (2000). Efficient generation of midbrain and hindbrain neurons from mouse embryonic stem cells. *Nature Biotechnol*, 18(6), 675–679. doi:10.1038/76536

Lee, S. M., Danielian, P. S., Fritzsch, B., & McMahon, A. P. (1997). Evidence that FGF8 signalling from the midbrain-hindbrain junction regulates growth and polarity in the developing midbrain. *Development*, 124(5), 959–969.

Leimeister, C., Bach, A., & Gessler, M. (1998). Developmental expression patterns of mouse sFRP genes encoding members of the secreted frizzled related protein family. *Mechanisms of Development*, 75(1-2), 29–42.

Lev, S., Kehat, I., & Gepstein, L. (2005). Differentiation pathways in human embryonic stem cell-derived cardiomyocytes. *Annals of the New York Academy of Sciences*, 1047, 50–65. doi:10.1196/annals.1341.005

Levenberg, S., Burdick, J. A., Kraehenbuehl, T., & Langer, R. (2005). Neurotrophin-induced differentiation of human embryonic stem cells on three-dimensional polymeric scaffolds. *Tissue engineering*, 11(3-4), 506–512. doi:10.1089/ten.2005.11.506

Levenstein, M. E., Ludwig, T. E., Xu, R.-H., Llanas, R. A., VanDenHeuvel-Kramer, K., Manning, D., & Thomson, J. A. (2006). Basic fibroblast growth factor support of human embryonic stem cell self-renewal. *Stem cells (Dayton, Ohio)*, *24*(3), 568–574. doi:10.1634/stemcells.2005-0247

Levivier, M., Dethy, S., Rodesch, F., Peschanski, M., Vandesteene, A., David, P., et al. (1997). Intracerebral Transplantation of Fetal Ventral Mesencephalon for Patients with Advanced Parkinson's Disease Methodology and 6-Month to 1-Year Follow-Up in 3 Patients. *Stereotact Funct Neurosurg*, *69*, 99–111.

Levy, G., Burra, P., Cavallari, A., Duvoux, C., Lake, J., Mayer, A. D., et al. (2002). Improved clinical outcomes for liver transplant recipients using cyclosporine monitoring based on 2-hr post-dose levels (C2). *Transplantation*, 73(6), 953–959.

Leyns, L., Bouwmeester, T., Kim, S. H., Piccolo, S., & De Robertis, E. M. (1997). Frzb-1 is a secreted antagonist of Wnt signalling expressed in the Spemann organizer. *Cell*, 88(6), 747–756.

Li, J. Y. H., & Joyner, A. L. (2001). Otx2 and Gbx2 are required for refinement and not induction of mid-hindbrain gene expression. *Development* 128:4979-4991

Li, X., Zhao, X., Fang, Y., Jiang, X., Duong, T., Fan, C., et al. (1998). Generation of destabilized green fluorescent protein as a transcription reporter. *Journal of Biological Chemistry*, 273(52), 34970–34975.

Li, X.-J., Du, Z.-W., Zarnowska, E. D., Pankratz, M., Hansen, L. O., Pearce, R. A., & Zhang, S.-C. (2005). Specification of motoneurons from human embryonic stem cells. *Nature biotechnology*, 23(2), 215–221. doi:10.1038/nbt1063

Li, Y., Chen, J., Wang, L., Zhang, L., Lu, M., & Chopp, M. (2001). Intracerebral transplantation of bone marrow stromal cells in a 1-methyl-4-phenyl-1,2,3,6-tetrahydropyridine mouse model of Parkinson's disease. *Neuroscience letters,* 316(2), 67–70. doi:10.1016/S0304-3940(01)02384-9

Li, Y., Liu, W., Oo, T. F., Wang, L., & Tang, Y. (2009). Mutant LRRK2R1441G BAC transgenic mice recapitulate cardinal features of Parkinson's disease. *Nature*.

Liberatore, G., Przedborski, S., Jackson-Lewis, V., Vukosavic, S., Mandir, A., Vila, M., et al. (1999). Inducible nitric oxide synthase stimulates dopaminergic neurodegeneration in the MPTP model of Parkinson disease. *Nature Med*, 5, 1403–1409.

Lin, W., Metzakopian, E., Mavromatakis, Y., Gao, N., Balaskas, N., Sasaki, H., et al. (2009). Foxa1 and Foxa2 function both upstream of and cooperatively with *Lmx1a* and Lmx1b in a feedforward loop promoting mesodiencephalic dopaminergic neuron development. *Developmental Biology*, 333(2), 386–396.

Lindholm, P., Voutilainen, M. H., Laurén, J., Peränen, J., Leppänen, V.-M., Andressoo, J.-O., et al. (2007). Novel neurotrophic factor CDNF protects and rescues midbrain dopamine neurons *in vitro*. *Nature*, 448(7149), 73–77. doi:10.1038/nature05957

Lindvall, O., & Björklund, A. (2011). Cell Therapeutics in Parkinson's Disease. *Neurotherapeutics* : the journal of the American Society for Experimental NeuroTherapeutics. doi:10.1007/s13311-011-0069-6

Lindvall, O., & Kokaia, Z. (2010). Stem cells in human neurodegenerative disorders — time for clinical translation? *The Journal of Clinical Investigation*, 120(1), 29. doi:10.1172/JCI40543

Lindvall, O., Rehncrona, S., Brundin, P., Gustavii, B., Astedt, B., Widner, H., et al. (1989). Human fetal dopamine neurons grafted into the striatum in two patients with severe Parkinson's disease. A detailed account of methodology and a 6-month follow-up. *Arch Neurol*, 46(6), 615–631.

Lindvall, O., Brundin, P., Widner, H., Rehncrona, S., Gustavii, B., Frackowiak, R., et al. (1990). Grafts of fetal dopamine neurons survive and improve motor function in Parkinson's disease. *Science*, *247*(4942), 574–577.

Lindvall, O., Widner, H., Rehncrona, S., Brundin, P., Odin, P., Gustavii, B., et al. (1992). Transplantation of fetal dopamine neurons in Parkinson's disease: one-year clinical and neurophysiological observations in two patients with putaminal implants. *Annals of neurology*, *31*(2).

Lindvall, O., & Björklund, A. (2011). Cell Therapeutics in Parkinson's Disease. *Neurotherapeutics : the journal of the American Society for Experimental NeuroTherapeutics*. doi:10.1007/s13311-011-0069-6

Liou, H. H., Tsai, M. C., Chen, C. J., Jeng, J. S., Chang, Y. C., Chen, S. Y., & Chen, R. C. (1997). Environmental risk factors and Parkinson's disease: a case-control study in Taiwan. *Neurology*, 48(6), 1583–1588.

Liu, X., Li, F., Stubblefield, E., & Blanchard, B. (2011). Direct reprogramming of human fibroblasts into dopaminergic neuron-like cells. *Cell research*.

Liu, Y., Roghani, A., & Edwards, R. H. (1992). Gene transfer of a reserpine-sensitive mechanism of resistance to N-methyl-4-phenylpyridinium. *Proceedings of the National Academy of Sciences*, 89(19), 9074–9078.

Livak, K. (2001). Analysis of relative gene expression data using real-time quantitative PCR and the 2-[Delta][Delta] CT method. *Methods*.

Logan, C. Y., & Nusse, R. (2004). The Wnt signalling pathway in development and disease. *Annual Review of Cell and Developmental* Biology, 20, 781–810. doi:10.1146/annurev.cellbio.20.010403.113126

López-Lozano J. J., Bravo, G., Abascal, J,. & de Hierro Neural Transplantation Group, T. C. P. (1991). Grafting of perfused adrenal medullary tissue into the caudate nucleus of patients with Parkinson's disease. Journal of Neurosurgery 75(2) 234-243

Louvi, A., & Artavanis-Tsakonas, S. (2006). Notch signalling in vertebrate neural development. *Nature Reviews Neuroscience.*

Lujan, E., Chanda, S., Ahlenius, H., Südhof, T. C., & Wernig, M. (2012). Direct conversion of mouse fibroblasts to self-renewing, tripotent neural precursor cells. *Proceedings of the National Academy of Sciences of the United States of America*, 109(7), 2527–2532. doi:10.1073/pnas.1121003109

Luo, J. (2002). Subthalamic GAD Gene Therapy in a Parkinson's Disease Rat Model. *Science*, 298(5592), 425–429. doi:10.1126/science.1074549

Lyashenko, N., Winter, M., Migliorini, D., & Biechele, T. (2011). Differential requirement for the dual functions of [beta]-catenin in embryonic stem cell self-renewal and germ layer formation. *Nature cell Biology*

Mahlapuu, M., Enerbäck, S., & Carlsson, P. (2001). Haploinsufficiency of the forkhead gene Foxf1, a target for sonic hedgehog signalling, causes lung and foregut malformations. *Development*.

Mak, S. K., Huang, Y. A., Iranmanesh, S., Vangipuram, M., Sundararajan, R., Nguyen, L., et al. (2012). Small molecules greatly improve conversion of human-induced pluripotent stem cells to the neuronal lineage. *Stem cells international*, 2012, 140427. doi:10.1155/2012/140427

Mangale, V. S., Hirokawa, K. E., Satyaki, P. R. V., Gokulchandran, N., Chikbire, S., Subramanian, L., et al. (2008). Lhx2 selector activity specifies cortical identity and suppresses hippocampal organizer fate. *Science*, 319(5861), 304–309. doi:10.1126/science.1151695

Mann, D. M., & Yates, P. O. (1983). Pathological basis for neurotransmitter changes in Parkinson's disease. *Neuropathology and Applied Neurobiology*, 9(1), 3–19.

Manning-Bog, A., McCormack, A., Li, J., Uversky, V., Fink, A., & Di Monte, D. (2002). The Herbicide Paraquat Causes Up-regulation and Aggregation of alpha -Synuclein in Mice. Paraquat and alpha -SYNUCLEIN. *J Biol Chem*, 277(3), 1641–1644. doi:10.1074/jbc.C100560200

Marcelle, C., & Stark, M. (1997). Coordinate actions of BMPs, Wnts, Shh and noggin mediate patterning of the dorsal somite. *Development*.

Madrazo, I., Franco-Bourland, R., Ostrosky-Solis, F., Aguilera, M., Cuevas, C., Zamorano, C., et al. (1990). Fetal Homotransplants (Ventral Mesencephalon and Adrenal Tissue) to the Striatum of Parkinsonian Subjects. *Archives of Neurology*, *47*(12), 1281. doi:10.1001/archneur.1990.00530120025005

Markey, S., Johannessen, J., Chiueh, C., Burns, R., & Herkenham, M. (1984). Intraneuronal generation of a pyridinium metabolite may cause drug-induced parkinsonism. *Nature*, 311(5985), 464–467.

Marro, S., Pang, Z. P., Yang, N., Tsai, M.-C., Qu, K., Chang, H. Y., et al. (2011). Direct lineage conversion of terminally differentiated hepatocytes to functional neurons. *Cell stem cell*, 9(4), 374–382. doi:10.1016/j.stem.2011.09.002

Martinat, C., Bacci, J.-J., Leete, T., Kim, J., Vanti, W. B., Newman, A. H., et al. (2006). Cooperative transcription activation by Nurr1 and Pitx3 induces embryonic stem cell maturation to the midbrain dopamine neuron phenotype. *Proceedings of the National Academy of Sciences*, 103(8), 2874–2879. doi:10.1073/pnas.0511153103

Martinez, S., Crossley, P. H., Cobos, I., Rubenstein, J. L., & Martin, G. R. (1999). FGF8 induces formation of an ectopic isthmic organizer and isthmocerebellar development via a repressive effect on Otx2 expression. *Development*, 126(6), 1189–1200.

Matsui, T., Takano, M., Yoshida, K., Ono, S., Fujisaki, C., Matsuzaki, Y., et al. (2012). Neural Stem Cells Directly Differentiated from Partially Reprogrammed Fibroblasts Rapidly Acquire Gliogenic Competency. *Stem cells,* doi:10.1002/stem.1091

Matsuura, K., Kabuto, H., Makino, H., & Ogawa, N. (1997). Pole test is a useful method for evaluating the mouse movement disorder caused by striatal dopamine depletion. *Journal of Neuroscience Methods*, 73(1), 45–48.

Maxwell, S. L., Ho, H. Y., Kuehner, E., Zhao, S., & Li, M. (2005). Pitx3 regulates tyrosine hydroxylase expression in the substantia nigra and identifies a subgroup of mesencephalic dopaminergic progenitor neurons during mouse development. *Developmental Biology*, 282(2), 467–479.

Männistö, P., & Kaakkola, S. (1989). New selective COMT inhibitors: useful adjuncts for Parkinson's disease? *Trends in Pharmacological Sciences*.

McCormack, A. L., Thiruchelvam, M., Manning-Bog, A. B., Thiffault, C., Langston, J. W., Cory-Slechta, D. A., & Di Monte, D. A. (2002). Environmental risk factors and

Parkinson's disease: selective degeneration of nigral dopaminergic neurons caused by the herbicide paraquat. *Neurobiology of disease*, 10(2), 119–127.

McGeer, P. L., Itagaki, S., Akiyama, H., & McGeer, E. G. (1988). Rate of cell death in parkinsonism indicates active neuropathological process. *Ann Neurol*, 24(4), 574–576. doi:10.1002/ana.410240415

McGrew, L. L., Hoppler, S., & Moon, R. T. (1997). Wnt and FGF pathways cooperatively pattern anteroposterior neural ectoderm in Xenopus. M*echanisms of Development*, 69(1-2), 105–114.

McGrew, L., & Lai, C. (1995). Specification of the Anteroposterior Neural Axis through Synergistic Interaction of the Wnt Signalling Cascade with noggin and follistatin. *Developmental Biology*.

McGrew, L., & Otte, A. (1992). Analysis of Xwnt-4 in embryos of Xenopus laevis: a Wnt family member expressed in the brain and floor plate. *Development*.

Megason, S. G., & McMahon, A. P. (2002). A mitogen gradient of dorsal midline Wnts organizes growth in the CNS. *Development*, 129(9), 2087–2098.

Meng, F., Chen, S., Miao, Q., Zhou, K., & Lao, Q. (2011). Induction of fibroblasts to neurons through adenoviral gene delivery. *Cell research*.

Meredith, G. E., Halliday, G. M., & Totterdell, S. (2004). A critical review of the development and importance of proteinaceous aggregates in animal models of Parkinson's disease: new insights into Lewy body formation. *Parkinsonism & Related Disorders*, 10(4), 191–202. doi:10.1016/j.parkreldis.2004.01.001

Meredith, G. E., Sonsalla, P. K., & Chesselet, M.-F. (2008). Animal models of Parkinson's disease progression. *Acta neuropathologica*, 115(4), 385–398. doi:10.1007/s00401-008-0350-x

Millonig, J. H., Millen, K. J., & Hatten, M. E. (2000). The mouse Dreher gene *Lmx1a* controls formation of the roof plate in the vertebrate CNS. *Nature*, 403(6771), 764–769. doi:10.1038/35001573

Min, N., Joh, T. H., Kim, K. S., Peng, C., & Son, J. H. (1994). 5′ Upstream DNA sequence of the rat tyrosine hydroxylase gene directs high-level and tissue-specific expression to catecholaminergic neurons in the central nervous system of transgenic mice. *Molecular Brain Research*, *27*(2), 281–289. doi:10.1016/0169-328X(94)90011-6

Minkovsky, A., & Patel, S. (2011). Pluripotency and the Transcriptional Inactivation of the Female Mammalian X Chromosome. *Stem cells*.

Misgeld, U. (2004). Innervation of the substantia nigra. *Cell and Tissue Research*.

Mishima, Y., Lindgren, A. G., Chizhikov, V. V., Johnson, R. L., & Millen, K. J. (2009). Overlapping function of *Lmx1a* and Lmx1b in anterior hindbrain roof plate formation and cerebellar growth. *The Journal of neuroscience*, 29(36), 11377–11384. doi:10.1523/JNEUROSCI.0969-09.2009

Miyoshi, N., Ishii, H., Nagano, H., Haraguchi, N., Dewi, D. L., Kano, Y., et al. (2011). Reprogramming of mouse and human cells to pluripotency using mature microRNAs. *Cell stem cell,* 8(6), 633–638. doi:10.1016/j.stem.2011.05.001

Monville, C., Torres, E. M., & Dunnett, S. B. (2006). Comparison of incremental and accelerating protocols of the rotarod test for the assessment of motor deficits in the 6-OHDA model. *Journal of Neuroscience Methods*, 158(2), 219–223. doi:10.1016/j.jneumeth.2006.06.001

Morón, J. A., Brockington, A., Wise, R. A., Rocha, B. A., & Hope, B. T. (2002). Dopamine uptake through the norepinephrine transporter in brain regions with low levels of the dopamine transporter: evidence from knock-out mouse lines. *The Journal of neuroscience*, 22(2), 389–395.

Mortiboys, H., Johansen, K. K., Aasly, J. O., & Bandmann, O. (2010). Mitochondrial impairment in patients with Parkinson disease with the G2019S mutation in LRRK2. *Neurology*, 75(22), 2017–2020. doi:10.1212/WNL.0b013e3181ff9685

Moses, H. L., Ganote, C. E., Beaver, D. L., & Schuffman, S. S. (1966). Light and electron microscopic studies of pigment in human and rhesus monkey substantia nigra and locus coeruleus. *The Anatomical Record,* 155(2), 167–183. doi:10.1002/ar.1091550205

Munemitsu, S., Albert, I., Souza, B., Rubinfeld, B., & Polakis, P. (1995). Regulation of intracellular beta-catenin levels by the adenomatous polyposis coli (APC) tumor-suppressor protein. *Proceedings of the National Academy of Sciences*, 92(7), 3046–3050.

Muramatsu, S. I., Okuno, T., Suzuki, Y., & Nakayama, T. (2009). Multitracer assessment of dopamine function after transplantation of embryonic stem cell-derived neural stem cells in a primate model of Parkinson's disease. *Synapse*.

Müller, U. (1999). Ten years of gene targeting: targeted mouse mutants, from vector design to phenotype analysis. *Mechanisms of Development*, 82(1-2), 3–21.

Nakamura, T., Hamada, F., Ishidate, T., & Anai, K. (1998). Axin, an inhibitor of the Wnt signalling pathway, interacts with β-catenin, GSK-3β and APC and reduces the β-catenin level. Genes to ….

Nakano, I. (1984). Parkinson“s disease: neuron loss in the nucleus basalis without concomitant Alzheimer”s disease. *Annals of neurology*.

Nakatani, T., Kumai, M., Mizuhara, E., Minaki, Y., & Ono, Y. (2010). *Lmx1a* and Lmx1b cooperate with Foxa2 to coordinate the specification of dopaminergic neurons and control of floor plate cell differentiation in the developing mesencephalon. *Developmental Biology*, 339(1), 101–113.

Nefzger, C. M., Haynes, J. M., & Pouton, C. W. (2011). Directed Expression of Gata2, Mash1, and Foxa2 Synergize to Induce the Serotonergic Neuron Phenotype During In vitro Differentiation of Embryonic Stem Cells. *Stem cells*, 29(6), 928–939. doi:10.1002/stem.640

Nefzger, C. M., Su, C. T., Fabb, S. A., Hartley, B. J., Beh, S. J., Zeng, W. R., et al. (2012). *Lmx1a* Allows Context-Specific Isolation of Progenitors of GABAergic or Dopaminergic Neurons During Neural Differentiation of Embryonic Stem Cells. *Stem cells*, 30(7), 1349–1361. doi:10.1002/stem.1105

Nelander, J., Hebsgaard, J. B., & Parmar, M. (2009). Organization of the human embryonic ventral mesencephalon. *Gene expression pattern*: GEP, 9(8), 555–561. doi:10.1016/j.gep.2009.10.002

Neman, J., & De Vellis, J. (2012). A method for deriving homogenous population of oligodendrocytes from mouse embryonic stem cells. *Developmental Neurobiology*. doi:10.1002/dneu.22008

Ngwuluka, N., Pillay, V., Toit, Du, L. C., Ndesendo, V., Choonara, Y., Modi, G., & Naidoo, D. (2010). Levodopa delivery systems: advancements in delivery of the gold standard. *Expert opinion on drug delivery*, 7(2), 203–224. doi:10.1517/17425240903483166

Niederreither, K., Fraulob, V., & Garnier, J. (2002). Differential expression of retinoic acid-synthesizing (RALDH) enzymes during fetal development and organ differentiation in the mouse. … of development.

Nikkhah, G., Olsson, M., Eberhard, J., Bentlage, C., Cunningham, M., & Bjorklund, A. (1994). A microtransplantation approach for cell suspension grafting in the rat Parkinson model: a detailed account of the methodology. *Neuroscience*, 63(1), 57.

Nirenberg, M. J., Vaughan, R. A., Uhl, G. R., Kuhar, M. J., & Pickel, V. M. (1996). The dopamine transporter is localized to dendritic and axonal plasma membranes of nigrostriatal dopaminergic neurons. *The Journal of Neuroscience*, 16(2), 436–447.

Nishimura, F., Yoshikawa, M., & Kanda, S. (2003). Potential Use of Embryonic Stem Cells for the Treatment of Mouse Parkinsonian Models: Improved Behavior by Transplantation of In vitro Differentiated Dopaminergic Neurons from Embryonic Stem Cells. *Stem Cells* -

Niwa, H., Burdon, T., Chambers, I., & Smith, A. (1998). Self-renewal of pluripotent embryonic stem cells is mediated via activation of STAT3. Genes & development, *12*(13), 2048–2060.

Nunes, I., Tovmasian, L. T., Silva, R. M., Burke, R. E., & Goff, S. P. (2003). Pitx3 is required for development of substantia nigra dopaminergic neurons. *Proceedings of the National Academy of Sciences*, 100(7), 4245–4250. doi:10.1073/pnas.0230529100

Ogawa, N., Hirose, Y., Ohara, S., Ono, T., & Watanabe, Y. (1985). A simple quantitative bradykinesia test in MPTP-treated mice. R*es Commun Chem Path*, 50(3), 435–441.

Ogura, T., Ogata, M., Akita, H., Jitsuki, S., Akiba, L., Noda, K., et al. (2005). Impaired acquisition of skilled behavior in rotarod task by moderate depletion of striatal dopamine in a pre-symptomatic stage model of Parkinson's disease. *Neuroscience research*, 51(3), 299–308. doi:10.1016/j.neures.2004.12.006

Ohgushi, M., & Sasai, Y. (2011). Lonely death dance of human pluripotent stem cells: ROCKing between metastable cell states. *Trends in cell biology*, 21(5), 274–282. doi:10.1016/j.tcb.2011.02.004

Okada, Y., Shimazaki, T., Sobue, G., & Okano, H. (2004). Retinoic-acid-concentration-dependent acquisition of neural cell identity during *in vitro* differentiation of mouse embryonic stem cells. *Developmental Biology*, 275(1), 124–142. doi:10.1016/j.ydbio.2004.07.038

Okita, K., Nakagawa, M., Hyenjong, H., Ichisaka, T., & Yamanaka, S. (2008). Generation of mouse induced pluripotent stem cells without viral vectors. *Science*, 322(5903), 949–953. doi:10.1126/science.1164270

Olanow, C., Brin, M., & Obeso, J. (2000). The role of deep brain stimulation as a surgical treatment for Parkinson's disease. *Neurology*.

Ono, Y., Nakatani, T., Sakamoto, Y., Mizuhara, E., Minaki, Y., Kumai, M., et al. (2007). Differences in neurogenic potential in floor plate cells along an anteroposterior location: midbrain dopaminergic neurons originate from mesencephalic floor plate cells. *Development*, 134(17), 3213.

Pagano, S. F., Impagnatiello, F., Girelli, M., Cova, L., Grioni, E., Onofri, M., et al. (2000). Isolation and characterization of neural stem cells from the adult human olfactory bulb. *Stem cells*, 18(4), 295–300. doi:10.1634/stemcells.18-4-295

Palacino, J. J., Sagi, D., Goldberg, M. S., Krauss, S., Motz, C., Wacker, M., et al. (2004). Mitochondrial dysfunction and oxidative damage in parkin-deficient mice. Journal of Biological Chemistry, 279(18), 18614–18622. doi:10.1074/jbc.M401135200

Pan, G. (2007). Nanog and transcriptional networks in embryonic stem cell pluripotency. Cell research.

Pang, Z. P., Yang, N., Vierbuchen, T., Ostermeier, A., Fuentes, D. R., Yang, T. Q., et al. (2011). Induction of human neuronal cells by defined transcription factors. Nature, 476(7359), 220–223. doi:10.1038/nature10202

Parish, C., Castelo-Branco, G., Rawal, N., Tonnesen, J., Sorensen, A., Salto, C., et al. (2008). Wnt5a-treated midbrain neural stem cells improve dopamine cell replacement therapy in parkinsonian mice. J Clin Invest, 118(1), 149–160.

Parmar, M., & Li, M. (2007). Early specification of dopaminergic phenotype during ES cell differentiation. BMC developmental biology, 7(1), 86.

Parr, B., Shea, M., & Vassileva, G. (1993). Mouse Wnt genes exhibit discrete domains of expression in the early embryonic CNS and limb buds. Development (Cambridge, England).

Patel, A., Uhl, G., & Kuhar, M. J. (1993). Species differences in dopamine transporters: postmortem changes and glycosylation differences. Journal of Neurochemistry, 61(2), 496–500.

Patthey, C., & Gunhaga, L. (2011). Specification and regionalisation of the neural plate border. The European journal of neuroscience, 34(10), 1516–1528. doi:10.1111/j.1460-9568.2011.07871.x

Pawley, J. B. (2006). Handbook of biological confocal microscopy.

Paxinos, G., & Franklin, K. (2003). The mouse brain in stereotaxic coordinates: compact second edition. San Diego: Academic.

Peschanski, M., Defer, G., N'Guyen, J. P., Ricolfi, F., Monfort, J. C., Remy, P., et al. (1994). Bilateral motor improvement and alteration of L-dopa effect in two patients with Parkinson's disease following intrastriatal transplantation of fetalventral mesencephalon. *Brain : a journal of neurology*, *117 (Pt 3)*(3), 487–499.

Peng, G., & Westerfield, M. (2006). Lhx5 promotes forebrain development and activates transcription of secreted Wnt antagonists. Development (Cambridge, England), 133(16), 3191–3200. doi:10.1242/dev.02485

Perrier, A. L., Tabar, V., Barberi, T., Rubio, M. E., Bruses, J., Topf, N., et al. (2004). Derivation of midbrain dopamine neurons from human embryonic stem cells. Proceedings of the National Academy of Sciences of the United States of America, 101(34), 12543.

Petroske, E., Meredith, G. E., Callen, S., Totterdell, S., & Lau, Y. S. (2001). Mouse model of Parkinsonism: a comparison between subacute MPTP and chronic MPTP/probenecid treatment. Neuroscience, 106(3), 589–601.

Pevny, LH, Sockanathan, S., & Placzek, M. (1998). A role for SOX1 in neural determination. ….

Pezzoli, G., Fahn, S., Dwork, A., & Truong, D. D. (1988). Non-chromaffin tissue plus nerve growth factor reduces experimental parkinsonism in aged rats. Brain research.

Pfisterer, U., Kirkeby, A., Torper, O., Wood, J., Nelander, J., Dufour, A., et al. (2011). Direct conversion of human fibroblasts to dopaminergic neurons. Proceedings of the National Academy of Sciences, 108(25), 10343–10348. doi:10.1073/pnas.1105135108

Piccolo, S., Agius, E., Leyns, L., & Bhattacharyya, S. (1999). The head inducer Cerberus is a multifunctional antagonist of Nodal, BMP and Wnt signals. Nature.

Pincus, D., & Keyoung, H. (1998). Fibroblast growth factor-2/brain-derived neurotrophic factor—associated maturation of new neurons generated from adult human subependymal cells. Annals of ….

Pinson, K. I., Brennan, J., Monkley, S., Avery, B. J., & Skarnes, W. C. (2000). An LDL-receptor-related protein mediates Wnt signalling in mice. Nature, 407(6803), 535–538. doi:10.1038/35035124

Plews, J. R., Li, J., Jones, M., Moore, H. D., Mason, C., Andrews, P. W., & Na, J. (2010). Activation of pluripotency genes in human fibroblast cells by a novel mRNA based approach. PLoS ONE, 5(12), e14397. doi:10.1371/journal.pone.0014397

Politis, M., Oertel, W. H., Wu, K., Quinn, N. P., Pogarell, O., Brooks, D. J., et al. (2011). Graft-induced dyskinesias in Parkinson's disease: High striatal serotonin/dopamine transporter ratio. Movement Disorders, 26(11), 1997–2003. doi:10.1002/mds.23743

Potashkin, J., Kang, U., Loomis, P., Jodelka, F., Ding, Y., & Meredith, G. (2007). MPTP administration in mice changes the ratio of splice isoforms of fosB and rgs9. Brain Res, 1182, 1–10.

Pouton, C. W., & Haynes, J. M. (2007). Embryonic stem cells as a source of models for drug discovery. Nature Reviews Drug Discovery, 6(8), 605–616. doi:10.1038/nrd2194

Prakash, N., Brodski, C., Naserke, T., & Puelles, E. (2006). A Wnt1-regulated genetic network controls the identity and fate of midbrain-dopaminergic progenitors *in vitro*. ….

Price, K. S., Farley, I. J., & Hornykiewicz, O. (1978). Neurochemistry of Parkinson's di... [Adv Biochem Psychopharmacol. 1978] - PubMed - NCBI. Advances in biochemical ….

Priyadarshi, A., Khuder, S. A., Schaub, E. A., & Priyadarshi, S. S. (2001). Environmental risk factors and Parkinson's disease: a metaanalysis. Environmental research, 86(2), 122–127. doi:10.1006/enrs.2001.4264

Przedborski, S., & Vila, M. (2003). The 1-Methyl-4-Phenyl-1, 2, 3, 6-Tetrahydropyridine Mouse Model A Tool to Explore the Pathogenesis of Parkinson's Disease. Ann Ny Acad Sci, 991(1), 189–198.

Przedborski, S., Jackson-Lewis, V., Naini, AB, Jakowec, M., Petzinger, G., Miller, R., & Akram, M. (2001). The parkinsonian toxin 1-methyl-4-phenyl-1, 2, 3, 6-tetrahydropyridine (MPTP): a technical review of its utility and safety. Journal of Neurochemistry, 76(5), 1265.

Przedborski, S., Jackson-Lewis, V., Yokoyama, R., Shibata, T., Dawson, V., & Dawson, T. (1996). Role of neuronal nitric oxide in 1-methyl-4-phenyl-1, 2, 3, 6-tetrahydropyridine (MPTP)-induced dopaminergic neurotoxicity, 93(10), 4565–4571.

Przedborski, S., Kostic, V., Jackson-Lewis, V., Naini, A. B., Simonetti, S., Fahn, S., et al. (1992). Transgenic mice with increased Cu/Zn-superoxide dismutase activity are resistant to N-methyl-4-phenyl-1, 2, 3, 6-tetrahydropyridine-induced neurotoxicity. The Journal of Neuroscience, 12(5), 1658–1667.

Puelles, E., Annino, A., Tuorto, F., Usiello, A., Acampora, D., Czerny, T., et al. (2004). Otx2 regulates the extent, identity and fate of neuronal progenitor domains in the ventral midbrain. Development (Cambridge, England), 131(9), 2037–2048. doi:10.1242/dev.01107

Puelles, L., & Rubenstein, J. (2003). Forebrain gene expression domains and the evolving prosomeric model. Trends in Neurosciences, 26(9), 469–476.

Ramalho-Santos, M., Yoon, S., Matsuzaki, Y., & Mulligan, R. C. (2002). " Stemness": transcriptional profiling of embryonic and adult stem cells. Science.

Rambhatla, L., Chiu, C.-P., Kundu, P., Peng, Y., & Carpenter, M. K. (2003). Generation of hepatocyte-like cells from human embryonic stem cells. Cell Transplant, 12(1), 1–11.

Ramsay, R. R., Salach, J. I., Dadgar, J., & Singer, T. P. (1986a). Inhibition of mitochondrial NADH dehydrogenase by pyridine derivatives and its possible relation to experimental and idiopathic parkinsonism. Biochem Biophys Res Commun, 135(1), 269–275.

Ramsay, R., Dadgar, J., Trevor, A., & Singer, T. (1986b). Energy-driven uptake on N-methyl-4-phenylpyridine by brain mitochondria mediates the neurotoxicity of MPTP. Life sciences(1973), 39(7), 581–588.

Rao, M. (2004). Conserved and divergent paths that regulate self-renewal in mouse and human embryonic stem cells. Developmental Biology.

Rascol, O., Brooks, D., & Korczyn, A. (2000). A five-year study of the incidence of dyskinesia in patients with early Parkinson's disease who were treated with ropinirole or levodopa. … England Journal of ….

Rattner, A., Hsieh, J. C., Smallwood, P. M., Gilbert, D. J., Copeland, N. G., Jenkins, N. A., & Nathans, J. (1997). A family of secreted proteins contains homology to the cysteine-rich ligand-binding domain of frizzled receptors. Proceedings of the National Academy of Sciences, 94(7), 2859–2863.

Raye, W., Tochon-Danguy, N., Pouton, C., & Haynes, J. (2007). Heterogeneous population of dopaminergic neurons derived from mouse embryonic stem cells: preliminary phenotyping based on receptor expression and function. The European journal of neuroscience, 25(7), 1961–1970.

Richardson, J. R., Quan, Y., Sherer, T. B., Greenamyre, J. T., & Miller, G. W. (2005). Paraquat neurotoxicity is distinct from that of MPTP and rotenone. Toxicological sciences : an official journal of the Society of Toxicology, 88(1), 193–201. doi:10.1093/toxsci/kfi304

Robinson, T. E., & Becker, J. B. (1983). The rotational behavior model: asymmetry in the effects of unilateral 6-OHDA lesions of the substantia nigra in rats. Brain research, 264(1), 127–131.

Robinton, D. A., & Daley, G. Q. (2012). The promise of induced pluripotent stem cells in research and therapy. Nature, 481(7381), 295–305. doi:10.1038/nature10761

Rodriguez-Gomez, J. A., Lu, J.-Q., Velasco, I., Rivera, S., Zoghbi, S. S., Liow, J.-S., et al. (2007). Persistent Dopamine Functions of Neurons Derived from Embryonic Stem Cells in a Rodent Model of Parkinson Disease. Stem cells (Dayton, Ohio), 25(4), 918–928. doi:10.1634/stemcells.2006-0386

Roelink, H., & Nusse, R. (1991). Expression of two members of the Wnt family during mouse development--restricted temporal and spatial patterns in the developing neural tube.

Roelink, H., Porter, J., Chiang, C., & Tanabe, Y. (1995). Floor plate and motor neuron induction by different concentrations of the amino-terminal cleavage product of sonic hedgehog autoproteolysis. Cell.

Rosa, A., & Brivanlou, A. H. (2010). Synthetic mRNAs: powerful tools for reprogramming and differentiation of human cells. Cell stem cell, 7(5), 549–550. doi:10.1016/j.stem.2010.10.002

Rossant, J. (2004). Lineage development and polar asymmetries in the peri-implantation mouse blastocyst. Seminars in cell & developmental biology, 15(5), 573–581. doi:10.1016/j.semcdb.2004.04.003

Rossant, J. (2008). Stem cells and early lineage development. Cell.

Roy, N., Cleren, C., Singh, S., Yang, L., Beal, M., & Goldman, S. (2006). Functional engraftment of human ES cell-derived dopaminergic neurons enriched by coculture with telomerase-immortalized midbrain astrocytes. Nature Med, 12(11), 1259–1268.

Rozas, G., López-Martín, E., Guerra, M. J., & Labandeira-García, J. L. (1998). The overall rod performance test in the MPTP-treated-mouse model of Parkinsonism. Journal of Neuroscience Methods, 83(2), 165–175.

Ruby, K. M., & Zheng, B. (2009). Gene targeting in a HUES line of human embryonic stem cells via electroporation. Stem cells (Dayton, Ohio), 27(7), 1496–1506. doi:10.1002/stem.73

Sacchetti, P., Brownschidle, L. A., Granneman, J. G., & Bannon, M. J. (1999). Characterization of the 5'-flanking region of the human dopamine transporter gene. Mol Brain Res, 74(1-2), 167–174.

Saha, S., Guillily, M. D., Ferree, A., Lanceta, J., Chan, D., Ghosh, J., et al. (2009). LRRK2 modulates vulnerability to mitochondrial dysfunction in Caenorhabditis elegans. The Journal of neuroscience : the official journal of the Society for Neuroscience, 29(29), 9210–9218. doi:10.1523/JNEUROSCI.2281-09.2009

Sakai, Y. (1989). Neurulation in the mouse: Manner and timing of neural tube closure. The Anatomical Record, 223(2), 194–203. doi:10.1002/ar.1092230212

Sander, M., Paydar, S., Ericson, J., Briscoe, J., Berber, E., German, M., et al. (2000). Ventral neural patterning by Nkx homeobox genes: Nkx6.1 controls somatic motor neuron and ventral interneuron fates. Genes & development, 14(17), 2134–2139.

Sasai, Y., Lu, B., Steinbeisser, H., & De Robertis, E. M. (1995). Regulation of neural induction by the Chd and Bmp-4 antagonistic patterning signals in Xenopus. Nature, 377(6551), 757. doi:10.1038/377757a0

Satoh, N., Yonezawa, A., Tadano, T., Kisara, K., & Arai, Y. (1987a). Acute effects of a parkinsonism-inducing neurotoxin, 1-methyl-4-phenyl-1, 2, 3, 6-tetrahydropyridine (MPTP) on mouse body temperature. *Life Sciences*.

Satoh, N., Yonezawa, A., Tadano, T., Kisara, K., & Arai, Y. (1987b). Central hypothermic effects of some analogues of 1-methyl-4-phenyl-1, 2, 3, 6-tetrahydropyridine (MPTP) and 1-methyl-4-phenylpyridinium ion (MPP+). *Neuroscience*.

Schallert, T., & Woodlee, M. (2002). Disentangling multiple types of recovery from brain injury. … of cerebral ischemia.

Schapira, A. H., & Jenner, P. (2011). Etiology and pathogenesis of Parkinson's disease. Movement Disorders, 26(6), 1049–1055. doi:10.1002/mds.23732

Schatten, G., Smith, J., Navara, C., Park, J.-H., & Pedersen, R. (2005). Culture of human embryonic stem cells. Nature methods, 2(6), 455–463. doi:10.1038/nmeth0605-455

Schober, A. (2004). Classic toxin-induced animal models of Parkinson's disease: 6-OHDA and MPTP. Cell and Tissue Research, 318(1), 215–224.

Schulz, J., Matthews, R., & Muqit, M. (1995). Inhibition of neuronal nitric oxide synthase by 7-nitroindazole protects against MPTP-induced neurotoxicity in mice. Journal of ….

Schulz, T. C., Noggle, S. A., Palmarini, G. M., Weiler, D. A., Lyons, I. G., Pensa, K. A., et al. (2004). Differentiation of Human Embryonic Stem Cells to Dopaminergic Neurons in Serum-Free Suspension Culture. Stem cells (Dayton, Ohio), 22(7), 1218–1238. doi:10.1634/stemcells.2004-0114

Sedelis, M., Hofele, K., Auburger, G. W., Morgan, S., Huston, J. P., & Schwarting, R. K. (2000). MPTP susceptibility in the mouse: behavioral, neurochemical, and histological analysis of gender and strain differences. Behavior genetics, 30(3), 171–182.

Sedelis, M., Schwarting, R. K., & Huston, J. P. (2001). Behavioral phenotyping of the MPTP mouse model of Parkinson's disease. Behav Brain Res, 125(1-2), 109–125.

Semchuk, K. M., Love, E. J., & Lee, R. G. (1991). Parkinson's disease and exposure to rural environmental factors: a population based case-control study. The Canadian journal of neurological sciences. Le journal canadien des sciences neurologiques, 18(3), 279–286.

Semina, E. V., Murray, J. C., Reiter, R., Hrstka, R. F., & Graw, J. (2000). Deletion in the promoter region and altered expression of Pitx3 homeobox gene in aphakia mice. Human Molecular Genetics, 9(11), 1575–1585.

Shachar, D. B., Kahana, N., Kampel, V., Warshawsky, A., & Youdim, M. B. H. (2004). Neuroprotection by a novel brain permeable iron chelator, VK-28, against 6-hydroxydopamine lession in rats. Neuropharmacology, 46(2), 254–263.

Shahed, J., & Jankovic, J. (2007). Motor symptoms in Parkinson's disease. Handbook of Clinical Neurology.

Shen, Y., Muramatsu, S., & Ikeguchi, K. (2000). … -associated virus vectors expressing tyrosine hydroxylase, aromatic-L-amino-acid decarboxylase, and GTP cyclohydrolase I for gene therapy of Parkinson's disease. … gene therapy.

Sherer, T. B., Kim, J.-H., Betarbet, R., & Greenamyre, J. T. (2003a). Subcutaneous Rotenone Exposure Causes Highly Selective Dopaminergic Degeneration and [alpha]-Synuclein Aggregation. Experimental neurology, 179(1), 9–16. Retrieved from http://www.sciencedirect.com/science/article/pii/S0014488602980726

Sherer, T., Betarbet, R., & Testa, C. (2003b). Mechanism of toxicity in rotenone models of Parkinson's disease. The Journal of ….

Shi, Y., Desponts, C., Do, J. T., Hahm, H. S., Schöler, H. R., & Ding, S. (2008). Induction of pluripotent stem cells from mouse embryonic fibroblasts by Oct4 and Klf4 with small-molecule compounds. Cell stem cell, 3(5), 568–574. doi:10.1016/j.stem.2008.10.004

Simon, H. H., Saueressig, H., Wurst, W., Goulding, M. D., & O'Leary, D. D. (2001). Fate of midbrain dopaminergic neurons controlled by the engrailed genes. The Journal of neuroscience : the official journal of the Society for Neuroscience, 21(9), 3126–3134.

Simon, H. H., Thuret, S., & Alberi, L. (2004). Midbrain dopaminergic neurons: control of their cell fate by the engrailed transcription factors. Cell and Tissue Research, 318(1), 53–61. doi:10.1007/s00441-004-0973-8

Sinha, S., & Chen, J. K. (2006). Purmorphamine activates the Hedgehog pathway by targeting Smoothened. Nature chemical biology, 2(1), 29–30. doi:10.1038/nchembio753

Smidt, M., Asbreuk, C., Cox, J., Chen, H., Johnson, R., & Burbach, J. (2000). A second independent pathway for development of mesencephalic dopaminergic neurons requires Lmx1b. Nature neuroscience, 3(4), 337–341.

Smidt, M., Van Schaick, H., Lancto, t, C., Tremblay, J., Cox, J., et al. (1997). A homeodomain gene Ptx3 has highly restricted brain expression in mesencephalic dopaminergic neurons, 94(24), 13305–13310.

Smith, A. G., Heath, J. K., Donaldson, D. D., Wong, G. G., Moreau, J., Stahl, M., & Rogers, D. (1988). Inhibition of pluripotential embryonic stem cell differentiation by purified polypeptides. Nature, 336(6200), 688–690. doi:10.1038/336688a0

Smith, T. (1997). Mitochondrial toxins in models of neurodegenerative diseases. I: *in vitro* brain hydroxyl radical production during sytemic MPTP treatment or following microdialysis …. Brain research.

Smith, Y., & Parent, A. (1988). Neurons of the subthalamic nucleus in primates display glutamate but not GABA immunoreactivity. Brain research.

Smits, S. M., Ponnio, T., Conneely, O. M., Burbach, J. P. H., & Smidt, M. P. (2003). Involvement of Nurr1 in specifying the neurotransmitter identity of ventral midbrain dopaminergic neurons. The European journal of neuroscience, 18(7), 1731–1738.

Soldner, F., Hockemeyer, D., Beard, C., Gao, Q., Bell, G. W., Cook, E. G., et al. (2009). Parkinson's disease patient-derived induced pluripotent stem cells free of viral reprogramming factors. Cell, 136(5), 964–977. doi:10.1016/j.cell.2009.02.013

Somers, A., Jean, J.-C., Sommer, C. A., Omari, A., Ford, C. C., Mills, J. A., et al. (2010). Generation of transgene-free lung disease-specific human induced pluripotent stem cells using a single excisable lentiviral stem cell cassette. Stem cells (Dayton, Ohio), 28(10), 1728–1740. doi:10.1002/stem.495

Sommer, C. A., Sommer, A. G., Longmire, T. A., Christodoulou, C., Thomas, D. D., Gostissa, M., et al. (2010). Excision of reprogramming transgenes improves the differentiation potential of iPS cells generated with a single excisable vector. Stem cells (Dayton, Ohio), 28(1), 64–74. doi:10.1002/stem.255

Song, D. D., & Haber, S. N. (2000). Striatal responses to partial dopaminergic lesion: evidence for compensatory sprouting. The Journal of neuroscience : the official journal of the Society for Neuroscience, 20(13), 5102–5114.

Song, W. J., Sullivan, M. G., Legare, R. D., & Hutchings, S. (1999). Haploinsufficiency of CBFA2 causes familial thrombocytopenia with propensity to develop acute myelogenous leukaemia. Nature.

Sonntag, K. C., Pruszak, J., Yoshizaki, T., van Arensbergen, J., Sánchez-Pernaute, R., & Isacson, O. (2007). Enhanced yield of neuroepithelial precursors and midbrain-like dopaminergic neurons from human embryonic stem cells using the bone morphogenic protein antagonist noggin. Stem cells (Dayton, Ohio), 25(2), 411–418. doi:10.1634/stemcells.2006-0380

Staal, R. G., Hogan, K. A., Liang, C. L., German, D. C., & Sonsalla, P. K. (2000). In vitro studies of striatal vesicles containing the vesicular monoamine transporter (VMAT2): rat versus mouse differences in sequestration of 1-methyl-4-phenylpyridinium. J Pharmacol Exp Ther, 293(2), 329–335.

Stanic, D., Tripanichkul, W., Drago, J., Finkelstein, D. I., & Horne, M. K. (2004). Glial responses associated with dopaminergic striatal reinnervation following lesions of the rat substantia nigra. Brain research, 1023(1), 83–91. doi:10.1016/j.brainres.2004.07.012

Sul, J.-Y., Wu, C.-W. K., Zeng, F., Jochems, J., Lee, M. T., Kim, T. K., et al. (2009). Transcriptome transfer produces a predictable cellular phenotype. Proceedings of the National Academy of Sciences of the United States of America, 106(18), 7624–7629. doi:10.1073/pnas.0902161106

Sullivan, G. J., Bai, Y., Fletcher, J., & Wilmut, I. (2010). Induced pluripotent stem cells: epigenetic memories and practical implications. Molecular human reproduction, 16(12), 880–885. doi:10.1093/molehr/gaq091

Sundstrom, E., Fredriksson, A., & Archer, T. (1990). Chronic neurochemical and behavioral changes in MPTP-lesioned C57BL/6 mice: a model for Parkinson's disease. Brain research, 528(2), 181–188.

Swijnenburg, R.-J., Tanaka, M., Vogel, H., Baker, J., Kofidis, T., Gunawan, F., et al. (2005). Embryonic stem cell immunogenicity increases upon differentiation after transplantation into ischemic myocardium. Circulation, 112(9 Suppl), I166–72. doi:10.1161/CIRCULATIONAHA.104.525824

Swistowska, A., da Cruz, AB, Han, Y., Swistowski, A., Liu, Y., Shin, S., et al. (2010). Stage-specific role for Shh in dopaminergic differentiation of human embryonic stem cells induced by stromal cells. Stem Cells and Development, 19(1), 71–82.

Tadano, T., Satoh, N., Oyama, K., Kisara, K., & Arai, Y. (1991). Acute Effects of 1-Methyl-4-Phenyl-1, 2, 3, 6-Tetrahydropyridine (MPTP) on Body Temperature of Various Strains of Mice. *Basic, Clinical, and Therapeutic Aspects of Alzheimer's and Parkinson's Diseases* Advances in Behavioral Biology Volume 38A, 1991, pp 297-300

Takahashi, J., Takagi, Y., & Saiki, H. (2009). Transplantation of Embryonic Stem Cell-Derived Dopaminergic Neurons in MPTP-Treated Monkeys. Methods in molecular biology (Clifton, N.J.), 482, 199.

Takahashi, K., & Yamanaka, S. (2006). Induction of pluripotent stem cells from mouse embryonic and adult fibroblast cultures by defined factors. Cell, 126(4), 663–676. doi:10.1016/j.cell.2006.07.024

Takahashi, K., Tanabe, K., Ohnuki, M., Narita, M., Ichisaka, T., Tomoda, K., & Yamanaka, S. (2007). Induction of pluripotent stem cells from adult human fibroblasts by defined factors. Cell, 131(5), 861–872. doi:10.1016/j.cell.2007.11.019

Takahashi, N., Miner, L., & Sora, I. (1997). VMAT2 knockout mice: heterozygotes display reduced amphetamine-conditioned reward, enhanced amphetamine locomotion, and enhanced MPTP toxicity. Presented at the Proceedings of the ….

Tamai, K., Zeng, X., Liu, C., Zhang, X., & Harada, Y. (2004). A mechanism for Wnt coreceptor activation. Molecular ….

Tang, M., Villaescusa, J. C., Luo, S. X., Guitarte, C., Lei, S., Miyamoto, Y., et al. (2010). Interactions of Wnt/beta-catenin signalling and sonic hedgehog regulate the neurogenesis of ventral midbrain dopamine neurons. The Journal of neuroscience : the official journal of the Society for Neuroscience, 30(27), 9280–9291. doi:10.1523/JNEUROSCI.0860-10.2010

Taupin, P. (2002). Adult neurogenesis and neural stem cells of the central nervous system in mammals. Journal of Neuroscience Research.

Teismann, P., & Schulz, J. B. (2004). Cellular pathology of Parkinson's disease: astrocytes, microglia and inflammation. Cell and Tissue Research, 318(1), 149–161. doi:10.1007/s00441-004-0944-0

Temel, Y., Kessels, A., Tan, S., Topdag, A., Boon, P., & Visser-Vandewalle, V. (2006). Behavioural changes after bilateral subthalamic stimulation in advanced Parkinson disease: a systematic review. Parkinsonism & Related Disorders, 12(5), 265–272. doi:10.1016/j.parkreldis.2006.01.004

Terzioglu, M., & Galter, D. (2008). Parkinson's disease: genetic versus toxin-induced rodent models. The FEBS journal, 275(7), 1384–1391. doi:10.1111/j.1742-4658.2008.06302.x

Tesar, P. J., Chenoweth, J. G., Brook, F. A., Davies, T. J., Evans, E. P., Mack, D. L., et al. (2007). New cell lines from mouse epiblast share defining features with human embryonic stem cells. Nature, 448(7150), 196–199. doi:10.1038/nature05972

Thameem, F., Wolford, J. K., Wang, J., German, M. S., Bogardus, C., & Prochazka, M. (2002). Cloning, expression and genomic structure of human *LMX1A*, and variant screening in Pima Indians. Gene, 290(1-2), 217–225.

Thier, M., Wörsdörfer, P., Lakes, Y. B., Gorris, R., Herms, S., Opitz, T., et al. (2012). Direct Conversion of Fibroblasts into Stably Expandable Neural Stem Cells. Cell stem cell. doi:10.1016/j.stem.2012.03.003

Thiruchelvam, M., Richfield, E. K., Baggs, R. B., Tank, A. W., & Cory-Slechta, D. A. (2000). The nigrostriatal dopaminergic system as a preferential target of repeated exposures to combined paraquat and maneb: implications for Parkinson's disease. The Journal of neuroscience : the official journal of the Society for Neuroscience, 20(24), 9207–9214.

Thomas, K. R., Folger, K. R., & Capecchi, M. R. (1986). High frequency targeting of genes to specific sites in the mammalian genome. Cell, 44(3), 419–428.

Thompson, L. H., Andersson, E., Jensen, J. B., Barraud, P., Guillemot, F., Parmar, M., & Björklund, A. (2006). Neurogenin2 identifies a transplantable dopamine neuron precursor in the developing ventral mesencephalon. Experimental neurology, 198(1), 183–198. doi:10.1016/j.expneurol.2005.11.025

Thompson, L. H., Grealish, S., Kirik, D., & Björklund, A. (2009). Reconstruction of the nigrostriatal dopamine pathway in the adult mouse brain. The European journal of neuroscience, 30(4), 625–638. doi:10.1111/j.1460-9568.2009.06878.x

Thompson, L. H., Kirik, D., & Björklund, A. (2008). Non-dopaminergic neurons in ventral mesencephalic transplants make widespread axonal connections in the host brain. Experimental neurology, 213(1), 220–228. doi:10.1016/j.expneurol.2008.06.005

Thompson, L., Barraud, P., Andersson, E., Kirik, D., & Björklund, A. (2005). Identification of dopaminergic neurons of nigral and ventral tegmental area subtypes in grafts of fetal ventral mesencephalon based on cell morphology, protein expression, and efferent projections. The Journal of neuroscience : the official journal of the Society for Neuroscience, 25(27), 6467–6477. doi:10.1523/JNEUROSCI.1676-05.2005

Thomson, J. A., Itskovitz-Eldor, J., Shapiro, S. S., Waknitz, M. A., Swiergiel, J. J., Marshall, V. S., & Jones, J. M. (1998). Embryonic stem cell lines derived from human blastocysts. Science, 282(5391), 1145–1147.

Tolwinski, N. S., & Wieschaus, E. (2004). A Nuclear Function for Armadillo/β-Catenin. PLoS Biol, 2(4), e95. doi:10.1371/journal.pbio.0020095

Trépanier, L., Kumar, R., Lozano, A., & Lang, A. (2000). Neuropsychological outcome of GPi pallidotomy and GPi or STN deep brain stimulation in Parkinson's disease. Brain and Cognition.

Tripanichkul, W., Sripanichkulchai, K., & Finkelstein, D. I. (2006). Estrogen down-regulates glial activation in male mice following 1-methyl-4-phenyl-1,2,3,6-tetrahydropyridine intoxication. Brain research, 1084(1), 28–37. doi:10.1016/j.brainres.2006.02.029

Ugrumov, M. (2008). Brain neurons partly expressing monoaminergic phenotype: distribution, development, and functional significance in norm and pathology. Handbook of Neurochemistry and Molecular ….

Ungar, A. R., Kelly, G. M., & Moon, R. T. (1995). Wnt4 affects morphogenesis when misexpressed in the zebrafish embryo. Mechanisms of Development, 52(2-3), 153–164.

Ungerstedt, U. (1968). 6-Hydroxydopamine induced degeneration of central monoamine neurons. European Journal of Pharmacology, 5(1), 107–110.

Urbach, A., Schuldiner, M., & Benvenisty, N. (2004). Modeling for Lesch-Nyhan disease by gene targeting in human embryonic stem cells. Stem cells (Dayton, Ohio), 22(4), 635–641. doi:10.1634/stemcells.22-4-635

Urbánek, P., Fetka, I., Meisler, M. H., & Busslinger, M. (1997). Cooperation of Pax2 and Pax5 in midbrain and cerebellum development. Proceedings of the National Academy of Sciences, 94(11), 5703–5708.

Vallier, L., Alexander, M., & Pedersen, R. A. (2005). Activin/Nodal and FGF pathways cooperate to maintain pluripotency of human embryonic stem cells. Journal of Cell Science, 118(Pt 19), 4495–4509. doi:10.1242/jcs.02553

van de Wetering, M., Cavallo, R., Dooijes, D., van Beest, M., van Es, J., Loureiro, J., et al. (1997). Armadillo coactivates transcription driven by the product of the Drosophila segment polarity gene dTCF. Cell, 88(6), 789–799.

Van Woert, M. H., Prasad, K. N., & Borg, D. C. (1967). Spectroscopic studies of substantia nigra pigment in human subjects. Journal of Neurochemistry, 14(7), 707–716.

VanDunk, C., Hunter, L. A., & Gray, P. A. (2011). Development, maturation, and necessity of transcription factors in the mouse suprachiasmatic nucleus. The Journal of neuroscience : the official journal of the Society for Neuroscience, 31(17), 6457–6467. doi:10.1523/JNEUROSCI.5385-10.2011

Vazin, T., Becker, K. G., Chen, J., Spivak, C. E., Lupica, C. R., Zhang, Y., et al. (2009). A Novel Combination of Factors, Termed SPIE, which Promotes Dopaminergic Neuron Differentiation from Human Embryonic Stem Cells. PLoS ONE, 4(8), e6606.

Vermeren, M., & Keynes, R. (2001). Veterbrate Central Nervous System: Pattern Formation. (John Wiley & Sons, Ltd, Ed.). Chichester, UK: John Wiley & Sons, Ltd. doi:10.1002/9780470015902.a0000794.pub2

Vierbuchen, T., Ostermeier, A., Pang, Z. P., Kokubu, Y., S ºdhof, T. C., & Wernig, M. (2010). Direct conversion of fibroblasts to functional neurons by defined factors. *Nature*, 463(7284), 1035–1041. doi:10.1038/nature08797

Vila, M., Jackson-Lewis, V., Vukosavic, S., Djaldetti, R., Liberatore, G., Offen, D., et al. (2001). Bax ablation prevents dopaminergic neurodegeneration in the 1-methyl- 4-phenyl-1,2,3,6-tetrahydropyridine mouse model of Parkinson's disease. *Proceedings of the National Academy of Sciences*, 98(5), 2837–2842. doi:10.1073/pnas.051633998

Villaescusa, J. C., & Arenas, E. (2010). Transplantable midbrain dopamine neurons: A moving target. *Experimental neurology*, *222*(2), 173–178.

Vogt, J., Traynor, R., & Sapkota, G. P. (2011). The specificities of small molecule inhibitors of the TGFß and BMP pathways. *Cellular signalling*, *23*(11), 1831–1842. doi:10.1016/j.cellsig.2011.06.019

Voon, V., Fernagut, P.-O., Wickens, J., Baunez, C., Rodríguez, M., Pavon, N., et al. (2009). Chronic dopaminergic stimulation in Parkinson's disease: from dyskinesias to impulse control disorders. *Lancet neurology*, 8(12), 1140–1149. doi:10.1016/S1474-4422(09)70287-X

Waddington, C. H., & Schmidt, G. A. (1933). Induction by heteroplastic grafts of the primitive streak in birds. Archiv für Mikroskopische Anatomie und Entwicklungsmechanik, 128(3), 522–563. doi:10.1007/BF00649863

Wang, S., Bates, J., Li, X., Schanz, S., Chandler-Militello, D., Levine, C., et al. (2013). Human iPSC-Derived Oligodendrocyte Progenitor Cells Can Myelinate and Rescue a Mouse Model of Congenital Hypomyelination. *Cell stem cell*, 12(2), 252–264. doi:10.1016/j.stem.2012.12.002

Warren, L., Manos, P. D., Ahfeldt, T., Loh, Y.-H., Li, H., Lau, F., et al. (2010). Highly efficient reprogramming to pluripotency and directed differentiation of human cells with synthetic modified mRNA. *Cell stem cell*, 7(5), 618–630. doi:10.1016/j.stem.2010.08.012

Wassef, M., & Joyner, A. (1997). Perspectives on Developmental Neurobiology

Watanabe, K., Kamiya, D., Nishiyama, A., Katayama, T., Nozaki, S., Kawasaki, H., et al. (2005). Directed differentiation of telencephalic precursors from embryonic stem cells. *Nature neuroscience*, 8(3), 288–296. doi:10.1038/nn1402

Watanabe, K., Ueno, M., Kamiya, D., Nishiyama, A., Matsumura, M., Wataya, T., et al. (2007). A ROCK inhibitor permits survival of dissociated human embryonic stem cells. Nature biotechnology, 25(6), 681–686. doi:10.1038/nbt1310

Watmuff, B., Pouton, C. W., & Haynes, J. M. (2012). In vitro maturation of dopaminergic neurons derived from mouse embryonic stem cells: implications for transplantation. *PLoS ONE*, 7(2), e31999. doi:10.1371/journal.pone.0031999

Wehrli, M., Dougan, S. T., Caldwell, K., O'Keefe, L., Schwartz, S., Vaizel-Ohayon, D., et al. (2000). arrow encodes an LDL-receptor-related protein essential for Wingless signalling. *Nature*, 407(6803), 527–530. doi:10.1038/35035110

Weinstein, D. C., & Hemmati-Brivanlou, A. (1999). Neural induction. Annual Review of Cell and Developmental, 15, 411–433. doi:10.1146/annurev.cellbio.15.1.411

Wessely, O., Agius, E., & Oelgeschläger, M. (2001). Neural Induction in the Absence of Mesoderm: β-Catenin-Dependent Expression of Secreted BMP Antagonists at the Blastula Stage in Xenopus. *Developmental Biology*

West, M. J., & Gundersen, H. J. (1990). Unbiased stereological estimation of the number of neurons in the human hippocampus. *The Journal of Comparative Neurology*, 296(1), 1–22. doi:10.1002/cne.902960102

Wichterle, H., Lieberam, I., Porter, J. A., & Jessell, T. M. (2002). Directed differentiation of embryonic stem cells into motor neurons. *Cell*, 110(3), 385–397.

Wiesmann, C., Ultsch, M. H., Bass, S. H., & de Vos, A. M. (1999). Crystal structure of nerve growth factor in complex with the ligand-binding domain of the TrkA receptor. *Nature*, 401(6749), 184–188. doi:10.1038/43705

Wilson, S. I., & Edlund, T. (2001). Neural induction: toward a unifying mechanism. *Nature neuroscience.*

Winter, C. G., Wang, B., Ballew, A., Royou, A., Karess, R., Axelrod, J. D., & Luo, L. (2001). Drosophila Rho-associated kinase (Drok) links Frizzled-mediated planar cell polarity signalling to the actin cytoskeleton. *Cell*, 105(1), 81–91.

Wobus, A. M. (2001). Potential of embryonic stem cells. *Molecular aspects of medicine.*

Woltjen, K., Hämäläinen, R., Kibschull, M., Mileikovsky, M., & Nagy, A. (2011). Transgene-free production of pluripotent stem cells using piggyBac transposons. *Methods in molecular biology*, 767, 87–103. doi:10.1007/978-1-61779-201-4_7

Wu, D., & Boyd, A. (2007). Embryonic stem cell transplantation: potential applicability in cell replacement therapy and regenerative medicine. *Front Biosci.*

Wu, D., Teismann, P., Tieu, K., Vila, M., Jackson-Lewis, V., Ischiropoulos, H., & Przedborski, S. (2003). NADPH oxidase mediates oxidative stress in the 1-methyl-4-phenyl-1, 2, 3, 6-tetrahydropyridine model of Parkinson's disease. *Proceedings of the National Academy of Sciences*, 100(10), 6145–6150.

Wurst, W., & Bally-Cuif, L. (2001). Neural plate patterning: upstream and downstream of the isthmic organizer. *Nat Rev Neurosci*, 2(2), 99–108. doi:10.1038/35053516

Xi, J., Liu, Y., Liu, H., Chen, H., Emborg, M. E., & Zhang, S.-C. (2012). Specification of midbrain dopamine neurons from primate pluripotent stem cells. *Stem cells*, 30(8), 1655–1663. doi:10.1002/stem.1152

Xilouri, M., Vogiatzi, T., Vekrellis, K., Park, D., & Stefanis, L. (2009). Abberant alpha-synuclein confers toxicity to neurons in part through inhibition of chaperone-mediated autophagy. *PLoS ONE*, 4(5), e5515. doi:10.1371/journal.pone.0005515

Xu, R. H., Kim, J. B., Taira, M., Zhan, S. I., Sredni, D., & Kung, H. F. (1995). A Dominant Negative Bone Morphogenetic Protein 4 Receptor Causes Neuralization in Xenopus Ectoderm. *Biochemical and Biophysical Research Communications*, *212*(1), 212–219. doi:10.1006/bbrc.1995.1958

Xu, R.-H., Chen, X., Li, D. S., Li, R., Addicks, G. C., Glennon, C., et al. (2002). BMP4 initiates human embryonic stem cell differentiation to trophoblast. *Nature biotechnology*, *20*(12), 1261–1264. doi:10.1038/nbt761

Yamazoe, H., Murakami, Y., Mizuseki, K., Sasai, Y., & Iwata, H. (2005). Collection of neural inducing factors from PA6 cells using heparin solution and their immobilization on plastic culture dishes for the induction of neurons from embryonic stem cells. Biomaterials, 26(28), 5746–5754. doi:10.1016/j.biomaterials.2005.02.021

Yan, C. H., Levesque, M., Claxton, S., Johnson, R. L., & Ang, S.-L. (2011). *Lmx1a* and lmx1b function cooperatively to regulate proliferation, specification, and differentiation of midbrain dopaminergic progenitors. *The Journal of neuroscience* 31(35), 12413–12425. doi:10.1523/JNEUROSCI.1077-11.2011

Yang, D., Zhang, Z., Oldenburg, M., & Ayala, M. (2008). Human Embryonic Stem Cell-Derived Dopaminergic Neurons Reverse Functional Deficit in Parkinsonian Rats. *Stem cells*

Yang, L., Matthews, R. T., Schulz, J. B., Klockgether, T., Liao, A. W., Martinou, J. C., et al. (1998). 1-Methyl-4-phenyl-1,2,3,6-tetrahydropyride neurotoxicity is attenuated in mice overexpressing Bcl-2. *The Journal of Neuroscience*, 18(20), 8145–8152.

Yang, N., Ng, Y. H., Pang, Z. P., Südhof, T. C., & Wernig, M. (2011). Induced neuronal cells: how to make and define a neuron. *Cell stem cell,* 9(6), 517–525. doi:10.1016/j.stem.2011.11.015

Yang-Snyder, J., Miller, J. R., Brown, J. D., & Lai, C. J. (1996). A frizzled homolog functions in a vertebrate Wnt signalling pathway. *Current Biology*

Ying, Q. L., Nichols, J., Chambers, I., & Smith, A. (2003). BMP induction of Id proteins suppresses differentiation and sustains embryonic stem cell self-renewal in collaboration with STAT3. *Cell*, *115*(3), 281–292.

Ying, Q., Wray, J., Nichols, J., Batlle-Morera, L., Doble, B., Woodgett, J., et al. (2008). The ground state of embryonic stem cell self-renewal. *Nature*, 453(7194), 519–523.

Yoshimoto, Y., Lin, Q., Collier, T., & Frim, D. (1995). Astrocytes retrovirally transduced with BDNF elicit behavioral improvement in a rat model of Parkinson's disease. *Brain research*.

Yu, J., Vodyanik, M. A., Smuga-Otto, K., Antosiewicz-Bourget, J., Frane, J. L., Tian, S., et al. (2007). Induced pluripotent stem cell lines derived from human somatic cells. *Science*, *318*(5858), 1917–1920. doi:10.1126/science.1151526

Yuan, S. H., Martin, J., Elia, J., Flippin, J., Paramban, R. I., Hefferan, M. P., et al. (2011a). Cell-surface marker signatures for the isolation of neural stem cells, glia and neurons derived from human pluripotent stem cells. *PLoS ONE*, 6(3), e17540. doi:10.1371/journal.pone.0017540

Yuan, X., Wan, H., Zhao, X., Zhu, S., Zhou, Q., & Ding, S. (2011b). Combined Chemical Treatment Enables Oct4-Induced Reprogramming from Mouse Embryonic Fibroblasts. *Stem cells*. doi:10.1002/stem.594

Zeng, W. R., Fabb, S. R. A., Haynes, J. M., & Pouton, C. W. (2011). Extended periods of neural induction and propagation of embryonic stem cell-derived neural progenitors with EGF and FGF2 enhances *Lmx1a* expression and neurogenic potential. *Neurochemistry international*, 59(3), 394–403. doi:10.1016/j.neuint.2011.04.002

Zeng, X., Cai, J., Chen, J., Luo, Y., You, Z.-B., Fotter, E., et al. (2004). Dopaminergic differentiation of human embryonic stem cells. *Stem cells*, 22(6), 925–940. doi:10.1634/stemcells.22-6-925

Zeng, X., Chen, J., Deng, X., Liu, Y., Rao, M. S., Cadet, J.-L., & Freed, W. J. (2006). An *in vitro* model of human dopaminergic neurons derived from embryonic stem cells: MPP+ toxicity and GDNF neuroprotection. *Neuropsychopharmacology*, 31(12), 2708–2715. doi:10.1038/sj.npp.1301125

Zetterström, R. H., Solomin, L., Jansson, L., Hoffer, B. J., Olson, L., & Perlmann, T. (1997). Dopamine neuron agenesis in Nurr1-deficient mice. *Science*, 276(5310), 248.

Zetterström, R. H., Williams, R., Perlmann, T., & Olson, L. (1996). Cellular expression of the immediate early transcription factors Nurr1 and NGFI-B suggests a gene regulatory role in several brain regions including the nigrostriatal dopamine system. *Mol Brain Res*, 41(1-2), 111–120.

Zhang, W., Wang, T., Qin, L., Gao, H.-M., Wilson, B., Ali, S. F., et al. (2004). Neuroprotective effect of dextromethorphan in the MPTP Parkinson's disease model: role of NADPH oxidase. *FASEB journal: official publication of the Federation of American Societies for Experimental Biology*, *18*(3), 589–591. doi:10.1096/fj.03-0983fje

Zhang, D, Jiang, W., Liu, M., Sui, X., Yin, X., Chen, S., & Shi, Y. (2009). Highly efficient differentiation of human ES cells and iPS cells into mature pancreatic insulin-producing cells. *Cell research*.

Zhang, Jingzhong, Giesert, F., Kloos, K., Vogt Weisenhorn, D. M., Aigner, L., Wurst, W., & Couillard-Despres, S. (2010). A powerful transgenic tool for fate mapping and functional analysis of newly generated neurons. *BMC neuroscience*, 11, 158. doi:10.1186/1471-2202-11-158

Zhao, T., Zhang, Z., & Rong, Z. (2011). Immunogenicity of induced pluripotent stem cells. *Nature*.

Zhou, H., Wu, S., Joo, J. Y., Zhu, S., Han, D. W., Lin, T., et al. (2009). Generation of induced pluripotent stem cells using recombinant proteins. *Cell stem cell*, 4(5), 381–384. doi:10.1016/j.stem.2009.04.005

Zhu, Q., Ma, J., Yu, L., & Yuan, C. (2009). Grafted neural stem cells migrate to substantia nigra and improve behavior in Parkinsonian rats. *Neurosci Lett*, 462(3), 213–218. doi:10.1016/j.neulet.2009.07.008

Zhu, S., Wurdak, H., & Schultz, P. G. (2010). Directed embryonic stem cell differentiation with small molecules. *Future medicinal chemistry*, 2(6), 965–973. doi:10.4155/fmc.10.190

Zimprich, A. (2011). Genetics of Parkinson's disease and essential tremor. Curr *Opin Neurol*, 24(4), 318–323. doi:10.1097/WCO.0b013e3283484b87

Zlokarnik, G., Negulescu, P. A., Knapp, T. E., Mere, L., Burres, N., Feng, L., et al. (1998). Quantitation of transcription and clonal selection of single living cells with beta-lactamase as reporter. *Science*, 279(5347), 84–88.

Zorzon, M., Capus, L., & Pellegrino, A. (2002). Familial and environmental risk factors in Parkinson's disease: a case–control study in north-east Italy. *Acta neurologica*

Zou, J., Maeder, M. L., Mali, P., Pruett-Miller, S. M., Thibodeau-Beganny, S., Chou, B.-K., et al. (2009). Gene targeting of a disease-related gene in human induced pluripotent stem and embryonic stem cells. *Cell stem cell*, 5(1), 97–110. doi:10.1016/j.stem.2009.05.023

Zwaka, T. P., & Thomson, J. A. (2003). Homologous recombination in human embryonic stem cells. *Nature biotechnology* 21:319–321. doi:10.1038/nbt788

Appendix I

STEM CELLS®

EMBRYONIC STEM CELLS/INDUCED PLURIPOTENT STEM CELLS

Lmx1a Allows Context-Specific Isolation of Progenitors of GABAergic Or Dopaminergic Neurons During Neural Differentiation of Embryonic Stem Cells

CHRISTIAN M. NEFZGER, COLIN T. SU, STEWART A. FABB, BRIGHAM J. HARTLEY, SIEW J. BEH, WENDY R. ZENG, JOHN M. HAYNES, COLIN W. POUTON

Drug Discovery Biology, Monash Institute of Pharmaceutical Sciences, Monash University (Parkville Campus), Melbourne, Australia

Key Words. Embryonic stem cells · Differentiation · Lmx1a · Msx1 · GABAergic neurons · Dopaminergic neurons

ABSTRACT

LIM homeobox transcription factor 1 alpha (Lmx1a) is required for the development of midbrain dopaminergic neurons, roof plate formation, and cortical hem development. We generated a reporter embryonic stem cell (ESC) line for Lmx1a and used it to track differentiation and extract neural progenitors from differentiating mouse ESCs. Lmx1a^1 cells gave rise to functional cortical upper layer GABAergic neurons or dopaminergic neurons depending on the culture conditions used for differentiation. Under chemically defined neurobasal conditions, ESC differentiation resulted in widespread and transient expression of Lmx1a, without the addition of exogenous factors such as sonic hedgehog (Shh), Wnts, and/or bone morphogenic proteins (BMPs). Under neutral conditions, Lmx1a^1 cells express genes known to be downstream of Lmx1a and cortical hem markers Wnt3a and p73. The majority of these cells did not express the ventral midbrain dopaminergic marker Foxa2 or dorsal roof plate marker BMP-2. Lmx1a^1-Foxa2^2 cells were primed to become Satb2^1 GABAergic neurons and appeared to be resistant to dopaminergic patterning cues. PA6 coculture produced a substantial population of Lmx1a^1 progenitors that also expressed Foxa2 and on further differentiation gave rise to dopaminergic neurons at high frequency. We conclude that Lmx1a is a useful marker for the extraction of progenitors of GABAergic or dopaminergic neurons. We caution against the assumption that it indicates dopaminergic commitment during in vitro differentiation of ESCs. Indeed, in monolayer culture under neurobasal conditions, with or without the addition of Shh and fibroblast growth factor 8 (FGF8), Lmx1a^1 cells were predominantly progenitors of forebrain GABAergic neurons. We obtained dopaminergic cells in large numbers only by coculture with PA6 cells. STEM CELLS 2012; 30:1349–1361

Disclosure of potential conflicts of interest is found at the end of this article.

INTRODUCTION

Parkinson's disease (PD) and schizophrenia are common diseases of the central nervous system, the main symptoms resulting largely from a progressive loss of midbrain dopaminergic neurons in PD [1, 2] and impaired function of cortical GABAergic neurons in schizophrenia [3–6]. Derivation of these neuronal subtypes in high purity from embryonic stem cells (ESCs) could pave the way to alleviate these conditions directly, through cell transplantation strategies, or indirectly through the development of in vitro models suitable for screening of novel therapeutic compounds [7]. Various strategies have been used to derive mature subtypes of neurons from ESCs, including: culture in the presence of specific growth factors [8–10], coculture with a stromal cell line [11, 12], or forced expression of developmental genes [13, 14]. A major obstacle that thwarts progress with cell transplantation or screening studies is the common observation that neuronal differentiation protocols produce heterogeneous populations. The cultures may contain the desired cell type but also contain other neuronal subtypes, non-neural derivatives, undifferentiated cells, and unwanted types of neural cells. Cell grafts contaminated with undifferentiated cells are unacceptable due to their predisposition to form tumors [15, 16], while for in vitro applications, in particular the screening of novel compounds, the presence of high numbers of unwanted cell types is likely to obscure results. The notion of extracting

Author contributions: C.N.: conception and design, collection and/or assembly of data, data analysis and interpretation, and manuscript writing; C.S.: collection and/or assembly of data, data analysis and interpretation, and manuscript writing; S.F.: provision of study material or patients and collection and/or assembly of data; B.H., S.B., and W.Z.: collection and/or assembly of data; J.H. and C.P.: conception and design, data analysis and interpretation, manuscript writing, and final approval of manuscript. C.M.N. and C.T.S. contributed equally to this article.

Correspondence: John M. Haynes, B.Sc., Ph.D., Monash Institute of Pharmaceutical Sciences, Monash University (Parkville Campus), 381 Royal Parade, Parkville, Victoria 3052, Australia. Telephone: þ61-3-9903-9562; Fax: þ61-3-9903-9638; e-mail: John.haynes@monash.edu; or Colin W. Pouton, B.Pharm., PhD., Monash Institute of Pharmaceutical Sciences, Monash University (Parkville Campus), 381 Royal Parade, Parkville, Victoria 3052, Australia. Telephone: þ61-3-9903-9562; Fax: þ61-3-9903-9638; e-mail: colin.pouton@monash.edu Received October 6, 2011; accepted for publication March 22, 2012; first published online in STEM CELLS EXPRESS April 11, 2012. ¥ AlphaMed Press 1066-5099/2012/$30.00/0 doi: 10.1002/stem.01105

committed mitotic progenitors is attractive since their proliferative potential makes subsequent expansion for in vitro and in vivo applications a possibility. The derivation of ESC reporter lines via homologous recombination has the potential to enable isolation of a specific progenitor subpopulation by fluorescence-activated cell sorting (FACS), and we chose to use this strategy to investigate whether we could identify midbrain dopaminergic progenitors. In recent years, LIM homeobox transcription factor 1 alpha (Lmx1a) has gained prominence as a key transcription factor in dopaminergic neuron differentiation. Midbrain dopaminergic neurons arise in vivo in the ventral midline from $Foxa2^{+}$ floor plate cells established by sonic hedgehog (Shh) signaling from the notochord [17–19]. In this context, Lmx1a activates downstream determinants of the dopaminergic phenotype by binding to the promoter sequences of Msx1, Lmx1b, Wnt1, and potentially other target genes [20, 21]. Although Lmx1a is prominent in dopaminergic neuron differentiation, it is also expressed in three unrelated neural tissues during development: (a) the cortical hem, a forebrain structure that gives rise to cortical and hippocampal neurons [22], (b) the roof plate of the developing cerebellum [22, 23], and (c) the non-neurogenic roof plate of the neural tube [24, 25].

In recent studies, we have shown that nominal midbrain differentiation protocols give rise to heterogeneous populations of dopaminergic and GABAergic neurons [26, 27]. In this study, we investigate the phenotypic potential of $Lmx1a^{+}$ cells that arise during in vitro differentiation, in monolayers, or in coculture with stromal cells. We report that Lmx1a expression is early and widespread when ESCs are removed from maintenance medium and are subjected to neural differentiation protocols in vitro. The propensity of these cells to give rise to GABAergic or dopaminergic neuron fates is highly dependent on the culture paradigm used for differentiation.

Methods

Generation of Targeted Genetic Reporter ESC Lines

The methods used are described in detail in Supporting Information.

Cell Culture and Neural Differentiation

Before differentiation, E14-tg2a, Lmx1a-AMP-IRES-GFP, Msx1-AMP-IRES-GFP, and Lmx1a-IRES-eGFP ESCs were maintained in Dulbecco's modified Eagle's medium supplemented with 10% fetal calf serum (FCS) (ESC qualified), Pen/Strep (1,000 units/ml), 2 mM Glutamax, 0.1 mM b-mercaptoethanol, and leukemia inhibitory factor (LIF) (10^{3} units/ml). Sox1-GFP ESCs (a modified version of E14-tg2a, received as a courtesy of Stem Cell Sciences) were maintained in Glasgow's minimum essential medium (GMEM) supplemented with 10% FCS, 1 mM sodium pyruvate, 0.1 mM modified eagle media (MEM) nonessential amino acids, 0.1 mM b-mercaptoethanol, 2.75 g/l sodium bicarbonate, and LIF (10^{3} units/ml). Cells were passaged every other day and replated at 2.5×10^{4} cells per square centimeter.

Monolayer neural differentiation was undertaken using a modified version of a previously described protocol [28]. The logic of using a monolayer is that it offers the potential to produce an enriched culture of differentiated cells without a contaminating feeder layer. Briefly, ESCs were dissociated with accutase and replated onto 0.1% (vol/vol) gelatin-coated plates at 4.5×10^{3} cells per square centimeter and cultured in ESC culture media for 24 hours. The culture medium was changed to N2B27 neurobasal medium and supplemented with BMP-4 (10 ng/ml), Noggin (500 ng/ml), Shh (200 ng/ml), SANT-1 (1 μM, Tocris Bioscience, Bristol, U.K., www.tocris.com), Cyclopamine (1 μM, Sigma-Aldrich, Sydney, Australia, www.sigma.com), Wnt1 (50 ng/ml), Wnt3a (50 ng/ml), CHIR99021 (3 μM, Axon Medchem, Groningen, The Netherlands, www.axonmedchem.com), or Dkk1 (100 ng/ml), as indicated. The N2B27 medium was supplemented with L-ascorbic acid (200 μM, Merck, Melbourne, Australia, www.merck.com.au) from day 12 onward. All cytokines were purchased from Peprotech (Rehovot, Israel, www.peprotech.com) unless stated otherwise.

PA6 stromal cells (Riken, Tokyo, Japan, www.riken.go.jp) were maintained in minimum essential medium a supplemented with 10% FCS and Pen/Strep (1,000 units/ml). Prior to differentiation of ESCs, PA6 cells were seeded at 5×10^{4} cells per square centimeter in maintenance medium and then switched to GMEM supplemented with 15% KSR, 2 mM Glutamax, 1 mM sodium pyruvate, 0.1 mM MEM nonessential amino acids, and 0.1 mM b-mercaptoethanol. ESCs were seeded at 100 cells per square centimeter onto PA6-containing wells. After 8 days, the medium was switched to N2B27. From day 3 of differentiation onward, medium was renewed at least every other day. Hela cells were cultured in Eagle's Minimum Essential Medium in the presence of 10% FCS (Invitrogen, Melbourne, Australia, www.invitrogen.com).

Immunocytochemistry

Details are provided in Supporting Information.

Imaging and Cell Counting

Images were taken with an A1R confocal microscope (Nikon, Tokyo, Japan, www.nikon.com). For quantification, TH^{+} or $GABA^{+}$ neurons were counted manually on nine random fields of view (×6 magnification) taken from three separate experiments. To quantify $Foxa2^{+}/TH^{+}$-cells, stacks (50 μm, 2.5 μm per step) were taken at ×10 magnifications to confirm colabeling for both markers.

As described previously [14], in order to assess cell proliferation under different growth conditions, cultured cells were stained with a nuclear dye (TOPRO-3, Invitrogen) and plates scanned with an Odyssey Infrared Imaging System (Li-cor Biosciences, Lincoln, www.licor.com, BD Biosciences) at 700 nm. Emission values of each well were standardized to control wells.

Flow Cytometry

Lmx1a-AMP-IRES-GFP and Msx1-AMP-IRES-GFP cultures were dissociated into single cells with accutase (Sigma-Aldrich) in preparation for FACS analysis. Cells were loaded with substrate using the LiveBLAzer-FRET B/G Loading Kit (Invitrogen) according to manufacturer's specifications for 2–3 hours prior to analysis. Wild-type cells submitted to the staining procedure were used as the control for flow cytometry.

The Click-iT EdU Alexa Fluor 647 Flow Cytometry Assay Kit (Invitrogen) was used to detect dividing cells in culture according to manufacturer's specifications. Briefly, cells of the reporter line were incubated with Click-iT EdU (10 μM) for 2 hours, dissociated into single cells, submitted to b-lactamase staining, fixed with 4% paraformaldehyde, permeabilized with 0.5% Triton X-100, and then incubated with the Click-iT reaction cocktail for 30 minutes. Wild-type cells (controls for flow cytometry) were processed in the same way with the exception that they were not exposed to Click-iT EdU.

Cell cultures were dissociated with accutase, resuspended in phosphate buffered saline (PBS) with 5% FCS (vol/vol) and run through a 40 μm strainer (BD Biosciences, Sydney, Australia, www.bdbiosciences.com) to remove clumps. Flow cytometry was performed with a FACS Canto II analyzer (BD Biosciences) or a FACS Aria I (BD Biosciences) for cell sorting experiments. After FACS extraction, $Lmx1a^{+}$ and $Lmx1a^{-}$ fractions were either used for RNA extraction (>1 million cells per sample) or replated onto laminin/fibronectin/poly(D-lysine) (1 μg/cm^{2} each)-coated wells at 3×10^{5} cells per square centimeter (low density) or 1.5×10^{6} cells per square centimeter (high density). For the monolayer differentiation paradigm, extracted cells were plated in

N2B27 supplemented with fibroblast growth factor 2 (FGF2) (20 ng/ml) alone or in combination with Shh (200 ng/ml) and FGF8 (100 ng/ml; Peprotech). Five days later, the medium was replaced with N2B27 supplemented with brain-derived neurotrophic factor (BDNF) (20 ng/ml) and L-ascorbic acid (200 μM) for another 7 days. For experiments on PA6-mediated differentiation, cells were seeded in PA6-preconditioned N2B27 medium supplemented with FGF2 (20 ng/ml). Two days later cells were switched to PA6-preconditioned N2B27 media supplemented with BDNF (20 ng/ml) and L-ascorbic acid (200 μM) for another 5 days. Medium was renewed at least every other day.

RNA Extraction and Quantitative-PCR Methods

These methods are described in Supporting Information.

Calcium Imaging

Calcium imaging was undertaken as described previously [26, 29]. Briefly, cells were washed twice with HEPES buffer (containing in mM; NaCl 145; 3 KCl 5; $MgSO_4$ 1; HEPES 10; D-glucose 10; $CaCl_2$ 2.5) at pH 7.4 and incubated with FLUO-4AM (10 μM, Invitrogen) in HEPES buffer for 30 minutes at 37°C. After incubation, cells were viewed using a Nikon Eclipse Ti camera (Nikon) coupled to an A1 Nikon confocal microscope (Nikon). Cells were illuminated at 488 nm and emission was recorded at 515 nm. Cellular fluorescent intensities were captured with NIS-elements-AR software (Nikon) 30 times per second. Background fluorescence was subtracted from each neuron and fluorescence intensity was calculated. During experiments, cultures were first exposed to vehicle control, glutamate (30 μM), and then KCl (30 mM).

Statistical Analysis

For all experiments, results are presented as mean with SEM of at least three independent experiments. Statistical analyses were performed using PRISM v5.00 (Graphpad Software, La Jolla, California, www.graphpad.com). All raw data were analyzed by Student's t test or one-way analysis of variance with post hoc Dunnett's test. In all cases, $p < .05$ was considered to be statistically significant.

RESULTS

Expression of *Lmx1a* and *Msx1* Is Widespread in Differentiating ESC Cultures Under Chemically Defined Neurobasal Conditions

We used an Lmx1a-AMP-IRES-GFP ESC line to examine *Lmx1a* expression during neural differentiation of ESCs. The sensitive catalytic reporter β-lactamase (e.g., the ampicilin resistance gene, AMP) and enhanced green fluorescent protein (GFP) were coexpressed under control of the endogenous *Lmx1a* promoter (Fig. 1A). We chose to study reporter expression in detail during monolayer differentiation [28], since this approach makes use of chemically defined conditions, without the unpredictable interference of animal serum or coculture with a stromal cell line. During differentiation of the reporter line for 20 days, AMP and GFP expression peaked on day 8 and day 10, respectively, with approximately 40% cells positive for each reporter (Fig. 1B, 1C). Considering that detection of GFP by flow cytometry requires 3 orders of magnitude more molecules of GFP per cell than the catalytic reporter AMP [30], AMP expression was detected at earlier time points than GFP, resulting in an apparent lag in the proportion of cells expressing GFP (Fig. 1C). At the peak, day 8 for AMP and day 10 for GFP, 35%–40% of cells were positive for reporter expression. We observed that GFP expression peaked at day 10, a time when the percentage of AMP-positive cells was already in decline, reflecting the considerably shorter half-life of AMP (~3.5 hours [30]) compared to GFP (~26 hours [31]). To further substantiate that the *Lmx1a* promoter was activated in 35%–40% of cells, we established an analogous reporter line for *Msx1*, the direct downstream target of *Lmx1a*. The expression profile of AMP in the *Msx1* reporter line was indistinguishable from that obtained with the *Lmx1a* reporter line (Fig. 1D), implying that the endogenous *Lmx1a* transcript translates into functional protein at levels sufficient for activation of downstream gene expression. To determine whether expression of *Lmx1a* or *Msx-1* correlates with exit from the proliferative state, differentiating cultures were pulsed with DNA-base analog EdU for 2 hours at various time points (Supporting Information Fig. S1A). The overall percentage of cycling cells in the culture decreased gradually during differentiation from approximately 70% (day 0) to 10% (day 20) (Supporting Information Fig. S1B). The percentage of Lmx1a-AMP$^+$ or Msx1-AMP$^+$ cells that incorporated EdU decreased progressively during differentiation and no significant differences were found between AMP$^+$ and AMP$^-$ cells (Supporting Information Fig. S1C, S1D). This indicates that Lmx1a$^+$ and Msx-1$^+$ cells are in general a proliferating population up to day 20 and suggests that the gradual reduction in cell division over time was a consequence of contact inhibition in the two-dimensional cultures.

Transient *Lmx1a* Expression on Day 8 Is Not Predictive of Dopaminergic Neuron Differentiation

To put the time course of expression of *Lmx1a* in context with the state of neural differentiation, we established the time course for conversion of ESCs into neuroectoderm using a Sox1-GFP reporter line. Sixty-five percentage of cells expressed Sox1-GFP by day 4, indicating that the first stages of commitment to neural lineages had taken place. The maximum percentage of Sox1$^+$ cells was observed at day 8 (75%), but this was not significantly higher than the estimate on day 4 (Fig. 1E). Less than 10% of cells were Lmx1a$^+$ on day 4 indicating that *Lmx1a* expression occurred well after neural conversion of ESCs (Fig. 1C, 1E). Immunocytochemical labeling of day 8 cultures showed that *Lmx1a*-expressing cells (GFP reporter) were positive for the neural progenitor marker nestin but did not label for pluripotency marker Oct-4 or mature neuron marker TUJ-1 (Fig. 1F–1J). Considering the previous experience of ourselves and others [32] that monolayer differentiation produces limited numbers of dopaminergic neurons, we were surprised to see widespread expression of *Lmx1a*. To investigate whether *Lmx1a* expression on day 8 was a marker of dopaminergic progenitors, we investigated the effect of various growth factors on induction of *Lmx1a* expression at day 8 and investigated whether there was a correlation with the numbers of TH$^+$ cells present on day 20. We chose factors modulating pathways that have been associated with the induction of *Lmx1a* expression in vivo, namely canonical Wnt signaling and Shh signaling (both ventral midline), and bone morphogenic protein (BMP) signaling (roof plate) [21, 24, 33, 34]. Pathway agonists and antagonists were added to cultures either at the start of differentiation process (day 0) or after neural conversion (day 4). After treatment with each of the factors, we allowed cultures to progress toward terminal differentiation in the presence of ascorbic acid from days 12 to 20. Results indicated that none of the factors tested induced a significant increase in the percentage of Lmx1a$^+$ cells present on day 8 of differentiation (Fig. 2A, 2B). We found that stimulation of the BMP pathway or the canonical Wnt pathway reduced the percentage of Lmx1a$^+$ cells present on day 8. Decreases were much more pronounced when factors were added from day 0. In view of the

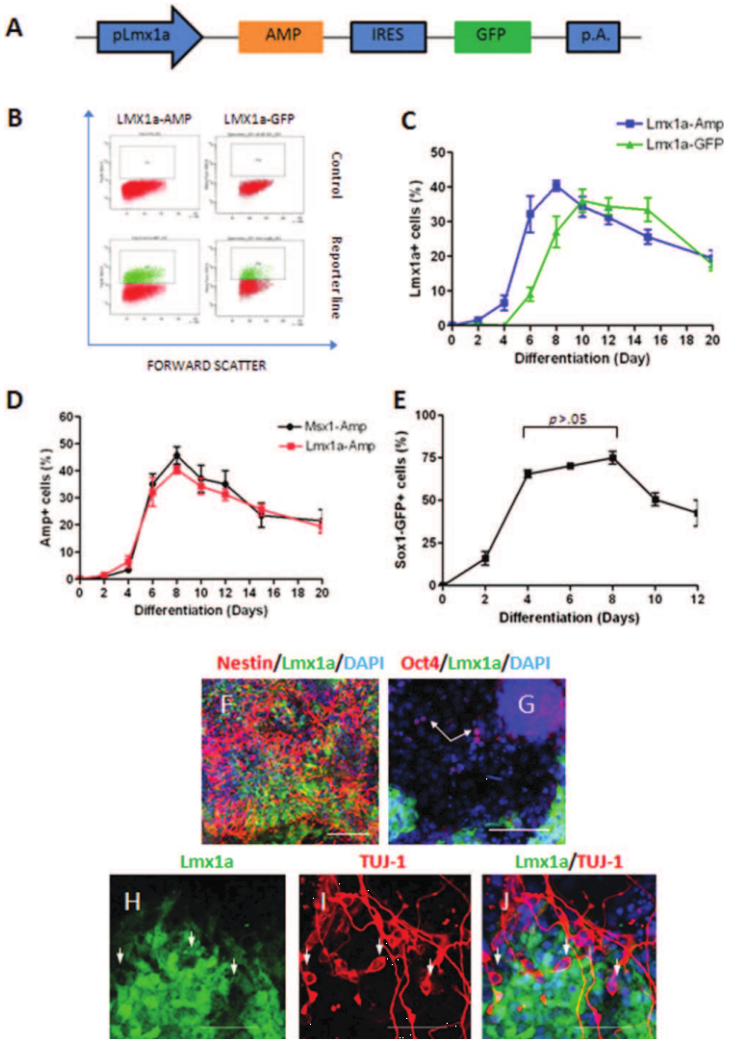

Figure 1. Reporter expression during embryonic stem cell differentiation in N2B27. (A): Outline of the expression construct that was coupled to the endogenous Lmx1a promoter via homologous recombination. (B): Typical flow cytometry blots for reporter detection of AMP and GFP on day 8 of differentiation. (C): Time courses for AMP and GFP expression under control of the Lmx1a promoter. (D): Comparison of AMP expression under control of the Lmx1a or Msx1 promoter. (E): Time course for Sox1-GFP expression during differentiation. (F–J): Labeling of Lmx1a-GFP cultures on day 8 for (F) Nestin and DAPI, (G) Oct-4 and DAPI, and (H–J) TUJ-1 and DAPI (arrows indicate the location of cell bodies of TUJ-1^{p} cells). Scale bar ¼ 100 l m. Abbreviations: AMP, ampicilin resistance gene/b-lactamase; GFP, green fluorescent protein; IRES, internal ribosome entry site; Lmx1a, LIM homeobox transcription factor 1 alpha; p.A., polyadenylation site; DAPI, 4^{0},6-diamidino-2-phenylindole; pLmx1a, Lmx1a promoter; N.S., not significant.

fact that BMP and canonical Wnt signaling are known to antagonize neural commitment of ESCs, we also investigated the percentage of Sox1-GFP^{p} cells present on day 8 after treatment with the various factors (Fig. 2C, 2D). Decreases in Lmx1a expression correlated with reductions in numbers of Sox1^{p} cells, suggesting that agonism of BMP or canonical Wnt pathways reduced the occurrence of Lmx1a^{p} cells indirectly, by inhibiting neural conversion. Interestingly, while none of the treatments increased Lmx1a expression at day 8, exposure to Noggin or Dkk1 (days 0–12) significantly increased numbers of TH^{p} cells on day 20 (Fig. 2E–2L). We concluded that Lmx1a expression on day 8 was not predictive

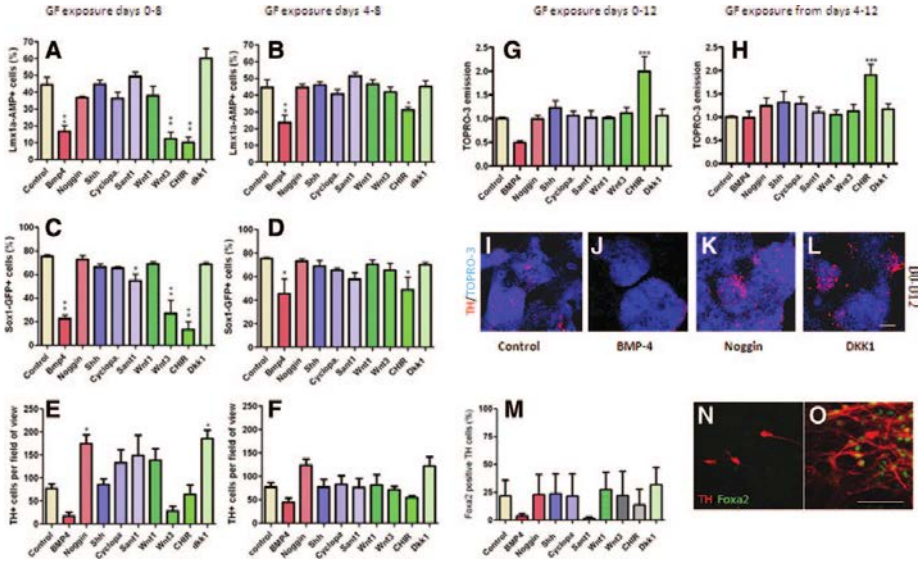

mase; BMP, bone morphogenic protein; GFP, green fluorescent protein; Lmx1a, LIM homeobox transcription factor 1 alpha; Shh, sonic hedgehog.

of subsequent development of TH^+ neurons by day 20. Furthermore, induction of *Lmx1a* expression under chemically defined conditions occurred independently of signaling pathways that are known to be implicated with the induction of *Lmx1a* expression in vivo in the ventral midline or the roof plate [24, 33, 34].

It is noteworthy that inhibition of Shh signaling (either by SANT-1 or Cyclopamine) did not alter the number of TH^+ neurons on day 20. This was surprising because of the obligatory role of Shh during the in vivo differentiation of midbrain dopaminergic neurons [19, 34]. Closer examination of monolayer-derived TH^+ neurons indicated that the majority did not express Foxa2, a marker present in all midbrain dopaminergic neurons [35], implying that most monolayer-derived TH^+ cells are not bona fide midbrain dopaminergic neurons (Fig. 2M–2O).

Analysis of $Lmx1a^+$ and $Lmx1a^-$ Cells Sorted at Day 8 of Differentiation

To study $Lmx1a^+$ cells in more detail and to investigate which cell types they were able to give rise to, we separated $Lmx1a^+$ and negative cells on day 8 using the AMP reporter (Fig. 3A). Plating of $Lmx1a^+$-cells produced homogenous cultures with morphology consistent with our expectation that these were neural progenitors. Immunocytochemistry supported this hypothesis, showing that approximately 80% percent of cells labeled positive for nestin, while very few TUJ-1^+ neurons could be found in these cultures (Fig. 3B–3D). $Lmx1a^-$ cells produced cultures with mixed cell morphologies and significantly fewer cells labeling for nestin (Fig. 3E, 3F). Although few TUJ-1 immunoreactive cells in day 8 cultures seemed to survive dissociation and FACS separation, these cells were primarily found in the negative fraction (Fig. 3G) providing further support that $Lmx1a^+$ cells (day 8) were primarily neural progenitors and not primitive neurons. A remarkable feature of the $Lmx1a^+$ fraction, when seeded at high density, was the formation of neural rosettes, characterized by ZO-1^+ foci surrounded by $nestin^+$ cells, within 3–4 days of plating (Fig. 3H). This was rarely observed in cultures of the $Lmx1a^-$ fraction (Fig. 3I). Interestingly, after 5 days of culture in neurobasal medium supplemented with FGF2, only 30% cells of the positive fraction still expressed *Lmx1a* (AMP reporter), while 5% $Lmx1a^+$ cells could now be detected in cells grown from the negative fraction (Fig. 3J). To investigate changes in *Lmx1a* expression after sorting, we tracked the presence of Lmx1a-GFP-positive/negative cells using confocal microscopy. Consistent with the flow cytometry results shown in Figure 3J, a gradual downregulation of GFP expression could be observed in the positive fraction (Fig. 3K). In the negative fraction, clusters of $Lmx1a^+$ cells could be detected after 96 hours. Retrospective analysis of white light images taken 72 hours after replating showed that many of the GFP^+ clusters, produced by cells that were AMP^- at day 8, originated from spherical colonies with distinctly

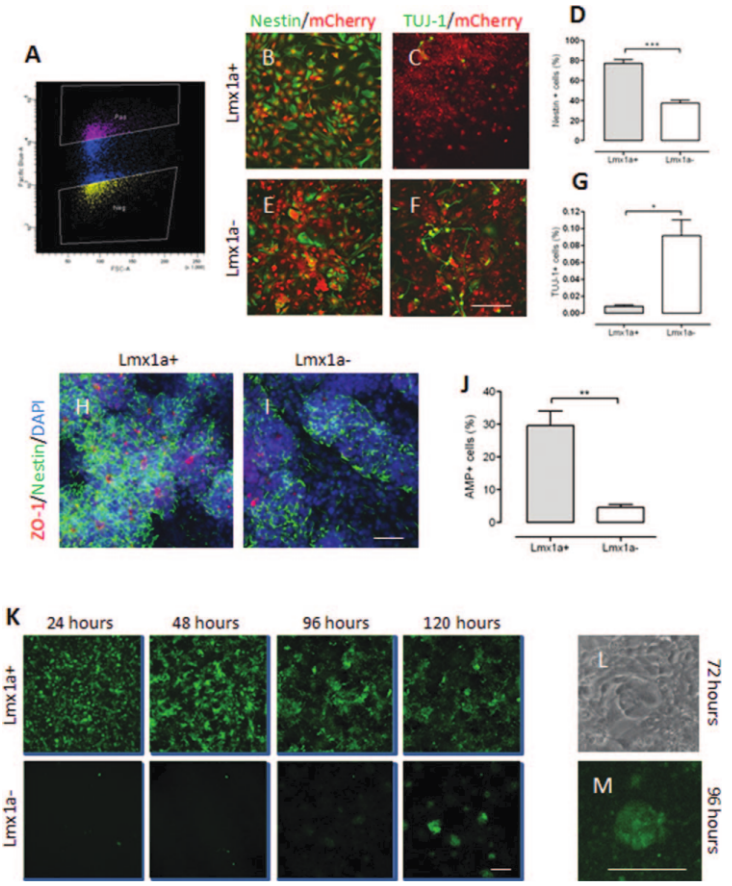

Figure 3. Culture of FACS separated Lmx1a^{P} and Lmx1a^{-} cells (at day 8 of differentiation in N2B27). (A): Fluorescence-activated cell sorting (FACS) extraction and culture of Lmx1a^{P} cells. Typical flow cytometry blot (FACS ARIA II) for the extraction of Lmx1a-AMP-positive (pos) and -negative (neg) cells (day 8 of differentiation), gates were set generously to only extract cells that were unambiguously positive or negative. Note: For some experiments, a Lmx1a reporter line that constitutively expresses mCherry from the Rosa26 locus was used. (B, C): Labeling of the AMP-positive fraction (48 hours after extraction) for (B) nestin and (C) TUJ-1; (D) percentage of cells labeling for Nestin in the positive and negative fraction. (E, F): Labeling of the AMP-negative fraction for (E) nestin and (F) TUJ-1. (G): Percentage of cells labeling for TUJ-1 in the positive and negative fraction. (H, I): Labeling of the positive and negative fraction for ZO-1, Nestin, and DAPI 5 days after extraction. (J): Reassessment of AMP reporter expression 5 days after FACS extraction. (K): Changes in GFP expression during the first 5 days following FACS separation. (L): White light image of cell colony with distinctly undifferentiated morphology (negative fraction/72 hours after FACS separation); (M) GFP fluorescence 96 hours after separation (same field of view as depicted in panel L). *, $p < .05$; **, $p < .01$; and ***, $p < .001$. Scale bar ¼ 100 l m. Abbreviations: AMP, ampicillin resistance gene; DAPI, 4^{0},6-diamidino-2-phenylindole; Lmx1a, LIM homeobox transcription factor 1 alpha.

undifferentiated morphology (Fig. 3L, 3M). We hypothesize that Oct-4^{P}/Lmx1a^{-} cells were present in day 8 cultures, giving rise to a second wave of Lmx1a^{P} cells, indicative of a degree of asynchronous differentiation during monolayer culture.

The Majority of Lmx1a^{1} Cells Express Expected Downstream Genes But Not Early Dopaminergic Neuron Marker Foxa2 or Roofplate Marker BMP-2

Quantitative polymerase chain reaction (PCR) analysis of the Lmx1a^{P} and Lmx1a fractions (AMP reporter, day 8) showed that transcript levels of Lmx1a are over 2 orders of magnitude higher in the positive fraction compared to the negative fraction (Fig. 4A), demonstrating that our reporter line allowed robust separation of Lmx1a-expressing cells from the rest of the population. Probing for direct downstream targets of Lmx1a [20, 21] showed that the positive fraction was significantly enriched with transcripts of Wnt1, Wnt3a, Msx-1, and Lmx1b (Fig. 4B, 4C). The expression level of neural stem cell/progenitor marker nestin was more than twofold higher in the positive fraction (Fig. 4B, 4C) reflecting our immunocytochemical data for the distribution of nestin-labeled cells in

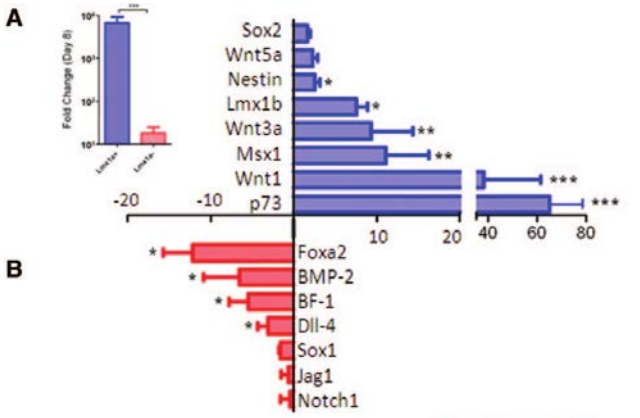

C

Gene	Lmx1a+ cells	Lmx1a- cells
Sox2	1.1 ± 1.2	- 1.7 ± 0.54
Jag1	2.7 ± 1.3	3.7 ± 0.9
p73	2.8 ± 0.8	- 36.7 ± 10.6
Wnt5a	2.9 ± 1.3	1.7 ± 0.4
BF-1	3.4 ± 1.5	21.3 ± 13.7
Dll4	3.4 ± 1.5	10.6 ± 3.1
Notch1	4.3 ± 1.5	6.0 ± 3.4
Bmp2	6.5 ± 4.9	21.1 ± 9.1
Foxa2	16.3 ± 2.5	263.8 ± 150.3
Sox1	21.6 ± 8.0	40.2 ± 6.9
Nestin	57.5 ± 25.7	31.5 ± 16.7
Lmx1b	321.0 ± 186.4	53.2 ± 35.2
Wnt3a	903.7 ± 286.5	177.8 ± 105.1
Msx1	1428.0 ± 1182.7	123.0 ± 52.7
Lmx1a	6612.52 ± 4680.69	18.41 ± 11.65
Wnt1	101303.3 ± 68276.0	7482.7 ± 7192.3

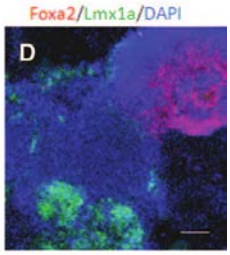

FACS separated cultures (Fig. 3D). Roof plate marker *BMP-2* and ventral marker *Foxa2*, which is known to be expressed in the ventral midline well before *Lmx1a* [34], were primarily upregulated in the negative fraction (Fig. 4B, 4C). Given the significance of *Foxa2*, we confirmed this finding by immunocytochemistry, showing that *Foxa2* and *Lmx1a*-GFP expressing domains in day 8 cultures did not overlap (Fig. 4D). The expression of cortical hem marker *Wnt3a* [36] was strongly upregulated in the positive fraction, while genes associated with multipotent rosette neural stem cells and their maintenance (*BF-1, Notch-1, Jag-1, and Dll-1*) [37] were upregulated in the negative fraction (Fig. 4B, 4C).

Lmx1a$^+$ Neural Progenitors Primarily Give Rise to Cortical GABAergic Neurons

Since Lmx1a$^+$ cells (day 8) did not highly express key markers associated with early dopaminergic progenitors or roofplate identity, we speculated that they might correspond to cells of the cortical hem. In the developing forebrain, this structure is a putative signaling center at the interface of the future hippocampus and the choroid plexus [38]. Furthermore, it is the origin of a migratory population of neural progenitors that give rise to marginal zone cortical neurons [38]. In agreement with our hypothesis, the Lmx1a$^+$ cell fraction showed upregulated expression of *p73*, a marker expressed in the hippocampus and by cortical hem-derived marginal neurons [38] (Fig. 4B, 4C). In order to determine the developmental potential of Lmx1a$^+$ and negative cells, we terminally differentiated FACS-separated day 8 cultures. The positive fraction gave rise to cultures with highly neuronal morphology that labeled strongly for TUJ-1 (Fig. 5A, 5B). Despite the fact that the plated negative fraction also contained nestin$^+$ cells that we presumed were neural progenitors (Fig. 3D, 3E), at the end of the differentiation period, rapidly proliferating cells with non-neural morphology dominated the cultures (Fig. 5F–5J). At this stage, the terminally differentiated positive fraction contained predominantly neural cells labeling for TUJ-1, GABA, TH, and glial fibrillary acidic protein (GFAP), which were mostly Lmx1a-GFP$^-$ (Fig. 5B–5E). The vast majority of neurons produced by day 8 Lmx1a$^+$ cells were GABA$^+$/GAD67$^+$ GABAergic neurons (Fig. 5K, 5L) that frequently

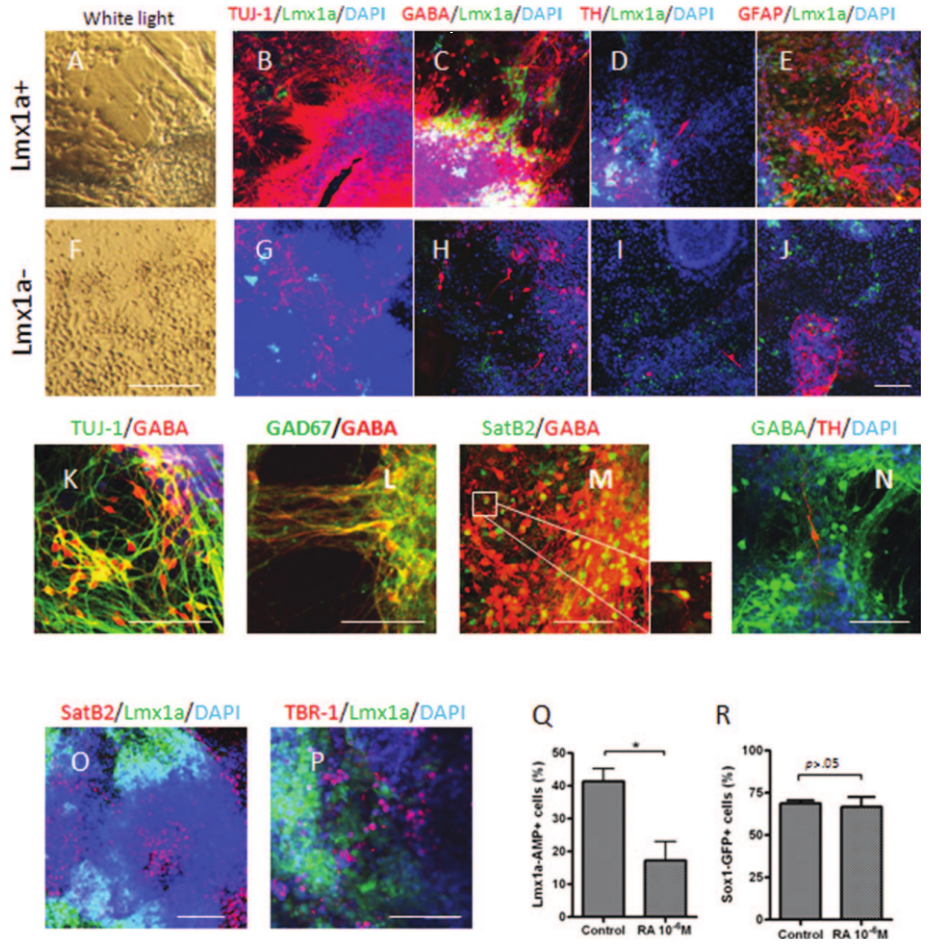

Figure 5. Characterization of monolayer-derived Lmx1a^{P} cells. Positive and negative cells were fluorescence-activated cell sorting separated and terminally differentiated; panels (A) and (F) show white light images of respective cultures. Both fractions were labeled for (B, G) TUJ-1, (C, H) GABA, (D, I) TH, and (E, J) GFPA; DAPI was used as nuclear counter stain. (K–N): The positive fraction was also labeled for (K) TUJ-1 and GABA, (L) GABA and SatB2, (M) GAD67 and GABA, and (N) TH and GABA. (O, P): Labeling of unsorted day 8 cultures (Lmx1a reporter line) for (O) SatB2 and (P) TBR-1; DAPI was used as nuclear counter stain. (Q, R): Effect of RA treatment on the percentage of Lmx1a^{P} and Sox1p cells on day 8 of differentiation. *, $p < .05$. Scale bar ¼ 100 l m. Abbreviations: DAPI, 4^{0},6-diamidino-2-phenylindole; GFAP, glial fibrillary acidic protein; Lmx1a, LIM homeobox transcription factor 1 alpha.

labeled for upper layer cortical marker SatB2 (Fig. 5M), while expression of TBR-1, a transcription factor found in other layers, was rare. Expression of p73 could not be detected in terminally differentiated cultures using immunocytochemistry (Supporting Information Fig. S2A–S2E). Very few TH^{P} cells could be detected among the GABAergic cells (Fig. 5N). At day 8, the Lmx1a^{P} cells, while giving rise to neurons with forebrain identity, did not yet label for SatB2 or TBR-1 (Fig. 5O, 5P). When the positive fraction was exposed to the caudalizing agent retinoic acid (day 4), the percentage of Lmx1a^{P} cells by day 8 (Fig. 5Q, 5R) was reduced, which implies that the untreated cells were destined for an anterior identity, whereas retinoic acid-treatment promoted more posterior fates. The observation that transcripts for forebrain marker BF-1/FoxG1 were primarily upregulated in the negative fraction by day 8 (Fig. 4B, 4C) is not necessarily paradoxical as this marker is only very early expressed throughout the forebrain; by embryonic day 10.5, BF-1 expression is excluded from the dorsomedial telencephalon that includes the cortical hem [39]. Considering that Lmx1a^{P} cells give rise to neural rosettes (Fig. 3H), a morphology that has been associated with multipotent neural stem cells [37], we tried to pattern extracted Lmx1a^{P} cells toward a dopaminergic fate by exposure to Shh and FGF8. Regardless of the absence or presence

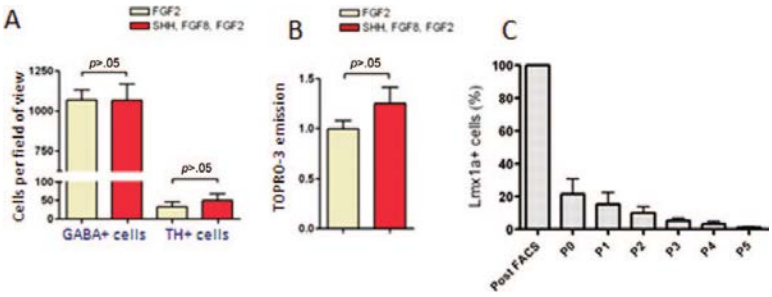

tor 1 alpha; P, Passage number.

of morphogens after sorting at day 8, Lmx1a$^+$ cells produced GABAergic and dopaminergic neurons at a ratio of 20:1 implying that the day 8 Lmx1a$^+$ cells were already committed to give rise to a specific neuronal subtype (Fig. 6A, 6B). To further test whether day 8 Lmx1a$^+$ cells had neural stem cell properties, we attempted their maintenance after extraction in the presence of FGF2 and epidermal growth factor (EGF), factors shown to allow the propagation of neural stem cells [40]. In agreement with our working hypothesis that the majority of the Lmx1a$^+$ cells were at a transient stage during the differentiation of SatB2$^+$ GABA$^+$ neurons, *Lmx1a* expression decreased rapidly during successive passages following FACS extraction (Fig. 6C). By passage, five cultures were Lmx1a$^-$ and had stopped proliferating. Substitution of EGF with rosette stem cell maintenance factors [37] yielded similar results (data not shown).

PA6-Coculture Produces Lmx1a$^+$ Cells Biased Toward a Dopaminergic Neuron Fate

Since monolayer differentiation, a culture method strongly associated with the occurrence of forebrain phenotypes [41] produced Lmx1a$^+$ cells that appeared to be predisposed to become GABAergic neurons, we wanted to explore the fate of Lmx1a$^+$ cells produced during PA6 coculture, a method that has been reported to produce midbrain dopaminergic neurons at high frequency within 2 weeks [12, 42]. Analysis of *Lmx1a* expression under these culture conditions showed that the percentage of Lmx1a$^+$ cells did not transiently peak on day 8, as observed for monolayer differentiation, but gradually increased to >20% positive cells by the end of the differentiation period (AMP reporter, day 15, Fig. 7A). Immunocytochemistry at day 8 showed that Lmx1a-GFP$^+$ cells were TUJ-1$^-$, nestin$^+$, and frequently labeled for ventral marker Foxa2 (Fig. 7B–7D). By day 15 of a typical differentiation experiment, 70.0% ± 5.0% of the TUJ-1$^+$ colonies contained patches of Lmx1a-GFP$^+$ cells. We observed a strong correlation between the presence of Lmx1a and the occurrence of TH$^+$ neurons in these cultures, and coexpression of the two markers was observed frequently at the edges of colonies (Fig. 7E, 7F). Furthermore, colonies that contained ≥10 TH$^+$ neurons were more likely to be positive for Lmx1a than colonies with <10 TH$^+$ neurons ($p < .01$) (Fig. 7G). To verify that Lmx1a$^+$ cells produced by PA6 differentiation were committed to the dopaminergic neuron fate, we performed FACS extraction. We chose to do this on day 10 since published PA6 differentiation protocols that recommend enhancement of dopaminergic differentiation by supplementation with Shh and Fgf8 recommend removal of patterning factors at approximately day 10 [42, 43]. We hypothesized that commitment to a dopaminergic fate during PA6 coculture is likely to be completed by this time. Making use of an Lmx1a$^+$ reporter line that also constitutively expresses mCherry under control of the *Rosa26* promoter, we were able to purify ESC-derived Lmx1a$^+$ and negative cells by FACS while excluding the remaining PA6 stromal feeder cells. Terminal differentiation of either fraction for 7 days produced neuronal cultures with few GFAP$^+$ glial cells (Fig. 7H–7O). Strikingly, Lmx1a$^+$ cells gave rise to TH$^+$ neurons at threefold higher frequency than GABA$^+$ neurons (Fig. 7P, 7Q). This trend was reversed for the negative fraction where GABA$^+$ neurons were produced at approximately three times higher frequency than TH$^+$ cells (Fig. 7P, 7Q). Lmx1a-GFP expression was commonly observed in terminally differentiated cultures of the positive fraction (Fig. 7J) that contrasted with our observations during differentiation of monolayer cultures, where substantial downregulation of reporter expression occurred in the days following extraction (Fig. 3K). It is also noteworthy that the few TH$^+$ cells produced after differentiation of the PA6 coculture-derived negative fraction were associated with secondary clusters of *Lmx1a*-expressing cells that arose subsequent to FACS separation (Fig. 7K). To substantiate that the neurons produced from extracted Lmx1a$^+$ cells (monolayer or PA6 coculture) possess functional properties, we performed calcium imaging studies. As would be expected for neuronal cells in vivo, stimulation with glutamate, the major excitatory neurotransmitter of the central nervous system, or depolarization by KCl elicited significant elevations in intracellular calcium compared to vehicle control (in all cases $p < .01$, Supporting Information Fig. S3).

Discussion

Genetic reporters offer a powerful means to track differentiation of ESCs, provided that the expression of the reporter faithfully reproduces endogenous patterns of expression. We chose to use the most robust method to ensure high-fidelity expression by targeting the reporter construct to replace exon 1 of a single allele of the gene in question. The endogenous protein is expressed by the second allele only; however, this did not appear to result in haploinsufficiency. Neither the ability of the reporter ESCs to differentiate into neurons nor the ability of the reporter ESCs to specify either the GABAergic

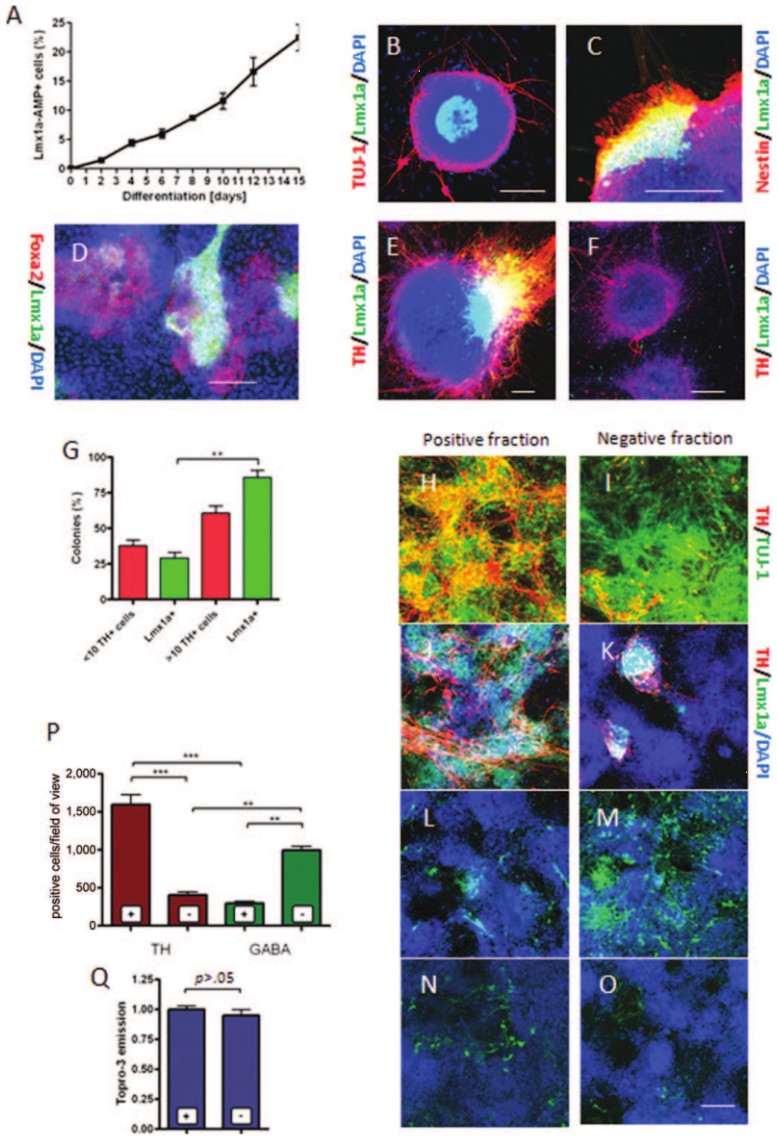

Figure 7. Lmx1a^{p} cells in the context of PA-6 coculture. (A): Time course showing the percentage of Lmx1a-AMP^{p} cells during differentiation. (B, C): Labeling of day 8 cultures (reporter line) for (B) TUJ-1 and (C) Nestin; DAPI was used as nuclear counter stain. (D): Labeling of day 10 cells (Lmx1a reporter line) for Foxa2; DAPI was used as nuclear counter stain. (E, F): Labeling of day 15 cultures (Lmx1a reporter line) for TH; DAPI was used as nuclear counter stain. (G): Percentage of TUJ-1^{p} colonies (day 15) that contain more or less than 10 THþ cells (red bars); neighboring bars (green) indicate the percentage of these colonies that are positive for Lmx1a reporter green fluorescent protein. Panels (H–O) show terminally differentiated cultures of fluorescence-activated cell sorting (FACS) extracted Lmx1a^{p} and Lmx1a^{-} cells labeled for (H, I) TH and TUJ-1, (J, K) TH, (L , M) GABA, (N, O) glial fibrillary acidic protein; DAPI was used as nuclear counter stain. (P): Numbers of TH-positive (red bars) and GABAþ (green bars) cells per field of view in terminally differentiated cultures of FACS extracted Lmx1a^{p} and Lmx1a^{-} cells. Panel (Q) depicts TOPRO-3 (nuclear dye) emission values for terminally differentiated cultures of the positive and negative fraction as a measure of cell density for both conditions. *, $p < .05$; **, $p < .01$; and ***, $p < .001$. Scale bar ¼ 100 l m. Abbreviations: DAPI, 4^{0},6-diamidino-2-phenylindole; Lmx1a, LIM homeobox transcription factor 1 alpha.

or dopaminergic phenotypes were affected (Supporting Information Fig. S4). Our interest in targeting the *Lmx1a* gene was raised by its reported ability to identify precursors of dopaminergic neurons in the ventral midbrain [20, 44, 45]. There is considerable interest in research that can establish the best cells for use in cell therapy of PD. Neural stem cell implants produce a beneficial effect by way of the "chaperone effect," but these cells do not produce new dopaminergic neurons [46]. There may be a need to implant dopaminergic neurons or their precursors, and to test this there is a need for methods to enrich cell cultures for these cells. We hypothesized that an *Lmx1a* reporter might allow us to track development of dopaminergic precursors and also sort them using flow cytometry, to enrich and to allow detailed analysis of their phenotype. To this end, we targeted the dual reporter, AMP-IRES-eGFP, so that we could visualize cells using GFP if expression was strong enough, but could also introduce a substrate for β-lactamase (i.e., using the AMP reporter gene) to give a very sensitive assay or FACS sorting method (Figs. 1B, 3A).

Initially, we chose to study differentiation of ESCs in monolayer culture, reasoning that this approach would ultimately give the best control over differentiation, as opposed to the alternative use of differentiation in embryoid bodies [47, 48]. Using an ESC reporter line for *Lmx1a*, we demonstrated that depending on the culture conditions, Lmx1a$^+$ cells gave rise to GABAergic or dopaminergic neurons. To our knowledge, this is the first time that *Lmx1a* has been implicated with GABAergic neuron differentiation in vitro. Indeed, we observed that unless conditions were optimized for the generation of midbrain phenotypes, *Lmx1a* is predominantly a marker for forebrain GABAergic neurons during monolayer differentiation of ESCs.

Monolayer culture is a chemically defined approach that has been reported to be prone to production of anterior neuron fates [41]. Under neurobasal conditions in the absence of patterning cues, we observed that expression of *Lmx1a* was widespread and transient (Fig. 1). The vast majority of neurons produced by Lmx1a$^+$ cells were GABAergic neurons that were labeled for SatB2 but not for TBR-1 (Fig. 5), indicating an upper layer cortical identity [41, 49, 50]. Some of the Lmx1a$^+$ cells derived by monolayer culture did in fact give rise to TH$^+$ neurons, albeit at very low frequency. However, most of these cells were not midbrain dopaminergic neurons, as their differentiation was independent of Shh signaling and, crucially, the majority of these TH$^+$ cells were not immunopositive for Foxa2. Our results reflect previous reports that monolayer differentiation in neurobasal medium, with or without patterning factors, is a poor source of midbrain dopaminergic neurons [32, 41]. We hypothesize that monolayer-derived TH+ neurons correspond mostly to forebrain dopaminergic neurons [51]. In support of this concept, differentiation in the presence of either Dkk1 or Noggin increased the numbers of TH$^+$ neurons. Both Noggin, in the context of "dual smad" inhibition in the absence of caudalizing factors, as well as Dkk1, have been reported to promote or enhance the generation of anterior neural fates from ES cells [52–54].

As the cortical hem is the primary site of *Lmx1a* expression in the developing forebrain [22], it is tempting to speculate that monolayer-derived Lmx1a$^+$ cells are the in vitro equivalent of this structure. In support of this hypothesis; (a) the occurrence of Lmx1a$^+$ cells (day 8) was not enhanced by factors implicated in dopaminergic neuron or roof plate differentiation (Fig. 2); (b) consistent with the concept that Lmx1a$^+$ cells were an anterior population, the caudalizing factor retinoic acid reduced *Lmx1a* expression (Fig. 5P); and (c) Lmx1a$^+$ strongly expressed cortical hem markers *Wnt3a* [36] and *p73* [55]. This assumption is complicated by reports indicating that the cortical hem is also a site of *BMP-2* expression [56]. In this study, during monolayer differentiation, *BMP-2* expression was primarily upregulated in the negative fraction (Fig. 4B) with only modest increases in the Lmx1a$^+$ fraction (6.5 $\pm$ 4.9-fold) compared to day 1 (Fig. 4C). Furthermore, we detected high levels of *Wnt1* expression in Lmx1a$^+$ cells (Fig. 4B, 4C), which has been implicated as a cortical hem marker in the chick [57] but not in mouse system [58]. Most importantly, in vivo cortical hem is primarily a source of p73$^+$ Cajal-Retzius cells, a type of marginal zone glutamatergic neuron [36], while our monolayer-derived Lmx1a$^+$ cells predominantly give rise to p73$^-$/GAD67$^+$/GABA$^+$ neurons with upper layer identity (Fig. 5K–5M). We surmise that these differences might be an artifact of the in vitro differentiation process due to the absence of one or many factors present during forebrain embryonic development. In a permissive environment, like the embryonic brain, in vitro-derived Lmx1a$^+$ cells (day 8) might very well be capable of giving rise to cortical hem derivates. But until this possibility has been explored, it is uncertain whether there is a direct in vivo equivalent for monolayer-derived Lmx1a$^+$ cells. Furthermore, the primary differentiation product that we obtained from Lmx1a$^+$ cells, for example, SatB2$^+$ GABAergic neurons, is of questionable physiological relevance since SatB2$^+$ neurons in the cortex are unlikely to be GABAergic [59]. GABAergic interneurons labeling for SatB2 have been reported in the mammalian retina [60]; however, there are no reports implicating *Lmx1a* with eye development in vivo. At this stage, we are not aware of any other reports of SatB2$^+$ GABAergic neurons.

Friling et al. reported that monolayer cultures can be coaxed to give rise to dopaminergic neurons at high frequency under the influence of forced expression of *Lmx1a* [13]. In this experiment, *Lmx1a* was expressed under control of the *nestin* promoter that is active as early as 24 hours after neural induction. The recent study by Chung et al. [21] demonstrated that two independent transcription factors cascades, one characterized by *Lmx1a* and the second by Shh-induced *Foxa2*, are required for midbrain dopaminergic differentiation. This explains the observation by the former group that efficient derivation of TH$^+$ neurons by misexpression of *Lmx1a* was only possible in the presence of Shh [61]. We showed in this work that monolayer differentiation gives rise to cultures in which typically 40% cells endogenously expressed *Lmx1a* (days 8–10). While this does not translate into widespread dopaminergic differentiation, even in the presence of Shh, it marks the generation of a cortical progenitor population. We conclude that there is only a brief early period during monolayer differentiation, before the expression of endogenous *Lmx1a*, when forced expression of *Lmx1a* has the capacity to induce dopaminergic neuron specification.

We conclude that the majority of the Lmx1a$^+$ cells produced in monolayers express downstream targets *Msx1*, *Lmx1b*, and *Wnt1*, but not *Foxa2*, and that these cells are primarily committed and restricted to GABAergic neuron and astrocyte differentiation. They cannot be patterened toward the dopaminergic fate and *Lmx1a* expression is not maintained after extraction. In contrast to monolayer culture, we identified a striking association between *Lmx1a* expression and dopaminergic neuron differentiation in PA6 cocultures, as Lmx1a$^+$ colonies were more likely to contain dopaminergic neurons than Lmx1a$^-$ colonies. Furthermore, Lmx1a$^+$ cells (day 10) expressed *Foxa2* and when extracted gave rise to dopaminergic neurons at high frequency. Our findings are in line with the concept that coexpression of *Lmx1a* and *Foxa2* is required for the specification of dopaminergic neurons in

vitro. We show here that the PA6 coculture method, a robust method for the differentiation of dopaminergic neurons with midbrain identity [62, 63], provides the appropriate patterning cues for the generation of Lmx1a^{P} dopaminergic progenitors. Interestingly, even in PA6 coculture, some of the Lmx1a^{P} cells gave rise to GABAergic neurons. Since these neurons do not express cortical marker SatB2 (Supporting Information Fig. S5), we believe that they possess a different regional identity compared to their monolayer-derived counterparts. This observation indicates that regardless of culture conditions and their associated regional identity, Lmx1a^{P} cells can differentiate into GABAergic neurons. This occurs at markedly different frequencies during monolayer differentiation (ratio GABA^{P} to TH^{P} neurons—20:1) and PA6 coculture (ratio GABA^{P} to TH^{P} neurons—1:3). Taken as a whole, the data indicate that extraction of midbrain dopaminergic progenitors by flow cytometry will require at least one more reporter gene to identify the correct subpopulation of Lmx1a^{P} cells. At present, Foxa2 appears to be a good candidate for use in a future dual reporter system.

Lmx1a has also a pivitol role during dopaminergic neuron differentiation from human ESCs [64–66]; however, there is conflicting evidence about the requirement of Lmx1a and Foxa2 coexpression for the generation of this neuronal subtype. In the context of a five-stage protocol that produced up to 20% TH^{P} cells, Cai et al. [64] noted that barely any neural progenitors colabeled for Lmx1a and Foxa2. On the other hand, two very recent studies report that only early coexpression of both factors is indicative of dopaminergic neuron differentiation. Jaeger et al. [65] showed that under standard monolayer differentiation conditions, mouse epiblast stem cells as well as human ESCs produced Lmx1a^{P}/Foxa2^{-} cells and generated cultures with only moderate numbers of TH^{P} cells. Modulation of FGF/ERK signaling early during differentiation followed by exposure to Shh and FGF8 facilitated the generation of Lmx1a^{P}/Foxa2^{P} cells and concomitantly increased the percentage of dopaminergic neurons. Kriks et al. ([66] a study that was published after this manuscript was submitted for review) showed that dual similar to Mothers Against Decapentaplegic (SMAD) inhibition produced cultures with Lmx1a^{P}/Foxa2^{-} cells that rarely gave rise to TH^{P} cells, whereas dual SMAD inhibition plus stimulation of Shh and canonical Wnt pathways allowed efficient generation of cultures with Lmx1a^{P} Foxa2^{P} cells that produced dopaminergic neurons at high frequency.

Conclusions

In this study, we show that a reporter line for Lmx1a can be used to isolate neural progenitors biased toward the GABAergic or the dopaminergic neuron fate depending on the culture method used for differentiation. By doing so, we demonstrate the limitations of Lmx1a as a marker for dopaminergic neuron differentiation in vitro. Furthermore, we provide convincing evidence that the widespread expression of Lmx1a during differentiation under chemically defined conditions signifies the rise of a forebrain progenitor population that gives rise to functional GABAergic neurons, albeit with aberrant marker expression. This highlights that artificial culture condition can result in cells with no physiological relevance. Nevertheless this does not negate the potential of PA6 coculture-derived dopaminergic neurons to become valuable research tools for the study PD with applications ranging from in vitro drug screening to transplantation work. While enrichment for progenitors of either GABAergic or dopaminergic neurons was feasible, we acknowledge that the use of a single reporter was not sufficient to produce pure cultures. Optimized growth factor treatment and/or a dual reporter line for Lmx1a and a transcription factor differentially expressed in GABAergic and dopaminergic progenitors should enable isolation of considerably enriched populations. This is desirable to enable global gene expression analysis, and identification of selectively expressed surface markers, particularly of dopaminergic neuron progenitors, to facilitate extraction from mouse and human sources without the need for genetic modifications.

Acknowledgments

This work was supported by a research grant gratefully received from Pfizer (Australia). C.S. and W.R.Z. received Ph.D. Scholarships from Monash University.

Disclosure of Potential Conflicts of Interest

The authors indicate no potential conflicts of interest.

References

1 Dauer W, Przedborski S. Parkinson's disease: Mechanisms and models. Neuron 2003;39:889–909.
2 Olanow CW, Tatton WG. Etiology and pathogenesis of Parkinson's disease. Annu Rev Neurosci 1999;22:123–144.
3 Benes FM, Berretta S. GABAergic interneurons: Implications for understanding schizophrenia and bipolar disorder. Neuropsychopharmacology 2001;25:1–27.
4 Costa E, Chen Y, Dong E et al. GABAergic promoter hypermethylation as a model to study the neurochemistry of schizophrenia vulnerability. Expert Rev Neurother 2009;9:87–98.
5 Guidotti A, Auta J, Davis JM et al. GABAergic dysfunction in schizophrenia: New treatment strategies on the horizon. Psychopharmacology (Berl) 2005;180:191–205.
6 Lewis DA, Hashimoto T, Volk DW. Cortical inhibitory neurons and schizophrenia. Nat Rev Neurosci 2005;6:312–324.
7 Pouton CW, Haynes JM. Embryonic stem cells as a source of models for drug discovery. Nat Rev Drug Discov 2007;6:605–616.
8 Bissonnette CJ, Lyass L, Bhattacharyya BJ et al. The controlled generation of functional basal forebrain cholinergic neurons from human embryonic stem cells. Stem Cells 2011;29:802–811.
9 Chatzi C, Scott RH, Pu J et al. Derivation of homogeneous GABAergic neurons from mouse embryonic stem cells. Exp Neurol 2009;217:407–416.
10 Wichterle H, Peljto M. Differentiation of mouse embryonic stem cells to spinal motor neurons. Curr Protoc Stem Cell Biol. 2008;Chapter 1:Unit 1H. 1.1–1H.1.9.
11 Kawasaki H, Suemori H, Mizuseki K et al. Generation of dopaminergic neurons and pigmented epithelia from primate ES cells by stromal cell-derived inducing activity. Proc Natl Acad Sci USA 2002;99:1580–1585.
12 Kawasaki H, Mizuseki K, Nishikawa S et al. Induction of midbrain dopaminergic neurons from ES cells by stromal cell-derived inducing activity. Neuron 2000;28:31–40.
13 Friling S, Andersson E, Thompson LH et al. Efficient production of mesencephalic dopamine neurons by Lmx1a expression in embryonic stem cells. Proc Natl Acad Sci USA 2009;106:7613–7618.
14 Nefzger CM, Haynes JM, Pouton CW. Directed expression of Gata2, Mash1, and Foxa2 synergize to induce the serotonergic neuron phenotype during in vitro differentiation of embryonic. Stem Cells 2011;29:928–939.
15 Nishimura F, Yoshikawa M, Kanda S et al. Potential use of embryonic stem cells for the treatment of mouse parkinsonian models: Improved behavior by transplantation of in vitro differentiated dopaminergic neurons from embryonic stem cells. Stem Cells 2003;21:171–180.

16 Bjorklund LM, Sanchez-Pernaute R, Chung S et al. Embryonic stem cells develop into functional dopaminergic neurons after transplantation in a Parkinson rat model. PNAS 2002;9:2344–2349.
17 Bonilla S, Hall AC, Pinto L et al. Identification of midbrain floor plate radial glia-like cells as dopaminergic progenitors. Glia 2008;56:809–820.
18 Joksimovic M, Anderegg A, Roy A et al. Spatiotemporally separable Shh domains in the midbrain define distinct dopaminergic progenitor pools. Proc Natl Acad Sci USA 2009;106:19185–19190.
19 Ono Y, Nakatani T, Sakamoto Y et al. Differences in neurogenic potential in floor plate cells along an anteroposterior location: Midbrain dopaminergic neurons originate from mesencephalic floor plate cells. Development 2007;134:3213–3225.
20 Andersson E, Tryggvason U, Deng Q et al. Identification of intrinsic determinants of midbrain dopamine neurons. Cell 2006;124: 393–405.
21 Chung S, Leung A, Han BS et al. Wnt1-lmx1a forms a novel autoregulatory loop and controls midbrain dopaminergic differentiation synergistically with the SHH-FoxA2 pathway. Cell Stem Cell 2009;5: 646–658.
22 Chizhikov VV, Lindgren AG, Mishima Y et al. Lmx1a regulates fates and location of cells originating from the cerebellar rhombic lip and telencephalic cortical hem. Proc Natl Acad Sci USA 2010;107: 10725–10730.
23 Mishima Y, Lindgren AG, Chizhikov VV et al. Overlapping function of Lmx1a and Lmx1b in anterior hindbrain roof plate formation and cerebellar growth. J Neurosci 2009;29:11377–11384.
24 Chizhikov VV, Millen KJ. Control of roof plate formation by Lmx1a in the developing spinal cord. Development 2004;131:2693–2705.
25 Millonig JH, Millen KJ, Hatten ME. The mouse Dreher gene Lmx1a controls formation of the roof plate in the vertebrate CNS. Nature 2000;403:764–769.
26 Khaira SK, Pouton CW, Haynes JM. P2X2, P2X4 and P2Y1 receptors elevate intracellular Ca2+ in mouse embryonic stem cell-derived gabaergic neurons. Br J Pharmacol 2009;158:1922–1931.
27 Raye WS, Tochon-Danguy N, Pouton CW et al. Heterogeneous population of dopaminergic neurons derived from mouse embryonic stem cells: Preliminary phenotyping based on receptor expression and function. Eur J Neurosci 2007;25:1961–1970.
28 Ying QL, Stavridis M, Griffiths D et al. Conversion of embryonic stem cells into neuroectodermal precursors in adherent monoculture. Nat Biotechnol 2003;21:183–186.
29 Khaira SK, Nefzger CM, Beh SJ et al. Midbrain and forebrain patterning delivers immunocytochemically and functionally similar populations of neuropeptide Y containing GABAergic neurons. Neurochem Int 2011;59:413–420.
30 Zlokarnik G, Negulescu PA, Knapp TE et al. Quantitation of transcription and clonal selection of single living cells with beta-lactamase as reporter. Science 1998;279:84–88.
31 Corish P, Tyler-Smith C. Attenuation of green fluorescent protein half-life in mammalian cells. Protein Eng 1999;12:1035–1040.
32 Konstantoulas CJ, Parmar M, Li M. FoxP1 promotes midbrain identity in embryonic stem cell-derived dopamine neurons by regulating Pitx3. J Neurochem 2010;113:836–847.
33 Arenas E. Foxa2: The rise and fall of dopamine neurons. Cell Stem Cell 2008;2:110–112.
34 Joksimovic M, Yun BA, Kittappa R et al. Wnt antagonism of Shh facilitates midbrain floor plate neurogenesis. Nat Neurosci 2009;12: 125–131.
35 Kittappa R, Chang WW, Awatramani RB et al. The foxa2 gene controls the birth and spontaneous degeneration of dopamine neurons in old age. PLoS Biol 2007;5:e325.
36 Yoshida M, Assimacopoulos S, Jones KR et al. Massive loss of Cajal-Retzius cells does not disrupt neocortical layer order. Development 2006;133:537–545.
37 Elkabetz Y, Panagiotakos G, Al Shamy G et al. Human ES cell-derived neural rosettes reveal a functionally distinct early neural stem cell stage. Genes Dev 2008;22:152–165.
38 Meyer G. Building a human cortex: The evolutionary differentiation of Cajal-Retzius cells and the cortical hem. J Anat 2010;217:334–343.
39 Furuta Y, Piston D, Hogan B. Bone morphogenetic proteins (BMPs) as regulators of dorsal forebrain development. Development 1997;124: 2203–2212.
40 Conti L, Pollard SM, Gorba T et al. Niche-independent symmetrical self-renewal of a mammalian tissue stem cell. PLoS Biol 2005;3:e283.
41 Gaspard N, Bouschet T, Hourez R et al. An intrinsic mechanism of corticogenesis from embryonic stem cells. Nature 2008;455:351–357.
42 Barberi T, Klivenyi P, Calingasan NY et al. Neural subtype specification of fertilization and nuclear transfer embryonic stem cells and application in parkinsonian mice. Nat Biotechnol 2003;21:1200–1207.
43 Kim DW, Chung S, Hwang M et al. Stromal cell-derived inducing activity, Nurr1, and signaling molecules synergistically induce dopaminergic neurons from mouse embryonic. Stem Cells 2006;24:557–567.
44 Lin W, Metzakopian E, Mavromatakis YE et al. Foxa1 and Foxa2 function both upstream of and cooperatively with Lmx1a and Lmx1b in a feedforward loop promoting mesodiencephalic dopaminergic neuron development. Dev Biol 2009;333:386–396.
45 Nakatani T, Kumai M, Mizuhara E et al. Lmx1a and Lmx1b cooperate with Foxa2 to coordinate the specification of dopaminergic neurons and control of floor plate cell differentiation in the developing mesencephalon. Dev Biol 2009;339:101–113.
46 Ourednik J, Ourednik V, Lynch WP et al. Neural stem cells display an inherent mechanism for rescuing dysfunctional neurons. Nat Biotechnol 2002;20:1103–1110.
47 Bain G, Ray WJ, Yao M et al. Retinoic acid promotes neural and represses mesodermal gene expression in mouse embryonic stem cells in culture. Biochem Biophys Res Commun 1996;223:691–694.
48 Lee SH, Lumelsky N, Studer L et al. Efficient generation of midbrain and hindbrain neurons from mouse embryonic stem cells. Nat Biotechnol 2000;18:675–679.
49 Hevner RF, Daza RA, Rubenstein JL et al. Beyond laminar fate: Toward a molecular classification of cortical projection/pyramidal neurons. Dev Neurosci 2003;25:139–151.
50 Shen Q, Wang Y, Dimos JT et al. The timing of cortical neurogenesis is encoded within lineages of individual progenitor cells. Nat Neurosci 2006;9:743–751.
51 Björklund A, Dunnett SB. Dopamine neuron systems in the brain: an update. Trends Neurosci 2007;30:194–202.
52 Chambers SM, Fasano CA, Papapetrou EP et al. Highly efficient neural conversion of human ES and iPS cells by dual inhibition of SMAD signaling. Nat Biotechnol 2009;27:275–280.
53 Fasano CA, Chambers SM, Lee G et al. Efficient derivation of functional floor plate tissue from human embryonic stem cells. Cell Stem Cell 2010;6:336–347.
54 Watanabe K, Kamiya D, Nishiyama A et al. Directed differentiation of telencephalic precursors from embryonic stem cells. Nat Neurosci 2005;8:288–296.
55 Meyer G, Perez-Garcia CG, Abraham H et al. Expression of p73 and Reelin in the developing human cortex. J Neurosci 2002;22: 4973–4986.
56 Grove EA, Tole S. Patterning events and specification signals in the developing hippocampus. Cereb Cortex 1999;9:551–561.
57 Ligon KL, Echelard Y, Assimacopoulos S et al. Loss of Emx2 function leads to ectopic expression of Wnt1 in the developing telencephalon and cortical dysplasia. Development 2003;130:2275–2287.
58 Grove EA, Tole S, Limon J et al. The hem of the embryonic cerebral cortex is defined by the expression of multiple Wnt genes and is compromised in Gli3-deficient mice. Development 1998;125:2315–2325.
59 Alcamo EA, Chirivella L, Dautzenberg M et al. Satb2 regulates callosal projection neuron identity in the developing cerebral cortex. Neuron 2008;57:364–377.
60 Kay JN, Voinescu PE, Chu MW et al. Neurod6 expression defines new retinal amacrine cell subtypes and regulates their fate. Nat Neurosci 2011;14:965–972.
61 Panman L, Andersson E, Alekseenko Z et al. Transcription factor-induced lineage selection of stem-cell-derived neural progenitor cells. Cell Stem Cell 2011;8:663–675.
62 Perrier AL, Tabar V, Barberi T et al. Derivation of midbrain dopamine neurons from human embryonic stem cells. Proc Natl Acad Sci USA 2004;101:12543–12548.
63 Zeng X, Cai J, Chen J et al. Dopaminergic differentiation of human embryonic stem cells. Stem Cells 2004;22:925–940.
64 Cai J, Donaldson A, Yang M et al. The role of Lmx1a in the differentiation of human embryonic stem cells into midbrain dopamine neurons in culture and after transplantation into a Parkinson's disease model. Stem Cells 2009;27:220–229.
65 Jaeger I, Arber C, Risner-Janiczek JR et al. Temporally controlled modulation of FGF/ERK signaling directs midbrain dopaminergic neural progenitor fate in mouse and human pluripotent stem cells. Development 2011;138:4363–4374.
66 Kriks S, Shim JW, Piao J et al. Dopamine neurons derived from human ES cells efficiently engraft in animal models of Parkinson's disease. Nature 2011;480:547–551.

See www.StemCells.com for supporting information available online.

Appendix II

In vitro differentiation of pluripotent stem cells towards either forebrain GABAergic or midbrain dopaminergic neurons

Brigham J Hartley, Bradley Watmuff, Cameron PJ Hunt, John M Haynes and Colin W Pouton

Drug Discovery Biology, Monash Institute of Pharmaceutical Sciences, Monash University (Parkville Campus), Melbourne, Australia

Summary

There is considerable interest in the derivation of neuronal cells from pluripotent stem cells (PSCs). Cells produced in this way have potential uses in the treatment of neurodegenerative diseases, drug discovery studies, or for basic research in neuroscience. Here we describe protocols for the directed differentiation of forebrain GABAergic and midbrain dopaminergic neurons, using murine and human PSCs.

Key Words

Directed differentiation, neural differentiation, mouse pluripotent stem cells, human pluripotent stem cells, GABAergic neurons, dopaminergic neurons

1. Introduction

The directed differentiation of pluripotent stem cells from either embryonic stem cells (ESCs) or induced pluripotent stem cells (iPSCs) may be a source of cells for transplantation therapy, but may also become a powerful tool for *in vitro* modeling of disease. The advantage of PSCs cultures is that they can be, (i) expanded indefinitely and, (ii) directed to differentiate into post-mitotic mature neurons.

Given the limitations of primary culture (Klimanskaya et al., 2008) and the scarce availability of fetal tissue, PSC cultures are a powerful resource with the potential to provide a virtually inexhaustible source of functional neuronal cells. Forebrain γ-aminobutyric acid (GABA), and midbrain dopaminergic neurons, are two distinct neurochemical phenotypes that have been the subject of intense interest. This is not surprising given their roles in a variety of neurological disorders, including epilepsy (Naegele et al., 2010) and Parkinson's disease (Lindvall, 2012). In monolayer culture, and

in the absence of external patterning, differentiating stem cells default to an anterior neuroectodermal fate (Fasano et al., 2010), with dorsal forebrain GABAergic neurons the predominant neuron type (Jain, 2003; Khaira et al., 2011; Ying et al., 2003). Redirecting this differentiation towards alternative fates requires natural protein morphogens, small molecules, and/or stromal feeder layers. In this Chapter we describe the efficient derivation of forebrain GABA, and midbrain dopaminergic neurons using mouse and human PSCs.

2. Materials

2.1 Equipment

1. Cell Culture Consumables: Cell culture flasks, multi-well plates, centrifuge tubes, pipettes, pipette tips, stripettes, 45μm cell strainers caps, 0.22μm syringe filters, motorized pipette gun.
2. Bench-top Class II Biosafety cabinet with HEPA filter and integrated inverted microscope.
3. CO_2 incubator with CO_2, humidity and temperature control.
4. Cell Culture centrifuge capable of spinning 15-50 mL tubes at speeds of at least 200*xg.*
5. Glass haemocytometer.

2.2 PSC Culture

1. Pluripotent stem cells: we have routinely used the murine ESC line E14Tg2a (mESC; ATCC) or the H9 hESC cells (hESC; WARF) but many other PSC lines are available (Kim et al., 2011).
2. MEF CF-1 mitomycin treated mouse embryonic fibroblasts (MEFs; GlobalStem Inc.).
3. mESC Medium: Dulbecco's modified eagle medium (DMEM, Cat no. 10569-044, Life Technologies), 15% fetal bovine serum (FBS, Cat no. HYC15-010.02, Thermo Scientific), Penicillin/Streptomycin (Pen/Step, 1,000 units mL^{-1}, Cat no. 15140-122, Life Technologies), 2 mM Glutamax™ (Cat no. 35050-061, Life Technologies) and 0.1 mM β-mercaptoethanol (Cat no. 21985-023, Life Technologies).
4. Leukemia inhibitory factor (LIF, Cat no. ESG1107, Millipore).
5. hESC Medium: DMEM/F12 Medium (Cat no. 11330-032), 20% (v/v) Knockout Serum Replacement (KSR, Cat no. 10828-028), 1 mM GlutaMAX™, 0.1 mM MEM non-essential amino acids (MEM-NEAA, Cat no. 11140-050, Life Technologies), 55 μM β-

mercaptoethanol and 6 ng mL^{-1} recombinant human FGF2 (Cat no. 233-FB-025, R&D Systems). [See Note 1]

6. Accutase (Cat no. A11105-01, Life Technologies)
7. Sterile 1 x PBS (Cat no. 70011-044, Life technologies)
8. Gelatin coated dishes: made by covering the surface of flask or well with 0.1% gelatin (pre-dilute 2% v/v Cat no. G1393, Sigma-Aldrich) in PBS. Allow the coating to bind by storing in an incubator for at least 15 min at 37°C before aspirating.

2.3 Forebrain GABAergic differentiation

2.3.1 Mouse PSC:

1. N2B27 medium: a 1:1 mixture of DMEM/F12 supplemented with 5mL L^{-1} N2 supplement (Cat no. 17502-048, Life Technologies), 50 μg mL^{-1} bovine albumin fraction V (BSA-FV; Cat no. 15260-037, Life Technologies), 25 μg mL^{-1} insulin (Cat no. I6634, Sigma-Aldrich) and Neurobasal medium (NBM, Cat no. 21103-049) supplemented with 10mL L^{-1} B-27 serum-free additive (Cat no. 17504-044, both Life Technologies).
2. Recombinant mFGF2 (Cat no. 3139-FB-025, R&D Systems). [See Note 1]
3. Matrigel-coated wells: Defrost matrigel (Cat no. 356231, BD Biosciences) aliquot on ice for 2 hrs. With pre-cooled P1000 tips transfer defrosted 300 μL Matrigel aliquot in 10 mL of cold DMEM/F12 basal medium. Add sufficient matrigel to cover wells and set aside for 1 hr at room temperature. [See note 2]

2.3.2 Human PSC:

1. Differentiation Medium for human PSCs (HD1): Knockout DMEM (Cat no. 10829-018, Life Technologies), 15% (v/v) KSR, 1mM GlutaMAX™, 0.1mM MEM-NEAA, 1,000 units mL^{-1} Pen/Strep and 55 μM β-mercaptoethanol.
2. HD2: DMEM/F12, 5mL L^{-1} N2 supplement, 25 μg mL^{-1} insulin, 50 μg/mL BSA-FV.
3. Neurobasal medium: Neurobasal® medium with 10mL L^{-1} B27 supplement, 1,000 units mL^{-2} Pen/Step and 1mM GlutaMAX™
4. Y-27632 (10 μM, Cat no. C9127-2s, Cellagen Technology).
5. SB431542 (10 μM, Cat no. 1661, Axon Medchem).
6. LDN193189 (100 nM, Cat no. 1509, Axon Medchem).
7. Ascorbic acid, (AA, 200μM, Cat no. A4034, Sigma-Aldrich).

8. Dibutyryl cyclic AMP (db- cAMP, 500μM, Cat no. 28745, Calbiochem).
9. *N*-[(3,5-Difluorophenyl)acetyl]-L-alanyl-2-phenylglycine-1,1-dimethylethyl ester (DAPT, 10 nM, Cat no. 1484, Axon Medchem).
10. Brain-derived neurotrophic factor (BDNF, 20 ng mL^{-1}, Cat no. 248-8D, R&D Systems) [See note 1].

2.4 Midbrain dopaminergic differentiation

2.4.1 For differentiation of mouse PSC:

1. Mitomycin-C treated PA6 stromal cells (Riken, Tokyo, Japan, www.riken.go.jp)
2. PA6 medium: Minimum essential medium α (α-MEM, Cat no. 32571-036) supplemented with 10% (v/v) FBS and 1,000 units mL-1 Pen/Strep.
3. PA6 Neural Induction Medium (PNIM): Glasgow's minimum essential medium (GMEM, Cat no. 11710-035) supplemented with 15% KSR, 2 mM GlutaMAX, 1 mM sodium pyruvate (Cat no. 11360-070, Life Technologies), 0.1 mM MEM nonessential amino acids, and 0.1 mM β-mercaptoethanol.
4. PA6 conditioned medium (CM) is collected from PA6-coated flasks. The PA6 stromal cells (ATCC) are plated at 55,000 cells cm-2 in a T25 flask in PA6 medium. The following day the flask is washed with 1 x PBS before the addition of 10 mL of N2B27 medium. Cells are then incubated for 24 h before the medium is removed and replaced with fresh N2B27. The medium is passed through a 0.22μm syringe filter; the resulting CM can be used immediately or stored at 4°C for 1 week. PA6 CM should not be collected from the same flask for more than 7 days.
5. Poly-L-ornithine (PLO)/laminin (LAM)/fibronectin (FN) coated plates: Dilute PLO (Cat no. P3655, Sigma-Aldrich) to 15 μg mL-1 in PBS and add to wells. Twenty-four hours later wash PLO coated wells three times with PBS. Make up natural mouse LAM,1 μg mL-1 (Cat no. 23017-015) and natural human FN, 10 μg mL-1 (Cat no. PHE0023, both Life technologies) in PBS. Add to PLO coated wells for a minimum of 6 hrs (best left over night). Aspirate the LAM/FN from the PLO coated wells and let dry prior plating cells.

2.4.2 Differentiation of human PSC:

1. Human Differentiation Medium (HD1): as above.
2. Human Differentiation medium (HD2): as above.

3. Neurobasal medium, as above.SB431542, as above.
4. LDN193189, as above.
5. Purmorphamine (2 μM, Cat no. 540220, Calbiochem).
6. CHIR99021 (3 μM, Cat no. 04-0004, Stemgent).
7. Sonic hedgehog C25-II (SHH-C25II, 200 ng mL^{-1}, Cat no. 464-SH-025, R&D Systems) [See note 1].
8. BDNF, as above.
9. Ascorbic acid, as above.
10. Glial cell line-derived neurotrophic factor (GDNF, 20 ng mL^{-1}, Cat no. 423-FB-025, R&D Systems) [See note 1]
11. db-cAMP, as above.
12. Transforming growth factor 3 β (TGF-β3, 1 ng mL^{-1}, Cat no. 243-B3, R&D Systems) [See note 3].

    DAPT, as above.

3. Methods

3.1 PSC Maintenance

mESC: Passage mouse PSCs every three days and replate on to gelatin coated wells at a density of 2.5 x 10^4 in mESC medium supplemented with 10^3 units mL^{-1} LIF. [See Note 4].

hESC: Culture hESCs on mitomycin-C treated fibroblasts in hESC medium. Change medium daily. Passage by dissecting colonies into 0.5 mm^2 fragments; using a P200 pipette tip transfer colony pieces onto freshly plated feeders every 5-7 days. [See note 5].

3.2 GABAergic Differentiation:

3.2.1 Mouse PSC:

1. Aspirate mESC medium, wash cells with PBS and add sufficient Accutase to cover cells. Incubate at 37°C until a single cell suspension is achieved (5 – 10 min). Usual volume used: 500μLs per well for a 6-well plate, 1.5mL for a T25 or 3mL of a 60mm dish.
2. Gently pipette cells up and down with a P1000 pipette tip to achieve a homogenous single cell suspension, add mESC medium to cell culture vessel and transfer cell suspension to a 15mL tube.

3. Centrifuge (200x*g* for 5 min).
4. Resuspend centrifuged cells in 1mL of mESC medium and perform a trypan blue count using a haemocytometer to assess cell viability and concentration.
5. Plate mESC cells at 4.5 x 10^3 cells per cm^2 in mESC medium supplemented with LIF.
6. Twenty-four hours following plating, wash cells with 1 X PBS and add N2B27 medium. We denote this as day 0 of differentiation.
7. On day 3 of differentiation supplement with fresh N2B27. Do not perform a complete media change.
8. On day 5 of differentiation, using a P1000 remove half of the medium from the well and add the same volume of fresh N2B27 medium.
9. On day 7 of differentiation, using a P1000 pipette remove half of the medium from the well and add the same volume of fresh N2B27 medium. Continue half media changes daily until cells are used. Typical functional maturation of GABAergic neurons occurs at day 24 of differentiation (Khaira et al., 2011).

3.2.2 Human PSC:

1. Coat wells with diluted Matrigel, (see step 4 under materials).
2. To select the best colonies for differentiation, clean up hESCs using the laminar flow class II hood with HEPA filter and integrated inverted microscope. Remove any pluripotent colonies that contain differentiated cells, inconsistent borders or cores with a transparent appearance using a P200 pipette tip.
3. Following aspiration of hESC medium, add sufficient Accutase to cover colonies and incubate for 10-15 mins at 37°C until a single cell suspension is achieved.
4. Gently triturate cells with a P1000 pipette tip to achieve a homogenous single cell suspension, add hESC medium to cell culture vessel and transfer the cell suspension to a 15mL tube.
5. Centrifuge (160x*g* for 5 min).
6. Resuspend centrifuged cells in 1mL of hESC medium and add 9mL of hESC medium to wash cells.
7. Centrifuge (160x*g* for 5 min). Aspirate medium with Accutase, resuspend centrifuged cells in 1mL of hESC medium and add 9mL of hESC medium to wash cells for a second time.

8. Centrifuge (160x*g* for 5 min). Aspirate medium and resuspend centrifuged cells in 3 mL of hESC medium containing 10 μM of the Rock inhibitor, Y-27632 and filter using a 45μm cell strainer cap.
9. Plate cells on pre-gelatin coated culture vessel at a density of 200,000 cells per cm^2.
10. Following 30 min incubation at 37°C collect non-adherent cells and gently wash the cell culture vessel with hESC medium and centrifuge (160x*g* for 5 min).
11. Resuspend cells in filtered MEF-CM supplemented with 10 ng mL^{-1} rhFGF2 and 10 μM Y-27632. Using a haemocytometer determine viability and cell concentration.
12. Wash Matrigel coated plates by aspirating Matrigel, and rinsing at room temperature with DMEM/F12.
13. Plate hESCs on Matrigel coated wells at a density of 25,000 - 50,000 cells cm^{-2}. In our hands a higher density leads to better cell survival and more consistent differentiation.
14. Twenty fours later, aspirate medium and add fresh MEF-CM supplemented with 10 μM Y-27632.
15. Grow to 90% confluence before initiating differentiation. Y-27632 is not required after 48 hrs.
16. Add a sufficient amount of HD1 medium supplemented with 100 nM LDN193189 and 10 μM SB431452 to wells (this marks day 0 of differentiation).
17. Replace HD1 medium supplemented with 100 nM LDN193189 and 10 μM SB431452 daily.
18. On day 5 of differentiation, aspirated supplemented HD1 medium and add a mixture of HD1 medium (75%) and HD2 medium (25%) supplemented with 100 nM LDN193189.
19. On day 7 of differentiation, aspirated supplemented medium and add a mixture of HD1 medium (50%) and HD2 medium (50%) supplemented with 100 nM LDN193189.
20. On day 9 of differentiation, aspirated supplemented medium and add a mixture of HD1 medium (25%) and HD2 medium (75%) supplemented with 100 nM LDN193189.
21. On day 11 of differentiation, aspirate supplemented medium and NBM medium supplemented with 10 mM DAPT, 200 μM Ascorbic Acid and 1 mM dibutyryl cAMP.

22. Replace medium with fresh supplemented NBM daily.
23. At day 20-25 cells can be replated for terminal differentiation, if desired for further experiments replate Accutase digested cells on PLO/LAM/FN pre-coated wells at a density of 400,000 cells per cm^2 in supplemented NBM medium.

3.3 Dopaminergic differentiation:

3.3.1 Mouse PSC:

1. Plate out PA6 cells at 5.5 x 10^4 cells per cm^2 on pre-gelatin coated cell culture vessels in PA6 medium.
2. Twenty-four hours following, aspirate mESC medium, wash cells with PBS and add sufficient Accutase to cover cells. Incubate at 37°C until colonies are dissociate to single cells (5 – 10 min).
3. Triturate cells with a 1mL pipette to obtain a homogenous single cell suspension, add PIM to cell culture vessel and transfer cell suspension to a 15mL tube.
4. Centrifuge (200x*g* for 5 min).
5. Resuspend centrifuged cells in 1mL of PNIM and perform a trypan blue count using a haemocytometer to assess cell viability and concentration.
6. Wash PA6 stromal cells with PBS and seed mESC cells at 100 cells per cm^2 in PNIM. This is day 0 of differentiation.
7. On day 3 and every day there after aspirate medium and add fresh PNIM.
8. On day 8 of differentiation aspirate PNIM and replace with fresh N2B27 medium supplemented with 20 ng mL^{-1} GDNF, 20 ng mL^{-1} BDNF, and 200 µM ascorbic acid. Change media daily thereafter.
9. At this point cells can be separated from the PA6 stromal feeder layer. Add sufficient Accutase to cover cells and incubate for 15-30 min at 37°C until colonies dissociate.
10. Aspirate N2B27 and Accutase, resuspend in supplemented N2B27, and perform a trypan blue count to assess cell viability and concentration.
11. Replate on PLO/LAM/FN coated wells in N2B27 supplemented with 10 ng mL^{-1} rmFGF2 medium at a density of 400,000 cells per cm. [See note 6].
12. In this instance PA6 cells will contaminate the culture. To obtain pure mESC derived neural cultures, dissect colonies from the PA6 feeder layer using a 21-gauge needle and using a P-200 pipette tip transfer to a 15mL tube containing pre-warmed Accutase. Follow steps 10 and 11 as above.

3.3.2 Human PSC:

1. Follow steps 1-16 of the above section outlining the derivation of GABAergic neurons from hESCs. However, on day 2 of differentiation, add HD1 medium supplemented with 100 nM LDN193189, 10 μM SB431452, 200 ng mL^{-1} SHH-C25II and 2 μM purmorphamine.
2. Aspirate supplemented medium on day 3 and add fresh HD1 medium supplemented with 100 nM LDN193189, 10 μM SB431452, 200 ng mL^{-1} SHH-C25II and 2 μM purmorphamine.
3. Aspirate supplemented medium on day 4 and add fresh HD1 medium supplemented with 100 nM LDN193189, 10 μM SB431452, 200 ng mL^{-1} SHH-C25II, 2 μM purmorphamine and 3 μM CHIR99021.
4. Aspirate supplemented medium on day 5 and add a mixture of fresh HD1 (75%) and HD2 (25%) media supplemented with 100 nM LDN193189, 200 ng mL^{-1} SHH-C25II, 2 μM purmorphamine and 3 μM CHIR99021.
5. Aspirate supplemented medium on day 6 and add a mixture of fresh HD1 (75%) and HD2 (25%) media supplemented with 100 nM LDN193189, 200 ng mL^{-1} SHH-C25II, 2 μM purmorphamine and 3 μM CHIR99021.
6. Aspirate supplemented medium on day 7 and add a mixture of fresh HD1 (50%) and HD2 (50%) media supplemented with 100 nM LDN193189 and 3 μM CHIR99021.
7. Aspirate supplemented medium on day 8 and add a mixture of fresh HD1 (50%) and HD2 (50%) media supplemented with 100 nM LDN193189 and 3 μM CHIR99021.
8. Aspirate supplemented medium on day 9 and add a mixture of fresh HD1 (25%) and HD2 (25%) media supplemented with 100 nM LDN193189 and 3 μM CHIR99021.
9. Aspirate supplemented medium on day 10 and add a mixture of fresh HD1 (25%) and HD2 (25%) media supplemented with 100 nM LDN193189 and 3 μM CHIR99021.
10. Aspirate supplemented medium on day 11 and add NBM supplemented with 3 μM CHIR99021, 20 ng mL^{-1} BDNF, 20 ng mL^{-1} GDNF, 10 mM DAPT, 200 μM Ascorbic Acid and 1 mM db-cAMP.
11. Aspirate supplemented medium on day 12 and add fresh NBM medium supplemented with 20 ng mL^{-1} BDNF, 20 ng mL^{-1} GDNF, 10 mM DAPT, 200 μM ascorbic acid and 1 mM db-cAMP.

12. At day 20-25 cells can be replated for terminal differentiation. If desired for further experiments replate Accutase-digested cells on PLO/LAM/FN pre-coated wells at a density of 400,000 cells per cm^2 in supplemented NBM.

4. Notes

1. Unless described otherwise recombinant growth factors and morphogens are made up in sterile PBS containing 0.1% (w/v) BSA (A2153, Sigma-Aldrich). Following initial suspension solutions are aliquoted and stored at -80°C. Avoid sterile filtering as protein can stick to the membrane of filters altering the final concentration. Once thawed factors are stored at 4°C to avoid freeze-thaw cycles and used within 2 weeks.

2. We have had issues with using Matrigel at concentrations lower than 10 mg mL^{-1}. Do not let Matrigel-coated wells over dry.

3. Recombinant TGF3β is made up in sterile PBS containing 0.1% (w/v) BSA with 4 mM HCl.

4. The inhibitor cocktail "2i" (Ying et al., 2008) should not be used to maintain mESC cultures immediately prior to neural differentiation, as the stabilization of β-catenin affects early neural commitment when commencing neural induction. We find that 2i is the best medium for long-term propagation of mESCs, but recommend 1-2 passages in LIF/serum prior to neural differentiation.

5. hESC colonies can be grown on Matrigel coated plates in mTeSR, but we have found that chemically defined monolayer differentiation is more reproducible if cells are grown on MEFs in the first instance.

6. When replating mESCs differentiated under midbrain dopaminergic conditions, rmFGF2 is only required for the first two days.

5. Typical Results

A working culture of putative PSC-derived neurons is ready to use from ~day 20 of differentiation onwards. The majority of cells in murine cultures will be mature at this point (Watmuff et al., 2012); it is likely that human cells at day 20 are still maturing.

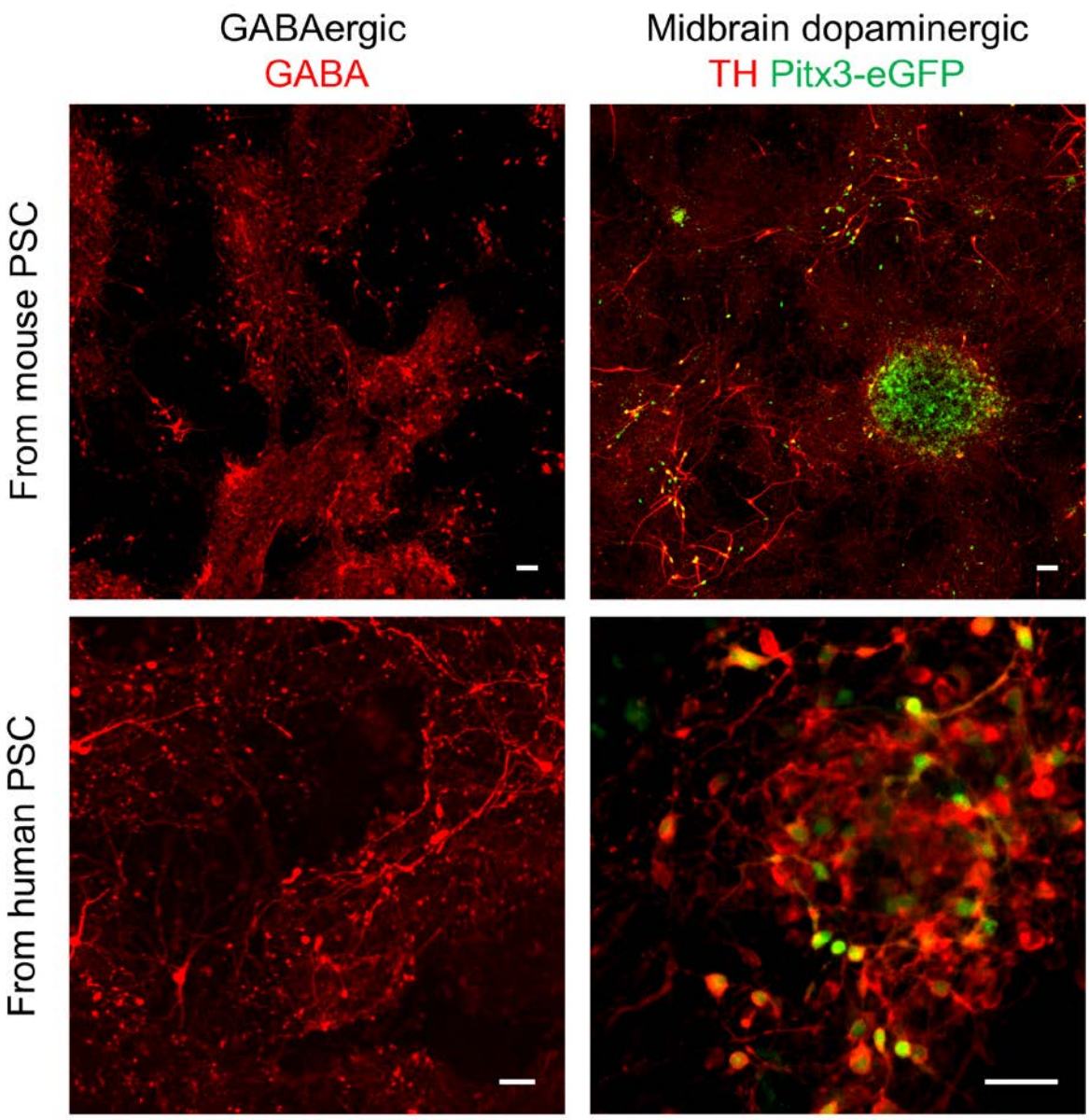

Figure 1: Immunocytochemical characterization of PSC-derived neurons.
Cells express typical markers of GABAergic (A and C) and dopaminergic (B and D) neurons after ~3 weeks of *in vitro* differentiation under conditions outlined herein. Scale bars; 100μm.

References

Fasano, C.A., Chambers, S.M., Lee, G., Tomishima, M.J., and Studer, L. (2010). Efficient derivation of functional floor plate tissue from human embryonic stem cells. Cell Stem Cell *6*, 336–347.

Jain, M. (2003). GABAergic immunoreactivity is predominant in neurons derived

from expanded human neural precursor cells in vitro. Experimental Neurology *182*, 113–123.

Khaira, S.K., Nefzger, C.M., Beh, S.J., Pouton, C.W., and Haynes, J.M. (2011). Midbrain and forebrain patterning delivers immunocytochemically and functionally similar populations of neuropeptide Y containing GABAergic neurons. Neurochemistry International *59*, 413–420.

Kim, H., Lee, G., Ganat, Y., Papapetrou, E.P., Lipchina, I., Socci, N.D., Sadelain, M., and Studer, L. (2011). miR-371-3 Expression Predicts Neural Differentiation Propensity in Human Pluripotent Stem Cells. Cell Stem Cell *8*, 695–706.

Klimanskaya, I., Rosenthal, N., and Lanza, R. (2008). Derive and conquer: sourcing and differentiating stem cells for therapeutic applications. Nature Reviews Drug Discovery *7*, 131–142.

Lindvall, O. (2012). Dopaminergic neurons for Parkinson's therapy. Nat Biotechnol *30*, 56–58.

Naegele, J.R., Maisano, X., Yang, J., Royston, S., and Ribeiro, E. (2010). Recent advancements in stem cell and gene therapies for neurological disorders and intractable epilepsy. Neuropharmacology *58*, 855–864.

Watmuff, B., Pouton, C.W., and Haynes, J.M. (2012). In vitro maturation of dopaminergic neurons derived from mouse embryonic stem cells: implications for transplantation. PLoS One *7*, e31999–e31999.

Ying, Q.L., Stavridis, M., Griffiths, D., Li, M., and Smith, A. (2003). Conversion of embryonic stem cells into neuroectodermal precursors in adherent monoculture. Nat Biotechnol *21*, 183–186.

Ying, Q.L., Wray, J., Nichols, J., Batlle-Morera, L., Doble, B., Woodgett, J., Cohen, P., and Smith, A. (2008). The ground state of embryonic stem cell self-renewal. Nature *453*, 519–523.

Appendix III

Genetic reporter cell lines: tools for stem cell biology and drug discovery

Cameron PJ Hunt, Bradley Watmuff, Brigham J Hartley, Colin W Pouton and John M Haynes

Drug Discovery Biology, Monash Institute of Pharmaceutical Sciences, Monash University (Parkville Campus), Melbourne, Australia

1.0 Pluripotent stem cell reporter lines

The development of methods to enable the propagation and maintenance of pluripotent stem cells (PSCs) has permanently and profoundly altered developmental biology. Isolation of embryonic stem cells (ESCs) has allowed closer examination of the underlying differentiation and development events that have been difficult to define *in vivo*. The development of PSC genetic reporter technology is an essential part of the methodological arsenal that enables us to (i) identify and isolate specific populations of cells at particular stages of development, (ii) elucidate developmental consequences of genetic misregulation and (iii) establish the roles of specific signalling pathways in development, and investigate their mechanisms of action.

All of the current protocols for neural differentiation of ESCs generate multiple cell types. A fraction of these cells are of a desirable phenotype but, often, the majority of these cells are unwanted, ill-defined and possibly counterproductive to attempts to generate a homogeneous population of cells. These unwanted cells may be produced as a consequence of inefficient differentiation strategies that allow fractions of ESCs to drift away from commitment to the desired lineage. This heterogeneity of differentiation is a major consideration when developing strategies to generate specific neural cell types. Previously, investigators were forced to rely on cell surface immunolabelling strategies to isolate fractions of cells and immunocytochemistry with PCR to identify neural phenotypes. These methods are often time-consuming and cannot be performed on viable cells. The use of reporter cell lines in neural differentiation of ESCs enables tracking and isolation of specific neural subtypes, resulting in a more efficient optimisation of differentiation methods.

2.0 Choice of PSC genetic reporter systems

There are several current methods for generation of genetic reporters in PSCs; the most common include targeted homologous recombination (HR), integration of engineered bacterial artificial chromosomes (BACs) and use of viral transduction vectors (VTVs), typically lentiviral vectors.

The successful generation of genetic reporter ESC lines by HR is heavily dependent on the accessibility of the targeted genetic locus and design of the targeting vector [1]. Whilst BACs and lentiviral transfection integrate foreign DNA to random sites within the host genome, HR uses targeted sequences to insert a gene of interest into a specific genetic locus. Since this process is usually highly inefficient it, if successful, is likely to result in one endogenous and one modified allele for the target gene. The main disadvantages of this strategy are the need to isolate dozens, if not hundreds, of PSC clones to ensure correct site-specific integration, and also the unknown effects from haploinsufficient expression of target genes [2]. To circumvent this issue, the generation of reporter cell lines by integration of engineered BACs is becomingly increasingly popular. BAC-derived vectors are large enough to allow a significant length of DNA upstream of the reporter gene to be integrated, leading to high fidelity function of the promoter. However, the BAC strategy also requires substantial sub-cloning to allow positive selection of desired clones. In contrast, viral-mediated delivery of reporter constructs is a faster process, typically integrating at multiple sites and significantly increasing copy number of target genes [3]. However, most viral vectors integrate randomly, have unknown effects on regulatory sequences and disrupt vital signalling mechanisms [4]. Viral vectors are limited with respect to the size of the insert that can be accommodated, so that only the immediate upstream promoter sequences can be included. As a result the regulation of gene expression may not be faithfully reproduced in transduced PSC lines. This strategy is a quick way of screening for genes that are important for development, but subsequent HR or BAC transgenesis is likely to be desired for investigation of fine detail. Selection of an appropriate VTV system depends on several factors including; whether control over the site of vector integration is required, the size of the genetic construct to be integrated, and the efficiency of infection required [5]. In addition, conditional expression or silencing of the transgene may be required for downstream applications such as transplantation studies.

For the bulk of the work in our laboratory we have opted for HR. The advantage of this method is that it provides stable, context-specific expression of reporters. We have recently utilized zinc-finger nuclease (ZFN) targeting, an approach that can speed up the process of HR, but which has drawbacks. ZFN technology is relatively expensive and could lead to rare but unpredictable off-target effects. One aspect of HR that requires careful consideration is that targeting a reporter to one allele leaves the second unchanged, but usually results in the creation of a heterozygous knock-out cell line. This could result in a cell line that is haploinsufficient for the target gene, meaning that the levels of mRNA are unusually low, resulting in changes in the physiology of the cell line. Whether this introduces abnormal physiology is dependent on how the expression of each gene is regulated. We have used HR to introduce reporters, typically targeting exon 1 of a single allele, of several neural developmental genes without causing obvious developmental abnormalities. However, we have not probed for subtle changes in detail. To reduce the effects of haploinsufficiency, the cDNA of the target gene could be reintroduced within the targeting construct. To our knowledge this is not common practice and may not necessarily restore normal gene expression, because the introns present in the chromosomal DNA may play a role in natural gene regulation. Integration of modified BACs is an alternative way of avoiding potential haploinsufficiency but with BAC transgenesis there is the possibility that reporter gene expression is abnormal, either due to a lack of distant natural gene regulatory sequences, or direct influences of flanking DNA at the site of random integration. Our experience suggests that concerns about haploinsufficiency have not proven to be a major obstacle to use of HR.

Having chosen a method to introduce the reporter gene, the next task is to identify the optimal reporter system for the intended use. There are three basic types of reporter proteins: fluorescent proteins, enzymes, or proteins used to introduce more complex sensors of specific signalling systems.

3.0 Reporter systems

3.1 Fluorescent Proteins

Fluorescent proteins are a widely used and growing group of reporter proteins [6]. These proteins emit a distinct spectrum of light when excited with light from within a specific excitation spectrum, both excitation and emission having characteristic wavelength maxima. Selection of the fluorescent protein to be used as a reporter is

dependent on available equipment i.e. light source, excitation and emission filters. Whilst some fluorescent proteins may not be suitable due to poor stability or 'brightness', a significant number of fluorescent protein variants are available that span the visible spectrum from Sapphire & Cerulean proteins in the UV/blue range to Citrine & red fluorescence proteins (RFP) in the yellow & near-red ranges to mPlum & infra-RFP in the far-red & near infrared ranges respectively. For extensive lists of fluorescent proteins see [7, 8]. Table 1 shows a selection of reporters and why we have chosen them. The distinct advantage of fluorescent proteins is that they facilitate non-destructive imaging of live cells without the need for introduction of additional materials.

3.2 Enzyme Proteins

This class of reporter includes a series of older enzymes, such as □-galactosidase and alkaline phosphatase, which have associated substrates to allow colourimetric or fluorometric assays. However, the most useful enzymes for HR are more sensitive enzymes that are xenobiotic to the host cells, including the luciferase enzymes that were originally identified in fireflies and beetles [9] and □-lactamase. These enzymes can be targeted so that they are expressed under the control of a desired host cell promoter. Upon luciferase expression, the addition of a substrate, D-luciferin, causes a reaction with ATP to produce luciferyl adenylate which combines with molecular oxygen to produce oxyluciferin and light. The light is emitted within a range from 550 – 620 nm, depending on the choice of luciferase. An unwanted side effect of this reaction is the production of hydrogen peroxide (H_2O_2) and may need to be considered with repeated imaging or if long term survival of the cell population is required.

An alternative enzyme-based reporter is the ampicillin resistance (*AMP*^{R}) cDNA which encodes for β-lactamase. There are multiple substrates available for this system, including fluorescent & luminescent assays. We have used the GeneBlAzer® substrate loading kits (Invitrogen) to facilitate live cell imaging and flow cytometry with living cells. The LiveBlAzer® substrate for this system is a fusion of two fluorescent molecules that excite at (peaks of) 409nm and 494nm. In the absence of □-lactamase the 409nm excitation results in 447nm (peak) emission that is absorbed by the other fluorophore and as a consequence, emits green light at 520nm i.e. the result of a fluorescence resonance energy transfer (FRET) reaction. In the presence of □-lactamase the substrate

is cleaved, subsequent excitation at 409nm now results in 447nm (peak) blue emission. Both luciferase and β-lactamase reporters are highly sensitive as they are enzymes, so that a single molecule of protein when combined with substrate produces a considerable amplification of signal when compared with the sensitivity of a fluorescent protein. In our hands the sensitivity is an important consideration when investigating the temporal expression of transcription factors. For example, using identical ES cell differentiation protocols *Lmx1a* expression can be detected approximately 24 hours earlier in an Lmx1a-β-lactamase reporter line than the Lmx1a-eGFP reporter line.

Bioluminescent assays are also commonly used in plate-based assays where protein expression assayed after lysis marks a functional end point. Although these assays are highly sensitive, the need for substrates adds significant costs to reporter detection.

3.3 Complex reporter methodologies

Additional reporter technologies have been developed for more specific imaging needs. Bioluminescence resonance energy transfer (BRET) assays rely on a luciferase-luciferin light emission to excite a fluorophore such as Yellow Fluorescent Protein [10] Reporter assays can be developed to take advantage of BRET/FRET-compatible substrates allowing the generation of sensitive enzyme-based assays that can be used to identify cells and also investigate events downstream of the gene of interest. In addition, proteins that respond to intracellular calcium gradients by FRET-based emission (such as those described [11]) could be considered to track activation of signal transduction pathways.

Table 1: “Common reporters used in neural differentiation assays”…..here

4.0 Multiple reporter lines

Most fluorescent proteins are suitable for imaging applications and for counting or sorting using flow cytometry; the choice of protein is only limited by the analytical instrument available. In stem cell biology reporter genes are commonly used to identify cells at specific stages of differentiation [12-14]. The selection of reporter system can be tailored according to the relative levels of expression, making use of fluorescent proteins for high expression systems or enzyme-systems if needed, when levels of expression are

low. However, a single genetic reporter may not be enough to identify specific populations of cells, especially differentiating neurons [12]. To enable more precise identification of particular lineages during differentiation it may be necessary to consider a double or multiple reporter strategy, targeting more than one reporter to a single gene, or targeting more than one gene in a single cell line.

Targeting a dual reporter to a single gene allows the use of multiple analytical techniques, for example we routinely create cell lines with GFP and luciferase under the control of a single promoter using an internal ribosome entry site (IRES) to facilitate expression of both reporters from the transcript, such as the Lmx1a-eGFP-IRES-□-lactamase cell line previously reported [12]. There are alternatives to the use of constructs using IRES sequences. Separation of reporter genes by T2 or T2A sequences allows multiple reporters to be co-expressed, though gene expression levels of reports placed downstream of the first gene are generally a factor of 2-5 times lower. The use of multiple reporters at one integration site allows more than one analytical operation to be performed. For example, the eGFP-IRES-luciferase construct allows imaging of differentiation (eGFP), FACS isolation of living cells (GFP) and a sensitive plate based assay after cell lysis (luciferase).

Dual or multiple reporters designed to track expression of more than one gene are more complicated to generate since they involve at least two rounds of HR. The first round generates a single reporter (Lmx1a-eGFP, for example). The second round uses a positive (Lmx1a-eGFP) clone to target a second reporter (Fox2-mCherry, for example), to produce a cell line that marks for both Lmx1a and FoxA2 expression. This approach is powerful if the aim is to generate precise regional specification of cell populations. Our approach to using these cell lines is illustrated below.

5.0 Use of genetic reporter ESCs to study neural differentiation

The protocols described below were developed for use with our Lmx1a reporter cell lines, but in principle could be used for analysis of reporters targeted at any gene involved in neural differentiation. We carried out neural differentiation using an adherent monolayer protocol (see Hartley BJ et al in this volume.

5.1 Utilising reporter cell lines to quantify expression of Lmx1a in neuronal progenitors

The following protocols describe different quantitative assays of Lmx1a+ expression during differentiation of PSCs to form neuronal progenitors. Flow cytometry (FACS) can be used to analyse the proportion of cells positive for the reporter gene. Alternatively plate-based assays for luciferase can be used to quantify, with high sensitivity, the total amount of gene expression in a single well, using either *e*GFP or □-lactamase reporter systems. Additionally, these cell lines could be used for imaging analysis if FACS is not available.

5.1.1 General method for preparation of cells prior to analysis

I) Differentiate reporter lines until the required day of analysis using the method of choice. We have used methods described in detail by Hartley BJ et al (this volume).

II) Wash adherent cells twice with PBS and harvest cells from the culture plate using Accutase®, pre-warmed to 37°C.

III) Return cells to incubator at 37°C for 5-10 min.

IV) Resuspended cells in complete mES medium & centrifuge at 200xg for 5 min to pellet cells.

5.1.2 FACS analysis using the eGFP reporter expressed in Lmx1a-luc-IRES-eGFP mouse ESCs

1) Aspirate supernatant and resuspend cells in FACS buffer (10% FCS v/v in 1x PBS) supplemented with 5 nm SYTOX® Red cell viability dye.

2) Incubate cells in the dark on ice for 10 min.

3) Analyse samples by flow cytometry using 488 and 633 nm excitation lasers with 510/20 & 660/20 emission filters for eGFP & SYTOX® Red respectively.

4) Analyse at least 1.0 x10^5 positive events using an appropriate FACS instrument for analysis using either inbuilt software or external cytometry data packages such as FlowJo (Tree Star Inc)

5.1.3 FACS analysis using β-lactamase (AMP^R) reporter expressed in Lmx1a-AMP-IRES-eGFP mouse ESCs

Follow steps I-IV outlined in 5.1.1

1) Aspirate the supernatant and then suspend the cells using the LiveBLAzer™-FRET β-lactamase labelling kit (Invitrogen).

2) Incubate cells in the dark at ambient temperature for 2-2.5 hrs.

3) After incubation, centrifuge cells at 200xg for 5 min and remove the supernatant.

4) Resuspend the cells in FACS buffer containing 5 nM SYTOX® Red and place on ice in the dark for 10 min

5) Analyse or sort the cells by FACS for reaction product (450/50), eGFP from loaded cells (510/20) and viable cells (660/20) using 405, 488 & 633 nm excitation lasers, respectively.

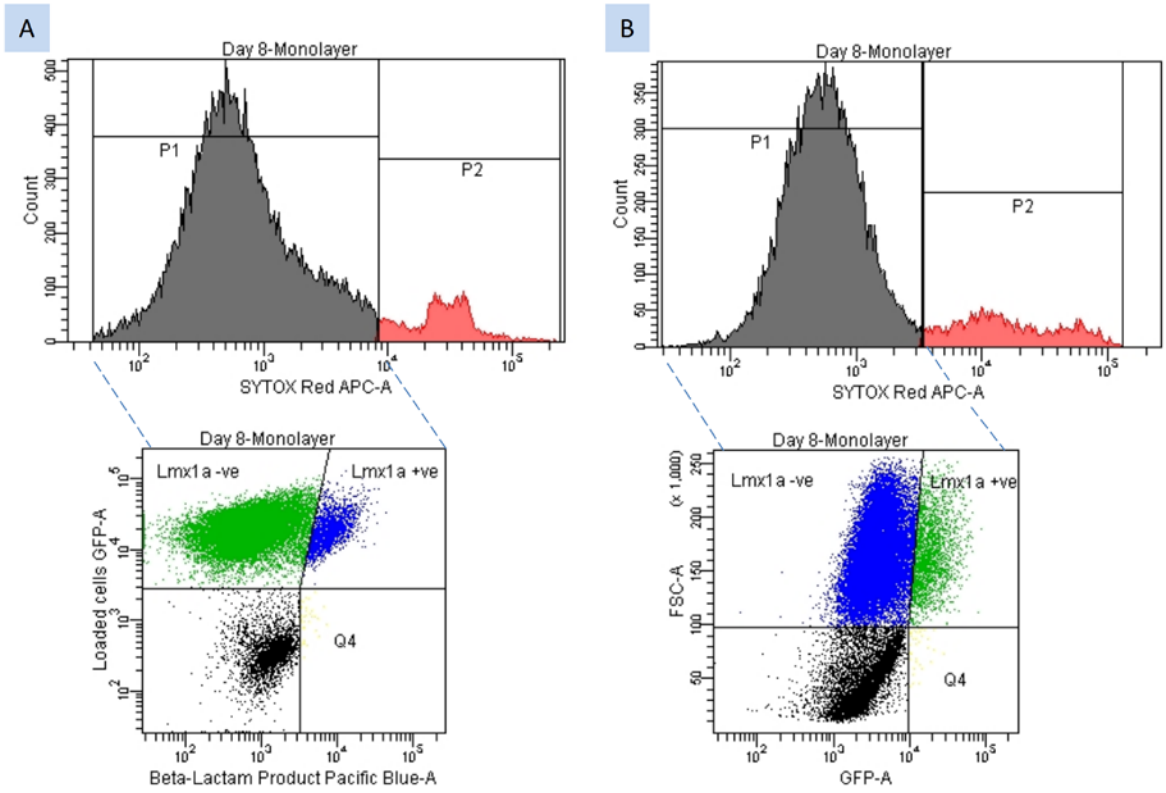

Figure 1: Quantitative analysis of Lmx1a+ progenitors. (A) assay of Lmx1a-□-lactamse⁺ cells, and (B) Lmx1a-eGFP⁺ cells. ESCs were differentiated using an adherent monolayer protocol and analysed on day 8.

The FACS plots in Figure 1 demonstrate that the above method is suitable for the isolation of Lmx1a-eGFP+ or Lmx1a-AMP+ cells. However, eGFP may not sensitive

enough for some applications requiring the AMP reporter system. In addition, over incubation of AMP substrate may provide false-positives and should be empirically determined.

5.1.4 Analysis of luciferase expression in Lmx1a-luc-IRES-eGFP mouse ESCs

The following method involves lysis of adherent or suspended cells, is rapid and suitable for large scale compound screens in microtitre plate format. We have found that a surrogate measure of cell number is necessary, to ensure that the expression of luciferase can be normalised if desired. We use the Cell Titer-Blue assay to provide a fast and simple assay for relative number of viable cells.

1) Seed cells into 96-well plates and differentiate using N2B27 media until the required day of assay.

2) Wash cells twice with 1x PBS.

3) Add Cell Titer-Blue® (CTB) reagent to quantify relative number of viable cells and return to incubator at 37°C for 2-4 hrs.

4) During incubation, remove Luciferase substrate (Steady-Glo®) from the freezer and bring to room temperature (RT).

5) After incubation, remove cells from the incubator and using an appropriate plate reader (we use Perkin Elmer, Wallac EnVision® 2101) to analyse for concentration of the CTB metabolised product at 590 nm.

6) Remove cells from the plate reader and wash with 1x PBS to remove quenching effects caused by the CTB[a].

7) Add 100 µL of PBS to each well, add 100 µL of Steady-Glo® luciferase substrate (Promega), and mix to combine reagents.

8) Incubate the plate in the dark at RT for 5-10 min[b]

9) After incubation, return the plate to the plate reader and analyse for luminescent signal at

The above methods illustrate that Lmx1a+ neural progenitors can be analysed quantitatively and isolated using genetic reporter systems. In addition, the generation of dual reporter systems such as Lmx1a-luc-IRES-eGFP allows both isolation (GFP+) & sensitive qualitative analysis (luc) of an enriched cell population. It should be noted that reporter expression is often weaker downstream of the IRES linker, thus the order of reporter genes may need to be considered. In the case of the Lmx1a cells line, both *luciferase* and *eGFP* reporters work well, but reporter gene expression may be lower when using some endogenous promoters, therefore an eGFP-IRES-luc may be more appropriate.

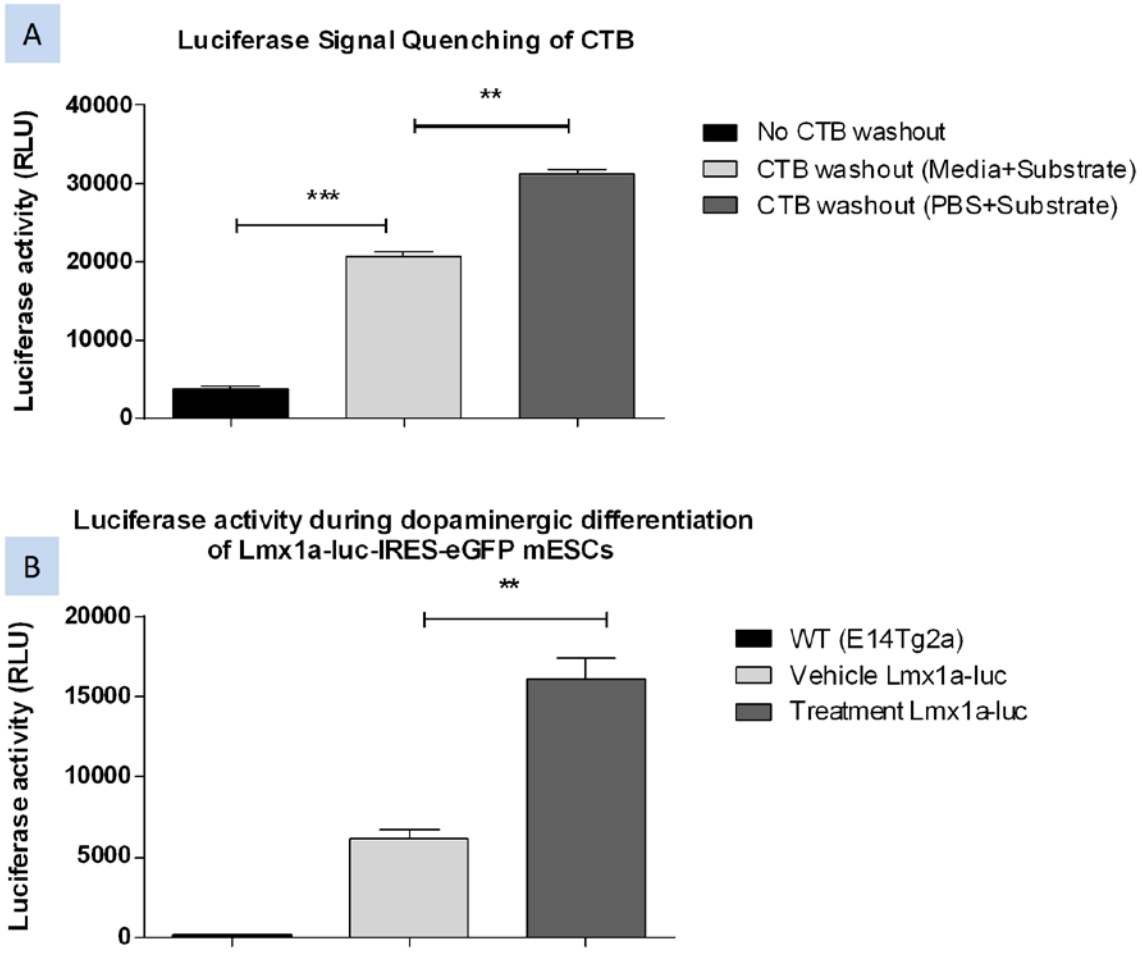

Figure 2: Luciferase as a reporter for screening assays. A) Effect of CTB washout on luciferase signal. B) Luciferase activity of Lmx1a-*luc* ES cells after 4 Days monolayer differentiation. [a] Figure 2 shows that the luciferase signal is increased after CTB wash out.

[b] In this protocol we recommend use of Steady-Glo® luciferase substrate (Promega) which is a variation of the classical luciferase substrate and is designed to extend the half-life of the luminescence signal. ****p<0 .001 p<0.01, one-way ANOVA compared to Vehicle, Bonferroni's post-test.*

5.2 Investigating neuronal development by sorting ESC-derived progenitors marked with a ubiquitously expressed reporter

In some cases it may be desirable to investigate the development of neural progenitors into mature neurons after placing the progenitors into a different environment, when the new environment could be *in vitro* or *in vivo*. The isolation of progenitors could then be achieved using an appropriate progenitor reporter such as the Lmx1a reporter used in section 5.1.3. Given that expression of the gene used for sorting may be down-regulated during differentiation, it is useful to mark the cells with a second reporter that is expressed in all cells derived from the sorted progenitors. This strategy could be particularly useful to track the survival and differentiation of implanted neurons *in vivo*. One approach we have used is to introduce a fluorescent protein at the Rosa26 locus in mouse cells. If a similar strategy is desired for use in human cells, the AAVS1 integration site could be utilised [15] as the site for the ubiquitously expressed reporter.

We have created a mESC line Lmx1a-*AMP*-IRES-eGFP/Rosa26-mCherry to allow isolation of Lmx1a+ cells during differentiation. The cells were then used to track their development into other lineages (which may become Lmx1a-) *in vitro*, or to image cells implanted into brain tissue using microscopic analysis of brain slices.

ES cells were grown as adherent monolayers and differentiated in accordance with the monolayer protocol (Hartley BJ et al, this volume). The following protocol is suitable for tracking development of cells *in vitro*, making use of the β-lactamase reporter for sorting progenitors.

1) On the day before a sorting experiment, coat cell culture wells, of required size, with laminin solution at 2 μg/cm^2.

2) On the day nominated for cell sorting, remove the medium from above the cell monolayers and filter using a 0.22 μm filter. This 'conditioned' medium can be stored at 4°C for later use. Wash cells with PBS and harvest using Accutase®, pre-warmed to 37^{o}C.

3) Return cells to an incubator at 37°C for 5-10 min to allow detachment from culture plate. Following incubation, resuspended cells using complete mES media and centrifuge at 200xg for 5 min to pellet cells.

4) After centrifugation, resuspend cells using LiveBLAzer™-FRET β-lactamase labelling solution (Invitrogen) and incubate in the dark at RT for 2-2.5 hrs.

5) After incubation, centrifuge cell suspension at 200xg for 5 min.

6) Remove supernatant and resuspend cells in FACS buffer with 5 nM SYTOX® Red. Incubate cell suspension on ice in the dark for 10 min.

7) Sort viable β-lactamase+ cells using a suitable FACS instrument and collect the isolated cells at RT in FACS buffer.

8) Centrifuge the resulting cell suspension again at 200xg for 5 min.

9) Resuspend the cell pellet in 1:1 mix of fresh N2B27 w/ Fgf-2(10ng/mL) & heparin sulphate (10μg/mL) and conditioned medium removed earlier (see (2)) warmed to 37°C. These cells are now ready to be replated for a differentiation experiment, or possible prepared for implantation. The protocol described immediately below is suitable for studying the fate of reporter+ and reporter- cells when recombined as a mixture.

10) Using a cell line that lacks the Rosa26-targeted fluorescent reporter (e.g. Lmx1a-*AMP*-IRES-eGFP), carry out steps 1-9 and capture cells that are β-lactamase- (i.e in the example shown cells that are Lmx1a-)

11) Mix isolated β-lactamase+/Rosa26-mCherry+ cells with β-lactamase-/Rosa26-mCherry- cells in the desired ratio.

12) Plate cells into laminin-coated tissue culture wells, as prepared earlier, at a density of 1.0×10^5 cells/cm^2.

13) Continue differentiation in this 1:1 media composition (described in 9) for 96 hrs, changing media every second day other day.

14) 96 hrs after replating, change media to N2B27 supplemented with Glial cell line-derived neurotrophic factor (GDNF, 10ng/mL) & Ascorbic Acid (AA, 200μM) until the day of analysis by immunocytochemistry.

15) On day of analysis, neuronal cultures can be fixed in 4%w/v paraformaldehyde, permeablised using 0.1%v/v Triton X-100, blocked (2%v/v Fetal bovine serum, or 2° antibody-host) and can be labeled for dopaminergic neurons using antibodies against markers such as tyrosine hydroxylase (TH).

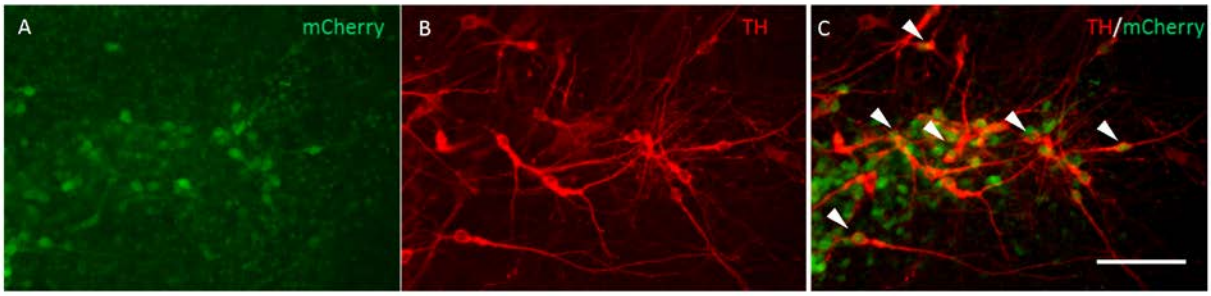

Figure 3: Immunocytochemistry of sorted Lmx1a-AMP:Rosa26-mCherry ES cells. (A) Rosa26-mCherry+ cells (B) Cells immunoreactive with anti-TH antibody (C) Superimposition of A and B. White arrows indicate double positive cells i.e. progenitors that were sorted as Lmx1a+ cells, which have given rise to TH+ neurons. Scale 100 µm.

	Brightness	*Photostability*	*Excitation*	*Emission*
Fluorescent assays			*λ*	*λ*
***eCFP*[1,2]**	Good	Good	405	470/15
***eGFP*[1,2]**	Very Good	Excellent	488	510/20
***Tomato*[1,2]**	Excellent	Poor	561	585/42
***DsRed*[1,2]**	Very Good	Good	561	595/20
***mCherry*[1,2]**	Good	Very Good	561	595/20
Luminescent assays				
***Luc*[3]**	Excellent	Poor	-	557
***CBR*[3]**	Excellent	Poor	-	617
Other Enzyme-based				
***AMP*[a 1,2,3]**	Very Good	Good	405	450/50
			488	510/20
***β-galactosidase*[b 1,2,3]**	Very Good	Good	488	510/20

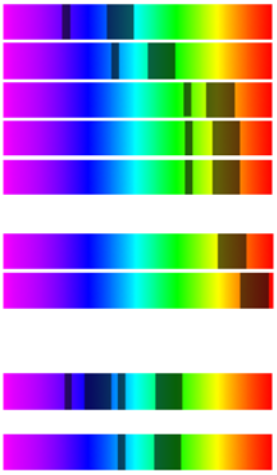

Table 1: Common reporter genes that can be used in neural differentiation assays. FACS: Fluorescence assisted cell sorting, CFP: Cyan Fluorescent protein, eGFP: enhanced fluorescent protein, Luc: Firefly luciferase enzyme, CBR: Click beetle red luciferase enzyme, AMP: AMP gene encoding B-lactamase. [1] protein suitable for imaging experiments, [2] FACS & [3] screening-based methods. In addition, luciferase & far red reporters are suitable for *in vivo* whole animal imaging.[16] [a] Substrates for β-Lactamase can vary, the LivBLAzer-FRET based substrate is described above. [b] Multiple fluorescent substrates for β-Galactosidase have been generated, ImaGene Green™ substrate (C12FDG) is shown above. Optimal emission filters reviewed [17] additional fluorophore data provided by [8, 18].

References

1. Bronson, S.K. and O. Smithies, *Altering mice by homologous recombination using embryonic stem cells.* Journal of Biological Chemistry, 1994. **269**(44): p. 27155-27158.
2. Sun, W. and J.R. Downing, *Haploinsufficiency of AML1 results in a decrease in the number of LTR-HSCs while simultaneously inducing an increase in more mature progenitors.* Blood, 2004. **104**(12): p. 3565-3572.
3. Zhang, Y. and B. Oliver, *Dosage compensation goes global.* Current Opinion in Genetics and Development, 2007. **17**(2): p. 113-120.
4. Mutskov, V. and G. Felsenfeld, *Silencing of transgene transcription precedes methylation of promoter DNA and histone H3 lysine 9.* EMBO Journal, 2004. **23**(1): p. 138-149.
5. Verma, I.M. and M.D. Weitzman, *Gene therapy: Twenty-first century medicine*, 2005. p. 711-738.
6. Bartlett, R.J., et al., *Long-term expression of a fluorescent reporter gene via direct injection of plasmid vector into mouse skeletal muscle: Comparison of human creatine kinase and CMV promoter expression levels in vivo.* Cell Transplantation, 1996. **5**(3): p. 411-419.
7. Shaner, N.C., et al., *Improved monomeric red, orange and yellow fluorescent proteins derived from Discosoma sp. red fluorescent protein.* Nat Biotech, 2004. **22**(12): p. 1567-1572.
8. Chudakov, D.M., et al., *Fluorescent Proteins and Their Applications in Imaging Living Cells and Tissues.* Physiological Reviews, 2010. **90**(3): p. 1103-1163.
9. De Wet, J.R., K.V. Wood, and M. DeLuca, *Firefly luciferase gene: Structure and expression in mammalian cells.* Molecular and Cellular Biology, 1987. **7**(2): p. 725-737.
10. Takakura, H., et al., *Development of luciferin analogues bearing an amino group and their application as BRET donors.* Chemistry, an Asian journal, 2010. **5**(9): p. 2053-2061.
11. Kerr, R.A. and W.R. Schafer, *Intracellular Ca2+ Imaging in C. elegans*, 2006. p. 253-264.

12. Nefzger, C.M., et al., *Lmx1a allows context-specific isolation of progenitors of GABAergic or dopaminergic neurons during neural differentiation of embryonic stem cells.* Stem Cells, 2012. **30**(7): p. 1349-1361.
13. Elliott, D.A., et al., *NKX2-5eGFP/w hESCs for isolation of human cardiac progenitors and cardiomyocytes.* Nat Meth, 2011. **8**(12): p. 1037-1040.
14. Goulburn, A.L., et al., *A Targeted NKX2.1 Human Embryonic Stem Cell Reporter Line Enables Identification of Human Basal Forebrain Derivatives.* Stem Cells, 2011. **29**(3): p. 462-473.
15. Hockemeyer, D., et al., *Efficient targeting of expressed and silent genes in human ESCs and iPSCs using zinc-finger nucleases.* Nat Biotech, 2009. **27**(9): p. 851-857.
16. Filonov, G.S., et al., *A bacteriophytochrome-based near infra-red fluorescent protein for in vivo imaging.* Molecular Biology of the Cell, 2011. **22**(24).
17. Shaner, N.C., P.A. Steinbach, and R.Y. Tsien, *A guide to choosing fluorescent proteins.* Nat Meth, 2005. **2**(12): p. 905-909.
18. Shaner, N.C., et al., *Improving the photostability of bright monomeric orange and red fluorescent proteins.* Nature Methods, 2008. **5**(6): p. 545-551.

Appendix IV

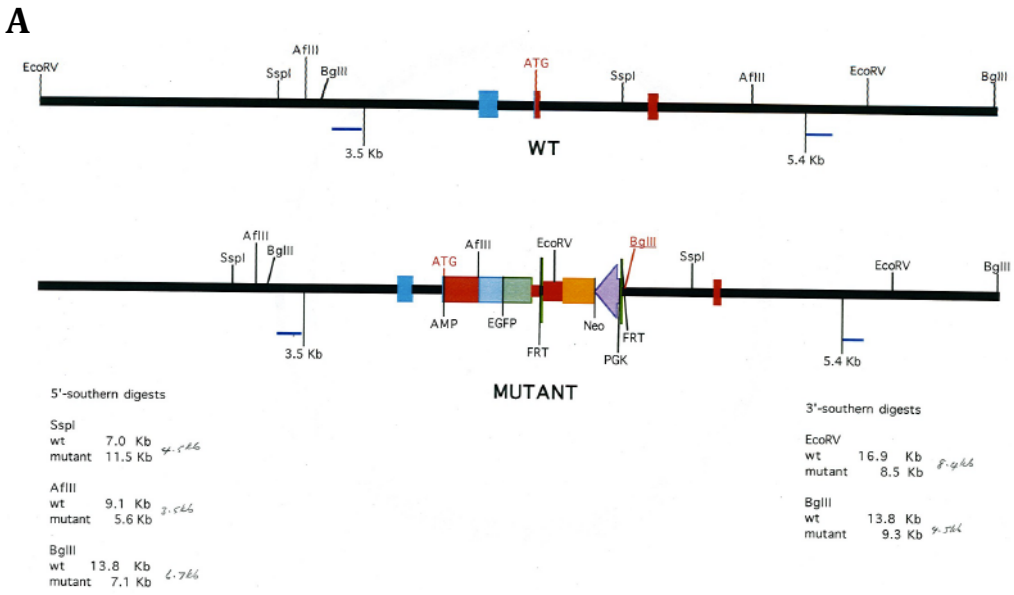

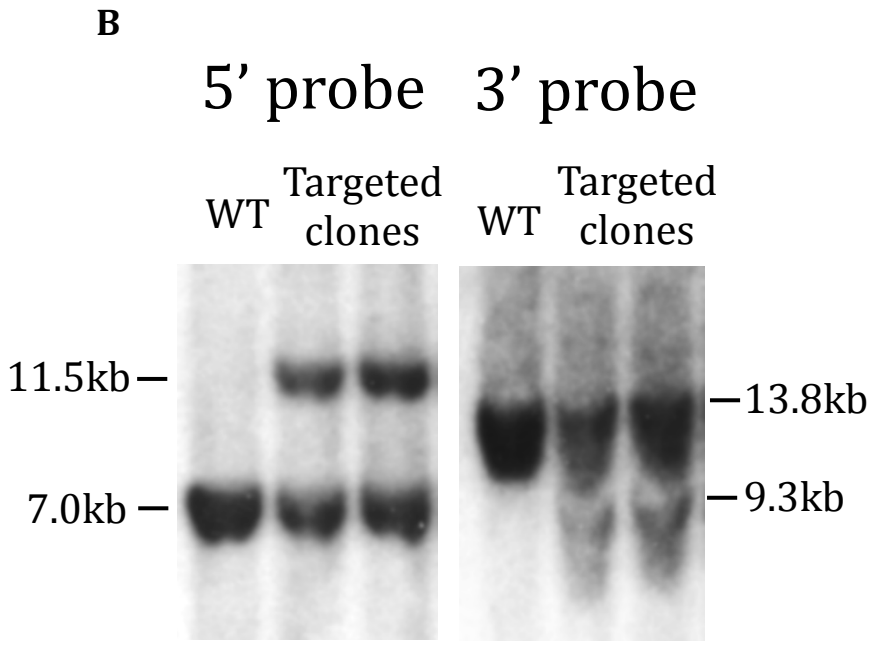

Appendix 4 Figure 1. hLMX1A-AIG *targeting validation in hESCs. (***A**) shows the schematic of the southern blot strategy employed to validate targeting of the *LMX1A* locus. (**B**) Correctly targeted colonies (as determined by PCR) were subsequently confirmed by Southern blot analysis.

Appendix V

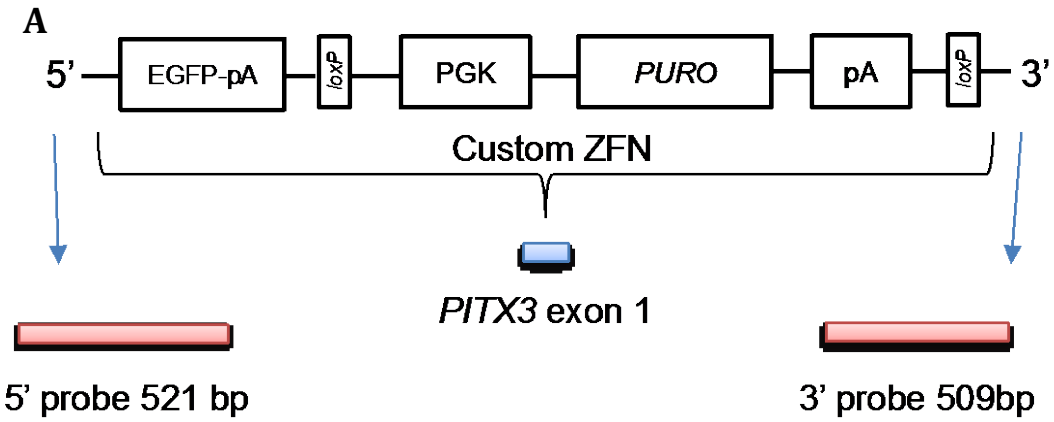

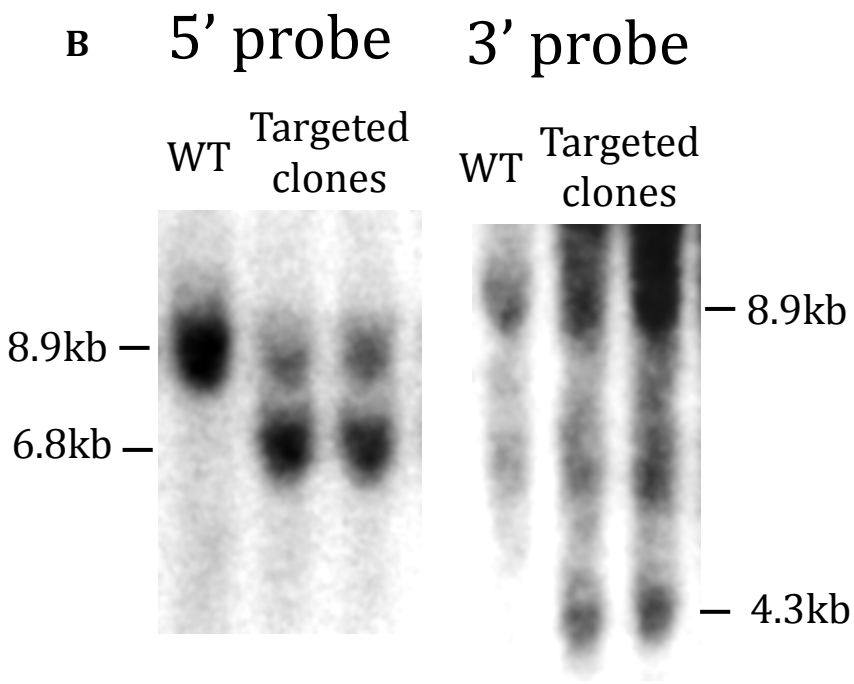

Appendix 5 Figure 1. hPITX3-EGFP *targeting using zinc finger nucleases validation in hESCs. (***A**) shows the schematic of the southern blot strategy employed to validate targeting of the *PITX3* locus (based on Hockemeyer et al., 2009). (**B**) Correctly targeted colonies (as determined by PCR) were subsequently confirmed by Southern blot analysis. Abbreviations: PGK, human phophoglycerol kinase promoter; PURO, puromycin resistance gene, loxP, loxP sites; pA, polyadenylation sequence.